Exploring new exchange-correlation kernels in the Bethe-Salpeter equation

Roberto Orlando

Université Fédérale
Toulouse Midi-Pyrénées

THÈSE

En vue de l'obtention du
DOCTORAT DE L'UNIVERSITÉ DE TOULOUSE
Délivré par l'Université Toulouse 3 - Paul Sabatier

Présentée et soutenue par

Roberto ORLANDO

Le 1 décembre 2023

Exploration de nouveaux noyaux d'échange-corrélation dans l'équation de Bethe-Salpeter

Ecole doctorale : **SDM - SCIENCES DE LA MATIERE - Toulouse**

Spécialité : **Physique de la Matière**

Unité de recherche :
LCPQ - Laboratoire de Chimie et Physique Quantiques

Thèse dirigée par
Pierre-François LOOS et Pina ROMANIELLO

Jury

M. Julien TOULOUSE, Rapporteur
M. Francesco SOTTILE, Rapporteur
Mme Nadine HALBERSTADT, Examinatrice
Mme Elisa REBOLINI, Examinatrice
M. Pierre-François LOOS, Directeur de thèse
Mme Pina ROMANIELLO, Co-directrice de thèse

Contents

1 Introduction **3**

2 The many-body problem **10**
2.1 The Born-Oppenheimer approximation . . . 10
2.2 Hartree-Fock theory . . . 12
2.2.1 Closed-Shell Hartree-Fock . . . 18
2.2.2 The Roothaan equations . . . 19
2.2.3 Koopmans' Theorem . . . 23

3 Post Hartree-Fock calculations **24**
3.1 Configuration Interaction . . . 24
3.2 Many-body perturbation theory . . . 26
3.2.1 Time-independent perturbation theory . . . 26
3.2.2 Time-dependent perturbation theory . . . 27
3.2.3 Green's functions . . . 31
3.2.4 Approximations of the self-energy . . . 38
3.2.5 Random Phase Approximation equations . . . 42
3.2.6 Stability problems . . . 48
3.3 The two-particle Green's function . . . 52
3.3.1 The two-body free response . . . 54
3.3.2 The two-body total response with a static kernel . . . 54

4 Exploring new approximations to the Bethe-Salpeter kernel **56**
4.1 The Hamiltonian of the Hubbard dimer . . . 56
4.2 Testing approximations to the self-energy and its derivative . . . 59
4.2.1 The symmetric dimer . . . 59
4.2.2 Asymmetric Hubbard dimer . . . 67

5 The GW, particle-particle, and electron-hole T-matrix self-energies **75**
5.1 The standard form of Hedin's equations . . . 75
5.2 An alternative form of Hedin's equations . . . 76
5.3 Hedin's equations from the equation-of-motion formalism . . . 77
5.4 Dyson equations . . . 78
5.5 Response functions . . . 80
5.6 Self-energies . . . 81
5.6.1 GW self-energy . . . 81
5.6.2 Particle-particle T-matrix self-energy . . . 82
5.6.3 Electron-hole T-matrix self-energy . . . 83
5.7 Results and discussion . . . 84

6 Conclusions and Perspectives **87**

7 Résumé en français **89**
7.1 L'approximation de Born-Oppenheimer . . . 92
7.2 Théorie Hartree-Fock . . . 93
7.3 Théorie des perturbations à N corps . . . 95
7.3.1 Approximations sur la self-énergie . . . 98
7.3.2 Calcul de la réponse depuis la polarisabilité reductible χ . . . 100
7.4 La fonction de Green à deux corps . . . 103
7.4.1 La réponse libre du système à deux corps . . . 104
7.4.2 La réponse totale du système à deux corps avec un noyau statique . 105
7.5 Le Hamiltonien du dimère de Hubbard . . . 106
7.5.1 Dimère de Hubbard symétrique . . . 107
7.5.2 Dimère de Hubbard asymétrique . . . 110

Appendices **129**

A Asymmetric dimer **130**
A.1 One electron . . . 130
A.2 Two electrons . . . 130
A.3 Three electrons . . . 132

B The electron-hole RPA **133**
B.1 GW . . . 134
B.2 G$\overline{T}^{eh}$ . . . 136

C The particle-particle RPA **140**

D Quasiparticles and neutral excitations of the symmetric Hubbard dimer **144**
D.1 Quasiparticles . . . 144
D.1.1 GW Quasiparticles . . . 145
D.1.2 GT^{pp} Quasiparticles . . . 145
D.1.3 $G\overline{T}^{eh}$ Quasiparticles . . . 146
D.2 Bethe-Salpeter calculation in the GW approximation . . . 147
D.3 Bethe-Salpeter calculation in the GT^{pp} approximation . . . 150
D.3.1 GW for the asymetric dimer . . . 153

E Resolution methods of a Bethe-Salpeter equation **155**
E.0.1 Quantum field theory . . . 155
E.0.2 DMFT . . . 160
E.0.3 Quantum electrodynamics . . . 162

Chapter 1

Introduction

Electrons determine many properties of materials. Therefore, to comprehend the properties of a stationary many-body system, one would need to solve the time-independent Schrödinger equation

$$\hat{H}\Psi = E\Psi \tag{1.1}$$

in order to access its many-body wave function Ψ. The (electronic) many-body Hamiltonian is given by

$$\hat{H} = \hat{T}_e + \hat{T}_n + \hat{V}_{en} + \hat{V}_{ee} + \hat{V}_{nn}, \tag{1.2}$$

where $\hat{T}_e$ is the electronic kinetic operator, $\hat{T}_n$ is the nuclear kinetic operator, $\hat{V}_{en}$ is the electron-nucleus interaction, $\hat{V}_{ee}$ is the electron-electron interaction, and $\hat{V}_{nn}$ is the nucleus-nucleus interaction. (Throughout this thesis we consider a non-relativistic framework.) However, this approach is not feasible because it necessitates solving a set of coupled equations with $4N$ degrees of freedom (stemming from the N particles defined by both their position $\boldsymbol{r}$ and their spin σ). Consequently, approximations to the many-body wave function or alternative many-body formalisms, such as density-functional theory (DFT) or many-body perturbation theory (MBPT) based on Green's functions (GFs), must be employed. These latter formalisms offer the advantage of simplifying the complexity of the problem by working with "reduced" quantities like the electron density or the one-body Green's function instead of the many-body wave function. These reduced quantities are simpler to handle than the many-body wave function, and yet they contain enough information to determine the observables of interest. However, in practical applications, approximations to the so-called many-body effects of the system, which characterize electron interactions, are necessary. Furthermore, it is not always straightforward to extract the properties of interest from these reduced quantities.

In this thesis, we will use the framework of MBPT to study neutral excitations or "bound states" of the system. These excitations correspond to transitions from the ground state to an excited state: the system is excited by a weak electric field and it responds to this perturbation within the framework of linear response (signifying that the system's response is directly proportional to the disturbance). In a simplified one-electron picture, neutral excitations can be described by transitions from occupied molecular orbitals (or bands in the case of solids) to unoccupied orbitals (see Fig. 1.1). These transitions encompass single electron-hole transitions, denoted as single excitations, or they can involve multiple electron-hole transitions. An example of the latter is the simultaneous promotion of two electrons to unoccupied orbitals, referred to as double excitations.

The advantage of using MBPT to describe neutral excitations is that, unlike DFT and its extension to the time domain, it offers a clearer physical framework to perform meaningful approximations to the many-body effects of the system. Relevant approximations are essential to get accurate results. Within MBPT, the one-body Green's function (1-GF) allows one to calculate the quasiparticle energies (related to ionization potentials and electron affinities), which are successively used to calculate neutral excitations through

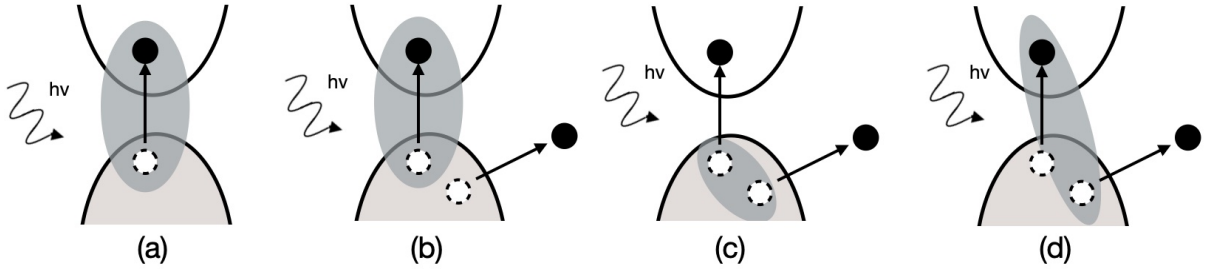

Figure 1.1 – Schematic representation of neutral and charged excitations: (a) creation of electron-hole pairs; (b) electron removal in GW; (c) electron removal in the particle-particle T-matrix; (d) electron removal in the electron-hole T-matrix. The shaded oval shape indicates the couple of particles that are correlated in the theoretical description.

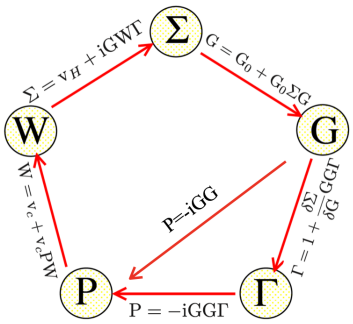

Figure 1.2 – The five Hedin equations of the self-energy (Σ), the one-body Green function (G), the irreducible vertex (Γ), the irreducible polarizability (P), and the dynamically screened Coulomb potential (W), represented as a pentagon. By setting the vertex to 1, one gets the GW approximation.

the two-body Green's function (2-GF). Each of these GFs fulfills a Dyson equation, which relates the non-interacting GF to the interacting one through a kernel. In the case of the 1-GF, this kernel is known as the self-energy (Σ), whereas in the case of the 2-GF this kernel is the functional derivative of the self-energy with respect to the 1-GF.

In practice, approximations of the self-energy and its derivative are required. A good starting point to make approximations are Hedin's equations (see Fig. 1.2). This is a set of five integro-differential equations which are, in principle, exact, but they have to be approximated in practice. A well-known approximation is the GW approximation to the self-energy, which hence reads $\Sigma = v_H + iGW$, where v_H is the classical Hartree potential, G is the 1-GF, and W the dynamically screened Coulomb potential. The structure is similar to the Hartree-Fock approximation to the self-energy ($\Sigma = v_H + iGv_c$, with v_c the Coulomb potential), but now there is correlation included through W which represents the fact that the Coulomb interaction between particles in the system is screened by the presence of the other particles. This is a physically motivated approximation in the case of a system with many electrons, but it shows failures at low density. In this case, other approximations, such as the T-matrix approximation, which describes multiple scattering between two particles (pp T-matrix) or an electron and a hole (eh T-matrix), are more suitable.

The three approximations can be put on equal footing by looking at the electron removal process (or equivalently the electron addition process): in a simplified picture the removed electron leaves a photohole which excites the system (creation of electron-hole pairs) (see Fig. 1.1b-d). This process can be seen as involving at least three particles, which, in a theoretical description, should be correlated together. This is usually expensive

and therefore one chooses to correlate only two of them, which hence dress the third one. In GW, the eh pairs created by the photohole are correlated (Fig. 1.1b), whereas, in the T-matrix formalism, one correlates the two holes (Fig. 1.1c) or the photohole and the excited electron (Fig. 1.1d).

These methods have been developed in the field of condensed matter to study solids. In particular, the GW method has been successful in many systems to study band structure and photoemission spectra as well as optical spectra using the Bethe-Salpeter equation (BSE) [1]. More recently this formalism has been imported into quantum chemistry to study the electronic properties of molecules [2, 3, 4, 5, 6, 7, 8, 9, 10, 11, 12, 13, 14, 15, 16, 17, 18, 19, 20, 21, 22, 23, 24]. However, when applied to finite systems like molecules, the GW method is often considered to be less effective. This perception arises from the fact that in the GW approximation, collective effects that screen the Coulomb interaction are taken into account. While this is a suitable approximation for solids where screening effects play a central role, it might be less applicable to smaller systems such as molecules, which exhibit less screening effects. In particular, the BSE within the GW approximation can show some failures, such as underestimated triplet excitation energies, lack of double excitations, ground-state energy instabilities in the dissociation limit, etc. Nonetheless, in this thesis, we aim to demonstrate the relevance of this approach in few-electron systems. To illustrate this, we will study neutral excitations in small molecules using the BSE within the GW, the pp T-matrix, and the eh T-matrix approximations.

Photoemission spectra

In the previous section, we mentioned that the 1-GF allows us to obtain ionization potentials and electron affinities. This is because it is strictly linked to photoemission spectra [25, 26].

Photoemission spectroscopy (PES) stands as one of the most pivotal methods for investigating the electronic properties of molecules and solids (see Fig. 1.3). Historically, the first experiment to unveil the connection between light and matter was the photoelectric effect. In this experiment, a photon with energy $h\nu$ is directed towards a sample. When the photon's energy surpasses a specific threshold V_0, corresponding to the work function of the sample, an electron is emitted with an energy E_{kin} satisfying the equation:

$$E_{\text{kin}} = h\nu - V_0 \tag{1.3}$$

Nowadays, employing the same underlying principle, photoemission experiments are conducted to explore the spectroscopic characteristics of electronic systems. Emitted electrons provide valuable information about the system under investigation. Various types of photoemission techniques are employed. For instance, ultraviolet photoemission spectroscopy (UPS) measures the kinetic energy of photoelectrons emitted by molecules upon absorbing ultraviolet photons. Another PES technique, X-ray photoelectron spectroscopy (XPS), employs X-rays to irradiate the sample and analyze the binding energy of core electrons.

The excitation of a photoelectron involves a complex process in which the sample, constituting a many-body system, acts as a collective entity. Nevertheless, it is often feasible to begin with a simplified one-particle model to comprehend many photoemission phenomena, particularly when electronic correlation effects are relatively insignificant or when the focus is on specific features like satellites.

The simplest method to study photoemission is based on Fermi's golden rule. In this approach, the photocurrent

$$J_{\boldsymbol{k}}(\omega) = \sum_n \left| \left\langle \Psi^{N-1}_{\boldsymbol{k}n} \middle| \hat{\Delta} \middle| \Psi^N_0 \right\rangle \right|^2 \delta(\varepsilon_{\boldsymbol{k}} - \varepsilon_n - \omega) \tag{1.4}$$

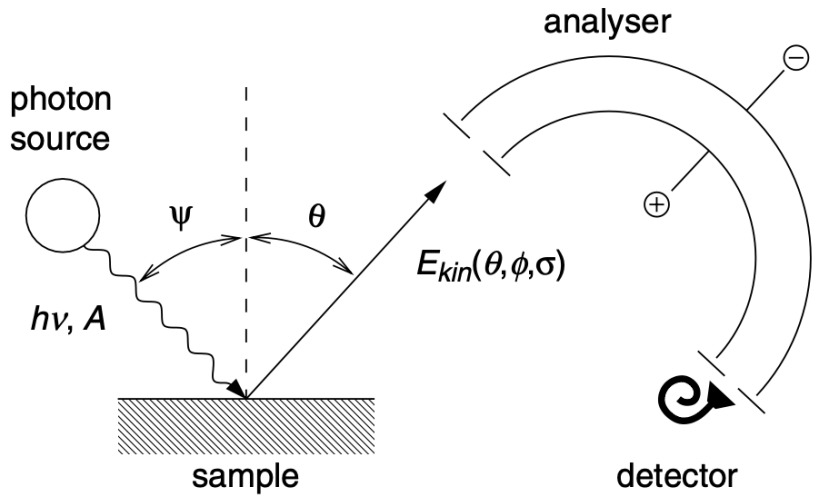

Figure 1.3 – Principle of a photoemission spectrometer. Monochromatic photons with energy $h\nu$ and polarization ($\boldsymbol{A}$ is the vector potential of the electromagnetic field) are produced by a light source and hit the sample surface with an angle ψ with respect to the surface normal. The kinetic energy E_{kin} of the photoelectrons can be analyzed by use of electrostatic analyzers as a function of the experimental parameters, e.g. emission angle (θ, ϕ), the electron spin orientation $\boldsymbol{\sigma}$ or the photon energy. The whole setup is evacuated to ultra-high vacuum (UHV, typically, $P \leq 10^{-10}$ mbar). (This picture is taken from Ref. [26])

is the result of a photon-induced excitation of the system from its ground state $\left|\Psi_0^N\right\rangle$ to a final state $\left|\Psi_f^{N-1}\right\rangle \equiv \left|\Psi_{\boldsymbol{k}n}^{N-1}\right\rangle$, resulting in a photoelectron with momentum $\boldsymbol{k}$ and kinetic energy $E_{\text{kin}} = \varepsilon_{\boldsymbol{k}} = \hbar^2 k^2 / 2m_e$ and the remaining $(N-1)$-electron system. The index n refers to a set of quantum numbers that contain all possible excitations to the final state, including phonons, plasmons, electron-hole pairs, and multiple excitations. The perturbation operator $\hat{\Delta}$ is the optical transition operator which describes the interaction of an electron in the system with the electromagnetic field, which is represented by the coupling $\boldsymbol{A} \cdot \boldsymbol{p}$ between the vector potential $\boldsymbol{A}$ and the momentum operator $\boldsymbol{p}$, and m_e is the electron's mass. For the calculation of the spectrum, we have to do a simplification known as the sudden approximation which decouples the final state (the photoelectron) from the remaining of the system, i.e.,

$$\left|\Psi_{\boldsymbol{k}n}^{N-1}\right\rangle \approx \hat{c}_{\boldsymbol{k}}^{\dagger} \left|\Psi_n^{N-1}\right\rangle \tag{1.5}$$

where $\hat{c}_{\boldsymbol{k}}^{\dagger}$ is a creation operator. Expanding the dipole transition operator $\hat{\Delta}$ in a basis of one-particle orbitals, we have

$$\hat{\Delta} = \sum_{pq} \Delta_{pq} \hat{c}_p^{\dagger} \hat{c}_q, \qquad \Delta_{pq} = \langle p | \boldsymbol{A} \cdot \boldsymbol{p} | q \rangle \tag{1.6}$$

which can be used to evaluate

$$\left\langle \Psi_{\boldsymbol{k}n}^{N-1} \middle| \hat{\Delta} \middle| \Psi_i^N \right\rangle = \sum_p \Delta_{kp} \left\langle \Psi_{\boldsymbol{k}n}^{N-1} \middle| \hat{c}_p \middle| \Psi_i^N \right\rangle \tag{1.7}$$

where we used the fact that $\hat{c}_{\boldsymbol{k}} \hat{c}_p^{\dagger} \hat{c}_q = \delta_{\boldsymbol{k}p} \hat{c}_q + \hat{c}_p^{\dagger} \hat{c}_q \hat{c}_{\boldsymbol{k}}$ thanks to the anticommutation relation of $\hat{c}_{\boldsymbol{k}}$ and $c_p^{\dagger}$, and we assumed that the ground state has no component in the state $|\boldsymbol{k}\rangle$, *i.e.*, $\hat{c}_{\boldsymbol{k}} \left|\Psi_0^N\right\rangle = 0$, as this state is of very high energy.

Introducing the matrix elements

$$A^{<}_{pq}(\omega) = \sum_{n}^{\varepsilon_n<\mu} \left\langle \Psi_i^N \middle| \hat{c}_p^\dagger \middle| \Psi_n^{N-1} \right\rangle \left\langle \Psi_n^{N-1} \middle| \hat{c}_q \middle| \Psi_i^N \right\rangle \delta(\omega - \varepsilon_n) \tag{1.8}$$

(where μ is the chemical potential), the photocurrent $J_{\boldsymbol{k}}(\omega)$ can thus be rewritten as

$$J_{\boldsymbol{k}}(\omega) = \sum_{pq} \Delta_{\boldsymbol{k}p} A^{<}_{pq}(\varepsilon_{\boldsymbol{k}} - \omega) \Delta_{q\boldsymbol{k}} \tag{1.9}$$

If we further assume that the matrix elements of the dipole transition operator Δ are constant and that the diagonal elements of $A^{<}_{pp}$ are the most relevant, we obtain

$$J_{\boldsymbol{k}}(\omega) = |\Delta|^2 \sum_{p} A^{<}_{pp}(\varepsilon_{\boldsymbol{k}} - \omega) \tag{1.10}$$

The photocurrent is thus given by the product of the trace of $A^<$ and $\hat{\Delta}$. In Chapter 2 we will see that $A^{<}_{pq}(\omega)$ are the matrix elements of the spectral function (for $\omega < \mu$), which can be directly obtained from the imaginary part of the 1-GF.

Linear response

As mentioned above, the 2-GF is related to the framework of linear response. In the context of quantum mechanics, a response function characterizes how a system reacts to an external perturbation. This response is quantified as the change in the expectation value of any arbitrary physical observable, denoted as $\hat{O}$, for a system initially in the ground state Ψ_0 of the Hamiltonian $\hat{H}_0$. The perturbation, represented as $\delta\hat{h}(t)$ and applied at time $t = t_0$, induces a change described as

$$\delta\langle\hat{O}\rangle(t) = \langle\Psi(t)|\hat{O}|\Psi(t)\rangle - \langle\Psi_0|\hat{O}|\Psi_0\rangle \tag{1.11}$$

Here, $\Psi(t)$ corresponds to the solution of the time-dependent Schrödinger equation

$$i\frac{\partial}{\partial t}\Psi(t) = [\hat{H}_0 + \delta\hat{h}(t)]\Psi(t) \tag{1.12}$$

To handle this equation effectively, we employ the Heisenberg picture relative to $\hat{H}_0$, where wavefunctions and operators are related to their counterparts in the Schrödinger picture through unitary transformations:

$$\Psi_H(t) = e^{i(t-t_0)\hat{H}_0}\Psi(t)e^{-i(t-t_0)\hat{H}_0} \tag{1.13}$$

$$\hat{O}_H(t) = e^{i(t-t_0)\hat{H}_0}\hat{O}e^{-i(t-t_0)\hat{H}_0} \tag{1.14}$$

The wavefunction $\Psi_H(t)$ follows the equation of motion

$$i\frac{\partial}{\partial t}\Psi_H(t) = \delta\hat{h}_H(t)\Psi_H(t) \tag{1.15}$$

that can be reformulated as an integral equation

$$\Psi_H(t) = \Psi(t_0) - i\int_{t_0}^{t} \delta\hat{h}_H(t')\Psi_H(t')dt' \tag{1.16}$$

where the causality constraint is inherently included. Notably, the wavefunctions in the Heisenberg and Schrödinger pictures coincide at $t = t_0$. Solving this integral equation iteratively, we obtain a solution up to terms linear in the perturbation

$$\Psi(t) = e^{-i(t-t_0)\hat{H}0}\left[1 - i\int_{t_0}^{t}\delta\hat{h}_H(t')dt'\right]\Psi_0 e^{i(t-t_0)\hat{H}_0} + O(\delta\hat{h}_H^2) \tag{1.17}$$

Consequently, the linear response equation (1.11) for the observable $\hat{O}$ is expressed as

$$\delta\langle\hat{O}\rangle(t) = -i\int_{t_0}^{t}\langle\Psi_0|[\hat{O}_H(t), \delta\hat{h}_H(t')]|\Psi_0\rangle dt' \tag{1.18}$$

where $[\hat{a}, \hat{b}]$ represents the commutator of operators $\hat{a}$ and $\hat{b}$. Considering the perturbation $\delta\hat{h}_H(t)$ as

$$\delta\hat{h}_H(t) = \sum_i \hat{O}_{iH}(t)\varphi_i(t) \tag{1.19}$$

with $\varphi_i(t)$ representing arbitrary time-dependent variables, the linear response for the operators $\hat{O}_i$ is given by

$$\delta\langle\hat{O}_i\rangle(t) = \sum_j \int_{t_0}^{\infty}\chi_{ij}(t, t')\varphi_j(t')dt' \tag{1.20}$$

Here, $\chi_{ij}(t, t')$ denotes the response functions and is defined as

$$\chi_{ij}(t, t') = -i\Theta(t - t')\langle\Psi_0|[\hat{O}_{iH}(t), \hat{O}_{jH}(t')]|\Psi_0\rangle \tag{1.21}$$

with $\Theta(\tau)$ ensuring the causality of the response functions by acting as the Heaviside step function, that is,

$$\Theta(\tau) = \begin{cases} 1 & \text{if } \tau > 0 \\ 0 & \text{if } \tau \leq 0 \end{cases} \tag{1.22}$$

If we consider the set denoted as $|\Psi_n\rangle$ that gathers all the eigenstates of the operator $\hat{H}_0$, we can make use of the closure relation

$$\sum_n |\Psi_n\rangle\langle\Psi_n| = 1 \tag{1.23}$$

and formulate the following relationship

$$\begin{aligned}\chi_{ij}(t - t') = -i\Theta(t - t')\sum_n \Big\{ & e^{i(E_0 - E_n)(t-t')}\langle\Psi_0|\hat{O}_i|\Psi_n\rangle\langle\Psi_n|\hat{O}_j|\Psi_0\rangle \\ & - e^{-i(E_0 - E_n)(t-t')}\langle\Psi_0|\hat{O}_j|\Psi_n\rangle\langle\Psi_n|\hat{O}_i|\Psi_0\rangle\Big\}\end{aligned} \tag{1.24}$$

It is important to note that this relationship holds true only when the operators $\hat{O}_i$ and $\hat{O}_j$ are independent of time. By employing the given expression for the Heaviside step function $\Theta(\tau)$:

$$\Theta(\tau) = -\frac{1}{2\pi i}\lim_{\eta\to 0^+}\int_{-\infty}^{\infty}\frac{e^{-i\omega\tau}}{\omega + i\eta}d\omega \tag{1.25}$$

leads to the following result

$$\chi_{ij}(t-t') = \lim_{\eta\to 0^+} \int_{-\infty}^{\infty} \frac{1}{2\pi} e^{-i\omega(t-t')} \chi_{ij}(\omega) d\omega \tag{1.26}$$

where

$$\chi_{ij}(\omega) = \lim_{\eta\to 0^+} \sum_{n=0} \left\{ \frac{\langle\Psi_0|\hat{O}_i|\Psi_n\rangle\langle\Psi_n|\hat{O}_j|\Psi_0\rangle}{\omega - (E_n - E_0) + i\eta} - \frac{\langle\Psi_0|\hat{O}_j|\Psi_n\rangle\langle\Psi_n|\hat{O}_i|\Psi_0\rangle}{\omega + (E_n - E_0) + i\eta} \right\} \tag{1.27}$$

represents the response functions in the frequency domain. The poles of χ correspond to the neutral excitations of the system. When the operators $\hat{O}_i$ and $\hat{O}_j$ are density operators, then $\chi_{\rho\rho} = \delta\rho/\delta V$, where V denotes a scalar potential derived from $\delta\hat{h}_H = \hat{\rho}_H(t)V(t)$. This is the density-density response function that we will focus on in this thesis.

Outline of the thesis

This thesis is organized as follows. In the first chapter, we describe the simplifications employed to investigate a many-body electronic system, including the Born-Oppenheimer approximation and Hartree-Fock theory. In the second chapter, we give a brief overview of post-Hartree-Fock methods in wave function-based approaches and in many-body perturbation theory based on Green's functions. In particular, we discuss the Dyson equation for the 1-GF and for the 2-GF (the Bethe-Salpeter equation) as well as the GW and T-matrix approximations to the self-energy and its derivative. In the third chapter, we use the exactly solvable asymmetric Hubbard dimer to test the GW and T-matrix approximations in the case of quasiparticle energies and neutral excitations. This model allows one to study various correlation regimes by varying the on-site Coulomb interaction as well as the degree of the asymmetry of the system by varying the difference of potential between the two sites. In Chapter 4, we derive a common practical framework for GW, particle-particle T-matrix, and electron-hole T-matrix and we use it to calculate quasiparticle energies and neutral excitations for the so-called $GW20$ set, which consists of atoms and molecules already explored in Refs.[27, 28, 29]. We finally draw our conclusions and provide some perspectives on the present work.

Chapter 2

The many-body problem

2.1 The Born-Oppenheimer approximation

In the following, we use atomic units $\hbar = m_e = e = 4\pi\epsilon_0 = 1$ (m_e is the electron's mass, e is the elementary charge, and ϵ_0 is vacuum permittivity). When we want to study a N-body system, one has to solve the many-body time-dependent Schrödinger equation [30]

$$i\frac{\partial}{\partial t}|\Phi\rangle = H|\Phi\rangle \tag{2.1}$$

where Φ is the many-body wave function of the system and H is the many-body (non-relativistic) Hamiltonian for a system of N electrons and M nuclei

$$H = -\sum_{i=1}^{N}\frac{1}{2}\nabla_i^2 - \sum_{A=1}^{M}\frac{1}{2M_A}\nabla_A^2 - \sum_{i=1}^{N}\sum_{A=1}^{M}\frac{Z_A}{r_{iA}} + \sum_{i=1}^{N}\sum_{i>j}^{N}\frac{1}{r_{ij}} + \sum_{A=1}^{M}\sum_{B>A}^{M}\frac{Z_A Z_B}{R_{AB}} \tag{2.2}$$

The first term of the right-hand side of (2.2) is the kinetic energy of the electrons, the second term is the kinetic energy of the nuclei, the third term is the electron-nucleus attraction, the fourth term is the electron-electron Coulomb repulsion and the fifth term is the nucleus-nucleus repulsion. $r_{iA} = |\mathbf{r}_i - \mathbf{R}_A|$ is the distance between the electron at position $\mathbf{r}_i$ and the nucleus at the position $\mathbf{R}_A$, $r_{ij} = |\mathbf{r}_i - \mathbf{r}_j|$ is the distance between the electron i at the position $\mathbf{r}_i$ and the electron j at the position $\mathbf{r}_j$, $R_{AB} = |\mathbf{R}_A - \mathbf{R}_B|$ is the distance between the nucleus A at the position $\mathbf{R}_A$ and the nucleus B at the position $\mathbf{R}_B$. M_A is the ratio of the mass of nucleus A to the mass of an electron and Z_A is the atomic number of nucleus A. The Laplacian operator ∇_i^2 differentiates with respect to the coordinates of the electron i and ∇_A^2 differentiates with respect to the coordinates of the nucleus A.

The state of the system is described by the wave function Φ which depends on the electrons' coordinates, the nuclei's coordinates, and the time t,

$$\Phi = \Phi(\{\mathbf{r}_i\}; \{\mathbf{R}_A\}, t) \tag{2.3}$$

The terms in the Hamiltonian (2.2) do not depend on the time; therefore, without any external time-dependent perturbation we can separate the space and the time dependence of (2.1) and study the time-independent Schrödinger equation

$$H|\Phi\rangle = E|\Phi\rangle \tag{2.4}$$

Since this eigenvalue equation is time-independent, its eigenstates are stationary states. Equation 2.4 is in general impossible to solve, so we can simplify the Hamiltonian with the Born-Oppenheimer approximation. We will consider that the "motion" of the electrons is

very fast with respect to the motion of the nuclei, which are much heavier, and therefore they will adjust instantaneously to a change of the positions of the nuclei, which are moving very slowly and therefore are taken to be fixed. With this approximation, the second term of (2.2) can be neglected. The fifth term of (2.2) can be considered to be constant so it does not change the operator, but since we are interested only in the electronic properties of the system, we will study the electronic Hamiltonian

$$H_{elec} = -\sum_{i=1}^{N} \frac{1}{2}\nabla_i^2 - \sum_{i=1}^{N}\sum_{A=1}^{M} \frac{Z_A}{r_{iA}} + \sum_{i=1}^{N}\sum_{i>j}^{N} \frac{1}{r_{ij}} \tag{2.5}$$

The eigenvalue problem (2.4) can be rewritten with (2.5) as

$$H_{elec}\,|\Phi_{elec}\rangle = E_{elec}\,|\Phi_{elec}\rangle \tag{2.6}$$

Φ_{elec} is the electronic wavefunction

$$\Phi_{elec} = \Phi_{elec}(\{\mathbf{r}_i\};\{\mathbf{R}_A\}) \tag{2.7}$$

which describes the motion of the electrons. It depends on the coordinates of the electrons $\{\mathbf{r}_i\}$ and, parametrically, on the coordinates of the nuclei $\{\mathbf{R}_A\}$. This means that for each set of nuclear coordinates $\{\mathbf{R}_A\}$ the electronic wavefunction has a different functional dependence on the electronic coordinates $\{\mathbf{r}_i\}$. The electronic energy also depends on $\{\mathbf{R}_A\}$

$$E_{elec} = E_{elec}(\{\mathbf{R}_A\}) \tag{2.8}$$

To obtain the total energy we add to (2.8) the nuclear-nuclear repulsion for fixed nuclei

$$E_{tot} = E_{elec} + \sum_{A=1}^{M}\sum_{B>A}^{M} \frac{Z_A Z_B}{R_{AB}} \tag{2.9}$$

If one can solve the electronic problem, then one can also solve the nuclear one. We write the nuclear Hamiltonian

$$H_{nucl} = -\sum_{A=1}^{M} \frac{1}{2M_A}\nabla_A^2 + E_{tot}(\{\mathbf{R}_A\}) \tag{2.10}$$

We solve the nuclear Schrödinger equation

$$H_{nucl}\,|\Phi_{nucl}\rangle = E\,|\Phi_{nucl}\rangle \tag{2.11}$$

with

$$\Phi_{nucl} = \Phi_{nucl}(\{\mathbf{R}_A\}) \tag{2.12}$$

This equation describes the vibration, rotation, and translation of a system. Therefore in the Born-Oppenheimer approximation, the total time-independent wavefunction is expressed as a product of an electronic wavefunction and a nuclear wavefunction

$$\Phi = \Phi_{elec}(\{\mathbf{r}_i\};\{\mathbf{R}_A\})\Phi_{nucl}(\{\mathbf{R}_A\}) \tag{2.13}$$

2.2 Hartree-Fock theory

The electronic Hamiltonian (2.5) depends only on the spatial coordinates of the electrons, but to describe them one has to take into account also the spin. We note $\alpha(\sigma)$ the spin up and $\beta(\sigma)$ the spin down. They have to verify the orthonormalisation properties

$$\sum_{\sigma} \alpha^*(\sigma)\alpha(\sigma) = \sum_{\sigma} \beta^*(\sigma)\beta(\sigma) = 1 \tag{2.14}$$

$$\sum_{\sigma} \alpha^*(\sigma)\beta(\sigma) = \sum_{\sigma} \beta^*(\sigma)\alpha(\sigma) = 0 \tag{2.15}$$

The coordinates of an electron are hence written as $\mathbf{x} = (\mathbf{r}, \sigma)$ and the many-body wavefunction of the system as $\Phi(\mathbf{x}_1, \ldots, \mathbf{x}_N)$. Because the electrons are fermions, they have to verify the Pauli exclusion principle for which two electrons cannot be in the same quantum state. This requires the wavefunction to be antisymmetric with respect to the interchange of electron coordinates, i.e.

$$\Phi(\mathbf{x}_1, \ldots, \mathbf{x}_i, \ldots, \mathbf{x}_j, \ldots, \mathbf{x}_N) = -\Phi(\mathbf{x}_1, \ldots, \mathbf{x}_j, \ldots, \mathbf{x}_i, \ldots, \mathbf{x}_N) \tag{2.16}$$

We define an orbital as a wavefunction for a single particle and we call the spatial orbital $\psi_i(\mathbf{r})$ the function of the position $\mathbf{r}$ which describes the spatial distribution of an electron. The probability of finding an electron in a volume element $d\mathbf{r}$ surrounding $\mathbf{r}$ is then $|\psi_i(\mathbf{r})|^2 d\mathbf{r}$. The set $\{\psi_i\}$ of the spatial orbitals verify the orthonormal properties

$$\int d\mathbf{r} \psi_i^*(\mathbf{r})\psi_j(\mathbf{r}) = \delta_{ij} \tag{2.17}$$

The set $\{\psi_i\}$ is infinite but in practice, we will use a finite set $\{\psi_i | i = 1, \ldots, K\}$. Therefore we will only span a certain region of the complete set and the results will be exact within the subspace spanned. We can place an electron in a spatial orbital $\psi_i(\mathbf{r})$ either with a spin up or a spin down, so to completely describe an electron we introduce the spin orbitals χ defined as

$$\chi_i(\mathbf{x}) = \begin{cases} \psi_i(\mathbf{r})\alpha(\sigma) \\ \psi_i(\mathbf{r})\beta(\sigma) \end{cases} \tag{2.18}$$

With a set of K spatial orbitals, we can form a set of $2K$ spin orbitals

$$\left.\begin{aligned} \chi_{2i-1}(\mathbf{x}) &= \psi_i(\mathbf{r})\alpha(\sigma) \\ \chi_{2i}(\mathbf{x}) &= \psi_i(\mathbf{r})\beta(\sigma) \end{aligned}\right\} i = 1, 2, \ldots, K \tag{2.19}$$

The orthonormality of the spatial orbitals implies

$$\int d\mathbf{x} \chi_i^*(\mathbf{x})\chi_j(\mathbf{x}) = \delta_{ij} \tag{2.20}$$

In Hartree-Fock theory, one describes the ground state of a many-body system with a single antisymmetric wavefunction called a Slater determinant

$$|\Psi_0\rangle = |\chi_1 \chi_2 \ldots \chi_i \chi_j \ldots \chi_N\rangle \tag{2.21}$$

or

$$\Psi_0(\mathbf{x}_1, \mathbf{x}_2, \ldots, \mathbf{x}_N) = \frac{1}{\sqrt{N!}} \begin{vmatrix} \chi_1(\mathbf{x}_1) & \chi_2(\mathbf{x}_1) & \cdots & \chi_N(\mathbf{x}_1) \\ \chi_1(\mathbf{x}_2) & \chi_2(\mathbf{x}_2) & \cdots & \chi_N(\mathbf{x}_2) \\ \vdots & \vdots & & \vdots \\ \chi_1(\mathbf{x}_N) & \chi_2(\mathbf{x}_N) & \cdots & \chi_N(\mathbf{x}_N) \end{vmatrix} \tag{2.22}$$

We note

$$\mathcal{O}_1 = \sum_{i=1}^{N} h_i = \sum_{i=1}^{N} \left(-\frac{1}{2}\nabla_i^2 - \sum_{A=1}^{M} \frac{Z_A}{r_{iA}} \right) \tag{2.23}$$

the one-electron terms of (2.5) and

$$\mathcal{O}_2 = \sum_{i<j}^{N} v_{ij} = \sum_{i=1}^{N} \sum_{i>j}^{N} \frac{1}{r_{ij}} \tag{2.24}$$

the two-electron terms of (2.5). One can show that for two determinants $|K\rangle$ and $|L\rangle$ we obtain the following Slater-Condon rules

Case 1 $|K\rangle = |\ldots \chi_m \chi_n \ldots\rangle$

$$\langle K|\mathcal{O}_1|K\rangle = \sum_{m}^{N} \langle \chi_m|h|\chi_m\rangle \tag{2.25}$$

$$\langle K|\mathcal{O}_2|K\rangle = \frac{1}{2}\sum_{m}^{N}\sum_{n}^{N} \langle \chi_m\chi_n||\chi_m\chi_n\rangle \tag{2.26}$$

Case 2 $|K\rangle = |\ldots \chi_m \chi_n \ldots\rangle$ and $|L\rangle = |\ldots \chi_p \chi_n \ldots\rangle$

$$\langle K|\mathcal{O}_1|L\rangle = \langle \chi_m|h|\chi_p\rangle \tag{2.27}$$

$$\langle K|\mathcal{O}_2|L\rangle = \sum_{n}^{N} \langle \chi_m\chi_n||\chi_p\chi_n\rangle \tag{2.28}$$

Case 3 $|K\rangle = |\ldots \chi_m \chi_n \ldots\rangle$ and $|L\rangle = |\ldots \chi_p \chi_q \ldots\rangle$

$$\langle K|\mathcal{O}_1|L\rangle = 0 \tag{2.29}$$

$$\langle K|\mathcal{O}_2|L\rangle = \langle \chi_m\chi_n||\chi_p\chi_q\rangle \tag{2.30}$$

where

$$\langle \chi_p\chi_q|\chi_r\chi_s\rangle = \int d\mathbf{x}_1 d\mathbf{x}_2 \chi_p^*(\mathbf{x}_1)\chi_q^*(\mathbf{x}_2)\frac{1}{|\mathbf{r}_1 - \mathbf{r}_2|}\chi_r(\mathbf{x}_1)\chi_s(\mathbf{x}_2) \tag{2.31}$$

and

$$\langle \chi_p\chi_q||\chi_r\chi_s\rangle = \langle \chi_p\chi_q|\chi_r\chi_s\rangle - \langle \chi_p\chi_q|\chi_s\chi_r\rangle \tag{2.32}$$

With the use of these rules, the ground-state total energy (within the Hartree-Fock approximation) reads

$$E_0 = \langle \Psi_0|H_{elec}|\Psi_0\rangle = \sum_i \langle \chi_i|h|\chi_i\rangle + \frac{1}{2}\sum_{ij} \langle \chi_i\chi_j||\chi_i\chi_j\rangle \tag{2.33}$$

The Schrödinger equation is simplified because the one-electron operators contain differential operators which select the coordinates of a particular electron or nucleus so the many-body wavefunction can reduce to a spin orbital for $\mathcal{O}_1$. The two-electron term $\mathcal{O}_2$ needs the coordinates of two electrons so it keeps two spin orbitals but the equation is still too complicated to solve.

To simplify more the problem we will apply a variational method on (2.33). Let us describe this for a general case. Let us call $\tilde{\Phi}$ a trial wavefunction. We saw in (2.33) that the energy depends on Ψ_0, so we write the energy as a functional of the many-body wavefunction

$$E[\tilde{\Phi}] = \left\langle \tilde{\Phi} \middle| H_{elec} \middle| \tilde{\Phi} \right\rangle \tag{2.34}$$

We apply a small variation on $\tilde{\Phi}$ such that

$$\tilde{\Phi} \to \tilde{\Phi} + \delta\tilde{\Phi} \tag{2.35}$$

This gives the energy

$$\begin{aligned} E[\tilde{\Phi} + \delta\tilde{\Phi}] &= \left\langle \tilde{\Phi} + \delta\tilde{\Phi} \middle| H_{elec} \middle| \tilde{\Phi} + \delta\tilde{\Phi} \right\rangle \\ &= E[\tilde{\Phi}] + \left\langle \delta\tilde{\Phi} \middle| H_{elec} \middle| \tilde{\Phi} \right\rangle + \left\langle \tilde{\Phi} \middle| H_{elec} \middle| \delta\tilde{\Phi} \right\rangle + \dots \\ &= E[\tilde{\Phi}] + \delta E + \dots \end{aligned} \tag{2.36}$$

δE represents the first-order variation of E. It includes the first-order terms in $\delta\tilde{\Phi}$. These terms are linear. In the variational method, we try to find a many-body wavefunction $\tilde{\Phi}$ which minimizes the energy. This means that the variation δE due to $\delta\tilde{\Phi}$ has to be equal to zero.

$$\delta E = 0 \tag{2.37}$$

We express the trial wavefunction as a linear combination of Slater determinants

$$\left| \tilde{\Phi} \right\rangle = \sum_{i=1}^{N} c_i \left| \Psi_i \right\rangle \tag{2.38}$$

Replacing this expression in (2.34) gives

$$E = \sum_{ij} c_i^* c_j \left\langle \Psi_i | H_{elec} | \Psi_j \right\rangle \tag{2.39}$$

We minimize this expression with the use of the Lagrange multipliers method with respect to the coefficients c_i and with the constraints that the trial wavefunction is normalized

$$\begin{aligned} \mathcal{L} &= \left\langle \tilde{\Phi} \middle| H_{elec} \middle| \tilde{\Phi} \right\rangle - E \left(\left\langle \tilde{\Phi} \middle| \tilde{\Phi} \right\rangle - 1 \right) \\ &= \sum_{ij} c_i^* c_j \left\langle \Psi_i | H_{elec} | \Psi_j \right\rangle - E \left(\sum_{ij} c_i^* c_j \left\langle \Psi_i | \Psi_j \right\rangle - 1 \right) \end{aligned} \tag{2.40}$$

We set the first-order variation in $\mathcal{L}$ equal to zero

$$\begin{aligned} \delta\mathcal{L} = &\sum_{ij} \delta c_i^* c_j \left\langle \Psi_i | H_{elec} | \Psi_j \right\rangle - E \sum_{ij} \delta c_i^* c_j \left\langle \Psi_i | \Psi_j \right\rangle \\ &+ \sum_{ij} c_i^* \delta c_j \left\langle \Psi_i | H_{elec} | \Psi_j \right\rangle - E \sum_{ij} c_i^* \delta c_j \left\langle \Psi_i | \Psi_j \right\rangle \\ = &\sum_{i} \delta c_i^* \left[\sum_j H_{ij} c_j - E S_{ij} c_j \right] + c.c = 0 \end{aligned} \tag{2.41}$$

where $H_{ij} = \langle \Psi_i | H_{elec} | \Psi_j \rangle$ and $S_{ij} = \langle \Psi_i | \Psi_j \rangle$. The quantity in the bracket in the last line of (2.41) has to be equal to zero, i.e.

$$\sum_j H_{ij} c_j = E \sum_j S_{ij} c_j \tag{2.42}$$

or, in a matrix form

$$\mathbf{Hc} = E\mathbf{Sc} \tag{2.43}$$

We now apply this variational process to (2.33). Since in the Hartree-Fock theory the ground state is described only by a single Slater determinant, to differentiate this equation implies to differentiate with respect to the spin orbitals (with the constraint of orthonormalization). This means that the spin orbitals will be optimized in such a way that they will give the lowest energy E_0:

$$\mathcal{L}[\{\chi_i\}] = E_0[\{\chi_i\}] - \sum_{ij} \varepsilon_{ji} \left(\langle \chi_i | \chi_j \rangle - \delta_{ij} \right) \tag{2.44}$$

The ε_{ji} constitute a set of Lagrange multipliers. Since $\mathcal{L}$ is real and $\langle \chi_i | \chi_j \rangle = \langle \chi_j | \chi_i \rangle^*$ we have that $\varepsilon_{ji} = \varepsilon_{ij}^*$. We apply an infinitesimal variation on the spin orbitals such that

$$\chi_i \to \chi_i + \delta\chi_i \tag{2.45}$$

and set the first-order variation of the Lagrangian equal to zero:

$$\delta\mathcal{L} = \delta E_0 - \sum_{ij} \varepsilon_{ji} \delta \langle \chi_i | \chi_j \rangle = 0 \tag{2.46}$$

with

$$\delta \langle \chi_i | \chi_j \rangle = \langle \delta\chi_i | \chi_j \rangle + \langle \chi_i | \delta\chi_j \rangle \tag{2.47}$$

From the right-hand side of (2.33) we have

$$\begin{aligned} \delta E_0 = & \sum_{i=1}^{N} \langle \delta\chi_i | h | \chi_i \rangle + \langle \chi_i | h | \delta\chi_i \rangle \\ & + \frac{1}{2} \sum_{i=1}^{N} \sum_{j=1}^{N} \langle \delta\chi_i \chi_j | \chi_i \chi_j \rangle + \langle \chi_i \delta\chi_j | \chi_i \chi_j \rangle + \langle \chi_i \chi_j | \delta\chi_i \chi_j \rangle + \langle \chi_i \chi_j | \chi_i \delta\chi_j \rangle \\ & - \frac{1}{2} \sum_{i=1}^{N} \sum_{j=1}^{N} \langle \delta\chi_i \chi_j | \chi_j \chi_i \rangle + \langle \chi_i \delta\chi_j | \chi_j \chi_i \rangle + \langle \chi_i \chi_j | \delta\chi_j \chi_i \rangle + \langle \chi_i \chi_j | \chi_j \delta\chi_i \rangle \end{aligned} \tag{2.48}$$

Moreover

$$\begin{aligned} \sum_{ij} \varepsilon_{ji} \left(\langle \delta\chi_i | \chi_j \rangle + \langle \chi_i | \delta\chi_j \rangle \right) &= \sum_{ij} \varepsilon_{ji} \langle \delta\chi_i | \chi_j \rangle + \sum_{ij} \varepsilon_{ji} \langle \chi_j | \delta\chi_i \rangle \\ &= \sum_{ij} \varepsilon_{ji} \langle \delta\chi_i | \chi_j \rangle + \sum_{ij} \varepsilon_{ji}^* \langle \chi_j | \delta\chi_i \rangle \\ &= \sum_{ij} \varepsilon_{ji} \langle \delta\chi_i | \chi_j \rangle + c.c \end{aligned} \tag{2.49}$$

Therefore (2.46) becomes

$$\begin{aligned} \delta\mathcal{L} = & \sum_{i=1}^{N} \langle \delta\chi_i | h | \chi_i \rangle + \sum_{i=1}^{N} \sum_{j=1}^{N} \left(\langle \delta\chi_i \chi_j | \chi_i \chi_j \rangle - \langle \delta\chi_i \chi_j | \chi_j \chi_i \rangle \right) - \sum_{ij} \varepsilon_{ji} \langle \delta\chi_i | \chi_j \rangle + c.c \\ = & \, 0 \end{aligned} \tag{2.50}$$

We define the Coulomb operator

$$\mathcal{J}_j(\mathbf{x}_1) = \int d\mathbf{x}_2 |\chi_j(\mathbf{x}_2)|^2 r_{12}^{-1} \tag{2.51}$$

This is a local potential which is the average of the classical Coulomb interaction that feels an electron located in $\mathbf{x}_1$ due to the charge distribution $|\chi_j(\mathbf{x}_2)|^2$ of electron 2 which occupies the volume element $d\mathbf{x}_2$. The action of the Coulomb operator on a spin orbital $\chi_i(\mathbf{x}_1)$ gives

$$\mathcal{J}_j(\mathbf{x}_1)\chi_i(\mathbf{x}_1) = \left[\int d\mathbf{x}_2 \chi_j^*(\mathbf{x}_2) r_{12}^{-1} \chi_j(\mathbf{x}_2)\right] \chi_i(\mathbf{x}_1) \tag{2.52}$$

We also define the exchange operator

$$\mathcal{K}_j(\mathbf{x}_1)\chi_i(\mathbf{x}_1) = \left[\int d\mathbf{x}_2 \chi_j^*(\mathbf{x}_2) r_{12}^{-1} \chi_i(\mathbf{x}_2)\right] \chi_j(\mathbf{x}_1) \tag{2.53}$$

This term is defined by its action on the spin orbital $\chi_i(\mathbf{x}_1)$. It is a non-classical term that arises from the antisymmetry of the Slater determinant wavefunction. The result of this action depends not only of the value of χ_i at the position $\mathbf{r}_1$ but also on the value of χ_i in the whole space; this implies for the exchange operator is non-local.

With these definitions, Eq.(2.50) can be rewritten as

$$\delta\mathcal{L} = \sum_{i=1}^{N} \int d\mathbf{x}_1 \delta\chi_i^*(\mathbf{x}_1) \left[h(\mathbf{x}_1)\chi_i(\mathbf{x}_1) + \sum_{j=1}^{N}(\mathcal{J}_j(\mathbf{x}_1) - \mathcal{K}_j(\mathbf{x}_1))\chi_i(\mathbf{x}_1) - \sum_{j=1}^{N} \varepsilon_{ji}\chi_j(\mathbf{x}_1)\right] + c.c = 0$$

$\delta\chi_i^*(\mathbf{x}_1)$ is arbitrary, so it is the quantity in the bracket that has to be equal to zero. We hence obtain

$$\left[h(\mathbf{x}_1) + \sum_{j=1}^{N}(\mathcal{J}_j(\mathbf{x}_1) - \mathcal{K}_j(\mathbf{x}_1))\right] \chi_i(\mathbf{x}_1) = \sum_{j=1}^{N} \varepsilon_{ji}\chi_j(\mathbf{x}_1) \tag{2.54}$$

We set $f(\mathbf{x}_1) = h(\mathbf{x}_1) + \sum_{j=1}^{N}(\mathcal{J}_j(\mathbf{x}_1) - \mathcal{K}_j(\mathbf{x}_1))$, where f is called the Fock operator. Equation (2.54) can be rewritten as

$$f\,|\chi_i\rangle = \sum_{j=1}^{N} \varepsilon_{ji}\,|\chi_j\rangle \tag{2.55}$$

Equations (2.55) are called Hartree-Fock equations. It is not an eigenvalue problem since there is not the same spin orbital on both sides of the equation. To obtain this equation in a canonical form we do a unitary transformation or a rotation on the spin orbitals. We call U the unitary transformation such that

$$\chi_i' = \sum_j \chi_j U_{ji} \tag{2.56}$$

where U has the following properties :

i) $U^\dagger = U^{-1}$;

ii) it preserves the orthonormality which means that if the old set χ_i of spin orbitals was orthonormal, the new set χ'_i is also orthonormal.

If we note $\mathbf{A}$ the following matrix

$$\mathbf{A} = \begin{pmatrix} \chi_1(\mathbf{x}_1) & \chi_2(\mathbf{x}_1) & \cdots & \chi_i(\mathbf{x}_1) & \cdots & \chi_N(\mathbf{x}_1) \\ \chi_1(\mathbf{x}_2) & \chi_2(\mathbf{x}_2) & \cdots & \chi_i(\mathbf{x}_2) & \cdots & \chi_N(\mathbf{x}_2) \\ \vdots & \vdots & & \vdots & & \vdots \\ \chi_1(\mathbf{x}_N) & \chi_2(\mathbf{x}_N) & \cdots & \chi_i(\mathbf{x}_N) & \cdots & \chi_N(\mathbf{x}_N) \end{pmatrix} \tag{2.57}$$

such that

$$|\Psi_0\rangle = \frac{1}{\sqrt{N!}} \det(\mathbf{A}) \tag{2.58}$$

then the new set of spin orbitals is given by the matrix

$$\mathbf{A}' = \mathbf{A}\mathbf{U} \tag{2.59}$$

Therefore we have

$$\det(\mathbf{A}') = \det(\mathbf{A}) \det(\mathbf{U}) \tag{2.60}$$

or equivalently

$$|\Psi'_0\rangle = \det(\mathbf{U}) |\Psi_0\rangle \tag{2.61}$$

Since

$$\mathbf{U}^\dagger\mathbf{U} = \mathbf{U}\mathbf{U}^\dagger = 1 \tag{2.62}$$

we have

$$\det\big(\mathbf{U}^\dagger\mathbf{U}\big) = (\det(\mathbf{U}))^* \det(\mathbf{U}) = |\det(\mathbf{U})|^2 = 1 \tag{2.63}$$

and

$$\det(\mathbf{U}) = e^{i\phi} \tag{2.64}$$

This means that the transformed single determinant $|\Psi'_0\rangle$ can at most differ from the original one by a phase factor. Since any observable depends on $|\Psi|^2$, the expectation values of observables are invariant under a unitary transformation of the spin orbitals. We can show that the Coulomb and the exchange operators do not change under a unitary transformation and, therefore, the Fock operator is invariant. For the Lagrange multipliers, we have

$$\begin{aligned} \varepsilon'_{ij} &= \int d\mathbf{x}_1 \chi'^*_i(\mathbf{x}_1) f(\mathbf{x}_1) \chi'_j(\mathbf{x}_1) \\ &= \sum_{kl} U^*_{ki} U_{lj} \int d\mathbf{x}_1 \chi^*_k(\mathbf{x}_1) f(\mathbf{x}_1) \chi_l(\mathbf{x}_1) \\ &= \sum_{kl} U^*_{ki} \varepsilon_{kl} U_{lj} \end{aligned} \tag{2.65}$$

In matrix form

$$\boldsymbol{\varepsilon}' = \mathbf{U}^\dagger \boldsymbol{\varepsilon} \mathbf{U} \tag{2.66}$$

$\boldsymbol{\varepsilon}$ is a Hermitian matrix, so it can be diagonalized by a unitary transformation. Therefore we can choose the matrix $\mathbf{U}$ to be a unitary transformation which diagonalizes the Lagrange multipliers. The matrix $\boldsymbol{\varepsilon}'$ is hence diagonal and we can make a unitary transformation of the spin orbitals such that the Hartree-Fock equation can be written in a canonical form

$$f\,|\chi'_i\rangle = \varepsilon'_i\,|\chi'_i\rangle \tag{2.67}$$

Equation (2.67) is now a (pseudo-)eigenvalue problem where the spin orbitals χ'_i are the eigenvectors of the Fock operator. The eigenvalues ε'_i of this operator are called orbital energies. It is the energy of one electron in the spin orbital χ'_i (or in a spatial orbital ψ'_i), interacting with all the other electrons of the system through Hartree and exchange.

2.2.1 Closed-Shell Hartree-Fock

By definition, in the restricted Hartree-Fock formalism, two spin orbitals with a spin α and a spin β will have the same spatial function, and all electrons are in a closed-shell configuration, which means that N electrons occupy $N/2$ spatial orbitals. In this configuration, the ground state is written as

$$|\Psi_0\rangle = |\chi_1\chi_2\dots\chi_i\chi_j\dots\chi_N\rangle = \left|\psi_1\overline{\psi}_1\dots\psi_i\overline{\psi}_i\dots\psi_{N/2}\overline{\psi}_{N/2}\right\rangle \tag{2.68}$$

where $\psi_i\overline{\psi}_i$ means that the same spatial orbital is occupied by a α spin electron (ψ_i) and a β spin electron ($\overline{\psi}_i$).

To obtain the Hartree-Fock equations in the spatial orbitals, we express (2.67) in terms of spatial orbitals. We choose a spin orbital with a spin α (choosing β would be the same), so the equation becomes

$$f(\mathbf{x}_1)\psi_j(\mathbf{r}_1)\alpha(\sigma_1) = \varepsilon_j\psi_j(\mathbf{r}_1)\alpha(\sigma_1) \tag{2.69}$$

We then multiply on the left by $\alpha^*(\sigma_1)$ and we sum over the spin

$$\sum_{\sigma_1}\alpha^*(\sigma_1)f(\mathbf{x}_1)\alpha(\sigma_1)\psi_j(\mathbf{r}_1) = \varepsilon_j\psi_j(\mathbf{r}_1) \tag{2.70}$$

We set

$$f(\mathbf{r}_1) = \sum_{\sigma_1}\alpha^*(\sigma_1)f(\mathbf{x}_1)\alpha(\sigma_1) \tag{2.71}$$

then

$$\begin{aligned} f(\mathbf{r}_1)\psi_j(\mathbf{r}_1) = h(\mathbf{r}_1)\psi_j(\mathbf{r}_1) &+ \sum_k^N\sum_{\sigma_1}\int d\mathbf{x}_2\alpha^*(\sigma_1)\chi_k^*(\mathbf{x}_2)r_{12}^{-1}\chi_k(\mathbf{x}_2)\alpha(\sigma_1)\psi_j(\mathbf{r}_1) \\ &- \sum_k^N\sum_{\sigma_1}\int d\mathbf{x}_2\alpha^*(\sigma_1)\chi_k^*(\mathbf{x}_2)r_{12}^{-1}\chi_k(\mathbf{x}_1)\alpha(\sigma_2)\psi_j(\mathbf{r}_2) \end{aligned} \tag{2.72}$$

Since we consider a closed-shell system we can decompose the sum over the spin orbitals in two equal sums over the spin α and the spin β, this gives

$$\begin{aligned} f(\mathbf{r}_1)\psi_j(\mathbf{r}_1) = h(\mathbf{r}_1)\psi_j(\mathbf{r}_1) &\\ &+ \sum_k^{N/2}\sum_{\sigma_1\sigma_2}\int d\mathbf{r}_2\alpha^*(\sigma_1)\psi_k^*(\mathbf{r}_2)\alpha^*(\sigma_2)r_{12}^{-1}\psi_k(\mathbf{r}_2)\alpha(\sigma_2)\alpha(\sigma_1)\psi_j(\mathbf{r}_1) \\ &+ \sum_k^{N/2}\sum_{\sigma_1\sigma_2}\int d\mathbf{r}_2\alpha^*(\sigma_1)\psi_k^*(\mathbf{r}_2)\beta^*(\sigma_2)r_{12}^{-1}\psi_k(\mathbf{r}_2)\beta(\sigma_2)\alpha(\sigma_1)\psi_j(\mathbf{r}_1) \\ &- \sum_k^{N/2}\sum_{\sigma_1\sigma_2}\int d\mathbf{r}_2\alpha^*(\sigma_1)\psi_k^*(\mathbf{r}_2)\alpha^*(\sigma_2)r_{12}^{-1}\psi_k(\mathbf{r}_1)\alpha(\sigma_1)\alpha(\sigma_2)\psi_j(\mathbf{r}_2) \\ &- \sum_k^{N/2}\sum_{\sigma_1\sigma_2}\int d\mathbf{r}_2\alpha^*(\sigma_1)\psi_k^*(\mathbf{r}_2)\beta^*(\sigma_2)r_{12}^{-1}\psi_k(\mathbf{r}_1)\beta(\sigma_1)\alpha(\sigma_2)\psi_j(\mathbf{r}_2) \end{aligned} \tag{2.73}$$

When we sum over the spin, the last term in (2.73) is zero because of spin orthogonality, whereas the second and third terms give the same result. We hence arrive at

$$f(\mathbf{r}_1)\psi_j(\mathbf{r}_1) = h(\mathbf{r}_1)\psi_j(\mathbf{r}_1) + 2\sum_k^{N/2}\int d\mathbf{r}_2\psi_k^*(\mathbf{r}_2)r_{12}^{-1}\psi_k(\mathbf{r}_2)\psi_j(\mathbf{r}_1) - \sum_k^{N/2}\int d\mathbf{r}_2\psi_k^*(\mathbf{r}_2)r_{12}^{-1}\psi_j(\mathbf{r}_2)\psi_k(\mathbf{r}_1) \tag{2.74}$$

Finally, the closed-shell Fock operator can be written as

$$f(\mathbf{r}_1) = h(\mathbf{r}_1) + \sum_k^{N/2}(2\mathcal{J}_k(\mathbf{r}_1) - \mathcal{K}_k(\mathbf{r}_1)) \tag{2.75}$$

The Hartree-Fock energy is

$$E_0 = \langle\Psi_0|H_{elec}|\Psi_0\rangle = 2\sum_i h_{ii} + \sum_{ij}(2\mathcal{J}_{ij} - \mathcal{K}_{ij}) \tag{2.76}$$

and the orbital energies are

$$\varepsilon_i = h_{ii} + \sum_j(2\mathcal{J}_{ij} - \mathcal{K}_{ij}) \tag{2.77}$$

where

$$\mathcal{J}_{ij} = \langle ij|ij\rangle \tag{2.78}$$

and

$$\mathcal{K}_{ij} = \langle ij|ji\rangle \tag{2.79}$$

Without the spin, the Hartree-Fock equations are written as

$$f(\mathbf{r}_1)\psi_i(\mathbf{r}_1) = \varepsilon_i\psi_i(\mathbf{r}_1) \tag{2.80}$$

We use these equations to obtain the molecular orbitals ψ_i and the energies ε_i. However, these equations have to be solved self-consistently since the Coulomb and exchange operators in f depend on the ψ_i's. We use a first guess for the wavefunction, which could be for instance the one of the non-interacting system and we solve (2.80) in a self-consistent procedure proposed by Roothaan and Hall.

2.2.2 The Roothaan equations

In 1951, Roothaan and Hall proposed to solve the Hartree-Fock equations by expanding the molecular orbitals $\{\psi_i\}$ in terms of atomic orbitals $\{\phi_i\}$. If we note K the number of basis functions spanned, the molecular orbitals are expressed as

$$\psi_i = \sum_{\mu=1}^{K} c_{\mu i}\phi_\mu \tag{2.81}$$

The number K has to be large enough so that every electron can be paired with another one in a spatial orbital, and so we can build the ground state of the system with a Slater determinant. Using this expansion in (2.80) gives

$$f(\mathbf{r}_1)\sum_\nu c_{\nu i}\phi_\nu(\mathbf{r}_1) = \varepsilon_i\sum_\nu c_{\nu i}\phi_\nu(\mathbf{r}_1) \tag{2.82}$$

If we multiply by $\phi_\mu^*(\mathbf{r}_1)$ and we integrate over $\mathbf{r}_1$ we get

$$\sum_\nu c_{\nu i} \int d\mathbf{r}_1 \phi_\mu^*(\mathbf{r}_1) f(\mathbf{r}_1) \phi_\nu(\mathbf{r}_1) = \varepsilon_i \sum_\nu c_{\nu i} \int d\mathbf{r}_1 \phi_\mu^*(\mathbf{r}_1) \phi_\nu(\mathbf{r}_1) \tag{2.83}$$

We define the elements of the overlap matrix $\mathbf{S}$

$$S_{\mu\nu} = \int d\mathbf{r}_1 \phi_\mu^*(\mathbf{r}_1) \phi_\nu(\mathbf{r}_1) \tag{2.84}$$

and the elements of the Fock matrix $\mathbf{F}$

$$F_{\mu\nu} = \int d\mathbf{r}_1 \phi_\mu^*(\mathbf{r}_1) f(\mathbf{r}_1) \phi_\nu(\mathbf{r}_1) = H_{\mu\nu}^{core} + \sum_i^{N/2} (2 \langle \mu i | \nu i \rangle - \langle \mu i | i \nu \rangle) \tag{2.85}$$

With these notations, the Roothaan equations can be rewritten as

$$\sum_\nu F_{\mu\nu} c_{\nu i} = \varepsilon_i \sum_\nu S_{\mu\nu} c_{\nu i} \tag{2.86}$$

or in the matrix form

$$\mathbf{FC} = \mathbf{SC}\boldsymbol{\varepsilon} \tag{2.87}$$

where $\mathbf{C}$ is a square matrix such that

$$\mathbf{C} = \begin{pmatrix} c_{11} & c_{12} & \cdots & c_{1K} \\ c_{21} & c_{22} & \cdots & c_{2K} \\ \vdots & \vdots & & \vdots \\ c_{K1} & c_{K2} & \cdots & c_{KK} \end{pmatrix} \tag{2.88}$$

and $\boldsymbol{\varepsilon}$ is a diagonal matrix. We expand the remaining molecular orbitals in the two-electron term of $F_{\mu\nu}$ as a linear combination of the spatial functions ϕ's; this gives

$$\begin{aligned} F_{\mu\nu} &= H_{\mu\nu}^{core} + \sum_i^{N/2} \sum_{\lambda\sigma}^{N/2} c_{\lambda i} c_{\sigma i}^* (2 \langle \mu\sigma | \nu\lambda \rangle - \langle \mu\sigma | \lambda\nu \rangle) \\ &= H_{\mu\nu}^{core} + \sum_{\lambda\sigma}^{N/2} P_{\lambda\sigma} (\langle \mu\sigma | \nu\lambda \rangle - \frac{1}{2} \langle \mu\sigma | \lambda\nu \rangle) \end{aligned} \tag{2.89}$$

where

$$P_{\lambda\sigma} = 2 \sum_i^{N/2} c_{\lambda i} c_{\sigma i}^* \tag{2.90}$$

$$\langle \mu\sigma | \nu\lambda \rangle = \int d\mathbf{r}_1 d\mathbf{r}_2 \phi_\mu^*(\mathbf{r}_1) \phi_\sigma^*(\mathbf{r}_2) r_{12}^{-1} \phi_\nu(\mathbf{r}_1) \phi_\lambda(\mathbf{r}_2) \tag{2.91}$$

The Roothaan equations allowed us to change the previous Hartree-Fock equations which were integro-differential equations into an algebraic system to solve. However (2.87) has not yet the structure of an eigenvalue equation because of the overlap matrix. To get an eigenvalue problem we can use this matrix to build an orthogonalizing matrix $\mathbf{X} = \mathbf{S}^{-1/2}$. We set

$$\mathbf{C}' = \mathbf{X}^{-1}\mathbf{C} \qquad \mathbf{C} = \mathbf{X}\mathbf{C}' \tag{2.92}$$

We replace this new expression for $\mathbf{C}$ in (2.87) and we multiply on the left by $\mathbf{X}^\dagger$

$$(\mathbf{X}^\dagger\mathbf{F}\mathbf{X})\mathbf{C}' = \underbrace{(\mathbf{X}^\dagger\mathbf{S}\mathbf{X})}_{=1}\mathbf{C}'\boldsymbol{\varepsilon} \tag{2.93}$$

We set $\mathbf{F}' = \mathbf{X}^\dagger\mathbf{F}\mathbf{X}$ and we obtain

$$\mathbf{F}'\mathbf{C}' = \mathbf{C}'\boldsymbol{\varepsilon} \tag{2.94}$$

We can now diagonalize $\mathbf{F}'$ to get the orbital energies and then we use the fact that $\mathbf{C} = \mathbf{X}\mathbf{C}'$, to obtain the coefficients of the initial molecular orbitals. The process to solve the Roothaan equation can be summarized in the following way: we start by diagonalizing the core Hamiltonian H^{core} to have a first guess for the coefficients c. We use these coefficients to get the molecular orbitals ψ, which are used to build the Fock matrix $\mathbf{F}$. We transform $\mathbf{F}$ into $\mathbf{F}'$, that we diagonalize, we transform back the matrix $\mathbf{C}'$ into $\mathbf{C}$ to obtain the new coefficients c, that we use to calculate a new Fock matrix $\mathbf{F}$ in another cycle. This is done until convergence is reached, which means that the new orbital energies and the new density matrix $\mathbf{P}$ do not change anymore (see Fig. 2.1).

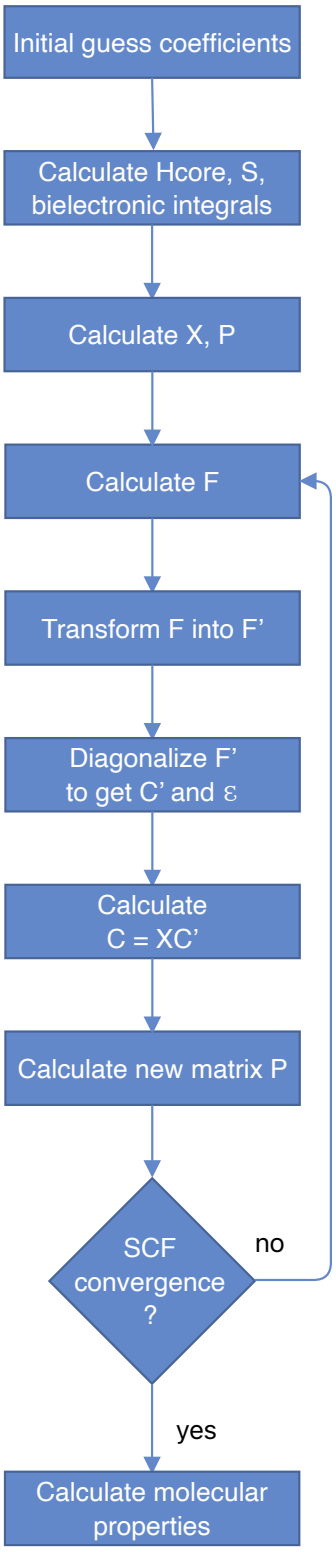

Figure 2.1 – Hartree-Fock self-consistent procedure.

2.2.3 Koopmans' Theorem

Once we know the orbitals and their associated energies in (2.67), we can use (2.75) to obtain

$$\varepsilon_p = \langle p|h|p\rangle + \sum_j \langle pj||pj\rangle \tag{2.95}$$

For an occupied orbital of energy ε_i and an unoccupied orbital of energy ε_a we have

$$\varepsilon_i = \langle i|h|i\rangle + \sum_{j\neq i} \langle ij||ij\rangle \tag{2.96}$$

$$\varepsilon_a = \langle a|h|a\rangle + \sum_j \langle aj||aj\rangle \tag{2.97}$$

In (2.96) the orbital energy ε_i contains the kinetic energy, the nuclei attraction, and a Coulomb-exchange interaction with $N-1$ other particles, whereas in (2.97) the Coulomb-exchange interaction is due to the N particles because we have added an extra electron to the N-electron system. If we note $\left|\Psi_i^{N-1}\right\rangle$ the single determinant state where we removed a particle from the system and $\left|\Psi_a^{N+1}\right\rangle$ the one where we have added a particle to the system

$$\left|\Psi_i^{N-1}\right\rangle = a_i \left|\Psi_0^N\right\rangle \tag{2.98}$$

$$\left|\Psi_a^{N+1}\right\rangle = a_a^\dagger \left|\Psi_0^N\right\rangle \tag{2.99}$$

we define the ionization potentials (IPs) and the electron affinities (EAs) such that

$$\mathrm{IP}_i = E_i^{N-1} - E_0^N = -\varepsilon_i \tag{2.100}$$

where

$$E_0^N = \left\langle \Psi_0^N \middle| H_{elec} \middle| \Psi_0^N \right\rangle \tag{2.101}$$

$$E_i^{N-1} = \left\langle \Psi_i^{N-1} \middle| H_{elec} \middle| \Psi_i^{N-1} \right\rangle \tag{2.102}$$

and

$$\mathrm{EA}_a = E_0^N - E_a^{N+1} = -\varepsilon_a \tag{2.103}$$

where

$$E_a^{N+1} = \left\langle \Psi_a^{N+1} \middle| H_{elec} \middle| \Psi_a^{N+1} \right\rangle \tag{2.104}$$

The expressions (4.9) and (2.104) where we have removed or added an electron to/from the N single determinant state with identical spin orbitals are the results of what is known as Koopmans' theorem.

Chapter 3

Post Hartree-Fock calculations

The Hartree-Fock method treats the interaction of the electrons with a mean-field approximation where each electron interacts with the others through an average static potential. As a consequence, this approximation overestimates the Coulomb interaction (and therefore we get higher electronic energies with respect to the exact ones) because it cannot describe correctly the electron-electron repulsion among particles.

To improve over Hartree-Fock, we need a theory that takes into account the fact that each electron, because of this repulsion, will influence the "motion" of the others and will be influenced by the others because they try to avoid each other. This is called the electron correlation. We will see two methods to include correlation. The first one presented is the configuration interaction [30] which is an exact way to treat correlations by giving a better description of the wavefunction. The second method will be a many-body perturbation theory based on Green's functions, which avoids the use of the many-body wavefunctions and uses Green's functions as fundamental variables of the theory. Correlations enter through an effective potential in which the Green's function moves.

3.1 Configuration Interaction

In Hartree-Fock theory, the wavefunction is described by one Slater determinant built with the occupied orbitals which represents the ground state of the system. What will change in the configuration interaction (CI) method is that we will add to the ground state Slater determinant the excited Slater determinants (single excitations, double excitations and so on) which will be built with occupied and unoccupied orbitals.

This takes into account electron correlation because a Slater determinant adds correlation among particles by preventing two particles from being in the same state at the same position. In a Hartree-Fock calculation, this correlation is included only through the ground state and now it is included also through excited states. So we take the previous basis of N spin orbitals and we increase it up to $2K$ spin orbitals $\{\chi_1, \ldots, \chi_i, \ldots, \chi_N, \chi_{N+1}, \ldots, \chi_a, \ldots, \chi_{2K}\}$. The indices i, j, k, l will refer to occupied orbitals and a, b, c, d to unoccupied orbitals. With this basis we form the basis of Slater determinants $\{|\Psi_0\rangle, |\Psi_i^a\rangle, |\Psi_{ij}^{ab}\rangle, |\Psi_{ijk}^{abc}\rangle, \ldots\}$ where the singly excited states are written as

$$|\Psi_i^a\rangle = |\chi_1 \cdots \chi_a \cdots \chi_N\rangle, \tag{3.1}$$

where the occupied spin orbital χ_i has been replaced by the empty one χ_a. The doubly excited states are written as

$$|\Psi_{ij}^{ab}\rangle = |\chi_1 \cdots \chi_a \cdots \chi_b \cdots \chi_N\rangle \tag{3.2}$$

where we replaced χ_i by χ_a and χ_j by χ_b and so on for the other excited states. If we note

Φ_0 the many-body ground state wavefunction of the system, its expression in CI reads

$$|\Phi_0\rangle = c_0 |\Psi_0\rangle + \sum_{ia} c_i^a |\Psi_i^a\rangle + \sum_{\substack{i<j \\ a<b}} c_{ij}^{ab} |\Psi_{ij}^{ab}\rangle + \sum_{\substack{i<j<k \\ a<b<c}} c_{ijk}^{abc} |\Psi_{ijk}^{abc}\rangle + \dots \tag{3.3}$$

The coefficients $\{c_0, c_i^a, c_{ij}^{ab}, \dots\}$ are called the CI coefficients. If we consider all excited determinants, the CI method is called the full CI (FCI) method. This gives exact energies within the space that we span with the finite basis set.

The total CI energy is given by

$$E_{CI} = \frac{\langle \Phi_0 | \hat{H} | \Phi_0 \rangle}{\langle \Phi_0 | \Phi_0 \rangle} \tag{3.4}$$

We can minimize the CI coefficients with a variational method

$$\frac{\partial E_{CI}}{\partial c_{ijk\cdots}^{abc\cdots}} = 0 \tag{3.5}$$

This affords, like for the Hartree-Fock equations, to write the CI Schrödinger equation

$$H |\Phi_0\rangle = \mathcal{E}_0 |\Phi_0\rangle \tag{3.6}$$

in a matrix formulation

$$\mathbf{HC} = \mathcal{E}\mathbf{C} \tag{3.7}$$

If we rewrite (3.3) in a symbolic form

$$|\Phi_0\rangle = c_0 |\Psi_0\rangle + c_S |S\rangle + c_D |D\rangle + c_T |T\rangle + \dots \tag{3.8}$$

the expression of the CI Hamiltonian is

$$\mathbf{H} = \begin{pmatrix} \langle \Psi_0 | \hat{H} | \Psi_0 \rangle & 0 & \langle \Psi_0 | \hat{H} | D \rangle & 0 & 0 & \cdots \\ 0 & \langle S | \hat{H} | S \rangle & \langle S | \hat{H} | D \rangle & \langle S | \hat{H} | T \rangle & 0 & \cdots \\ \langle D | \hat{H} | \Psi_0 \rangle & \langle D | \hat{H} | S \rangle & \langle D | \hat{H} | D \rangle & \langle D | \hat{H} | T \rangle & \langle D | \hat{H} | Q \rangle & \cdots \\ 0 & \langle T | \hat{H} | S \rangle & \langle T | \hat{H} | D \rangle & \langle T | \hat{H} | T \rangle & \langle T | \hat{H} | Q \rangle & \cdots \\ 0 & 0 & \langle Q | \hat{H} | D \rangle & \langle Q | \hat{H} | T \rangle & \langle Q | \hat{H} | Q \rangle & \cdots \\ \vdots & \vdots & \vdots & \vdots & \vdots & \ddots \end{pmatrix} \tag{3.9}$$

Due to Brillouin's theorem, the single excitations do not couple with the Hartree-Fock ground state. There is no coupling also between Slater determinants which differ by more than two spin orbitals.

We saw that we could obtain more accurate results than the Hartree-Fock method with the CI method by adding to the Hartree-Fock ground state wavefunction more Slater determinants, this gives a better description of the system since we have included electron correlation. However the CI method is computationally heavy, so one has to resort to other methods that are computationally more affordable such as perturbation theory based on Green's functions to treat correlation effects.

In this approach, we describe particles as quasiparticles, where we add to the particle an effective mass or self-energy written as Σ. This quantity will appear from the equation of motion of the one-body Green's function and will take into account all the

many-body effects of the system. This will afford us, as we did in the Hartree-Fock equations, to map the many-body system to an effective one-body system where the effective Schrödinger equation to solve is

$$(\mathbf{F} + \mathbf{\Sigma}(\omega))\psi^{QP}(\omega) = \omega\psi^{QP}(\omega) \tag{3.10}$$

where ψ^{QP} and ω (or ε^{QP}) are respectively the quasiparticle wavefunction and the quasiparticle energies.

3.2 Many-body perturbation theory

3.2.1 Time-independent perturbation theory

In order to obtain information on the electronic properties of a many-body system, one has to solve the many-body Schrödinger equation. This is not possible for problems of such complexity. Therefore one needs to break down the complex problem into a solvable one and a possibility to do so is to use the framework of perturbation theory [31, 32] which treats the interactions of the system as small perturbations of the non-interacting one.

In time-independent perturbation theory we split the Hamiltonian of the system into a non-interacting part H_0, and a perturbation $v = g\bar{v}$ which represents the particle-particle interactions:

$$H = H_0 + v \tag{3.11}$$

We solve the eigenvalue problem associated to H_0

$$H_0 \left|\Phi_n\right\rangle = W_n \left|\Phi_n\right\rangle \tag{3.12}$$

and then we treat the whole problem with expansions in a power series of the coupling constant g. The ground state of the complete problem verifies

$$H \left|\Psi_0\right\rangle = E_0 \left|\Psi_0\right\rangle \tag{3.13}$$

With these two equations, one can write

$$\langle\Phi_0|v|\Psi_0\rangle = \langle\Phi_0|E_0 - H_0|\Psi_0\rangle = (E_0 - W_0)\langle\Phi_0|\Psi_0\rangle \tag{3.14}$$

which gives

$$\Delta E = E_0 - W_0 = \frac{\langle\Phi_0|v|\Psi_0\rangle}{\langle\Phi_0|\Psi_0\rangle} \tag{3.15}$$

We define two projection operators P and Q

$$P = \left|\Phi_0\right\rangle\left\langle\Phi_0\right| \tag{3.16}$$

$$Q = 1 - P = \sum_{n\geq 0} \left|\Phi_n\right\rangle\left\langle\Phi_n\right| - \left|\Phi_0\right\rangle\left\langle\Phi_0\right| = \sum_{n\geq 1} \left|\Phi_n\right\rangle\left\langle\Phi_n\right| \tag{3.17}$$

If we define

$$|\xi\rangle = \frac{|\Psi_0\rangle}{\langle\Phi_0|\Psi_0\rangle} \tag{3.18}$$

one can show that

$$|\xi\rangle = \sum_{n\geq 0} \left[\frac{1}{E - H_0} Q(E - E_0 + v)\right]^n |\Phi_0\rangle \tag{3.19}$$

where we have expressed the solution of the complete problem on the ground state of the unperturbed system. Using this in the expression of the energy shift, we get

$$\Delta E = \langle\Phi_0|v|\xi\rangle = \sum_{n\geq 0} \langle\Phi_0|v \left[\frac{1}{E - H_0} Q(E - E_0 + v)\right]^n |\Phi_0\rangle \tag{3.20}$$

3.2.2 Time-dependent perturbation theory

This formalism can be extended to time-dependent problems where one has to solve the time-dependent Schrödinger equation

$$i\frac{\partial}{\partial t}\left|\Psi(t)\right\rangle_S = H_S\left|\Psi(t)\right\rangle_S \tag{3.21}$$

where the subscript S denotes the Schrödinger picture in which the operators and wave functions are time-dependent. We define the time-evolution operator $U(t,t_0)_S$ such that

$$\left|\Psi(t)\right\rangle_S = U(t,t_0)_S\left|\Psi(t_0)\right\rangle_S \tag{3.22}$$

Replacing this expression in the eigenvalue problem gives

$$i\frac{\partial}{\partial t}U(t,t_0)_S = H_S U(t,t_0)_S \tag{3.23}$$

One can show that U is an unitary operator which verifies $U(t,t_0)_S^{-1} = U(t_0,t)$ and

$$U(t,t_0) = e^{-iH_S(t-t_0)} \tag{3.24}$$

We represent the observables and wavefunction in the interaction picture denoted by the subscript I. We separate the Hamiltonian

$$H = H_0 + V_S \tag{3.25}$$

where H_0 is time independent. In this picture, the observables and wavefunctions are expressed as

$$O(t)_I = e^{iH_0t}O(t)_S e^{-iH_0t} \tag{3.26}$$

$$\left|\Psi(t)\right\rangle_I = e^{iH_0t}\left|\Psi(t)\right\rangle_S \tag{3.27}$$

Then, one can derive the equation of motion and obtain from it the Tomonoga-Schwinger equation

$$i\frac{\partial}{\partial t}\left|\Psi(t)\right\rangle_I = V(t)_I\left|\Psi(t)\right\rangle_I \tag{3.28}$$

which has the structure of a Schrödinger-like equation but contains only the interaction part. We define also a time-evolution operator in this picture

$$\left|\Psi(t)\right\rangle_I = U(t,t')\left|\Psi(t')\right\rangle_I \tag{3.29}$$

replacing this expression in (3.28) gives

$$i\frac{\partial}{\partial t}U(t,t') = V(t)_I U(t,t') \tag{3.30}$$

With the initial condition $U(t',t') = 1$, the solution of (3.30) is

$$U(t,t') = 1 - i\int_{t'}^{t} V(t_1)U(t_1,t')dt_1 \tag{3.31}$$

We can do successive iterations of this integral equation to obtain an approximation at a certain order, and if the successive approximations converge, then one can write

$$U(t,t') = 1 + \sum_{n=1}^{\infty} U^{(n)}(t,t') \tag{3.32}$$

where

$$U^{(n)}(t,t') = (i)^n \int_{t'}^{t} dt_1 \int_{t'}^{t_1} dt_2 \cdots \int_{t'}^{t_{n-1}} dt_n V(t_1)_I \cdots V(t_n)_I \tag{3.33}$$

Let us look at the second-order term

$$U^{(2)}(t,t') = (-i)^2 \int_{t'}^{t} dt_1 \int_{t'}^{t_1} dt_2 V(t_1)_I V(t_2)_I \tag{3.34}$$

The potentials V are functions of operators so they do not commute but to simplify the notations we can use mathematical tricks. We remove the integration limit t_1 so both integrations are on $[t,t']$. To do so, we decompose the integral in the following way

$$\int_{t'}^{t} dt_1 \int_{t'}^{t} dt_2 V(t_1)_I V(t_2)_I = \frac{1}{2}\int_{t'}^{t} dt_1 \int_{t'}^{t_1} dt_2 V(t_1)_I V(t_2)_I + \frac{1}{2}\int_{t'}^{t} dt_2 \int_{t_2}^{t} dt_1 V(t_1)_I V(t_2)_I \tag{3.35}$$

and we replace the triangular integration by integration on the whole square, where for the first term of the left-hand-side t_1 runs from t' to t and for each t_1, t_2 runs from t' to $t_2 = t_1$ and for the second term of the left-hand-side, t_2 runs from t' to t and for each t_2, t_1 runs from $t_1 = t_2$ to t. Then, we do a change of variable which allows us to write the left-hand-side as

$$\frac{1}{2}\int_{t'}^{t} dt_1 \int_{t'}^{t_1} dt_2 V(t_1)_I V(t_2)_I + \frac{1}{2}\int_{t'}^{t} dt_2 \int_{t_1}^{t} dt_1 V(t_2)_I V(t_1)_I \tag{3.36}$$

Introducing the time-ordering operator

$$T[A(t_1)B(t_2)] = \begin{cases} A(t_1)B(t_2) & t_1 > t_2 \\ B(t_2)A(t_1) & t_2 > t_1 \end{cases} \tag{3.37}$$

we can write

$$U^{(2)}(t,t') = \frac{1}{2}(-i)^2 \int_{t'}^{t} dt_1 \int_{t'}^{t} dt_2 T[V(t_1)_I V(t_2)_I] \tag{3.38}$$

For a product on n operators, we have

$$U^{(n)}(t,t') = \frac{1}{n!}(-i)^n \int_{t'}^{t} dt_1 \int_{t'}^{t} dt_2 \cdots \int_{t'}^{t} dt_n T[V(t_1)_I \cdots V(t_n)_I] \tag{3.39}$$

Using this expression in (3.32), we can write

$$U(t,t') = T\exp\left[-i\int_{t'}^{t} d\tau V(\tau)_I\right] \tag{3.40}$$

Using this evolution operator, we will obtain the wavefunction of the complete problem by introducing a fictitious time-dependence which allows us to connect this last one to the unperturbed wavefunction

$$|\Psi_0\rangle = U(0,-\infty)\,|\Phi_0\rangle \tag{3.41}$$

We define a time-dependent Hamiltonian in the Schrödinger picture

$$H_\epsilon(t) = H_0 + e^{-\epsilon|t|}v \tag{3.42}$$

where $\epsilon > 0$. This Hamiltonian has the following properties

$$H_\epsilon(t \to \pm\infty) = H_0$$
$$H_\epsilon(t \to 0) = H$$

The time-dependent Schrödinger equation

$$i\frac{\partial}{\partial t}\left|\Psi_\epsilon(t)\right\rangle_S = H_\epsilon(t)_S\left|\Psi_\epsilon(t)\right\rangle_S \tag{3.43}$$

at the limit $t \to \pm\infty$ tends to

$$i\frac{\partial}{\partial t}\left|\Psi_\epsilon(t)\right\rangle_S = H_0\left|\Psi_\epsilon(t)\right\rangle_S \tag{3.44}$$

For the initial condition $t \to -\infty$, the interacting ground state is obtained from the non-interacting one

$$\left|\Psi_\epsilon(t\to-\infty)\right\rangle_S = e^{-iW_0t}\left|\Phi_0\right\rangle \tag{3.45}$$

The equation of motion in the interaction picture is written

$$i\frac{\partial}{\partial t}\left|\Psi_\epsilon(t)\right\rangle_I = e^{-\epsilon|t|}v(t)_I\left|\Psi_\epsilon(t)\right\rangle_I \tag{3.46}$$

For $t \to \pm\infty$, we have

$$\lim_{t\to\pm\infty} i\frac{\partial}{\partial t}\left|\Psi_\epsilon(t)\right\rangle_I = 0 \tag{3.47}$$

In this limit, the wavefunction becomes time-independent

$$\left|\Psi_\epsilon(t\to\pm\infty)\right\rangle_I = \text{constant} \tag{3.48}$$

If we apply the initial condition $t \to -\infty$ in the expression (3.45), we get

$$\lim_{t\to\pm\infty}\left|\Psi_\epsilon(t)\right\rangle_I = \lim_{t\to\pm\infty} e^{iH_0t}\left|\Psi_\epsilon(t)\right\rangle_S = e^{iH_0t}e^{-iW_0t}\left|\Phi_0\right\rangle = \left|\Phi_0\right\rangle \tag{3.49}$$

so we can write (3.48) as

$$\left|\Psi_\epsilon(t)\right\rangle_I = U_\epsilon(0,-\infty)\left|\Phi_0\right\rangle \tag{3.50}$$

Now, we have to link $\left|\Psi_\epsilon(t)\right\rangle_I$ and $\left|\Psi_\epsilon(0)\right\rangle$. To do so, we drop the index I because at $t = 0$ all the pictures are the same, and we turn on the potential adiabatically. Under such conditions, we obtain

$$\left|\Psi_0\right\rangle = \lim_{\epsilon\to0}\left|\Psi_\epsilon(0)\right\rangle \tag{3.51}$$

This limit exists if we verify the Gell-Mann-Low theorem which says that the quantity

$$\left|\xi\right\rangle = \lim_{\epsilon\to0}\frac{\left|\Psi_\epsilon(0)\right\rangle}{\left\langle\Phi_0|\Psi_\epsilon(0)\right\rangle} \tag{3.52}$$

exists to all orders in perturbation theory, that is to say, if in the perturbation expansion

$$\frac{\left|\Psi_\epsilon(0)\right\rangle}{\left\langle\Phi_0|\Psi_\epsilon(0)\right\rangle} = \sum_{n=0}^{\infty}\left|\xi_\epsilon^{(n)}\right\rangle g^n \tag{3.53}$$

the limit $\lim_{\epsilon\to0}\left|\xi\right\rangle^{(n)}$ exists for each n, then $\left|\xi\right\rangle$ is an eigenstate of the perturbed Hamiltonian. However, it does not guarantee that this state is the ground state of the system. If we want to study the properties of a many-body system beyond its ground state, one has to resort to calculating the one-body Green's function with perturbation theory. To do so, we need to show first that the matrix elements of an operator O_H in the Heisenberg representation are related to its matrix elements in the interaction representation by

$$\begin{aligned}\frac{\left\langle\Psi_0|\hat{O}_H(t)|\Psi_0\right\rangle}{\left\langle\Psi_0|\Psi_0\right\rangle} = \lim_{\epsilon\to0}\frac{1}{\left\langle\Phi_0|\hat{S}_\epsilon|\Phi_0\right\rangle}\left\langle\Phi_0\right|\sum_{\nu=0}^{\infty}(-i)^\nu\frac{1}{\nu!}\int_{-\infty}^{\infty}dt_1\cdots\int_{-\infty}^{\infty}dt_\nu \\ \times e^{-\epsilon(|t_1|+\cdots+|t_\nu|)}T[\hat{H}_1(t_1)_I\cdots\hat{H}_1(t_\nu)_I\hat{O}_I(t)]\left|\Phi_0\right\rangle\end{aligned} \tag{3.54}$$

where $\hat{S}_\epsilon = U_\epsilon(\infty, -\infty)$ is the scattering matrix.

We start with the Gell-Mann and Low theorem

$$\frac{|\Psi_0\rangle}{\langle\Phi_0|\Psi_0\rangle} = \frac{U_\epsilon(0, \pm\infty)\,|\Phi_0\rangle}{\langle\Phi_0|U_\epsilon(0, \pm\infty)|\Phi_0\rangle} \tag{3.55}$$

With this expression, we can obtain an expression for the denominator of the left-hand-side of (3.54)

$$\begin{aligned}\frac{\langle\Psi_0|\Psi_0\rangle}{|\langle\Phi_0|\Psi_0\rangle|^2} &= \frac{\langle\Phi_0|U_\epsilon(0,\infty)^\dagger U_\epsilon(0,-\infty)|\Phi_0\rangle}{|\langle\Phi_0|\Psi_0\rangle|^2} \\ &= \frac{\langle\Phi_0|U_\epsilon(\infty,0)U_\epsilon(0,-\infty)|\Phi_0\rangle}{|\langle\Phi_0|\Psi_0\rangle|^2} \\ &= \frac{\langle\Phi_0|\hat{S}_\epsilon|\Phi_0\rangle}{|\langle\Phi_0|\Psi_0\rangle|^2}\end{aligned} \tag{3.56}$$

where

$$\langle\Phi_0|\hat{S}_\epsilon|\Phi_0\rangle = \langle\Phi_0|U_\epsilon(\infty,0)U_\epsilon(0,-\infty)|\Phi_0\rangle \tag{3.57}$$

An operator O_H in the Heisenberg representation is related to its interaction representation by

$$\hat{O}(t)_H = \hat{U}(0,t)\hat{O}(t)_I\hat{U}(t,0) \tag{3.58}$$

Using this expression in the numerator on the left side of (3.54) gives

$$\frac{\langle\Phi_0|\hat{U}_\epsilon(\infty,0)\hat{U}_\epsilon(0,t)\hat{O}_I(t)\hat{U}_\epsilon(t,0)\hat{U}_\epsilon(0,-\infty)|\Phi_0\rangle}{|\langle\Phi_0|\Psi_0\rangle|^2} = \frac{\langle\Phi_0|\hat{U}_\epsilon(\infty,t)\hat{O}_I(t)\hat{U}_\epsilon(t,-\infty)|\Phi_0\rangle}{|\langle\Phi_0|\Psi_0\rangle|^2} \tag{3.59}$$

We replace (3.59) and (3.56) in (3.54), we get

$$\frac{\langle\Psi_0|\hat{O}_H(t)|\Psi_0\rangle}{\langle\Psi_0|\Psi_0\rangle} = \lim_{\epsilon\to 0}\frac{\langle\Phi_0|\hat{U}_\epsilon(\infty,t)\hat{O}_I(t)\hat{U}_\epsilon(t,-\infty)|\Phi_0\rangle}{\langle\Phi_0|\hat{S}_\epsilon|\Phi_0\rangle} \tag{3.60}$$

Then, one can show that the numerator operator in the right-hand-side of (3.54) is equal to the following expression

$$\begin{aligned}&\hat{U}_\epsilon(\infty,t)\hat{O}_I(t)\hat{U}_\epsilon(t,-\infty) = \\ &\sum_{n=0}^{\infty}(-i)^n\frac{1}{n!}\int_{-\infty}^{\infty}dt_1\cdots\int_{-\infty}^{\infty}dt_n e^{-\epsilon(|t_1|+\cdots+|t_n|)}T[\hat{H}_1(t_1)_I\cdots\hat{H}_1(t_n)_I] \\ &\times\hat{O}_I(t)\sum_{n=0}^{\infty}(-i)^m\frac{1}{m!}\int_{-\infty}^{\infty}dt_1\cdots\int_{-\infty}^{\infty}dt_m \\ &\times e^{-\epsilon(|t_1|+\cdots+|t_m|)}T[\hat{H}_1(t_1)_I\cdots\hat{H}_1(t_m)_I]\end{aligned} \tag{3.61}$$

We obtain in the same way the expression of the expectation value of the time-ordered Heisenberg operators

$$\begin{aligned}\frac{\langle\Psi_0|T[\hat{O}_H(t)\hat{O}_H(t')]|\Psi_0\rangle}{\langle\Psi_0|\Psi_0\rangle} &= \lim_{\epsilon\to 0}\frac{1}{\langle\Phi_0|\hat{S}_\epsilon|\Phi_0\rangle}\langle\Phi_0|\sum_{\nu=0}^{\infty}(-i)^\nu\frac{1}{\nu!} \\ &\times\int_{-\infty}^{\infty}dt_1\cdots\int_{-\infty}^{\infty}dt_\nu e^{-\epsilon(|t_1|+\cdots+|t_\nu|)} \\ &\times T[\hat{H}_1(t_1)_I\cdots\hat{H}_1(t_\nu)_I\hat{O}_I(t)\hat{O}_I(t')]\,|\Phi_0\rangle\end{aligned} \tag{3.62}$$

3.2.3 Green's functions

The nth-body Green's function is defined as [33]

$$i^n G_n\left(1,2,\ldots,n;1',2',\ldots,n'\right) = \left\langle \Psi_0^N \left| T\left[\hat{\psi}_H(1)\cdots\hat{\psi}(n)\hat{\psi}_H^\dagger\left(n'\right)\cdots\hat{\psi}_H^\dagger\left(1'\right)\right] \right| \Psi_0^N \right\rangle \tag{3.63}$$

where Ψ_0^N is the normalized ground state many-body wavefunction of the interacting N-particle system and $1 = (\mathbf{x}_1, t_1) = (\mathbf{r}_1, \sigma_1, t_1)$ is a composite index gathering space, spin and time. The field operators $\hat{\psi}_H$ and $\hat{\psi}_H^\dagger$ are expressed in the Heisenberg picture as

$$\hat{\psi}_H(i) = e^{iHt_i}\hat{\psi}(\mathbf{x}_i)e^{-iHt_i} \tag{3.64}$$

$$\hat{\psi}_H^\dagger(i) = e^{iHt_i}\hat{\psi}^\dagger(\mathbf{x}_i)e^{-iHt_i} \tag{3.65}$$

where H in the exponential operator is the (time-independent) Hamiltonian of the system. The field operators can be expressed in the one-particle basis with the use of creation ($c_i^\dagger$) and annihilation (c_i) operators. In this way, $\chi_i^*(\mathbf{x})c_i^\dagger$ adds a particle in an orbital i at a position $\mathbf{x}$ and $\chi_i(\mathbf{x})c_i$ removes a particle from an orbital i at a position $\mathbf{x}$

$$\hat{\psi}(\mathbf{x}) = \sum_i \chi_i(\mathbf{x})c_i \tag{3.66}$$

$$\hat{\psi}^\dagger(\mathbf{x}) = \sum_i \chi_i^*(\mathbf{x})c_i^\dagger \tag{3.67}$$

T is the time-ordering operator which rearranges the field operators in the chronological order of their time arguments, with a multiplicative factor (± 1) depending on whether the chronological order is an even or odd permutation of the original order. From this general definition, we define the one-body Green's function (1-GF) [33, 32, 34] as

$$iG_1(1,2) = \left\langle \Psi_0^N \right| T[\hat{\psi}_H(1)\hat{\psi}_H^\dagger(2)] \left| \Psi_0^N \right\rangle \tag{3.68}$$

where

$$T[\hat{\psi}_H(1)\hat{\psi}_H^\dagger(2)] = \Theta(t_1 - t_2)\hat{\psi}_H(1)\hat{\psi}_H^\dagger(2) \pm \Theta(t_2 - t_1)\hat{\psi}_H^\dagger(2)\hat{\psi}_H(1) \tag{3.69}$$

The sign $\pm$ depends on the type of particles studied. Since the particles in our case are fermions we have a minus sign to take into account the Pauli principle. Replacing expression (3.69) in (3.68) gives

$$iG_1(1,2) = \Theta(t_1 - t_2)\left\langle \Psi_0^N \right| \hat{\psi}_H(1)\hat{\psi}_H^\dagger(2) \left| \Psi_0^N \right\rangle - \Theta(t_2 - t_1)\left\langle \Psi_0^N \right| \hat{\psi}_H^\dagger(2)\hat{\psi}_H(1) \left| \Psi_0^N \right\rangle \tag{3.70}$$

By replacing (3.64) in (3.70) we arrive at

$$\begin{aligned} iG_1(1,2) = {} & \Theta(t_1 - t_2)e^{iE_0^N(t_1-t_2)}\left\langle \Psi_0^N \right| \hat{\psi}(\mathbf{x}_1)e^{-iH(t_1-t_2)}\hat{\psi}^\dagger(\mathbf{x}_2) \left| \Psi_0^N \right\rangle \\ & -\Theta(t_2 - t_1)e^{iE_0^N(t_2-t_1)}\left\langle \Psi_0^N \right| \hat{\psi}^\dagger(\mathbf{x}_2)e^{-iH(t_2-t_1)}\hat{\psi}(\mathbf{x}_1) \left| \Psi_0^N \right\rangle \end{aligned} \tag{3.71}$$

where E_0^N is the ground-state energy of the N-electron system. We note that the one-body Green's function depends only on the time difference $t_1 - t_2$ because the Hamiltonian is time-independent and time is homogeneous.

In the first term in the right-hand side of the equation (3.71), we add to the N-particle system an electron in $\mathbf{x}_2$ at t_2. This particle propagates during a time $t_1 - t_2$ and it is then removed from the system in $\mathbf{x}_1$ at t_1. For the second term, an electron is removed at the position $\mathbf{x}_1$ at time t_1 leaving a hole. This hole propagates during a time $t_2 - t_1$ and

then it is removed from the system (i.e. an electron is added) in $\mathbf{x}_2$ at time t_1. Therefore the amplitudes in the Green's function represent the propagation of a particle (electron or hole) in a medium. As we saw, the one-body Green's function depends only on the time difference $\tau = t_1 - t_2$ so we have

$$G(1,2) = G(\mathbf{x}_1, \mathbf{x}_2, \tau) \tag{3.72}$$

Moreover, if the system is uniform and isotropic, we have that the Hamiltonian commutes with the momentum operator and so the one-body Green's function depends only of the difference $\mathbf{x}_1 - \mathbf{x}_2$.

Properties of interest from the one-body Green's function

With the one-body Green's function one can get access to the charged excitations [35, 1, 36, 37, 38] of a system, the expectation value of one particle-operators and the ground state total energy.

For instance, the density operator written in first quantization as

$$\hat{\rho}(\mathbf{x}) = \sum_{i=1}^{N} \delta(\mathbf{x} - \mathbf{x}_i) \tag{3.73}$$

is written in second quantization as

$$\hat{\rho}(\mathbf{x}) = \hat{\psi}^\dagger(\mathbf{x})\hat{\psi}(\mathbf{x}) \tag{3.74}$$

The density is obtained by averaging the previous quantity

$$\begin{aligned} \rho(\mathbf{x}, t) &= \left\langle \Psi_0^N \right| \hat{\psi}_H^\dagger(\mathbf{x}, t)\hat{\psi}_H(\mathbf{x}, t) \left| \Psi_0^N \right\rangle \\ &= \lim_{t' \to t^+} \left\langle \Psi_0^N \right| \hat{\psi}_H^\dagger\left(\mathbf{x}t'\right) \hat{\psi}_H(\mathbf{x}t) \left| \Psi_0^N \right\rangle \end{aligned} \tag{3.75}$$

With $t' > t$, then we introduce the operator T

$$\begin{aligned} \rho(\mathbf{x}) &= \lim_{t' \to t^+} \left\langle \Psi_0^N \right| T\left[\hat{\psi}_H^\dagger\left(\mathbf{x}t'\right) \hat{\psi}_H(\mathbf{x}t)\right] \left| \Psi_0^N \right\rangle \\ &= \lim_{t' \to t^+} -\left\langle \Psi_0^N \right| T\left[\hat{\psi}_H(\mathbf{x}t)\hat{\psi}_H^\dagger\left(\mathbf{x}t'\right)\right] \left| \Psi_0^N \right\rangle \\ &= \lim_{t' \to t^+} -iG(\mathbf{x}, \mathbf{x}, t - t') \end{aligned} \tag{3.76}$$

Thus, we have an expression that relates the density to the one-body Green's function. From this last expression, one can show that it is possible to get access to the average of any one-body operator in general.

Moreover, one can obtain the ionization potential (IP) and electron affinity (EA) of a system, as it is clear from the Lehmann representation of the one-body Green's function. We introduce two closure relations

$$\sum_{nM} \left| \Psi_n^M \right\rangle \left\langle \Psi_n^M \right| \tag{3.77}$$

in Fock space in (3.70), where $\left| \Psi_n^M \right\rangle$ is the n-th many-body wavefunction of the M-electron system, this gives

$$\begin{aligned} iG_1(1,2) = \Theta(t_1 - t_2) \sum_n \left\langle \Psi_0^N \right| \hat{\psi}_H(1) \left| \Psi_n^{N+1} \right\rangle \left\langle \Psi_n^{N+1} \right| \hat{\psi}_H^\dagger(2) \left| \Psi_0^N \right\rangle \\ - \Theta(t_2 - t_1) \sum_m \left\langle \Psi_0^N \right| \hat{\psi}_H^\dagger(2) \left| \Psi_m^{N-1} \right\rangle \left\langle \Psi_m^{N-1} \right| \hat{\psi}_H(1) \left| \Psi_0^N \right\rangle \end{aligned} \tag{3.78}$$

where Ψ_n^{N+1} is the n-th excited state of the $(N+1)$-particle system and Ψ_m^{N-1} is the m-th excited state of the $(N-1)$-particle system. We introduce the Feynman-Dyson amplitudes

$$\begin{aligned} f_n(1) &= \left\langle \Psi_0^N \right| \hat{\psi}(1) \left| \Psi_n^{N+1} \right\rangle \\ &= \left\langle \Psi_0^N \right| \hat{\psi}(\mathbf{x}_1) \left| \Psi_n^{N+1} \right\rangle e^{-i(E_n^{N+1}-E_0^N)t_1} \\ &= f_n(\mathbf{x}_1) e^{-i(E_n^{N+1}-E_0^N)t_1} \end{aligned} \tag{3.79}$$

$$\begin{aligned} g_n(1) &= \left\langle \Psi_n^{N-1} \right| \hat{\psi}(1) \left| \Psi_0^N \right\rangle \\ &= \left\langle \Psi_n^{N-1} \right| \hat{\psi}(\mathbf{x}_1) \left| \Psi_0^N \right\rangle e^{i(E_n^{N-1}-E_0^N)t_1} \\ &= g_n(\mathbf{x}_1) e^{i(E_n^{N-1}-E_0^N)t_1} \end{aligned} \tag{3.80}$$

With these amplitudes and setting $\tau = t_1 - t_2$, (3.80) is written as

$$\begin{aligned} iG_1(1,2) = \Theta(\tau) \sum_n f_n(\mathbf{x}_1) f_n^*(\mathbf{x}_2) e^{-i(E_n^{N+1}-E_0^N)\tau} \\ - \Theta(-\tau) \sum_m g_m(\mathbf{x}_1) g_m^*(\mathbf{x}_2) e^{-i(E_0^N-E_m^{N-1})\tau} \end{aligned} \tag{3.81}$$

The Feynman-Dyson amplitudes are not orthogonal nor linearly independent. It can be proved that the total set verifies the completeness relationship

$$\sum_n f_n(\mathbf{x}_1) f_n^*(\mathbf{x}_2) + \sum_m g_m(\mathbf{x}_1) g_m^*(\mathbf{x}_2) = \delta(\mathbf{x}_1 - \mathbf{x}_2) \tag{3.82}$$

Performing a Fourier transform of (3.81) one can obtain the Lehmann representation of the one-body Green's function as

$$G_1(\mathbf{x}_1, \mathbf{x}_2; \omega) = \lim_{\eta \to +0} \left[\sum_n \frac{f_n(\mathbf{x}_1) f_n^*(\mathbf{x}_2)}{\omega - (E_n^{N+1} - E_0^N) + i\eta} + \sum_m \frac{g_m(\mathbf{x}_1) g_m^*(\mathbf{x}_2)}{\omega - (E_0^N - E_m^{N-1}) - i\eta} \right] \tag{3.83}$$

where we used the following Fourier transform of the Heaviside step-function

$$\int_{-\infty}^{\infty} dt \left[\Theta(\pm t) e^{-i\alpha t} \right] e^{i\omega t} = \lim_{\eta \to +0} \frac{\pm i}{\omega - \alpha \pm i\eta} \tag{3.84}$$

The poles of the one-body Green's function are composed of discrete singularities which are represented by isolated points in the complex plane, which are the discrete states of the system (that is to say the bound states of the system). The continuous singularities represented by branches in the complex plane are the free states of the system.

The poles $\omega = E_0^N - E_m^{N-1}$ are the removal energies, they represent the energy that one must give to the system to remove one of its electrons. The pole $\omega = E_n^{N+1} - E_0^N$ are the addition energies, they represent the energy necessary to add an electron to the system. These poles are called the charged excitations of the system. They represent the fact that in a N-body system, to add a particle one needs to overcome the interaction of the particle with the rest of the system. The particle, therefore, is dressed with an effective "mass" which takes into account this interaction. From this, we can obtain the fundamental gap E_G of the system

$$E_G = \mathrm{IP} - \mathrm{EA} \tag{3.85}$$

where

$$\text{IP} = E_0^{N-1} - E_0^N \tag{3.86}$$

and

$$\text{EA} = E_0^{N+1} - E_0^N \tag{3.87}$$

We can use (3.83) to obtain the spectral function

$$A(\mathbf{x}_1, \mathbf{x}_2, \omega) = -\frac{1}{\pi}\text{sgn}(\omega)\text{Im}[G(\mathbf{x}_1, \mathbf{x}_2, \omega)] \tag{3.88}$$

which is related to the experimental photoemission spectra.

How to determine the one-body Green's function

In practice, we do not use (3.83) to get the one-body Green's function because it requires to know the eigenstates of the $(N-1)$-, N- and $(N+1)$-body system, which we want to avoid. Instead, we can use a simpler Green's function as a starting point such as the non-interacting Green's function G^0 or the Hartree-Fock Green's function G^{HF} for instance and use the Dyson equation to calculate an approximate Green's function.

Diagrammatic expansion

Using (3.62), we can write the expression of the exact one-body Green's function

$$\begin{aligned} &iG_{\alpha\beta}(x, x') \\ &= \lim_{\epsilon\to 0}\left[\frac{1}{\langle\Phi_0|\hat{S}_\epsilon|\Phi_0\rangle}\sum_{\nu=0}^{\infty}(-i)^\nu\frac{1}{\nu!}\int_{-\infty}^{\infty}dt_1\cdots\int_{-\infty}^{\infty}dt_\nu\right. \\ &\left.\times e^{-\epsilon(|t_1|+\cdots+|t_\nu|)}\langle\Phi_0|\,T[\hat{H}_1(t_1)_I\cdots\hat{H}_1(t_\nu)_I\psi_\alpha(x)_I\psi^\dagger_\beta(x')_I]\,|\Phi_0\rangle\right] \end{aligned} \tag{3.89}$$

where $x = (\boldsymbol{r}, t)$

We separate the first term of (3.89) written $iG^0_{\alpha\beta}(x, x')$ which refers to the non-interacting system from the rest of the sum

$$iG_{\alpha\beta}(x, x') = iG^0_{\alpha\beta}(x, x') + \cdots \tag{3.90}$$

where

$$iG^0_{\alpha\beta}(x, x') = \langle\Phi_0|\,T[\psi_\alpha(x)_I\psi^\dagger_\beta(x')_I]\,|\Phi_0\rangle \tag{3.91}$$

Then, one can show that by expressing the perturbation series in diagrams the sum in the numerator of (3.89) can be expressed as the product of the connected and disconnected diagrams, and the denominator contains the sum of all disconnected diagrams. Therefore, the disconnected diagrams are canceled and the perturbation series contains only connected diagrams. This is known as the linked-cluster theorem. Therefore, (3.89) becomes

$$\begin{aligned} iG_{\alpha\beta}(x, x') &= \sum_{\nu=0}^{\infty}(-i)^\nu\frac{1}{\nu!}\int_{-\infty}^{\infty}dt_1\cdots\int_{-\infty}^{\infty}dt_\nu \\ &\times\langle\Phi_0|\,T[\hat{H}_1(t_1)_I\cdots\hat{H}_1(t_\nu)_I\psi_\alpha(x)_I\psi^\dagger_\beta(x')_I]\,|\Phi_0\rangle_{\text{connected}} \end{aligned} \tag{3.92}$$

The expansions of the series are expressed as successive products of the non-interacting Green's function and an interaction term, for each order the interacting part represents the proper self-energy Σ. For instance, if we write the terms at first and second order, we get

$$G^{(1)}(x, y) = G^0(x, y) + \int d^4x_1 d^4x_{1'} G^0(x, x_1)\Sigma(x_1, x_{1'})G^0(x_{1'}, y) \tag{3.93}$$

and

$$G^{(2)}(x,y) = G^0(x,y) + \int d^4x_1 d^4x_{1'} G^0(x,x_1)\Sigma(x_1,x_{1'})G^0(x_{1'},y) + \int d^4x_1 d^4x_{1'} d^4x_2 d^4x_{2'} G^0(x,x_1)\Sigma(x_1,x_{1'}) \times G^0(x_{1'},x_2)\Sigma(x_2,x_{2'})G^0(x_{2'},y) \tag{3.94}$$

Therefore the final expression for the interacting 1-GF can be written as

$$G(x,y) = G^0(x,y) + \int d^4x_1 d^4x_{1'} G^0(x,x_1)\Sigma^{red}(x_1,x_{1'})G^0(x_{1'},y) \tag{3.95}$$

where Σ^{red} is the (reducible) self-energy and it contains the sum of all the proper terms

$$\Sigma^{red}(x,y) = \Sigma(x,y) + \int d^4x_1 d^4x_{1'} \Sigma(x,x_1)G^0(x_1,x_{1'})\Sigma(x_{1'},y) + \int d^4x_1 d^4x_{1'} d^4x_2 d^4x_{2'} \Sigma(x,x_1)G^0(x_1,x_{1'})\Sigma(x_{1'},x_2)G^0(x_2,x_{2'})\Sigma(x_{2'},y) + \cdots \tag{3.96}$$

Combining Eq. (3.95) and Eq. (3.96) one obtains the following Dyson equation

$$G(x,y) = G^0(x,y) + \int d^4x_1 d^4x_{1'} G^0(x,x_1)\Sigma(x_1,x_{1'};[G_0])G(x_{1'},y) \tag{3.97}$$

The first term of the right-hand-side in (3.95) is called the bare propagator. It is used in the second term of the right-hand side to obtain the interaction terms. Within this formalism, one says that the bare propagator has been dressed with the interaction which contains the collective effects due to the many-body system, and the effective system described by the dressed propagator is called a dressed particle or a quasiparticle.

Functional derivatives

In the following, we will derive the Dyson equation for the 1-GF using the functional approach.[34] The Dyson equation is obtained from the equation of motion (EoM) of the one-body Green's function [40]. To show this let us write the Hamiltonian of the system in second quantization as

$$H = \int d\mathbf{x}\hat{\psi}^\dagger(\mathbf{x})h(\mathbf{r})\hat{\psi}(\mathbf{x}) + \frac{1}{2}\int d\mathbf{x}d\mathbf{x}'\hat{\psi}^\dagger(\mathbf{x})\hat{\psi}^\dagger(\mathbf{x}')v(\mathbf{r},\mathbf{r}')\hat{\psi}(\mathbf{x}')\hat{\psi}(\mathbf{x}) \tag{3.98}$$

with

$$h(\mathbf{r}) = -\frac{1}{2}\nabla^2 + V(\mathbf{r}) \tag{3.99}$$

$$v(\mathbf{r},\mathbf{r}') = \frac{1}{|\mathbf{r}-\mathbf{r}'|} \tag{3.100}$$

where $h(\mathbf{r})$ is a one-particle operator that contains the kinetic energy operator and electron-nucleus interaction potential $V(\mathbf{r})$, and $v(\mathbf{r},\mathbf{r}')$ is the electron-electron Coulomb interaction. The EoM for the 1-GF can be obtained by differentiating the definition (3.68) with respect to t_1. One can use the equation of motion of the field operators in the Heisenberg picture

$$i\frac{\partial}{\partial t_1}\hat{\psi}_H(1) = [\hat{\psi}_H, H_H] \tag{3.101}$$

which, using (3.98), gives

$$i\frac{\partial}{\partial t_1}\hat{\psi}_H(1) = \left[h(1) + \int d3v(1,3)\hat{\psi}_H^\dagger(3)\hat{\psi}_H(3)\right]\hat{\psi}_H(1) \tag{3.102}$$

We now define the two-particle Green's function

$$G_2(1,2;1',2') = (-i)^2 \left\langle \Psi_0^N \right| T[\hat{\psi}_H(1)\hat{\psi}_H(2)\hat{\psi}_H^\dagger(1')\hat{\psi}_H^\dagger(2')] \left| \Psi_0^N \right\rangle \tag{3.103}$$

which represents the amplitude probability of adding and removing two bodies which can be electrons or holes depending on the channel we choose. Using (3.102) and (3.103) we can rewrite the equation of motion of the one-body Green's function as

$$\left[i\frac{\partial}{\partial t_1} - h(1)\right] G_1(1,2) + i\int d3v(1,3)G_2(1,3^+;2,3^{++}) = \delta(1,2) \tag{3.104}$$

The signs "$+$" in G_2 mean that we have choose the following time ordering

$$\begin{aligned} G_2(1,3^+;2,3^{++}) &= -\left\langle \Psi_0^N \right| T[\hat{\psi}_H(1)\hat{\psi}_H(3^+)\hat{\psi}_H^\dagger(2)\hat{\psi}_H^\dagger(3^{++})] \left| \Psi_0^N \right\rangle \\ &= \left\langle \Psi_0^N \right| T[\hat{\psi}_H^\dagger(3^{++})\hat{\psi}_H(3^+)\hat{\psi}_H(1)\hat{\psi}_H^\dagger(2)] \left| \Psi_0^N \right\rangle \end{aligned} \tag{3.105}$$

Note that $t_3 = t_1^+$ thanks to the Coulomb potential $v(1,3) = v(\mathbf{r}_1,\mathbf{r}_3)\delta(t_1 - t_3)$ in (3.104).

The equation (3.104) cannot be solved directly because it is not closed as it depends on the one-body Green's function and the two-body Green's function. To solve it, we need to determine the Green's function at higher orders but there is an infinity of them. Therefore, the hierarchy should be truncated, but how to do this is not trivial.

Another method was proposed by Schwinger [79]. It consists of introducing a fictitious external potential U in (3.104), which will be set to zero at the end. (The Green's functions are then a functional of this external potential, but we do not write it explicitly to lighten the notation.) This gives

$$\left[i\frac{\partial}{\partial t_1} - h(1)\right] G_1(1,2) - \int d3U(1,3)G_1(3,2) + i\int d3v(1,3)G_2(1,3^+;2,3^{++}) = \delta(1,2) \tag{3.106}$$

This external potential allows us to link the two-body Green's function to the one-body Green's function through the Schwinger relation

$$G_2(1,3;2,3^+) = G_1(1,2)G_1(3,3^+) - \frac{\delta G_1(1,2)}{\delta U(3)} \tag{3.107}$$

with

$$U(1,3) = U(\mathbf{x}_1,\mathbf{x}_3;t_1)\delta(t_1 - t_3) \tag{3.108}$$

In (3.107) we have $U(3) = U(3,3)$. With this expression, equation (3.106) is rewritten as

$$\left[i\frac{\partial}{\partial t_1} - h(1) - U(1) + i\int d3v(1,3)G_1(3,3^+)\right] G_1(1,2) - i\int d3v(1^+,3)\frac{\delta G_1(1,2)}{\delta U(3)} = \delta(1,2) \tag{3.109}$$

We define the self-energy

$$\Sigma(1,2) = \Sigma_H(1,2) + i\int d34\ \ v(1^+,3)\frac{\delta G_1(1,4)}{\delta U(3)}G_1^{-1}(4,2) \tag{3.110}$$

with

$$\Sigma_H(1,2) = \delta(1,2)\left[-i\int d3\ \ v(1,3)G_1(3,3^+)\right] \tag{3.111}$$

the Hartree contribution to the self-energy.

Σ is a non-local, non-hermitian, effective potential. Equation (3.110) is an exact expression that affords to take the interactions of a particle with the other particles in a medium reducing thus a many-particle equation into a one-particle equation. With this definition the expression (3.106) becomes

$$\left[i\frac{\partial}{\partial t_1} - h(1) - U(1)\right]G_1(1,2) - i\int d3\ \ \Sigma(1,3)G_1(3,2) = \delta(1,2) \tag{3.112}$$

From (3.112), we get the Dyson equation [33, 32, 34]

$$G_1(1,2) = G_1^0(1,2) + \int d34\ \ G_1^0(1,3)\Sigma(3,4)G_1(4,2) \tag{3.113}$$

where we used

$$\left[i\frac{\partial}{\partial t_1} - h(1)\right]\delta(1,2) = (G_1^0)^{-1}(1,2) \tag{3.114}$$

and we set $U = 0$.

We now define the total potential $V(1)$ and the inverse dielectric function as

$$V(1) = U(1) - i\int d3v(1,3)G_1(3,3^+) \tag{3.115}$$

and

$$\epsilon^{-1}(1,2) = \frac{\delta V(1)}{\delta U(2)} = \delta(1,2) + \int d3v(1,3)\frac{\delta\rho(3)}{\delta U(2)} \tag{3.116}$$

respectively, with

$$\rho(3) = -iG_1(3,3^+) \tag{3.117}$$

We now use the fact that

$$\chi(3,2) = \frac{\delta\rho(3)}{\delta U(2)} \tag{3.118}$$

to rewrite ϵ^{-1} as

$$\epsilon^{-1}(1,2) = \delta(1,2) + \int d3v(1,3)\chi(3,2) \tag{3.119}$$

where $\chi(3,2)$ is the reducible polarizability (or response function) of the system. It can be related to the irreducible polarizability $P = \frac{\delta\rho}{\delta V}$ as

$$\chi(1,2) = \int d3\frac{\delta\rho(1)}{\delta V(3)}\frac{\delta V(3)}{\delta U(2)} = P(1,2) + \int d34P(1,3)v(3,4)\chi(4,2) \tag{3.120}$$

With the properties of the functional derivatives, we can express Σ in terms of V

$$\Sigma(1,2) = \Sigma_H(1,2) - i\int d345\ \ v(1^+,3)G_1(1,4)\frac{\delta G_1^{-1}(4,2)}{\delta V(5)}\epsilon^{-1}(5,3) \tag{3.121}$$

where we used that $\frac{\delta G}{\delta U} = -G\frac{\delta G^{-1}}{\delta U}G$.

We set

$$\Sigma_{xc}(1,2) = -i\int d345v(1^+,3)G_1(1,4)\frac{\delta G_1^{-1}(4,2)}{\delta V(5)}\epsilon^{-1}(5,3) \tag{3.122}$$

where Σ_{xc} is the exchange-correlation part of the self-energy, and we define the irreducible vertex function such that

$$\Gamma(1,2,3) = -\frac{\delta G_1^{-1}(1,2)}{\delta V(3)} = \delta(1,3)\delta(2,3) + \frac{\delta \Sigma_{xc}(1,2)}{\delta V(3)} \tag{3.123}$$

where we used $G^{-1} = G_0^{-1} - V - \Sigma_{xc}$.

Using the chain rule $\frac{\delta \Sigma}{\delta V} = \frac{\delta \Sigma}{\delta G}\frac{\delta G}{\delta V}$ and again $\frac{\delta G}{\delta V} = -G\frac{\delta G^{-1}}{\delta V}G$, we arrive at

$$\Gamma(1,2,3) = \delta(1,3)\delta(2,3) + \int d4567 \frac{\delta \Sigma_{xc}(1,2)}{\delta G_1(4,5)} G_1(4,6)G_1(7,5)\Gamma(6,7,3) \tag{3.124}$$

We can relate also the irreducible polarizability to the vertex function by

$$P(1,2) = -i\frac{\delta G_1(1,1^+)}{\delta V(2)} = i\int d34 G_1(1,3)\frac{\delta G_1^{-1}(3,4)}{\delta V(2)} G_1(4,1^+) = -i\int d34 G_1(1,3)G_1(4,1)\Gamma(3,4,2) \tag{3.125}$$

At last, we introduce the dynamically screened Coulomb interaction W

$$\begin{aligned} W(1,2) &= \int d3 \epsilon^{-1}(1,3)v(3,2) \\ &= v(1,2) + \int d34 v(1,3)\chi(3,4)v(4,2) \\ &= v(1,2) + \int d34 v(1,3)P(3,4)W(4,2) \end{aligned} \tag{3.126}$$

where in the last line we used the relations $\chi = [1 - vP]^{-1}P$ and $[1 - vP]^{-1}v = W$.

W describes the fact that when a particle interacts with another one in a medium since the two particles are not alone, the Coulomb interaction between them is not the bare Coulomb interaction but a screened Coulomb interaction and the screening comes from the interaction with the rest of the system.

With these expressions, the self-energy can be written as

$$\Sigma(1,2) = \Sigma_H(1,2) + i\int d34 G_1(1,4)W(1^+,3)\Gamma(4,2,3) \tag{3.127}$$

The equations (3.113), (3.124), (3.125), (3.126) and (3.127) form a set of coupled equations called Hedin's equations [41] and can be schematically represented as the pentagon in Fig.1.2.

In this pentagon, we chose as input the non-interacting 1-GF, but in standard calculations, one usually uses a mean-field Green's function such as the Hartree-Fock Green's function G^{HF} or the Kohn-Sham Green's function G^{KS}. From this starting point, we should then calculate the vertex, the polarizability, the screened interaction, the self-energy, and iterate self-consistently until convergence is reached. In practice we rarely perform the full self-consistent procedure, we do only one cycle over the pentagon called a "one-shot" or we introduce some partial self-consistency by updating, for example, the energy poles of the 1-GF.

3.2.4 Approximations of the self-energy

In practice, we need approximations to the self-energy. In the following, we discuss some of these approximations.

GW approximation

By setting $\Gamma = 1$ in Hedin's equations we obtain the *GW* approximation. Within this approximation, the exchange-correlation part of the self-energy is written as

$$\Sigma_{xc}^{GW} = iGW \tag{3.128}$$

where W is built from the RPA polarizability

$$P(1,2) \approx -iG_1(1,2^+)G_1(2,1^+) \tag{3.129}$$

which describes the independent propagation of electron-hole pairs in a medium. The RPA irreducible polarizability is represented by bubble diagrams and the reducible polarizability

$$\chi(1,2) = P(1,2) + \int d34 P(1,3)v(3,4)\chi(4,2) \tag{3.130}$$

This produces an infinite summation of this particular diagram.

If we want to resum other types of diagrams and put the various approximations on an equal footing, it is convenient to express the self-energy as a generalized potential. To do so, we rewrite (3.110) as

$$\begin{aligned}\Sigma(1,2) &= \Sigma_H(1,2) + i\int d34\ \ v(1^+,3)\frac{\delta G_1(1,4)}{\delta U(3)}G_1^{-1}(4,2) \\ &= \Sigma_H(1,2) + iv(1,2^+)G_1(1,2) + i\int d2'345\ \ v(1,2'^+)G_1(1,3)\frac{\delta\Sigma(3,2)}{\delta G_1(4,5)}\frac{\delta G_1(4,5)}{\delta U(2')}\Big|_{U=0} \\ &= \Sigma_H(1,2) + iv(1,2^+)G_1(1,2) + i\int d2'345\ \ v(1,2'^+)G_1(1,3)\Xi(3,5,2,4)L(4,2',5,2'^+)\end{aligned} \tag{3.131}$$

where $\Xi(3,5,2,4) = \frac{\delta\Sigma(3,2)}{\delta G_1(4,5)}$ is called the kernel and $L(4,2',5,2'^+) = \frac{\delta G_1(4,5)}{\delta U(2',2')}$ is a generalised response function.

The last expression describes the following physical effects: the Hartree term Σ_H is the interaction of a particle with the density of the system, the term $\Sigma_x(1,2) = iv(1,2^+)G_1(1,2)$ exchanges two particles with the same spin, the last term (Σ_c) is the correlation one and can be seen as generalized induced non-local potential, caused by the propagation of a particle.

If in the kernel we approximate the self-energy as the Hartree term

$$\Xi(3,5,2,4) = \frac{\delta\Sigma(3,2)}{\delta G_1(4,5)} \approx \frac{\delta\Sigma_H(3,2)}{\delta G_1(4,5)} = -iv(3,4^+)\delta(4^+,5)\delta(3,2) \tag{3.132}$$

we obtain

$$\begin{aligned}\Sigma(1,2) &= \Sigma_H(1,2) + iv(1,2^+)G_1(1,2) + i\int d2'345\ \ v(1,2'^+)G_1(1,3)\Xi(3,5,2,4)L(4,2',5,2'^+) \\ &\approx \Sigma_H(12) + iv(12^+)G_1(12) + i\int d2'345 v(12'^+)G(13)\left[-iv(34^+)\delta(4^+5)\delta(32)L(42'4^+2'^+)\right] \\ &= \Sigma_H(1,2) + iv(1,2^+)G_1(1,2) + i\int d2'4 v(2,4^+)\chi(4,2')v(2'^+,1)G(1,2) \\ &= \Sigma_H(1,2) + iG_1(1,2)\left[\underbrace{v(1,2^+) + \int d2'4 v(1,2'^+)\chi(2',4)v(4^+,2)}_{W(1,2^+)}\right]\end{aligned} \tag{3.133}$$

where $\chi(1,2) = -iL(1,2,1^+,2^+)$, which is the *GW* form of the self-energy. Note that here χ is not necessarily the RPA response function but could also include vertex correction.

GT approximation

Another class of diagrams that we could consider is the ladder diagrams. To get them, in the first line of (7.58) we do the following approximation

$$L(4,2',5,2'^{+}) \approx G_1(4,2'^{+})G_1(2',5) \tag{3.134}$$

This gives

$$\Sigma(1,2) = \Sigma_H(1,2) + \Sigma_x(1,2) + i\int d2'345\ \ v(1,2'^{+})G_1(1,3)\frac{\delta\Sigma(3,1')}{\delta G_1(4,5)}G_1(4,2')G_1(2',5) \tag{3.135}$$

From this expression, we define the T-matrix operator T [42, 34] as a four point quantity such as [43, 44, 45, 46, 47, 48, 49, 50, 51, 52, 53, 54, 42, 55, 56, 57, 58, 59, 60]

$$\Sigma^{GT}(1,2) = \int d2'4 G_1(4,2')T(1,2',2,4) \tag{3.136}$$

When we derive the self-energy with respect to G_1, we get $\frac{\delta\Sigma}{\delta G_1} = \frac{\delta G_1}{\delta G_1}T + G_1\frac{\delta T}{\delta G_1}$, but we will neglect the derivative of T with respect to G_1 because this term gives terms of second order in T. This yields

$$\frac{\delta\Sigma}{\delta G_1} \approx T \tag{3.137}$$

in (3.135). The definition (3.136) gives respectively the particle-particle (pp) T-matrix T^{pp} and the electron-hole (eh) T-matrix $\overline{T}^{eh}$

$$T_1^{pp}(1,2,1',2') = -iv(12)\delta(11')\delta(22') + iv(12)\int d35 G(13)G(25)T_1^{pp}(3,5,1',2') \tag{3.138}$$

$$T_2^{pp}(1,2,1',2') = iv(12)\delta(21')\delta(12') + iv(12)\int d35 G_1(13)G_1(25)T_2^{pp}(3,5,1',2') \tag{3.139}$$

$$\overline{T}_1^{eh}(121'2') = -iv(1'2')\delta(11')\delta(22') + iv(12')\int d35 G_1(13)G_1(52')\overline{T}_1^{eh}(321'5) \tag{3.140}$$

$$\overline{T}_2^{eh}(121'2') = -iv(1'2')\delta(21')\delta(12') + iv(12')\int d35 G_1(13)G_1(52')\overline{T}_2^{eh}(321'5) \tag{3.141}$$

where T_1 is the direct term, T_2 is the exchange term, and T is written as

$$T = T_1 + T_2 \tag{3.142}$$

Spin structure of W

The screened Coulomb interaction is written in terms of the irreducible polarizability

$$W(\mathbf{r}_1,\mathbf{r}_2) = v_c(\mathbf{r}_1,\mathbf{r}_2) + \int d\mathbf{r}_3 d\mathbf{r}_4 v_c(\mathbf{r}_1,\mathbf{r}_3)P(\mathbf{r}_3,\mathbf{r}_4)W(\mathbf{r}_4,\mathbf{r}_2) \tag{3.143}$$

where we have omitted time arguments for simplicity and v_c is the bare Coulomb potential which is independent of the spin. Furthermore, when the GW approximation is used with the RPA form for the polarizability, this last one reduces to

$$P(\mathbf{r}_3,\mathbf{r}_4) \approx P_0(\mathbf{r}_3,\mathbf{r}_4) = -i\sum_{\sigma} G_\sigma(\mathbf{r}_3,\mathbf{r}_4)G_\sigma(\mathbf{r}_4,\mathbf{r}_3) \tag{3.144}$$

where we used the fact that the 1-GF is spin diagonal (because the Hamiltonian of the system is spin independent).

Therefore W does not depend on the spin, and the GW self-energy

$$\Sigma^{GW}_{xc,\sigma} = iG_\sigma W \tag{3.145}$$

is spin diagonal and its spin components are the ones of G_σ

Spin structure of T

The particle-particle and electron-hole T-matrix have the same spin structure [42, 34] with

$$T_{1,\sigma_1\sigma_2\sigma_1\sigma_2} = -v_c + iv_c G_{\sigma_1} G_{\sigma_2} T_{1,\sigma_1\sigma_2\sigma_1\sigma_2} \tag{3.146}$$

and

$$T_{2,\sigma_1\sigma_2\sigma_1\sigma_2} = v_c\delta_{\sigma_1\sigma_2} + iv_c G_{\sigma_1} G_{\sigma_2} T_{2,\sigma_1\sigma_2\sigma_1\sigma_2} \tag{3.147}$$

In both cases, the polarizability is a four-point quantity. So, with the approximation that the Green's function is spin diagonal, we have one spin for each Green's function. Therefore, the T-matrix is spin-dependent. When we sum T_1 and T_2, we keep the terms of opposite spins and so we have the same for the self-energy

$$\Sigma^{GT}_{\sigma_1} = \sum_{\bar{\sigma}_2} iG_{\bar{\sigma}_2} T_{\sigma_1\bar{\sigma}_2\sigma_1\bar{\sigma}_2} \tag{3.148}$$

Dyson equation in practice

With the self-energy Σ we introduce a shift in the particle energies such that

$$\omega = \varepsilon + \Sigma(\omega) \tag{3.149}$$

This turns the eigenvalue equation into a non-linear eigenvalue problem. It is due to the fact that when we add a particle (electron or hole) to the system we can obtain additional excitations called satellites which correspond to excited states of the $(N+1)$ or $(N-1)$-body system. In practical calculation to simplify this problem one can assume that at the quasiparticle resonance, the imaginary part of Σ is "small", so

$$\omega = \varepsilon + \mathrm{Re}[\Sigma(\omega)] \tag{3.150}$$

Furthermore one can show that the real part of Σ is linear close to the Fermi energy, so that one can do a Taylor expansion around ε to linear order as

$$\mathrm{Re}[\Sigma(\omega)] \approx \mathrm{Re}[\Sigma(\varepsilon)] + (\omega - \varepsilon)\frac{\partial\,\mathrm{Re}[\Sigma(\omega)]}{\partial\omega}\Big|_{\omega=\varepsilon} \tag{3.151}$$

We define the renormalization factor Z

$$Z = \frac{1}{1 - \frac{\partial\,\mathrm{Re}[\Sigma(\omega)]}{\partial\omega}\Big|_{\omega=\varepsilon}} \tag{3.152}$$

To rewrite the quasiparticle energies in the linear approximation as

$$\varepsilon^{QP} = \varepsilon + Z\Sigma(\omega = \varepsilon) \tag{3.153}$$

With perturbation theory we calculate the quasiparticle energies, which are related to electron addition and removal. We notice that the difference of these quasiparticle energies will not directly corresponds to the neutral excitations of the system because in the dressing, the interaction between the electron and the hole is not included. To add this interaction we will derive a two-body Dyson equation called the Bethe-Salpeter equation for the two-body Green's function. This is reported in Sec. 3.3.

3.2.5 Random Phase Approximation equations

In the previous section, we have introduced the Random Phase Approximation (RPA) in the context of the GW approximation. As we will see in Chapter 5 one can introduce RPA-like equations in the case of the particle-particle and electron-hole T matrix. In the following, we hence give a brief introduction to the original formulation of the RPA equations for the electron-hole (linked to GW) and particle-particle (linked to the pp T matrix) channels of the reducible polarizability χ[61, 62]. Note that for the eh T matrix the corresponding RPA-like equations, to the best of our knowledge, are not known. We will give their derivation in Chapter 5.

Tamm-Dancoff approximation

We will first introduce the well-known Tamm-Dancoff approximation in the electron-hole channel.

We start by doing a variational process similar to what we did previously, but with two differences. The quantities are expressed with the second quantization formalism and the variational process is not made on the Hartree-Fock ground state but rather on the deviation of the system with respect to the Hartree-Fock ground state.

We write an electron-hole pair built on the Hartree-Fock ground state as

$$|ai\rangle = \hat{a}_a^\dagger \hat{a}_i \, |\Psi_0\rangle \tag{3.154}$$

We study the variational problem

$$\delta \, \langle \Psi | \hat{H} | \Psi \rangle = 0 \tag{3.155}$$

where Ψ is a normalized wave function of the form

$$|\Psi\rangle = \sum_{ai} c_{ai} \, |ai\rangle = \sum_{ai} c_{ai} \hat{a}_a^\dagger \hat{a}_i \, |\Psi_0\rangle \tag{3.156}$$

and the general two-body Hamiltonian is

$$\hat{H} = \sum_{pq} t_{pq} \hat{a}_p^\dagger \hat{a}_q + \frac{1}{2} \sum_{pqrs} v_{pqrs} \hat{a}_p^\dagger \hat{a}_q^\dagger \hat{a}_s \hat{a}_r - \langle \Psi_0 | \hat{H} | \Psi_0 \rangle \tag{3.157}$$

where we removed the Hartree-Fock ground state energy to keep only excitation energies.

We do the following variation

$$\delta \Big(\langle \Psi | \hat{H} | \Psi \rangle - E \, \langle \Psi | \Psi \rangle = 0 \Big) \tag{3.158}$$

The variation in (3.158) can be carried out either with respect to $|\Psi\rangle$ or $\langle\Psi|$, since they correspond to two different degrees of freedom, like a number and its complex conjugate. Varying $\langle\Psi|$ yields

$$\Big(\langle \delta\Psi | \hat{H} | \Psi \rangle - E \, \langle \delta\Psi | \Psi \rangle = 0 \Big) \tag{3.159}$$

Varying with respect to c_{ai}^ν leads to

$$\sum_{bj} \left(\langle \Psi_0 | \hat{a}_i^\dagger \hat{a}_a \hat{H} \hat{a}_b^\dagger \hat{a}_j | \Psi_0 \rangle - E_\nu \underbrace{\langle \Psi_0 | \hat{a}_i^\dagger \hat{a}_a \hat{a}_b^\dagger \hat{a}_j | \Psi_0 \rangle}_{=\delta_{ij}\delta_{ab}} \right) c_{bj}^\nu = 0 \tag{3.160}$$

The first term gives for the diagonal part

$$\begin{aligned}\langle\Psi_0|\hat{a}_i^\dagger\hat{a}_a\hat{H}\hat{a}_a^\dagger\hat{a}_i|\Psi_0\rangle &= t_{aa} - t_{ii} + \sum_j \left(\langle aj||aj\rangle - \langle ij||ij\rangle\right) + \langle ai||ia\rangle \\ &= \varepsilon_a - \varepsilon_i + \langle ai||ia\rangle\end{aligned} \tag{3.161}$$

with

$$\varepsilon_k\delta_{kk'} = t_{kk'} + \sum_j \langle kj||k'j\rangle \tag{3.162}$$

The off-diagonal elements are

$$\langle\Psi_0|\hat{a}_i^\dagger\hat{a}_a\hat{H}\hat{a}_b^\dagger\hat{a}_j|\Psi_0\rangle = \langle aj||ib\rangle \tag{3.163}$$

As a result, we obtain what we call the Tamm-Dancoff equations

$$\sum_{bj}\left[(\varepsilon_a - \varepsilon_i)\delta_{ij}\delta_{ab} + \langle aj||ib\rangle\right]c_{bj}^\nu = E_\nu c_{ai}^\nu \tag{3.164}$$

To see how the collective excitations emerge from this equation, we make the assumption that the Coulomb potential is separable, that is,

$$\langle aj||ib\rangle = \overline{v}_{ajib} = \lambda D_{(ai)}D_{(jb)} \tag{3.165}$$

We get

$$c_{ai}^\nu = \frac{D_{(ai)}}{E_\nu - (\varepsilon_a - \varepsilon_i)}\lambda\sum_{bj} D_{(bj)}c_{bj}^\nu \tag{3.166}$$

then

$$\sum_{(ai)} D_{(ai)}c_{ai}^\nu = \sum_{(ai)}\frac{D_{(ai)}^2}{E_\nu - (\varepsilon_a - \varepsilon_i)}\lambda\sum_{bj} D_{(bj)}c_{bj}^\nu \tag{3.167}$$

which gives

$$\sum_{(ai)}\frac{D_{(ai)}^2}{E_\nu - (\varepsilon_a - \varepsilon_i)} = \frac{1}{\lambda} \tag{3.168}$$

The collective excitations occur at the electron-hole excitations, if we suppose these excitations to be degenerate and we set $\varepsilon = \varepsilon_a - \varepsilon_i$, we have

$$E = \varepsilon + \lambda\sum_{(ai)} D_{(ai)}^2 \tag{3.169}$$

In (3.166), the sum is a constant, so we can set

$$c_{ai}^\nu = \frac{D_{(ai)}}{E_\nu - (\varepsilon_a - \varepsilon_i)}N \tag{3.170}$$

with $N = \lambda\sum_{bj} D_{(bj)}c_{bj}^\nu$

We multiply by the complex conjugate $c_{ai}^{\nu*}$ and we use the fact that

$$\sum_{ai} c_{ai}^{\nu*}c_{ai}^{\nu'} = \delta_{\nu\nu'} \tag{3.171}$$

we find

$$\frac{1}{N^2} = \sum_{(ai)} \frac{\left|D_{(ai)}\right|^2}{E_\nu - (\varepsilon_a - \varepsilon_i)} \tag{3.172}$$

which gives the coefficients (with the approximation of degenerate levels)

$$c_{ai} = \frac{D_{(ai)}}{\sqrt{\sum_{(bj)} D^2_{(bj)}}} \tag{3.173}$$

This shows that the collective excited state is a coherent excitation of single particles.

Another way to derive (3.164) is by looking for the collective state $|\nu\rangle$ which solves the Schrödinger equation

$$\hat{H}\,|\nu\rangle = E_\nu\,|\nu\rangle \tag{3.174}$$

We define the operator $\hat{\mathcal{Q}}^\dagger_\nu$ such that

$$\hat{\mathcal{Q}}^\dagger_\nu\,|0\rangle = |\nu\rangle \qquad\qquad \hat{\mathcal{Q}}_\nu\,|0\rangle = 0 \tag{3.175}$$

where $|0\rangle$ is the vacuum. The variational equation becomes

$$\delta\,\langle\nu|\hat{H} - E_\nu|\nu\rangle = \delta\,\langle 0|\hat{\mathcal{Q}}_\nu \hat{H}\hat{\mathcal{Q}}^\dagger_\nu - E_\nu \hat{\mathcal{Q}}_\nu \hat{\mathcal{Q}}^\dagger_\nu|0\rangle = 0 \tag{3.176}$$

A variation of $\mathcal{Q}_\nu$ leads to

$$\langle 0|\delta\hat{\mathcal{Q}}_\nu \hat{H}\hat{\mathcal{Q}}^\dagger_\nu|0\rangle = E_\nu\,\langle 0|\delta\hat{\mathcal{Q}}_\nu \hat{\mathcal{Q}}^\dagger_\nu|0\rangle \tag{3.177}$$

We use the fact that

$$\hat{H}\hat{\mathcal{Q}}^\dagger_\nu\,|0\rangle = [\hat{H}, \hat{\mathcal{Q}}^\dagger_\nu]\,|0\rangle + E_0\hat{\mathcal{Q}}^\dagger_\nu\,|0\rangle \tag{3.178}$$

to rewrite (3.177)

$$\langle 0|\delta\hat{\mathcal{Q}}_\nu[\hat{H}, \hat{\mathcal{Q}}^\dagger_\nu]|0\rangle = (E_\nu - E_0)\,\langle 0|\delta\hat{\mathcal{Q}}_\nu \hat{\mathcal{Q}}^\dagger_\nu|0\rangle \tag{3.179}$$

At last, we write (3.179) in terms of commutators

$$\langle 0|\Big[\delta\hat{\mathcal{Q}}_\nu, [\hat{H}, \hat{\mathcal{Q}}^\dagger_\nu]\Big]|0\rangle = (E_\nu - E_0)\,\langle 0|[\delta\hat{\mathcal{Q}}_\nu, \hat{\mathcal{Q}}^\dagger_\nu]|0\rangle \tag{3.180}$$

This can be proven using

$$\langle 0|\,\hat{\mathcal{Q}}^\dagger_\nu = \langle 0|\,\hat{H}\hat{\mathcal{Q}}^\dagger_\nu = 0 \tag{3.181}$$

We define the operator $\hat{\mathcal{Q}}^\dagger_\nu$ as

$$\hat{\mathcal{Q}}^\dagger_\nu = \sum_{ai} c^\nu_{ai}\hat{a}^\dagger_a\hat{a}_i \tag{3.182}$$

This operator annihilates a particle below the Fermi level and creates a particle above the Fermi level. We define also the variation

$$\delta\hat{\mathcal{Q}}_\nu = \sum_{ai} \delta c^{\nu*}_{ai}\hat{a}^\dagger_i\hat{a}_a \tag{3.183}$$

With these definitions, we obtain

$$\sum_{ai}\delta c^{\nu*}_{ai}\sum_{bj}\,\langle\Psi_0|\hat{a}^\dagger_i\hat{a}_a(\hat{H} - E_\nu)\hat{a}^\dagger_b\hat{a}_j|\Psi_0\rangle\,c^\nu_{bj} = 0 \tag{3.184}$$

which is identical to (3.160).

In this procedure, we did some assumptions. As we saw in the full CI formalism, to get the solution of the Schrödinger equation by the variation of the coefficients of the wave function, this later should have the following general form

$$|0\rangle = c_0^0 |\Psi_0\rangle + \sum_{ai} c_{ai}^0 \hat{a}_a^\dagger \hat{a}_i |\Psi_0\rangle + \frac{1}{4} \sum_{abij} c_{ab,ij}^0 \hat{a}_a^\dagger \hat{a}_b^\dagger \hat{a}_i \hat{a}_j |\Psi_0\rangle + \dots \tag{3.185}$$

$$|\nu\rangle = c_0^\nu |\Psi_0\rangle + \sum_{ai} c_{ai}^\nu \hat{a}_a^\dagger \hat{a}_i |\Psi_0\rangle + \frac{1}{4} \sum_{abij} c_{ab,ij}^\nu \hat{a}_a^\dagger \hat{a}_b^\dagger \hat{a}_i \hat{a}_j |\Psi_0\rangle + \dots \tag{3.186}$$

but we suppose that the contribution of single excitations is dominant, so we restrict ourselves to the subset of 1 particle-1 hole and we write

$$|\nu\rangle \approx \sum_{ai} c_{ai}^\nu \hat{a}_a^\dagger \hat{a}_i |\Psi_0\rangle \tag{3.187}$$

Then we have an issue as we build correlations only for the excited states and we do not take into consideration the fact that correlations can also modify the ground state.

Electron-hole RPA with ground state correlations

Therefore we need a new ground state $|\text{RPA}\rangle$, on which we can built single excitations with electron-hole pairs $\hat{a}_a^\dagger \hat{a}_i$ and, which can be modified with electron-hole de-excitations $\hat{a}_i^\dagger \hat{a}_a$. The operator which generates collective states is then written as

$$\hat{\mathcal{Q}}_\nu^\dagger = \sum_{ai} X_{ai,\nu}^N \hat{a}_a^\dagger \hat{a}_i - \sum_{ai} Y_{ai,\nu}^N \hat{a}_i^\dagger \hat{a}_a \tag{3.188}$$

This operator and the new ground state verify the condition

$$\hat{\mathcal{Q}}_\nu |\text{RPA}\rangle = 0 \tag{3.189}$$

The variation of the operator implies a variation of the coefficients $X_{ai,\nu}^N$ or $Y_{ai,\nu}^N$. This gives the two following equations

$$\langle \text{RPA} | \left[\hat{a}_i^\dagger \hat{a}_a, [\hat{H}, \hat{\mathcal{Q}}_\nu^\dagger] \right] | \text{RPA} \rangle = (E_\nu - E_0) \langle \text{RPA} | [\hat{a}_i^\dagger \hat{a}_a, \hat{\mathcal{Q}}_\nu^\dagger] | \text{RPA} \rangle \tag{3.190}$$

$$\langle \text{RPA} | \left[\hat{a}_a^\dagger \hat{a}_i, [\hat{H}, \hat{\mathcal{Q}}_\nu^\dagger] \right] | \text{RPA} \rangle = (E_\nu - E_0) \langle \text{RPA} | [\hat{a}_a^\dagger \hat{a}_i, \hat{\mathcal{Q}}_\nu^\dagger] | \text{RPA} \rangle \tag{3.191}$$

To calculate the right-hand side, we use the commutation relation

$$[\hat{a}_i^\dagger \hat{a}_a, \hat{a}_b^\dagger \hat{a}_j] = \delta_{ab}\delta_{ij} - \delta_{ab} \hat{a}_j \hat{a}_i^\dagger - \delta_{ij} \hat{a}_b^\dagger \hat{a}_a \tag{3.192}$$

In the right-hand side of (3.192), the last term should be small when applied to the ground state, because there are no particles above the Fermi level. The second term is considered also to be small because we suppose for the same reason that there are no holes under the Fermi level. This leads to the following approximation

$$\begin{aligned} \langle \text{RPA} | [\hat{a}_i^\dagger \hat{a}_a, \hat{a}_b^\dagger \hat{a}_j] | \text{RPA} \rangle &= \delta_{ij}\delta_{ab} - \delta_{ab} \langle \text{RPA} | \hat{a}_j \hat{a}_i^\dagger | \text{RPA} \rangle - \delta_{ij} \langle \text{RPA} | \hat{a}_b^\dagger \hat{a}_a | \text{RPA} \rangle \\ &\approx \delta_{ij}\delta_{ab} \\ &= \langle \Psi_0 | [\hat{a}_i^\dagger \hat{a}_a, \hat{a}_b^\dagger \hat{a}_j] | \Psi_0 \rangle \end{aligned} \tag{3.193}$$

This has for consequences that the electron-hole creation operators behave as if they verify the boson commutation relation $[\hat{a}_i^\dagger \hat{a}_a, \hat{a}_b^\dagger \hat{a}_j] = \delta_{ij}\delta_{ab}$, but break the Pauli principle. This is known as the quasi-boson approximation. In this approximation, the square modulus of the amplitudes $X^N_{ai,\nu}$ and $Y^N_{ai,\nu}$ are the probabilities to find the states $\hat{a}_a^\dagger \hat{a}_i |0\rangle$ and $\hat{a}_i^\dagger \hat{a}_a |0\rangle$ in the excited state $|\nu\rangle$, which corresponds to the transition densities

$$\langle 0|\hat{a}_i^\dagger \hat{a}_a|\nu\rangle \approx \langle \Psi_0|[\hat{a}_i^\dagger \hat{a}_a, \hat{\mathcal{Q}}_\nu^\dagger]|\Psi_0\rangle = X^N_{ai,\nu} \tag{3.194}$$

$$\langle 0|\hat{a}_a^\dagger \hat{a}_i|\nu\rangle \approx \langle \Psi_0|[\hat{a}_a^\dagger \hat{a}_i, \hat{\mathcal{Q}}_\nu^\dagger]|\Psi_0\rangle = Y^N_{ai,\nu} \tag{3.195}$$

We evaluate the matrix elements and we set

$$\begin{aligned} A^{\text{eh}}_{ai,bj} &= \langle \Psi_0| \Big[\hat{a}_i^\dagger \hat{a}_a, [\hat{H}, \hat{a}_b^\dagger \hat{a}_j]\Big] |\Psi_0\rangle = (\varepsilon_a - \varepsilon_i)\delta_{ab}\delta_{ij} + \langle aj||ib\rangle \\ B^{\text{eh}}_{ai,bj} &= -\langle \Psi_0| \Big[\hat{a}_i^\dagger \hat{a}_a, [\hat{H}, \hat{a}_j^\dagger \hat{a}_b]\Big] |\Psi_0\rangle = \langle ab||ij\rangle \end{aligned} \tag{3.196}$$

The RPA equations become

$$\sum_{bj} \left(A^{\text{eh}}_{ai,bj} X^N_{bj,\nu} + B^{\text{eh}}_{ai,bj} Y^N_{bj,\nu}\right) = \Omega^N_\nu X^N_{ai,\nu} \tag{3.197}$$

$$\sum_{bj} \left(B^{\text{eh}*}_{ai,bj} X^N_{aj,\nu} + A^{\text{eh}*}_{ai,bj} Y^N_{bj,\nu}\right) = -\Omega^N_\nu Y^N_{ai,\nu} \tag{3.198}$$

where $\Omega_\nu = E_\nu - E_0$ is the excitation energy from the state $|0\rangle$ to the excited state $|\nu\rangle$. These equations can be written in the matrix form

$$\begin{pmatrix} \mathbf{A}^{\text{eh}} & \mathbf{B}^{\text{eh}} \\ -\mathbf{B}^{\text{eh}*} & -\mathbf{A}^{\text{eh}*} \end{pmatrix} \begin{pmatrix} \mathbf{X}^N_\nu \\ \mathbf{Y}^N_\nu \end{pmatrix} = \Omega^N_\nu \begin{pmatrix} \mathbf{X}^N_\nu \\ \mathbf{Y}^N_\nu \end{pmatrix} \tag{3.199}$$

The matrix $\mathbf{A}^{\text{eh}}$ is hermitian, the matrix $\mathbf{B}^{\text{eh}}$ is symmetric, they are of the same dimension and if we set $\mathbf{B}^{\text{eh}}$ to zero we retrieve the Tamm-Dancoff approximation. But the RPA matrix is not hermitian and the orthogonality on the excited states is not the usual one but rather

$$\langle \nu|\nu'\rangle = \delta_{\nu\nu'} = \langle \text{RPA}|[\hat{\mathcal{Q}}_\nu, \hat{\mathcal{Q}}_{\nu'}^\dagger]|\text{RPA}\rangle \approx \langle \Psi_0|[\hat{\mathcal{Q}}_\nu, \hat{\mathcal{Q}}_{\nu'}^\dagger]|\Psi_0\rangle \tag{3.200}$$

$$\delta_{\nu\nu'} = \sum_{ai} \left(X^{N*}_{ai,\nu} X^N_{ai,\nu'} - Y^{N*}_{ai,\nu} Y^N_{ai,\nu'}\right) \tag{3.201}$$

If we do the same approximation we did in (3.165) and we note $\mathcal{S}$ the sum

$$\mathcal{S} = \sum_{(bj)} D_{(bj)} X^N_{bj,\nu} + \sum_{(bj)} D_{(bj)} Y^N_{bj,\nu} \tag{3.202}$$

the eigenvectors can be expressed as

$$X^N_{ai,\nu} = \frac{\lambda \mathcal{S} D_{(ai)}}{\Omega_\nu - (\varepsilon_a - \varepsilon_i)} \tag{3.203}$$

and

$$Y^N_{ai,\nu} = \frac{\lambda \mathcal{S} D_{(ai)}}{-[\Omega_\nu - (\varepsilon_a - \varepsilon_i)]} \tag{3.204}$$

We retrieve the fact that collective excitations have their poles at the single particle excitations.

Particle-particle RPA

For the particle-particle RPA, we do an approach similar to the electron-hole excitations, but in this case, since the number of particles is not conserved, we have to do a variational process on the $(N+2)$-particle system and the $(N-2)$-particle system. We start with the $(N+2)$-particle system, which can be described in the Tamm-Dancoff approximation with

$$|N+2,\tau\rangle = \sum_{a<b} c_{ab}^{\tau} \hat{a}_a^\dagger \hat{a}_b^\dagger |\Psi_0\rangle \tag{3.205}$$

The restriction on the indices is there to prevent the removal of twice the same particle. To take into account the ground state correlations, we use an operator such as

$$\hat{\mathcal{Q}}_\tau^\dagger = \sum_{a<b} X_{ab,\tau}^{N+2} \hat{a}_a^\dagger \hat{a}_b^\dagger - \sum_{i<i} Y_{ij,\tau}^{N+2} \hat{a}_j^\dagger \hat{a}_i^\dagger \tag{3.206}$$

and

$$\hat{\mathcal{Q}}_\tau |\mathrm{RPA}\rangle = 0 \tag{3.207}$$

With these definitions, the same kind of derivations we did in the electron-hole case give for the amplitudes

$$X_{ab,\tau}^{N+2} = \langle 0|\hat{a}_b \hat{a}_a|N+2,\tau\rangle \tag{3.208}$$

$$Y_{ij,\tau}^{N+2} = \langle 0|\hat{a}_i \hat{a}_j|N+2,\tau\rangle \tag{3.209}$$

and leads to the following equations of motion

$$\sum_{a'<b'} A_{ab,a'b'}^{\mathrm{pp}} X_{a'b',\tau}^{N+2} - \sum_{i<j} B_{ab,ij}^{\mathrm{pp}} Y_{ij,\tau}^{N+2} = \Omega_\tau^{N+2} X_{ab,\tau}^{N+2} \tag{3.210}$$

$$\sum_{i'<j'} C_{ij,i'j'}^{\mathrm{pp}} Y_{i'j',\tau}^{N+2} - \sum_{a'<b'} B_{a'b',ij}^{\mathrm{pp}\dagger} X_{a'b',\tau}^{N+2} = -\Omega_\tau^{N+2} Y_{ij,\tau}^{N+2} \tag{3.211}$$

We obtain the same equations of motion for $(N-2)$-particle system with the following amplitudes

$$X_{ij,\lambda}^{N-2} = \langle N-2,\lambda|\hat{a}_j \hat{a}_i|0\rangle \tag{3.212}$$

$$Y_{ba,\lambda}^{N-2} = \langle N-2,\lambda|\hat{a}_a \hat{a}_b|0\rangle \tag{3.213}$$

This gives

$$\begin{pmatrix} \mathbf{A}^{\mathrm{pp}} & \mathbf{B}^{\mathrm{pp}} \\ -\mathbf{B}^{\mathrm{pp}\dagger} & -\mathbf{C}^{\mathrm{pp}} \end{pmatrix} \begin{pmatrix} \mathbf{X}_\nu^{N\pm2} \\ \mathbf{Y}_\nu^{N\pm2} \end{pmatrix} = \Omega_\nu^{N\pm2} \begin{pmatrix} \mathbf{X}_\nu^{N\pm2} \\ \mathbf{Y}_\nu^{N\pm2} \end{pmatrix} \tag{3.214}$$

where $\nu = \tau$ or $\nu = \lambda$ and

$$\begin{aligned} A_{ab,a'b'}^{\mathrm{pp}} &= (\varepsilon_a + \varepsilon_b)\delta_{aa'}\delta_{bb'} + \langle ab||a'b'\rangle \\ C_{ij,i'j'}^{\mathrm{pp}} &= -(\varepsilon_i + \varepsilon_j)\delta_{ii'}\delta_{jj'} + \langle ij||i'j'\rangle \\ B_{ab,ij}^{\mathrm{pp}} &= -\langle ab||ij\rangle \end{aligned} \tag{3.215}$$

Contrary to the previous matrix equation, the number of double additions and double removals are not related. Therefore the matrices $\mathbf{A}^{\mathrm{pp}}$ and $\mathbf{C}^{\mathrm{pp}}$ do not have the same dimension but they are still square matrices, and $\mathbf{B}^{\mathrm{pp}}$ is a rectangular matrix. The eigenvectors are normalized as in (3.201). From the equation of motion, we derived the electron-hole RPA and the particle-particle RPA. These will allow us to calculate the quasi-particle energies in the GW approximation and the particle-particle T-matrix T^{pp} but not in the electron-hole T-matrix $\overline{T}^{eh}$. To do so we will see another way to derive the RPA matrix equation of the system directly from the polarizability χ associated with the resummation of the particular class of diagrams concerned.

Normalization conditions

To calculate the intensities of the collective excitations one needs to have the normalized eigenvectors. For particle-hole excitations, we have a particle-hole symmetry, the number of excitations and de-excitations are directly related and we have $\Omega^{eh} = -\Omega^{he}$, so we can use the same eigenvectors to calculate the intensities. The normalization condition is [61, 62, 63]

$$\boldsymbol{S} = \boldsymbol{X}^T\boldsymbol{X} - \boldsymbol{Y}^T\boldsymbol{Y} \tag{3.216}$$

and the new eigenvectors are

$$\tilde{\boldsymbol{X}} = \boldsymbol{X}\boldsymbol{S}^{-1/2} \tag{3.217a}$$

$$\tilde{\boldsymbol{Y}} = \boldsymbol{Y}\boldsymbol{S}^{-1/2} \tag{3.217b}$$

For particle-particle excitations, the double additions and double removals are not related, so we have to calculate and normalize the eigenvectors for both processes separately. We note $\boldsymbol{Z}^{N+2} = (\boldsymbol{X}^{N+2}, \boldsymbol{Y}^{N+2})$ the eigenvectors for double additions and $\boldsymbol{Z}^{N-2} = (\boldsymbol{X}^{N-2}, \boldsymbol{Y}^{N-2})$ the eigenvectors for double removals. We introduce the metric $\boldsymbol{\mathcal{W}}$ such that

$$\boldsymbol{\mathcal{W}} = \begin{pmatrix} \boldsymbol{I}_{N+2} & \boldsymbol{0} \\ \boldsymbol{0} & -\boldsymbol{I}_{N-2} \end{pmatrix} \tag{3.218}$$

where $\boldsymbol{I}_{N+2}$ and $\boldsymbol{I}_{N-2}$ are respectively identity matrices of the size of the number of double additions possible and the number of double removals possible. We set

$$\boldsymbol{S}^{N+2} = +\boldsymbol{Z}^{N+2}\boldsymbol{\mathcal{W}}\boldsymbol{Z}^{N+2} \tag{3.219a}$$

$$\boldsymbol{S}^{N-2} = -\boldsymbol{Z}^{N-2}\boldsymbol{\mathcal{W}}\boldsymbol{Z}^{N-2} \tag{3.219b}$$

and the normalized eigenvectors are

$$\tilde{\boldsymbol{Z}}^{N+2} = +\boldsymbol{Z}^{N+2}\boldsymbol{S}^{N+2,-1/2} = \begin{pmatrix} \tilde{\boldsymbol{X}}^{N+2} \\ \tilde{\boldsymbol{Y}}^{N+2} \end{pmatrix} \tag{3.220a}$$

$$\tilde{\boldsymbol{Z}}^{N-2} = -\boldsymbol{Z}^{N-2}\boldsymbol{S}^{N-2,-1/2} = \begin{pmatrix} \tilde{\boldsymbol{X}}^{N-2} \\ \tilde{\boldsymbol{Y}}^{N-2} \end{pmatrix} \tag{3.220b}$$

In the following, we drop the tilde symbol to lighten the notations but the eigenvectors are normalized.

3.2.6 Stability problems

The crossing of energy levels

In the description of excited states, we coupled excitations and de-excitations with an off-diagonal term in the RPA matrices. This modifies the eigenstates that we obtained from the Tamm-Dancoff approximation. If we take a Hamiltonian of the form [62]

$$\boldsymbol{H} = \begin{pmatrix} a - bt & d \\ d & a + bt \end{pmatrix} \tag{3.221}$$

where a and b are fixed and t varies, the energies obtained when the coupling term d is set to zero are

$$\varepsilon_1^0(t) = a - bt \tag{3.222}$$

and

$$\varepsilon_2^0(t) = a + bt \tag{3.223}$$

whereas with the coupling term, we get

$$\varepsilon_1(t) = a - \sqrt{(bt)^2 + d^2} \tag{3.224}$$

and

$$\varepsilon_2(t) = a + \sqrt{(bt)^2 + d^2} \tag{3.225}$$

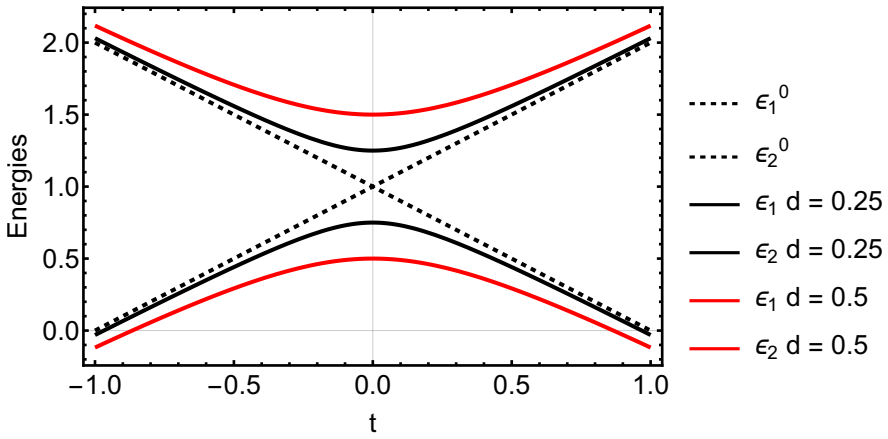

Figure 3.1 – Energies of the Hamiltonian H without coupling and with coupling

In Fig. 3.1, the dashed lines are the energies with $d = 0$, for the solid black lines $d = 0.25$ and for the red solid lines we have $d = 0.5$. The perturbed states tend to the unperturbed ones asymptotically far from the crossing and avoid each other near the crossing, and the more the coupling is important the more they avoid each other.

The critical value of the interaction strength λ

The polarizability χ in RPA is given by

$$\chi_{(pq)(rs)} = P_{(pq)(rs)} + \sum_{(ia)(jb)} P_{(pq)(ia)} v_{(ia)(jb)} \chi_{(jb)(rs)} \tag{3.226}$$

where, for the sake of notation convenience, we dropped the frequency dependence. We suppose the Coulomb potential separable [61] such that $v_{(ia)(jb)} = v_{ibaj} = \lambda D_{(ia)} D^*_{(jb)}$

$$\chi_{(pq)(rs)} = P_{(pq)(rs)} + \lambda \sum_{(ia)(jb)} P_{(pq)(ia)} D_{(ia)} D^*_{(jb)} \chi_{(jb)(rs)} \tag{3.227}$$

We multiply by $\sum_{(pq)} D^*_{(pq)}$ on the left and $\sum_{(rs)} D_{(rs)}$ on the right, we obtain

$$P_D = \tilde{P}_D + \lambda \tilde{P}_D P_D \tag{3.228}$$

where

$$P_D = \sum_{(pq)(rs)} D^*_{(pq)} \chi_{(pq)(rs)} D_{(rs)} \qquad \tilde{P}_D = \sum_{(pq)(rs)} D^*_{(pq)} P_{(pq)(rs)} D_{(rs)} \tag{3.229}$$

From (3.228) we get

$$P_D = \frac{\tilde{P}_D}{1 - \lambda \tilde{P}_D} \tag{3.230}$$

The poles of P_D gives the excitation energies Ω_ν. From $(1 - \lambda\tilde{P}_D) = 0$ we arrive at

$$\begin{aligned}\frac{1}{\lambda} = \tilde{P}_D &= \sum_{pqrs} D^*_{pq} P_{pqrs} D_{rs} \\ &= \sum_{pq} |D_{pq}|^2 \left[\frac{1}{\omega - (\varepsilon_q - \varepsilon_p) - i\eta} - \frac{1}{\omega + (\varepsilon_q - \varepsilon_p) + i\eta}\right] \\ &= \sum_{pq} |D_{pq}|^2 \frac{2\varepsilon_{qp}}{\omega^2 - \varepsilon^2_{qp}}\end{aligned} \tag{3.231}$$

where we used $P_{pqrs} = -iG_{pr}G_{qs}$. This gives the following relation dispersion (see Fig. 3.2)

$$\frac{1}{\lambda} = \tilde{P}_D(\Omega_\nu) = \sum_{pq} |D_{pq}|^2 \frac{2\varepsilon_{qp}}{\Omega^2_\nu - \varepsilon^2_{qp}} \tag{3.232}$$

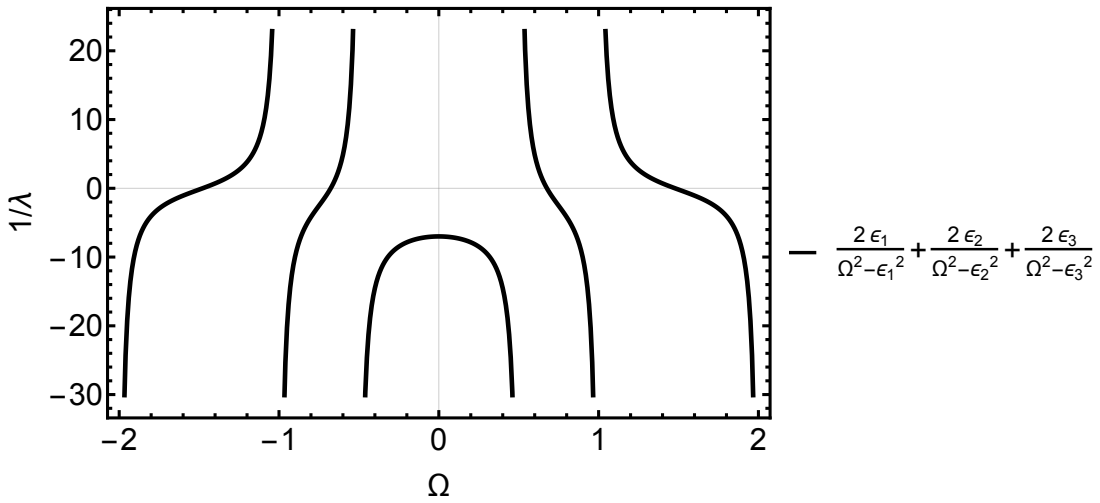

Figure 3.2 – Dispersion relation with, $\varepsilon_1 = 0.5$, $\varepsilon_2 = 0.1$ and $\varepsilon_3 = 2$

We observe on Fig.3.2 that when λ is under a critical value λ_{crit}, Ω becomes complex. To continue we suppose to have degenerate energies $\varepsilon_{qp} = \varepsilon$, from which

$$\Omega^{RPA}_\nu = \sqrt{\varepsilon^2 + 2\lambda\varepsilon \sum_{pq} |D_{pq}|^2} \tag{3.233}$$

In order that $\Omega^{RPA}_\nu > 0$, we should verify that $\lambda > \lambda_{crit}$ where

$$\lambda_{crit} = -\frac{\varepsilon}{2\sum_{pq} |D_{pq}|^2} \tag{3.234}$$

otherwise, the eigenvalues will become complex. For a fixed value of λ, the more λ is high, the more the TDA state and the RPA state are separated, as we can see in Fig. 3.3.

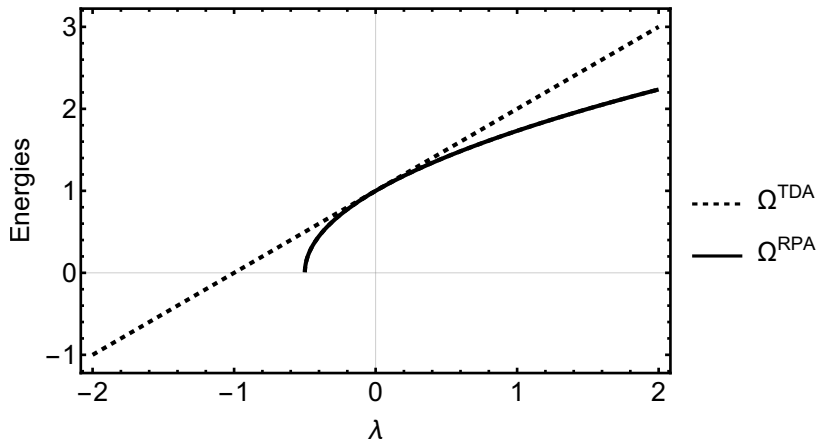

Figure 3.3 – Comparison of the collective excitations in TDA and RPA approximations

where the collective excitations in the Tamm-Dancoff approximation are given by

$$\Omega_{\nu}^{TDA} = \varepsilon + \lambda \sum_{pq} |D_{pq}|^2 \tag{3.235}$$

The poles of the two-body effective interaction

In this section, we show how to obtain the poles of a two-body effective interaction for the case of W. We write the integral equation projected in the one-particle site basis

$$W_{(rp)(qs)} = v_{(rp)(qs)} + \sum_{(bi)(ja)} v_{(rp)(bi)} P_{(bi)(ja)} W_{(ja)(qs)} \tag{3.236}$$

We suppose the potential separable as we did in the last section, we obtain

$$W_{(rp)(qs)} = \lambda D_{(rp)} D^*_{(qs)} + \sum_{(bi)(ja)} \lambda D_{(rp)} D^*_{(bi)} P_{(bi)(ja)} W_{(ja)(qs)} \tag{3.237}$$

Then we set

$$W_{(rp)(qs)} = D_{(rp)} B_{(qs)} \tag{3.238}$$

where

$$B_{(qs)} = \lambda D^*_{(qs)} + \lambda J B_{(qs)} \tag{3.239}$$

and

$$J = \sum_{(bi)(ja)} D^*_{(bi)} P_{(bi)(ja)} D_{(ja)} \tag{3.240}$$

We isolate $B_{(qs)}$ in (3.239) and we deduce an expression for W

$$W_{(rp)(qs)} = \frac{\lambda D_{(rp)} D^*_{(qs)}}{1 - \lambda J} \tag{3.241}$$

The poles of W are such that $J = 1/\lambda$, with a derivation similar to the previous one, we get

$$\sum_{(ij)} \left| D_{(ij)} \right|^2 \frac{2\varepsilon_{ij}}{\omega^2 - \varepsilon_{ij}^2} = \frac{1}{\lambda} \tag{3.242}$$

With the assumption that $\varepsilon_{ij} = \varepsilon$, we have

$$\omega = \sqrt{\varepsilon^2 + 2\lambda\varepsilon \sum_{(ij)} \left| D_{(ij)} \right|^2} \tag{3.243}$$

which are the poles of the response function.

3.3 The two-particle Green's function

The two-particle Green's function is a correlation function that allows us to study the correlation between an electron and a hole or two particles within a system that contains other particles. Its definition is [33, 40]

$$i^2 G_2\left(1,2;1',2'\right) = \left\langle \Psi_0^N \right| T[\hat{\psi}_H(1)\hat{\psi}(2)\hat{\psi}_H^\dagger\left(2'\right)\hat{\psi}_H^\dagger\left(1'\right)] \left| \Psi_0^N \right\rangle \tag{3.244}$$

It contains four field operators for which we have to choose the ordering in time such that this represents the correlations of the channel that we want to study. We have the following six possible orderings

$$\begin{aligned} G_2^{\mathrm{I}}\left(1,2;1',2'\right) &= (-i)^2 \left\langle \Psi_0^N \right| T[\hat{\psi}_H(1)\hat{\psi}_H^\dagger\left(1'\right)]T[\hat{\psi}_H(2)\hat{\psi}_H^\dagger\left(2'\right)] \left| \Psi_0^N \right\rangle \\ &\quad \cdot \Theta\left(\tau - \frac{1}{2}\left|\tau_1\right| - \frac{1}{2}\left|\tau_2\right|\right) \end{aligned} \tag{3.245a}$$

$$\begin{aligned} G_2^{\mathrm{II}}\left(1,2;1',2'\right) &= (-i)^2 \left\langle \Psi_0^N \right| T[\hat{\psi}_H(2)\hat{\psi}_H^\dagger\left(2'\right)]T[\hat{\psi}_H(1)\hat{\psi}_H^\dagger\left(1'\right)] \left| \Psi_0^N \right\rangle \\ &\quad \cdot \Theta\left(-\tau - \frac{1}{2}\left|\tau_1\right| - \frac{1}{2}\left|\tau_2\right|\right) \end{aligned} \tag{3.245b}$$

$$\begin{aligned} G_2^{\mathrm{III}}\left(1,2;1',2'\right) &= (-i)^2 \left\langle \Psi_0^N \right| T[\hat{\psi}_H(2)\hat{\psi}_H^\dagger\left(1'\right)]T[\hat{\psi}_H(1)\hat{\psi}_H^\dagger\left(2'\right)] \left| \Psi_0^N \right\rangle \\ &\quad \cdot \Theta\left(\frac{\tau_2}{2} - \frac{\tau_1}{2} - \frac{1}{2}\left|-\tau + \frac{\tau_1}{2} + \frac{\tau_2}{2}\right| - \frac{1}{2}\left|\tau + \frac{\tau_1}{2} + \frac{\tau_2}{2}\right|\right) \end{aligned} \tag{3.245c}$$

$$\begin{aligned} G_2^{\mathrm{IV}}\left(1,2;1',2'\right) &= (-i)^2 \left\langle \Psi_0^N \right| T[\hat{\psi}_H(1)\hat{\psi}_H^\dagger\left(2'\right)]T[\hat{\psi}_H(2)\hat{\psi}_H^\dagger\left(1'\right)] \left| \Psi_0^N \right\rangle \\ &\quad \cdot \Theta\left(\frac{\tau_1}{2} - \frac{\tau_2}{2} - \frac{1}{2}\left|-\tau + \frac{\tau_1}{2} + \frac{\tau_2}{2}\right| - \frac{1}{2}\left|\tau + \frac{\tau_1}{2} + \frac{\tau_2}{2}\right|\right) \end{aligned} \tag{3.245d}$$

$$\begin{aligned} G_2^{\mathrm{V}}\left(1,2;1',2'\right) &= (-i)^2 \left\langle \Psi_0^N \right| T[\hat{\psi}_H(1)\hat{\psi}_H\left(2\right)]T[\hat{\psi}_H^\dagger(2')\hat{\psi}_H^\dagger\left(1'\right)] \left| \Psi_0^N \right\rangle \\ &\quad \cdot \Theta\left(\frac{\tau_1}{2} + \frac{\tau_2}{2} - \frac{1}{2}\left|\tau + \frac{\tau_1}{2} - \frac{\tau_2}{2}\right| - \frac{1}{2}\left|\tau - \frac{\tau_1}{2} + \frac{\tau_2}{2}\right|\right) \end{aligned} \tag{3.245e}$$

$$\begin{aligned} G_2^{\mathrm{VI}}\left(1,2;1',2'\right) &= (-i)^2 \left\langle \Psi_0^N \right| T[\hat{\psi}_H^\dagger(2')\hat{\psi}_H^\dagger\left(1'\right)]T[\hat{\psi}_H(1)\hat{\psi}_H\left(2\right)] \left| \Psi_0^N \right\rangle \\ &\quad \cdot \Theta\left(-\frac{\tau_1}{2} - \frac{\tau_2}{2} - \frac{1}{2}\left|\tau + \frac{\tau_1}{2} - \frac{\tau_2}{2}\right| - \frac{1}{2}\left|\tau - \frac{\tau_1}{2} + \frac{\tau_2}{2}\right|\right) \end{aligned} \tag{3.245f}$$

where $\tau_1 = t_1 - t_{1'}$, $\tau_2 = t_2 - t_{2'}$, $\tau = t^1 - t^2$, $t^1 = \frac{t_1 + t_{1'}}{2}$ and $t^2 = \frac{t_2 + t_{2'}}{2}$

Here we focus on the electron-hole channel which corresponds to use the functions G_2^I and G_2^{II}, with the time ordering, respectively $t_1, t_{1'} > t_2, t_{2'}$ and $t_2, t_{2'} > t_1, t_{1'}$. We can write

$$G_2^I(1,2;1',2') = (-i)^2 \sum_n \chi_n(\mathbf{x}_1, \mathbf{x}_{1'}, \tau_1)\widetilde{\chi}_n(\mathbf{x}_2, \mathbf{x}_{2'}, \tau_2) e^{-i(E_n^N - E_0^N)\tau} \Theta\left(\tau - \frac{1}{2}|\tau_1| - \frac{1}{2}|\tau_2|\right) \tag{3.246}$$

and

$$G_2^{II}(1,2;1',2') = (-i)^2 \sum_n \widetilde{\chi}_n(\mathbf{x}_1, \mathbf{x}_{1'}, \tau_1)\chi_n(\mathbf{x}_2, \mathbf{x}_{2'}, \tau_2) e^{i(E_n^N - E_0^N)\tau} \Theta\left(-\tau - \frac{1}{2}|\tau_1| - \frac{1}{2}|\tau_2|\right) \tag{3.247}$$

with

$$\chi_n(1,1') = \left\langle \Psi_0^N \right| T[\hat{\psi}_H(\mathbf{x}_1)\hat{\psi}_H^\dagger\left(\mathbf{x}_{1'}\right)] \left| \Psi_n^N \right\rangle e^{-i\frac{(E_n^N - E_0^N)}{2}(t_1 + t_{1'})} \tag{3.248}$$

$$\widetilde{\chi}_n(2,2') = \left\langle \Psi_n^N \right| T[\hat{\psi}_H(\mathbf{x}_2)\hat{\psi}_H^\dagger\left(\mathbf{x}_{2'}\right)] \left| \Psi_0^N \right\rangle e^{i\frac{(E_n^N - E_0^N)}{2}(t_2 + t_{2'})} \tag{3.249}$$

The two-body Green's function in the electron-hole channel is

$$G_2^{eh}(1,2;1',2') = G_2^I(1,2;1',2') + G_2^{II}(1,2;1',2') \tag{3.250}$$

We now define the two-body correlation

$$L^{eh}(1,2;1',2') = -G_2^{eh}(1,2;1',2') + G_1(1,1')G_1(2,2') \tag{3.251}$$

The Fourier transform of L^{eh} with respect to τ is

$$L^{eh}(\mathbf{x}_1,\mathbf{x}_2,\mathbf{x}_{1'},\mathbf{x}_{2'};\tau_1,\tau_2,\omega) = \int \frac{d\omega}{2\pi}(L^I + L^{II})(\mathbf{x}_1,\mathbf{x}_2,\mathbf{x}_{1'},\mathbf{x}_{2'};\tau_1,\tau_2,\tau)e^{-i\omega\tau} \tag{3.252}$$

We obtain

$$\begin{aligned} L^{eh}(\tau_1,\tau_2,\omega) = & \\ & -i\lim_{\eta\to 0^+}\sum_{n\neq 0}\left[\frac{e^{\frac{i}{2}[\omega-(E_n^N-E_0^N)][|\tau_1|+|\tau_2|]}}{\omega-(E_n^N-E_0^N)+i\eta} - \frac{e^{-\frac{i}{2}[\omega+(E_n^N-E_0^N)][|\tau_1|+|\tau_2|]}}{\omega+(E_n^N-E_0^N)-i\eta}\right]\chi_n(\mathbf{x}_1,\mathbf{x}_{1'},\tau_1)\widetilde{\chi}_n(\mathbf{x}_2,\mathbf{x}_{2'},\tau_2) \end{aligned} \tag{3.253}$$

We take $\tau_1 \to 0^-$ and $\tau_2 \to 0^-$

$$\begin{aligned} L^{eh}(\omega) = & \\ & -i\lim_{\eta\to 0^+}\sum_{n\neq 0}\left[\frac{1}{\omega-(E_n^N-E_0^N)+i\eta} - \frac{1}{\omega+(E_n^N-E_0^N)-i\eta}\right]\chi_n(\mathbf{x}_1,\mathbf{x}_{1'})\widetilde{\chi}_n(\mathbf{x}_2,\mathbf{x}_{2'}) \end{aligned} \tag{3.254}$$

which is directly related to the response function $\chi(\omega) = -iL^{eh}(\omega)$.

This is the exact definition. We need however a practical equation to calculate L^{eh}. We can write a Dyson equation starting from (3.107). L^{eh} is then defined as

$$\begin{aligned} L^{eh}(1,2;1',2') &= -\int d34 G_1(1,3)\frac{\delta G_1^{-1}(3,4)}{\delta U(2',2)}G_1(4,1') \\ &= \int d34 G_1(1,3)\left[\delta(3,2')\delta(4,2)\delta(t_4-t_2)\frac{\delta\Sigma(3,4)}{\delta U(2',2)}\right]G_1(4,1') \\ &= G_1(1,2')G_1(2,1') + \int d3456 G_1(1,3)G_1(4,1')\frac{\delta\Sigma(3,4)}{\delta G_1(6,5)}L^{eh}(6,2;5,2') \end{aligned} \tag{3.255}$$

where the external potential U is supposed instantaneous, or for any variable t_2 and $t_{2'}$

$$L^{eh}(1,2;1',2') = L^0(1,2;1',2') + \int d3456 L^0(1,4;1',3)\Xi(3,5;4,6)L^{eh}(6,2;5,2') \tag{3.256}$$

where

$$L^0(1,2;1',2') = G_1(1,2')G_1(2,1') \tag{3.257}$$

This Dyson equation is called the Bethe-Salpeter equation (BSE) [64]. The first member of the right-hand side represents two bodies (the particle and the hole) propagating freely without interacting between them but each one interacting with the surrounding. The second member of the right-hand side is the homogeneous term, it represents the interaction of the two bodies.

3.3.1 The two-body free response

The Fourier transform of $L^0(1,2;1',2')$ is

$$L^0(\mathbf{x}_1,\mathbf{x}_2;\mathbf{x}_{1'},\mathbf{x}_{2'},\omega) = \int \frac{d\omega'}{2\pi} G_1(\mathbf{x}_1,\mathbf{x}_{2'},\omega'+\frac{\omega}{2}) G_1(\mathbf{x}_2,\mathbf{x}_{1'},\omega'-\frac{\omega}{2}) e^{i\omega'\eta} \tag{3.258}$$

We express the one-body Green's function in the quasiparticle approximation

$$G_1(\mathbf{x}_1,\mathbf{x}_2,\omega) = \sum_n \frac{\phi_n(\mathbf{x}_1)\phi_n^*(\mathbf{x}_2)}{\omega - \varepsilon_n^{QP} + i\eta\,\mathrm{sgn}(\varepsilon_n^{QP}-\mu)} \tag{3.259}$$

and we obtain

$$L^0(\mathbf{x}_1,\mathbf{x}_2;\mathbf{x}_{1'},\mathbf{x}_{2'},\omega) = i\sum_{nn'} \frac{(f_n - f_{n'})\phi_n(\mathbf{x}_1)\phi_n^*(\mathbf{x}_{2'})\phi_{n'}(\mathbf{x}_2)\phi_{n'}^*(\mathbf{x}_{1'})}{\varepsilon_n^{QP} - \varepsilon_{n'}^{QP} - \omega + i\eta\,\mathrm{sgn}(\varepsilon_{n'}^{QP} - \varepsilon_n^{QP})} \tag{3.260}$$

The poles of L^0 are at $\omega = \varepsilon_n^{QP} - \varepsilon_{n'}^{QP}$.

3.3.2 The two-body total response with a static kernel

In this section, we add to the independent propagation of the quasiparticle and the quasihole the interaction between them. To do so, we keep in the right-hand side of the Bethe-Salpeter equation, the homogeneous and nonhomogeneous terms. Its Fourier transform reads

$$L^{eh}(\omega,\omega',\omega'') = L^0(\omega,\omega',\omega'') + \int \frac{d\omega'''d\omega^{IV}}{(2\pi)^2} L^0(\omega,\omega',\omega''')\Xi(\omega,\omega''',\omega^{IV})L^{eh}(\omega,\omega^{IV},\omega'') \tag{3.261}$$

We can integrate only over ω' and ω'' because these variables are free. Then L^{eh} depends on ω on the left-hand side and of two frequencies ω and ω^{IV} on the right-hand side, therefore we cannot close the equation. To make the equation invertible, we enforce the static approximation of the kernel. We will consider it independent of the frequency $\Xi(\omega,\omega''',\omega^{IV}) \approx \Xi$ and we integrate over the last two frequencies. This gives

$$L^{eh}(\omega) = L^0(\omega) + L^0(\omega)\Xi L^{eh}(\omega) \tag{3.262}$$

In the one-particle orbital basis, the BSE reads

$$L^{eh}_{(pq)(rs)} = L^0_{(pq)(rs)} + \sum_{(ij)(kl)} L^0_{(pq)(ij)}\Xi_{(ij)(kl)}L^{eh}_{(kl)(rs)} \tag{3.263}$$

where

$$L^{eh}_{(pq)(rs)} = L^{eh}_{qrps} = \int dx_1 dx_2 dx_{1'} dx_{2'} L^{eh}(x_1,x_2,x_{1'},x_{2'})\phi_q^*(x_1)\phi_r^*(x_2)\phi_p(x_{1'})\phi_s(x_{2'}) \tag{3.264}$$

Using the same definition for L^0 and Ξ, we invert (3.263)

$$L^{eh-1}_{(pq)(rs)} = L^{0,-1}_{(pq)(rs)} - \Xi_{(pq)(rs)} \tag{3.265}$$

If we use the basis which diagonalizes L^0, we arrive at [65]

$$-iL^{eh}_{(pq)(rs)} = [(\varepsilon_n^{QP} - \varepsilon_{n'}^{QP} - \omega)\delta_{nm}\delta_{n'm'} + (f_{m'} - f_n)\Xi_{nn'm'm}]^{-1}_{(pq)(rs)}(f_s - f_r) \tag{3.266}$$

This can be written as a matrix eigenvalue equation

$$\begin{pmatrix} \boldsymbol{\mathcal{A}}^{\mathrm{eh}} & \boldsymbol{\mathcal{B}}^{\mathrm{eh}} \\ -\boldsymbol{\mathcal{B}}^{\mathrm{eh}} & -\boldsymbol{\mathcal{A}}^{\mathrm{eh}} \end{pmatrix} \begin{pmatrix} \boldsymbol{X}_n \\ \boldsymbol{Y}_n \end{pmatrix} = \omega_n \begin{pmatrix} \boldsymbol{X}_n \\ \boldsymbol{Y}_n \end{pmatrix} \tag{3.267}$$

where

$$\mathcal{A}^{\mathrm{eh}}_{ia,jb} = (\varepsilon^{QP}_a - \varepsilon^{QP}_i)\delta_{ij}\delta_{ab} + \Xi_{ibaj} \tag{3.268a}$$

$$\mathcal{B}^{\mathrm{eh}}_{ia,jb} = \Xi_{ijab} \tag{3.268b}$$

with i, j and a, b running over occupied and unoccupied orbitals, respectively.

The structure is similar to the RPA matrix equation that we use to build the GW self-energy but the quantities are different. The kernel Ξ goes beyond RPA since it contains the exchange and correlation effects. This is also a non-Hermitian eigenvalue problem, so the eigenvalues can become complex.

Chapter 4

Exploring new approximations to the Bethe-Salpeter kernel using the asymmetric Hubbard dimer

This chapter is an extended version of the following publication: R. Orlando, P. Romaniello, and P. F. Loos, *Adv. Quantum Chem.* **88** (2023) 183-211.

4.1 The Hamiltonian of the Hubbard dimer

The Hamiltonian of the asymmetric Hubbard dimer is

$$\hat{H} = -t \sum_{\sigma=\uparrow,\downarrow} \left(\hat{a}_{1\sigma}^{\dagger} \hat{a}_{2\sigma} + \hat{a}_{2\sigma}^{\dagger} \hat{a}_{1\sigma} \right) + U \sum_{i=1}^{2} \hat{n}_{i\uparrow} \hat{n}_{i\downarrow} + \Delta v \frac{\hat{n}_2 - \hat{n}_1}{2} \tag{4.1}$$

where $t > 0$ is the hopping parameter, $U \geq 0$ is the local Coulomb interaction, $\hat{n}_{i\sigma} = \hat{a}_{i\sigma}^{\dagger} \hat{a}_{i\sigma}$ is the spin density operator on site i, $\hat{n}_i = \hat{n}_{i\uparrow} + \hat{n}_{i\downarrow}$ is the density operator on site i, and $\Delta v = v_1 - v_2$ (with $v_1 > v_2$ and $v_1 + v_2 = 0$) is the potential difference between the two sites. The operator $\hat{a}_{i\sigma}^{\dagger}$ ($\hat{a}_{i\sigma}$) creates (annihilates) an electron of spin σ on site i. In the following, all quantities are reported in reduced units or, equivalently, in units of t.

For $N = 2$, the Hamiltonian in the site basis $|\uparrow_1\downarrow_2\rangle$, $|\uparrow\downarrow_1\, 0_2\rangle$, $|0_1\, \uparrow\downarrow_2\rangle$, $|\downarrow_1\uparrow_2\rangle$, is written as

$$H^{N=2} = \begin{array}{c} \begin{array}{cccc} |\uparrow_1\downarrow_2\rangle & |\uparrow\downarrow_1\, 0_2\rangle & |0_1\, \uparrow\downarrow_2\rangle & |\downarrow_1\uparrow_2\rangle \end{array} \\ \begin{pmatrix} 0 & -t & -t & 0 \\ -t & U + \Delta v & 0 & t \\ -t & 0 & U - \Delta v & t \\ 0 & t & t & 0 \end{pmatrix} \end{array} \tag{4.2}$$

The triplet excited-state wave function is

$$|^3\Psi^N\rangle = \frac{|\uparrow_1\downarrow_2\rangle + |\downarrow_1\uparrow_2\rangle}{\sqrt{2}} \tag{4.3}$$

while the wave functions of the singlet ground ($n = 0$) and excited ($n = 1$ and 2) states have the form

$$|^1\Psi_n^N\rangle = c_{1n} |\uparrow_1\downarrow_2\rangle + c_{2n} |\downarrow_1\uparrow_2\rangle + c_{3n} |0_1\, \uparrow\downarrow_2\rangle + c_{4n} |\uparrow\downarrow_1\, 0_2\rangle \tag{4.4}$$

with

$$c_{1n} = -c_{2n} = \frac{1}{\mathcal{N}_n} \tag{4.5a}$$

$$c_{3n} = \frac{1}{\mathcal{N}_n} \frac{2t}{U - \Delta v - E_n^N} \tag{4.5b}$$

$$c_{4n} = \frac{1}{\mathcal{N}_n} \frac{2t}{U + \Delta v - E_n^N} \tag{4.5c}$$

and

$$\mathcal{N}_n = \sqrt{2 + \left(\frac{2t}{U - \Delta v - E_n^N}\right)^2 + \left(\frac{2t}{U + \Delta v - E_n^N}\right)^2} \tag{4.6}$$

where the E_n^N's are the corresponding (exact) eigenenergies of Eq. (4.1). The differences between these N-electron energies allow us to compute the exact neutral excitation energies of the system as follows:

$${}^3\omega = E_1^{N=2} - E_0^{N=2} \tag{4.7}$$

$${}^1\omega = E_2^{N=2} - E_0^{N=2} \tag{4.8}$$

while the exact IP and EA are computed as energy differences with respect to the system with $N-1$ and $N+1$ electrons

$$\text{IP} = E_0^{N-1} - E_0^N = -\varepsilon_i \tag{4.9}$$

$$\text{EA} = E_0^N - E_0^{N+1} = -\varepsilon_a \tag{4.10}$$

We note that $|{}^1\Psi_2^N\rangle$ is the excited-state wave function associated with the so-called double excitation, which we will not address in the following since we will only focus on static approximations to the BSE kernel. The weights of the two first eigenstates are represented in Fig. 4.1

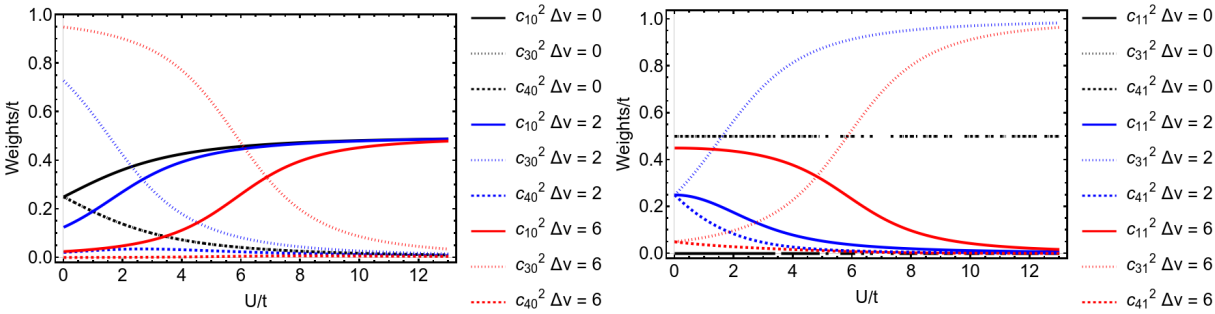

Figure 4.1 – Weights of ${}^1\Psi_0^N$ (left) and ${}^1\Psi_1^N$ (right) as functions of U/t. For $t = 1$ and several Δv, $c_{20}^2 = c_{10}^2$ and $c_{22}^2 = c_{12}^2$.

The transition probabilities are given by

$$f = \langle {}^1\Psi_0^N | \hat{n}_1 - \hat{n}_2 | {}^1\Psi_1^N \rangle \tag{4.11}$$

We look only at the singlet transition because the triplet transition is spin-forbidden.

Let us see what represents this matrix element. In (4.4), the coefficients are associated to singly-occupied configurations (s) or doubly-occupied configurations (d)

$$|{}^1\Psi_n^N\rangle = \underbrace{c_{1n}}_{s} |\uparrow_1\downarrow_2\rangle + \underbrace{c_{2n}}_{s} |\downarrow_1\uparrow_2\rangle + \underbrace{c_{3n}}_{d} |0_1\ \uparrow\downarrow_2\rangle + \underbrace{c_{4n}}_{d} |\uparrow\downarrow_1\ 0_2\rangle \tag{4.12}$$

Applying $\hat{n}_1$ to $|^1\Psi_n^N\rangle$ keeps the coefficients of configurations in which site 1 is occupied:

$$\hat{n}_1 |^1\Psi_n^N\rangle = \underbrace{c_{1n}}_{s} |\uparrow_1\downarrow_2\rangle + \underbrace{c_{2n}}_{s} |\downarrow_1\uparrow_2\rangle + 2\underbrace{c_{4n}}_{d} |\uparrow\downarrow_1\, 0_2\rangle \tag{4.13}$$

Similarly for $\hat{n}_2$, we have

$$\hat{n}_2 |^1\Psi_n^N\rangle = \underbrace{c_{1n}}_{s} |\uparrow_1\downarrow_2\rangle + \underbrace{c_{2n}}_{s} |\downarrow_1\uparrow_2\rangle + 2\underbrace{c_{3n}}_{d} |0_1\, \uparrow\downarrow_2\rangle \tag{4.14}$$

Hence, applying $\hat{n}_i$ to an eigenstate keeps the configurations where particles are located on the site i. Then, by projection on the ground state, one gets

$$\langle^1\Psi_0^N|\hat{n}_1|\Psi_n^N\rangle = \underbrace{c_{10}c_{1n}}_{s} + \underbrace{c_{20}c_{2n}}_{s} + 2\underbrace{c_{40}c_{4n}}_{d} \tag{4.15}$$

$$\langle^1\Psi_0^N|\hat{n}_2|\Psi_n^N\rangle = \underbrace{c_{10}c_{1n}}_{s} + \underbrace{c_{20}c_{2n}}_{s} + 2\underbrace{c_{30}c_{3n}}_{d} \tag{4.16}$$

These matrix elements consist of the sum of products of coefficients associated with the common configurations of both the ground and excited states, centered on a site i. The transition probability is calculated as the difference between these matrix elements

$$f = 2c_{40}c_{41} - 2c_{30}c_{31} \tag{4.17}$$

which keeps only the coefficients of doubly-occupied configurations.

In the case of the symmetric dimer, we have

$$\begin{aligned}
\left|^1\Psi_0^N\right\rangle &= \frac{4t}{a(c-U)}\left[|\uparrow_1\downarrow_2\rangle - |\downarrow_1\uparrow_2\rangle\right] + \frac{1}{a}\left[|\uparrow\downarrow_1\, 0_2\rangle - |0_1\, \uparrow\downarrow_2\rangle\right] \\
\left|^3\Psi^N\right\rangle &= \frac{1}{\sqrt{2}}\left[|\uparrow_1\downarrow_2\rangle + |\downarrow_1\uparrow_2\rangle\right] && \text{(4.18a)} \\
\left|^1\Psi_1^N\right\rangle &= \frac{1}{\sqrt{2}}\left[|\uparrow\downarrow_1\, 0_2\rangle - |0_1\, \uparrow\downarrow_2\rangle\right] && \text{(4.18b)}
\end{aligned}$$

where $c = \sqrt{(4t)^2 + U^2}$ and $a = \sqrt{2\left(\left(\frac{4t}{c-U}\right)^2 + 1\right)}$.

When we apply the number operators to the singlet excited state, we obtain

$$\hat{n}_1 \left|^1\Psi_1^N\right\rangle = \underbrace{\sqrt{2}}_{d} |\uparrow\downarrow_1\, 0_2\rangle \tag{4.19}$$

$$\hat{n}_2 \left|^1\Psi_1^N\right\rangle = -\underbrace{\sqrt{2}}_{d} |0_1\, \uparrow\downarrow_2\rangle \tag{4.20}$$

Furthermore, by projecting on the ground state, we end up with

$$\langle^1\Psi_0^N|\hat{n}_1|\Psi_n^N\rangle = \underbrace{\frac{\sqrt{2}}{a}}_{d} \tag{4.21}$$

$$\langle^1\Psi_0^N|\hat{n}_2|\Psi_n^N\rangle = -\underbrace{\frac{\sqrt{2}}{a}}_{d} \tag{4.22}$$

$$f = \frac{2\sqrt{2}}{a} \tag{4.23}$$

In the symmetric dimer, the singlet excited state consists only of doubly-occupied configurations. The triplet state, instead, exclusively comprises singly-occupied configurations (which is the case for any Δv).

We saw that W is a two-point quantity while T is a four-point quantity. Because the Coulomb interaction is local in the Hubbard model, i.e., $v(1,2) = U\delta(1,2)$, T also becomes a two-point quantity in this special case.

At the mean-field level, the system is composed of two orbitals: a bonding orbital $\varepsilon_{\text{HOMO}} = -\text{IP}$ and an anti-bonding orbital $\varepsilon_{\text{LUMO}} = -\text{EA}$. The approximated fundamental gap is thus $E_{\text{g}} = \text{IP} - \text{EA} = \varepsilon_{\text{LUMO}} - \varepsilon_{\text{HOMO}}$ and can be computed at the HF, GW, or T-matrix level depending on the choice of (quasi)particle energies.

Furthermore, we note ${}^1\boldsymbol{H}_{\text{exc}}$ and ${}^3\boldsymbol{H}_{\text{exc}}$ the singlet and triplet excitonic Hamiltonians of the dimer that are obtained by spin-resolving Eq. (5.6). [66, 67, 68] ${}^1\omega$ and ${}^3\omega$ are their corresponding positive eigenvalues that represent the excitation energies associated with the singlet-singlet and singlet-triplet transitions, respectively. We also define the binding energy of the singlet and triplet excitations as ${}^1E_{\text{b}} = E_{\text{g}} - {}^1\omega$ and ${}^3E_{\text{b}} = E_{\text{g}} - {}^3\omega$, respectively, where E_{g}, ${}^1\omega$, and ${}^3\omega$ are obtained at the same level of theory (i.e., exact, GW or T-matrix level).

From a general point of view, the excitonic Hamiltonian can be written as

$$\boldsymbol{H}_{\text{exc}} = \begin{pmatrix} E_{\text{g}} + a & b \\ -b & -E_{\text{g}} - a \end{pmatrix} \tag{4.24}$$

while the excitation energies are

$$\omega = \pm\sqrt{(E_{\text{g}} + a)^2 - b^2} \tag{4.25}$$

with "+" referring to excitations and "−" to the de-excitations.

4.2 Testing approximations to the self-energy and its derivative

4.2.1 The symmetric dimer

Quasiparticles

Let us first study the symmetric Hubbard dimer (i.e., $\Delta v = 0$) since it can be solved analytically in the case of a non-interacting or HF starting point, G_0 and G_{HF}, respectively, which further highlights the influence of the starting Green's function. Before commenting on the performance of GW and GT, let us first report some exact expressions for the symmetric Hubbard dimer at half-filling.

The exact IP, EA, and fundamental gap are

$$\text{IP} = -t - \frac{1}{2}\left[U - \sqrt{(4t)^2 + U^2}\right] \tag{4.26a}$$

$$\text{EA} = t - U + \frac{1}{2}\left[U - \sqrt{(4t)^2 + U^2}\right] \tag{4.26b}$$

$$E_{\text{g}} = -2t + \sqrt{(4t)^2 + U^2} \tag{4.26c}$$

It is instructive to study the small-U limit of these quantities. In particular, the fundamental gap behaves as

$$E_{\mathrm{g}} = 2t + \frac{U^2}{8t} - \frac{U^4}{512t^3} + \mathcal{O}\left(U^6\right) \tag{4.27}$$

The exact singlet and triplet excitation energies are

$$^1\omega = U - \frac{1}{2}\left[U - \sqrt{(4t)^2 + U^2}\right] \tag{4.28a}$$

$$^3\omega = -\frac{1}{2}\left[U - \sqrt{(4t)^2 + U^2}\right] \tag{4.28b}$$

which yields a singlet-triplet gap equals to U. In the small-U limit, these excitation energies behave as

$$^1\omega = 2t + \frac{U}{2} + \frac{U^2}{16t} - \frac{U^4}{1024t^3} + \mathcal{O}\left(U^6\right) \tag{4.29a}$$

$$^3\omega = 2t - \frac{U}{2} + \frac{U^2}{16t} - \frac{U^4}{1024t^3} + \mathcal{O}\left(U^6\right) \tag{4.29b}$$

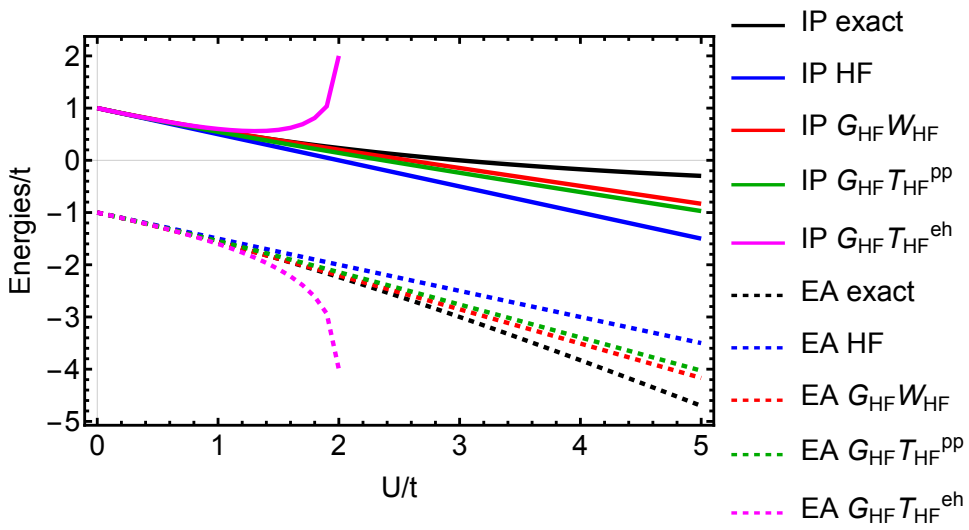

Figure 4.2 – IP and EA as functions of U/t in the symmetric Hubbard obtained at various levels of theory: exact (black), HF (blue), $G_{\mathrm{HF}}W$ (red), $G_{\mathrm{HF}}T^{pp}$ (green) and $G_{\mathrm{HF}}\overline{T}^{eh}$ (magenta).

We start by analyzing the charged excitation energies as functions of U/t. We are mainly interested in the quality of the quasiparticle energies (or, equivalently, the IP and EA) since they enter the BSE [see Eq. (3.268a)]. In Fig. 4.2, we compare the exact IP and EA with approximate IPs and EAs computed at the GW and GT levels with an HF starting Green's function. These two schemes are coined $G_{\mathrm{HF}}W_{\mathrm{HF}}$ and $G_{\mathrm{HF}}T_{\mathrm{HF}}$ in the following. Note that, in the specific case of the symmetric Hubbard dimer, one gets the same results using G_0 as the starting point.

In the weak correlation (i.e., small U/t) regime, all approximations are in good agreement with the exact results. In the strong correlation (i.e., large U/t) regime, both the GW and the T^{pp}-matrix approximations underestimate the fundamental gap quite significantly, while the T^{eh}-matrix approximation overestimates the gap and turn complex.

This observation can be rationalized by looking at the poles Ω of the response function in the RPA approximation:

$$\Omega^{GW,\mathrm{RPA}} = \sqrt{4t^2 + 4Ut} \tag{4.30a}$$

$$\Omega^{G\overline{T}^{eh},\mathrm{RPA}} = \sqrt{4t^2 - 2Ut} \tag{4.30b}$$

$$\Omega^{GT^{pp},\mathrm{RPA}} = \sqrt{4t^2 + 2Ut} \tag{4.30c}$$

The corresponding critical values for each approximation are

$$U^{GW}_{\mathrm{crit}} = -t \tag{4.31a}$$

$$U^{G\overline{T}^{eh}}_{\mathrm{crit}} = 2t \tag{4.31b}$$

$$U^{GT^{pp}}_{\mathrm{crit}} = -2t \tag{4.31c}$$

Since the Coulomb interaction U is positive, the collective excitations cannot turn complex for GW and GT^{pp}, while for $G\overline{T}^{eh}$, they become complex when $U > 2t$.

One would note, however, that GW is slightly better than the T-matrix approximations. For comparison, in Fig. 4.2, we report also the HF results, which are clearly worse than both $G_{\mathrm{HF}}W_{\mathrm{HF}}$ and $G_{\mathrm{HF}}T_{\mathrm{HF}}$. These observed trends are in line with previously reported results on the same model in which the quasiparticle energies are computed without linearizing the self-energy, [69, 42] as well as in more realistic molecular systems. [59, 70]

Based on these results, we can study analytically the small-U limits of the quantities of interest. For example, the $G_{\mathrm{HF}}W_{\mathrm{HF}}$ and $G_{\mathrm{HF}}T_{\mathrm{HF}}$ behave as

$$E_{\mathrm{g}}^{G_{\mathrm{HF}}W_{\mathrm{HF}}} = 2t + \frac{U^2}{4t} - \frac{3U^3}{16t^2} + \frac{19U^4}{128t^3} + \mathcal{O}\big(U^5\big) \tag{4.32a}$$

$$E_{\mathrm{g}}^{G_{\mathrm{HF}}T^{pp}_{\mathrm{HF}}} = 2t + \frac{U^2}{8t} - \frac{3U^3}{64t^2} + \frac{9U^4}{512t^3} + \mathcal{O}\big(U^5\big) \tag{4.32b}$$

$$E_{\mathrm{g}}^{G_{\mathrm{HF}}T^{eh}_{\mathrm{HF}}} = 2t + \frac{U^2}{8t} + \frac{3U^3}{64t^2} + \frac{9U^4}{512t^3} + \mathcal{O}\big(U^5\big) \tag{4.32c}$$

Compared with the exact gap reported in Eq. (4.27), one can see that $G_{\mathrm{HF}}W_{\mathrm{HF}}$ is already wrong at second-order in U, while the $G_{\mathrm{HF}}T_{\mathrm{HF}}$ gap is correct up to the quadratic term thanks to the inclusion of the second-order direct and exchange diagrams, as already mentioned in Ref. [42]. However, it exhibits a spurious cubic term and the wrong quartic coefficient. (Note that the renormalization factor only affects the value of the quartic coefficient.)

Neutral excitations

We now focus on the neutral excited states of the symmetric Hubbard dimer. Within the $G_{\mathrm{HF}}W_{\mathrm{HF}}$ approximation to the self-energy, the excitonic Hamiltonians read

$${}^3\boldsymbol{H}_{\mathrm{exc}}^{G_{\mathrm{HF}}W_{\mathrm{HF}}} = \begin{pmatrix} E_{\mathrm{g}}^{G_{\mathrm{HF}}W_{\mathrm{HF}}} - \frac{U}{2} & \frac{U}{2}\left(\frac{U}{t+U} - 1\right) \\ -\frac{U}{2}\left(\frac{U}{t+U} - 1\right) & -\left(E_{\mathrm{g}}^{G_{\mathrm{HF}}W_{\mathrm{HF}}} - \frac{U}{2}\right) \end{pmatrix} \tag{4.33a}$$

$${}^1\boldsymbol{H}_{\mathrm{exc}}^{G_{\mathrm{HF}}W_{\mathrm{HF}}} = \begin{pmatrix} E_{\mathrm{g}}^{G_{\mathrm{HF}}W_{\mathrm{HF}}} + \frac{U}{2} & \frac{U}{2}\left(\frac{U}{t+U} + 1\right) \\ -\frac{U}{2}\left(\frac{U}{t+U} + 1\right) & -\left(E_{\mathrm{g}}^{G_{\mathrm{HF}}W_{\mathrm{HF}}} + \frac{U}{2}\right) \end{pmatrix} \tag{4.33b}$$

When we use G_0 instead of G_{HF} as a starting Green's function, we obtain the same excitonic Hamiltonians. We see that the electron-hole polarisability induces an asymmetry

in the resonant and coupling terms due to the spin structure of W which implies that there is no Hartree term for the triplet state. The excitation energies are shown in Fig. 4.3 (top panel) alongside the binding energies of the singlet and triplet excitation energies.

The GW approximation (red curves) describes better the exact triplet excitation energy, ${}^3\omega$, than the exact singlet excitation energy, ${}^1\omega$. Between $U/t \approx 7$ and $U/t \approx 12$, however, ${}^3\omega^{GW}$ (solid red curve) turns complex due to a triplet instability in the BSE matrix. This occurs because the coupling term $b = \frac{U}{2}\left(\frac{U}{t+U} - 1\right)$ becomes larger than the resonant term $E_{\mathrm{g}} - a = E_{\mathrm{g}}^{G_{\mathrm{HF}}W_{\mathrm{HF}}} + U/2$, as it is clear from Eq. (4.25). Interestingly, in the same range, the GW binding energy ${}^3E_{\mathrm{b}}$ (solid blue curve) reaches the GW fundamental gap (solid magenta line). Moreover, at $U/t \approx 7$, ${}^1\omega^{GW}$ (dashed red curve) becomes lower than the fundamental gap and, hence, becomes, by definition, a "bound" state, while, at $U/t \approx 12$, it becomes complex (singlet instability) when ${}^1E_{\mathrm{b}}$ (dashed blue curve) reaches the GW fundamental gap (dashed magenta line).

Within the $G_{\mathrm{HF}}T^{pp}_{\mathrm{HF}}$ approximation to the self-energy, the excitonic Hamiltonians read

$$ {}^3\boldsymbol{H}^{G_{\mathrm{HF}}T^{pp}_{\mathrm{HF}}}_{\mathrm{exc}} = \begin{pmatrix} E_{\mathrm{g}}^{G_{\mathrm{HF}}T^{pp}_{\mathrm{HF}}} - \frac{U}{2} & \frac{U}{2}\left(\frac{Ut/2}{\Omega^2 - U^2} - 1\right) \\ -\frac{U}{2}\left(\frac{Ut/2}{\Omega^2 - U^2} - 1\right) & -\left(E_{\mathrm{g}}^{G_{\mathrm{HF}}T^{pp}_{\mathrm{HF}}} - \frac{U}{2}\right) \end{pmatrix} \tag{4.34a} $$

$$ {}^1\boldsymbol{H}^{G_{\mathrm{HF}}T^{pp}_{\mathrm{HF}}}_{\mathrm{exc}} = \begin{pmatrix} E_{\mathrm{g}}^{G_{\mathrm{HF}}T^{pp}_{\mathrm{HF}}} + \frac{U}{2} & -\frac{U}{2}\left(\frac{Ut/2}{\Omega^2 - U^2} - 1\right) \\ \frac{U}{2}\left(\frac{Ut/2}{\Omega^2 - U^2} - 1\right) & -\left(E_{\mathrm{g}}^{G_{\mathrm{HF}}T^{pp}_{\mathrm{HF}}} + \frac{U}{2}\right) \end{pmatrix} \tag{4.34b} $$

with $\Omega = \sqrt{4t^2 + 2Ut}$ and where one would notice a similar form as Eqs. (D.70a) and (D.70b) for the resonant and antiresonant blocks, and a very different expression for the coupling blocks due again to the difference in spin structure between W and T. In the case of G_0T_0, one gets similar expressions except that one must replace the coupling block by $\pm\frac{U}{2}\left(\frac{Ut/2}{\Omega^2} - 1\right)$ instead of $\pm\frac{U}{2}\left(\frac{Ut/2}{\Omega^2 - U^2} - 1\right)$.

For the electron-hole T-matrix, the excitonic Hamiltonians read

$$ {}^3\boldsymbol{H}^{G_{\mathrm{HF}}\overline{T}^{eh}_{\mathrm{HF}}}_{\mathrm{exc}} = \begin{pmatrix} E_{\mathrm{g}}^{G_{\mathrm{HF}}\overline{T}^{eh}_{\mathrm{HF}}} - \frac{U}{2} & -\frac{Ut}{2t-U} \\ \frac{Ut}{2t-U} & -\left(E_{\mathrm{g}}^{G_{\mathrm{HF}}\overline{T}^{eh}_{\mathrm{HF}}} - \frac{U}{2}\right) \end{pmatrix} \tag{4.35a} $$

$$ {}^1\boldsymbol{H}^{G_{\mathrm{HF}}\overline{T}^{eh}_{\mathrm{HF}}}_{\mathrm{exc}} = \begin{pmatrix} E_{\mathrm{g}}^{G_{\mathrm{HF}}\overline{T}^{eh}_{\mathrm{HF}}} + \frac{U}{2} & \frac{Ut}{2t-U} \\ -\frac{Ut}{2t-U} & -\left(E_{\mathrm{g}}^{G_{\mathrm{HF}}\overline{T}^{eh}_{\mathrm{HF}}} + \frac{U}{2}\right) \end{pmatrix} \tag{4.35b} $$

Similar to W, $\overline{T}^{eh}$ is constructed using an electron-hole polarizability, yielding the same expression whether we use G_0 or G_{HF}. Consequently, we obtain identical excitonic Hamiltonians regardless of our starting point. When we write the excitonic Hamiltonians for T^{pp} with G_0, they share the same structure as shown in (4.35a) and (4.35b). The only differences lie in the gap value and the coupling term, where the term $2t + U$ appears in the denominator.

Taylor expanding the singlet and triplet $G_{\mathrm{HF}}W_{\mathrm{HF}}$ excitations at small U shows that

$$ {}^1\omega^{G_{\mathrm{HF}}W_{\mathrm{HF}}} = 2t + \frac{U}{2} + \frac{3U^2}{16t} - \frac{19U^3}{64t^2} + \frac{251U^4}{1024t^3} + \mathcal{O}\left(U^5\right) \tag{4.36a} $$

$$ {}^3\omega^{G_{\mathrm{HF}}W_{\mathrm{HF}}} = 2t - \frac{U}{2} + \frac{3U^2}{16t} - \frac{5U^3}{64t^2} - \frac{5U^4}{1024t^3} + \mathcal{O}\left(U^5\right) \tag{4.36b} $$

which clearly do not have the right quadratic behavior in U/t when compared to Eqs. (4.29a) and (4.29b). At the $G_{\mathrm{HF}}T^{pp}_{\mathrm{HF}}$ level, we have

$$ {}^{1}\omega^{G_{\mathrm{HF}}T^{pp}_{\mathrm{HF}}} = 2t + \frac{U}{2} + \frac{U^2}{16t} - \frac{U^3}{64t^2} + \frac{3U^4}{512t^3} + \mathcal{O}(U^5) \tag{4.37a} $$

$$ {}^{3}\omega^{G_{\mathrm{HF}}T^{pp}_{\mathrm{HF}}} = 2t - \frac{U}{2} + \frac{U^2}{16t} - \frac{3U^3}{64t^2} + \frac{7U^4}{512t^3} + \mathcal{O}(U^5) \tag{4.37b} $$

which is correct up to second order in U/t. Interestingly, replacing the T-matrix quasiparticles with the HF one-particle energies changes the sign of the second-order term.

For $G_{\mathrm{HF}}\overline{T}^{eh}_{\mathrm{HF}}$, we have

$$ {}^{1}\omega^{G_{\mathrm{HF}}\overline{T}^{eh}_{\mathrm{HF}}} = 2t + \frac{U}{2} + \frac{U^2}{16t} - \frac{15U^4}{1024t^3} + \mathcal{O}(U^5) \tag{4.38a} $$

$$ {}^{3}\omega^{G_{\mathrm{HF}}\overline{T}^{eh}_{\mathrm{HF}}} = 2t - \frac{U}{2} + \frac{U^2}{16t} - \frac{3U^3}{32t^2} - \frac{47U^4}{1024t^3} + \mathcal{O}(U^5) \tag{4.38b} $$

which show the same behaviour as the $G_{\mathrm{HF}}T^{pp}_{\mathrm{HF}}$ excitation energies up to second order.

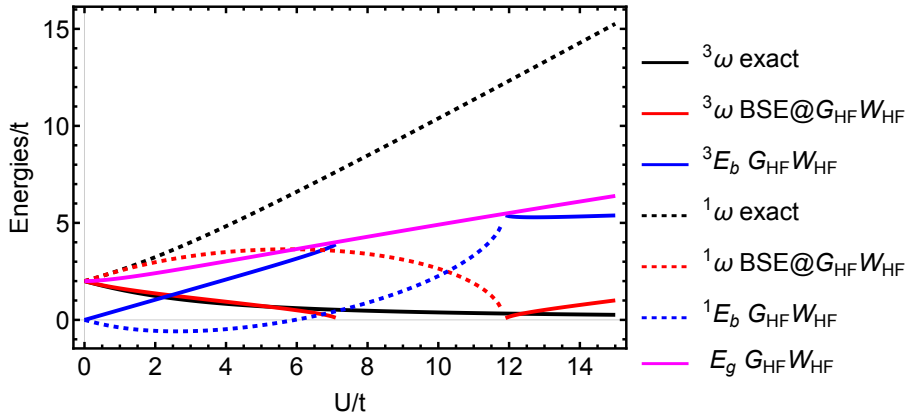

Figure 4.3 – Neutral excitation energies (red), binding energies (blue), and fundamental gap (magenta) as functions of U/t in the symmetric Hubbard dimer ($\Delta v = 0$) for the triplet (solid) and singlet (dashed) excited states at various levels of theory: exact (black) and BSE@$G_{\mathrm{HF}}W_{\mathrm{HF}}$.

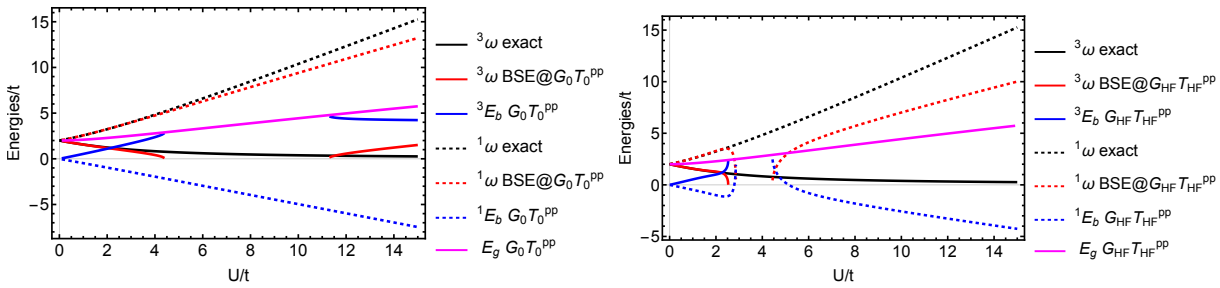

(a) Neutral excitation energies with G_0 **(b)** Neutral excitation energies with G_{HF}

Figure 4.4 – Neutral excitation energies (red), binding energies (blue), and fundamental gap (magenta) as functions of U/t in the symmetric Hubbard dimer ($\Delta v = 0$) for the triplet (solid) and singlet (dashed) excited states at various levels of theory: exact (black) and BSE@GT^{pp}.

The excitation energies are represented in Fig. 4.4a, Fig. 4.4b and Fig. 4.5 as functions of U/t. For the case of BSE@$G_{\mathrm{HF}}T^{pp}_{\mathrm{HF}}$ (top right panel), the exact singlet and triplet

transitions (black curves) are well described by ${}^1\omega^{G_{\rm HF}T^{pp}_{\rm HF}}$ and ${}^3\omega^{G_{\rm HF}T^{pp}_{\rm HF}}$ (red curves) until $U/t \approx 3$. After this, they both become complex, ${}^1\omega^{G_{\rm HF}T^{pp}_{\rm HF}}$ becoming real again at $U/t \approx 4.5$. As before ${}^1\omega^{G_{\rm HF}T^{pp}_{\rm HF}}$ and ${}^3\omega^{G_{\rm HF}T^{pp}_{\rm HF}}$ turn complex when their respective binding energy, ${}^1E_{\rm b}$ and ${}^3E_{\rm b}$ (magenta curves), reaches the value of the fundamental gap.

At the BSE@$G_0T^{pp}_0$ (top left panel), excitation energies are surprisingly more accurate. For example, ${}^1\omega^{G_0T^{pp}_0}$ (red dashed curve) is an excellent approximation of the exact singlet excitation energy until $U/t \approx 5$ at which it starts to deviate but remains decent. Likewise, ${}^3\omega^{G_0T^{pp}_0}$ (solid red curve) is accurate until $U/t \approx 4$ at which a triplet instability appears. Since the quality of the GW and GT quasiparticle energies as functions of U/t is very similar, and since the HF contribution to the GW and GT-based BSE kernels is the same, the difference between GW and GT excitation energies can be traced back to the difference in the correlation part of the GW- and GT-based kernels [see Eqs. (5.38) and (5.46), respectively].

These results show that, in order to get accurate neutral excitation energies, there is a subtle balance to fulfill between the quality of the fundamental gap and the correlation kernel. Altering one of them will result in instabilities in the BSE problem, hence complex excitation energies. In the next section, we will investigate this issue in more detail.

Finally, in the case of a BSE@$G_{\rm HF}\overline{T}^{eh}_{\rm HF}$ calculation, it is important to note that, as we have observed, the poles of the response function become complex when $U > 2t$. Consequently, the energies of the excitations in (4.35a) and (4.35b) will also become complex.

Overall, BSE@GW provides a better description of triplet excitations compared to BSE@GT^{pp}. Conversely, for singlet excitations, the opposite holds true. In the case of both T^{pp} and $\overline{T}^{eh}$, we encounter singularities.

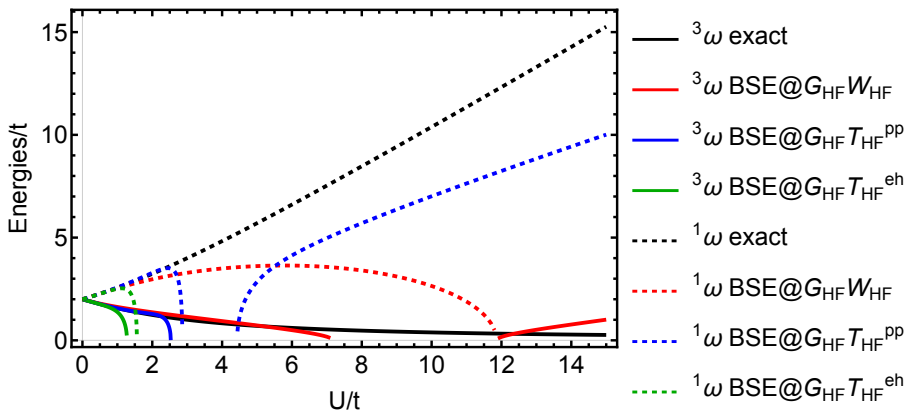

Figure 4.5 – Neutral excitation energies: exact (black), BSE@GW (red), BSE@GT^{pp} (blue) and BSE@$G\overline{T}^{eh}$ (green) as functions of U/t in the symmetric Hubbard dimer ($\Delta v = 0$) for the triplet (solid) and singlet (dashed) excited states.

Influence of approximate quasiparticles on the neutral excitations

In the eigenvalue expression given by (4.24), the terms a and b originate from the BSE kernel, which is consistently calculated using a static approximation. In this section, we calculate E_g with various levels of approximation for the self-energy. Figures 4.6a and 4.6b depict the triplet and singlet BSE@GW neutral excitations, respectively. Figures 4.6c and 4.6d illustrate the triplet and singlet BSE@GT^{pp} neutral excitations. In each figure, we compare the exact transition to the same BSE@GW or BSE@GT^{pp} transition

but with different quasiparticle energies. The orange curve corresponds to the poles of G_0 ($\Delta\varepsilon^0$), the blue curve to a linearized self-energy (Σ_{lin}), the green curve to a static self-energy (Σ_s), the red curve to a dynamical self-energy (Σ_d), and the purple curve to exact quasiparticles ($\Delta\varepsilon^{QP}$). (The derivations of Σ_s and Σ_d can be found in the Appendix.) The goal is to observe how the accuracy of the results changes as we improve the self-energy.

We notice that, as we enhance the self-energy, there is a shift in the point where the eigenvalues become complex. This also leads to an improvement in the accuracy of the results. This improvement is evident, for instance, in the case of the triplet excitation presented in Fig. 4.6a. The curve associated with the poles of G_0 performs worse compared to the others where we apply a self-energy correction. As we improve the self-energy, the approximated curve matches the exact one for a longer range, and the eigenvalues remain real for an extended period. With the exception of the dynamical self-energy (red curve), this behavior can be attributed to the fact that a dynamical correction includes satellite effects, resulting in smaller quasiparticle energies and consequently reducing E_g. However, since we do not apply a dynamical correction to the kernel in (4.25), the value of the term b remains unchanged. Therefore, even though the quasiparticles in the red curve are more accurate than those in the green curve, they turn complex more rapidly. It is important to note that obtaining quasiparticles from a dynamical self-energy should theoretically yield improved results compared to using a static or linearized self-energy. However, studies on the symmetric Hubbard dimer with a single spin-up electron have shown, for example, that when calculating quasiparticles with GW for the addition or removal of a spin-up electron, it can introduce spurious satellites. Thus, employing a dynamical self-energy does not guarantee the absence of errors when adding satellite effects [69].

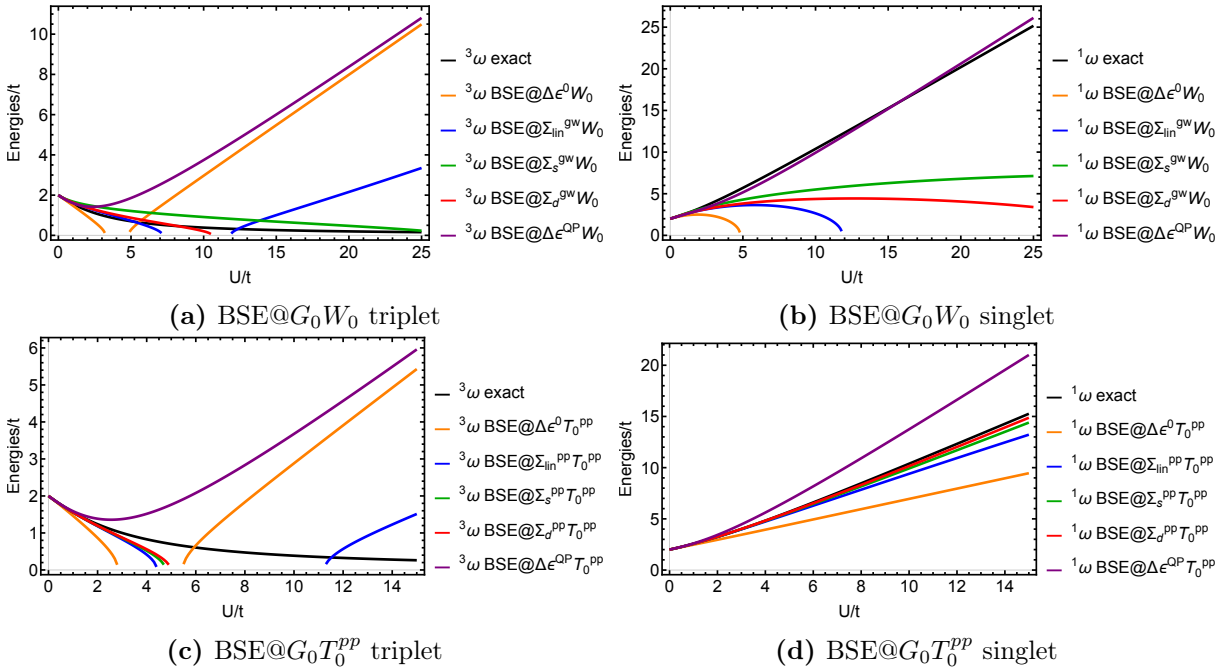

(a) BSE@G_0W_0 triplet **(b)** BSE@G_0W_0 singlet

(c) BSE@$G_0T_0^{pp}$ triplet **(d)** BSE@$G_0T_0^{pp}$ singlet

Figure 4.6 – Neutral excitations BSE@GW (top panels) and BSE@GT^{pp} (bottom panels) with different approximations to the self-energy: exact (black), orbital energies of G^0 (orange), linearized self-energy (blue), static self-energy (green), dynamical self-energy (red), exact quasiparticle (purple), for the triplet and singlet states.

We also observe that the results can be challenging to interpret. In the case of exact quasiparticles (the purple curve in Fig.4.6a), the results are nearly identical to the one obtained using the non-interacting Green's function (orange curve), while for the singlet excitation in Fig. 4.6b, the purple curve closely matches the exact curve shown in black.

It is important to note that when the value of E_g is significantly higher than that of a and b, it can potentially obscure certain issues. As seen in Fig. 4.2, the fundamental gaps for GW and GT^{pp} are similar. However, when comparing the BSE@GW and BSE@GT^{pp} excitations, they exhibit substantial differences, indicating that the results are primarily influenced by the choice of the kernel.

When conducting a BSE calculation with a GW self-energy and three different kernels, it becomes evident that the singlet excitation, which is inadequately described in a BSE@GW calculation, becomes much more accurate when the kernel W is replaced by the T^{pp} one (see Fig. 4.7). Consequently, the accuracy of the results depends on a compensatory error between the gap (where there is already a compensatory error between the ionization potential and the electron affinity) and the matrix elements of the kernel.

This implies that, even if we achieve favorable results when comparing with exact excitations, it is possibly a matter of chance. For example, in the GW approximation, the kernel correction is unsuitable for the singlet excitation and yields suboptimal results, as observed. However, for this kernel, if we use exact quasiparticles instead of GW quasiparticles (as represented by the purple curve in Fig. 4.6b), the approximation is in better agreement with the exact results this time. The GW kernel remains problematic, but the accuracy of the quasiparticles is sufficient to increase the gap and compensate for the errors introduced by the kernel.

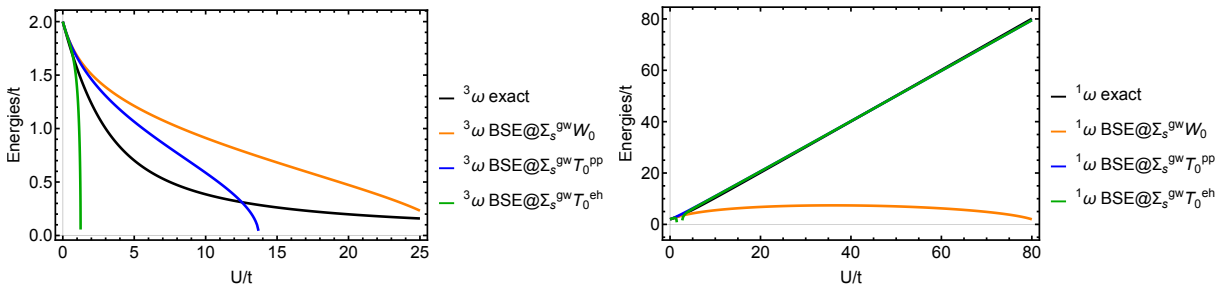

Figure 4.7 – Neutral excitations with a static GW self-energy and three different kernels.

In the following section, we examine the quasiparticle energies and neutral excitations of the asymmetric Hubbard dimer. We investigate the impact of introducing a non-zero Δv on the results. Next, we select a fixed value of U and vary the parameter Δv. Finally, we analyze the disparity between the isolated electron-hole system when utilizing G^0 and the electron-hole system interacting with the rest of the system when employing G_{HF}.

4.2.2 Asymmetric Hubbard dimer

We now turn our attention to the more general case of the asymmetric dimer for which we study G_{HF} as a starting point.

Charged excitations

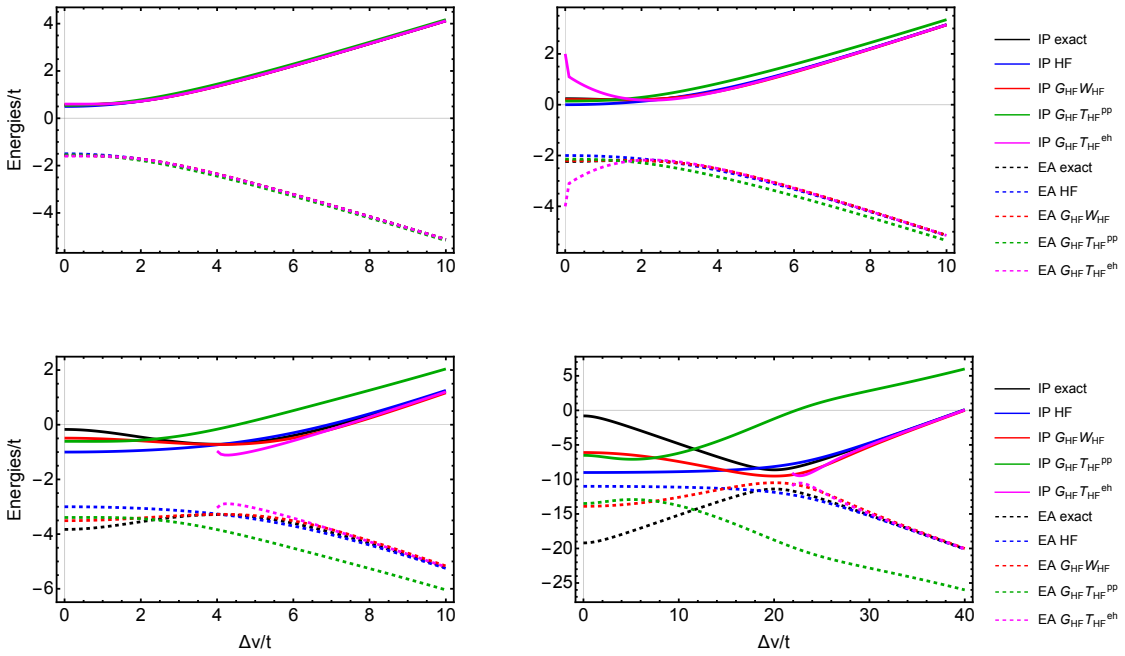

Figure 4.8 – IP and EA as functions of $\Delta v/t$ in the asymmetric Hubbard dimer for $U/t = 1$ (top left panel), $U/t = 2$ (top right panel), $U/t = 4$ (bottom left panel) and $U/t = 20$ (bottom right panel) obtained at various levels of theory: exact (black), HF (blue), $G_{\mathrm{HF}}W_{\mathrm{HF}}$ (red), $G_{\mathrm{HF}}T^{pp}_{\mathrm{HF}}$ (green) and $G_{\mathrm{HF}}\overline{T}^{eh}_{\mathrm{HF}}$ (magenta).

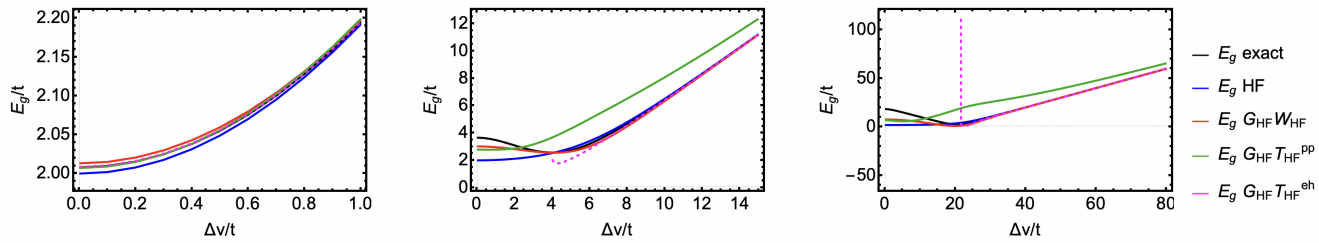

Figure 4.9 – Fundamental gap as a function of $\Delta v/t$ in the asymmetric Hubbard dimer for $U/t = 20$ (left), $U/t = 4$ (center) and $U/t = 1/4$ (right) at various levels of theory: exact (black), HF (blue), $G_{\mathrm{HF}}W_{\mathrm{HF}}$ (red), and $G_{\mathrm{HF}}T^{pp}_{\mathrm{HF}}$ (green) and $G_{\mathrm{HF}}\overline{T}^{eh}_{\mathrm{HF}}$ (magenta).

In Fig. 4.8, we report the IP and EA as functions of $\Delta v/t$. The ratio U/t is fixed at different values. For instance, if we set $U/t = 20$, for $\Delta v/t < 20$ (bottom right panel of Fig. 4.8), we can assume the system to be in a strongly-correlated regime, while, for $\Delta v/t > 20$, the electron correlation is weak. As for the symmetric case, we show that, in the strongly-correlated regime, all approximations underestimate the exact fundamental gap, with a slightly better performance of GW (red curves) as compared to GT^{pp} (green

curves). For $\Delta v/t > U/t$, HF, GW and GT^{eh} tend to the exact values, whereas GT^{pp} deviates from the exact result. Finally, $G\overline{T}^{eh}$ produces complex poles for $\Delta v/t$ smaller than a critical value.

In Fig. 4.9, we analyze this trend in more detail by looking at the evolution of the fundamental gap as a function of $\Delta v/t$ for various values of U/t: $U/t = 20$ (left panel), $U/t = 4$ (central panel), and $U/t = 1/4$ (right panel). We observe that the GT^{pp} and $G\overline{T}^{eh}$ gap merge to the exact one only for very small U/t. From Fig. 4.8, it becomes clear that the electron correlation is negligible for large $\Delta v/t$, which is also in line with the findings of Carrascal *et al.* [71] on the correlation energy. This explains why HF (blue curves) is exact for large $\Delta v/t$. Moreover, GW merges to HF since the screening tends to zero because of the large energy difference between the bonding and anti-bonding orbitals. The correlation part of the GT^{pp} self-energy, instead, is not negligible, and this can be attributed to the fact that the particle-particle polarizability that enters into the T-matrix expression does not go to zero in this limit.

Neutral excitations (Δv fixed)

We start by analyzing the triplet excitation. The triplet excited-state wave function $|^3\Psi^N\rangle$ [see Eq. (4.3)] does not depend on Δv, unlike the singlet ground-state wave function $|^1\Psi_0^N\rangle$. At $\Delta v = 0$ and $U = 0$, $|^1\Psi_0^N\rangle$ is a linear combination of $|\uparrow_1\downarrow_2\rangle$, $|\downarrow_1\uparrow_2\rangle$, $|\uparrow\downarrow_1\, 0_2\rangle$, and $|0_1\, \uparrow\downarrow_2\rangle$ with equal weights. The contribution from double occupancies, $|\uparrow\downarrow_1\, 0_2\rangle$ and $|0_1\, \uparrow\downarrow_2\rangle$, decreases by increasing U/t and increases by increasing $\Delta v/t$, as evidenced from Fig. 4.1. This excitation energy is well described by GW up to $U/t \approx 5$ for $\Delta v = 0$, as shown in Fig. 4.14 (top left panel); the error with respect to the exact result increases with $\Delta v/t$ (see top right panel of Fig. 4.14). In the case of the singlet excitation energy, instead, we observe that the GW error decreases by increasing $\Delta v/t$ (see bottom panels of Fig. 4.14). For the particle-particle T-matrix the results are shown in Fig. 4.15. For both the triplet and singlet transition energies, the error increases with Δv.

When we plot the neutral excitations of the electron-hole T-matrix as functions of U/t for different values of $\Delta v/t$ (as shown in Fig. 4.16), we observe that these neutral excitations become complex as U/t approaches the value of $\Delta v/t$. This behavior is consistent across all cases, occurring when the binding energy associated with the neutral excitation starts to rapidly increase. This increase indicates a significant strengthening of the electron-hole interaction, and it is observed for both triplet and singlet transitions. Previously, we found that GW provides a better description for triplet transitions compared to singlet ones. However, for T^{pp}, the opposite trend is observed. In the case of $\overline{T}^{eh}$, both types of excitations are described with roughly the same level of accuracy.

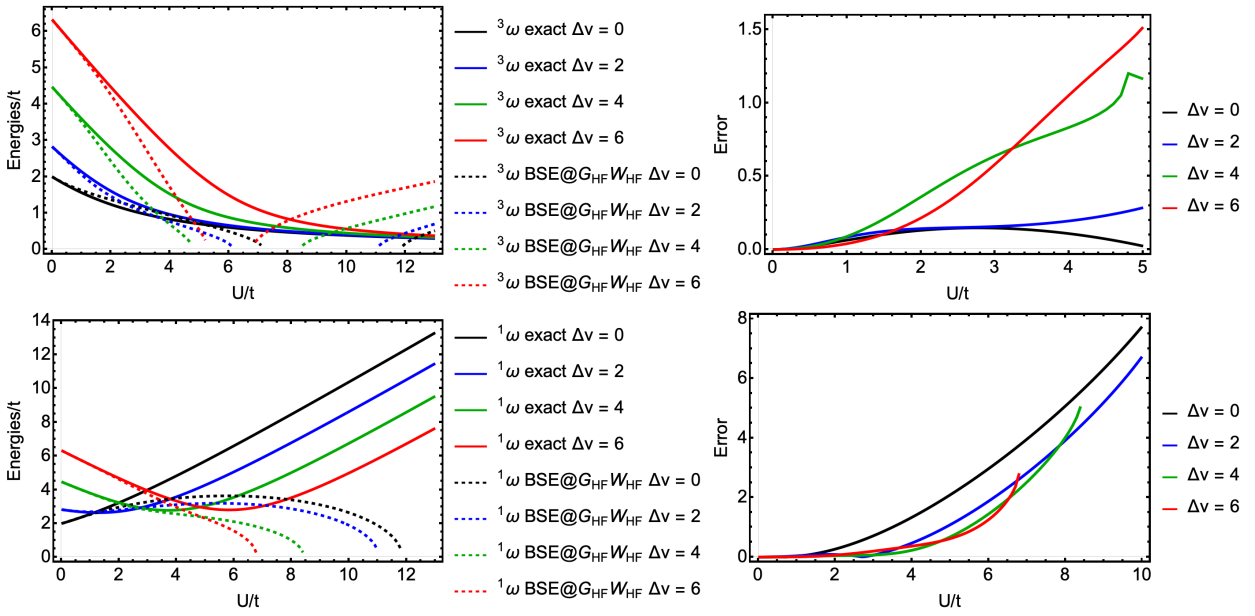

Figure 4.14 – Triplet (top) and singlet (bottom) BSE@$G_{\mathrm{HF}}W_{\mathrm{HF}}$ neutral excitations (left) and their corresponding error with respect to the exact results (right) as functions of U/t for various values of $\Delta v/t$.

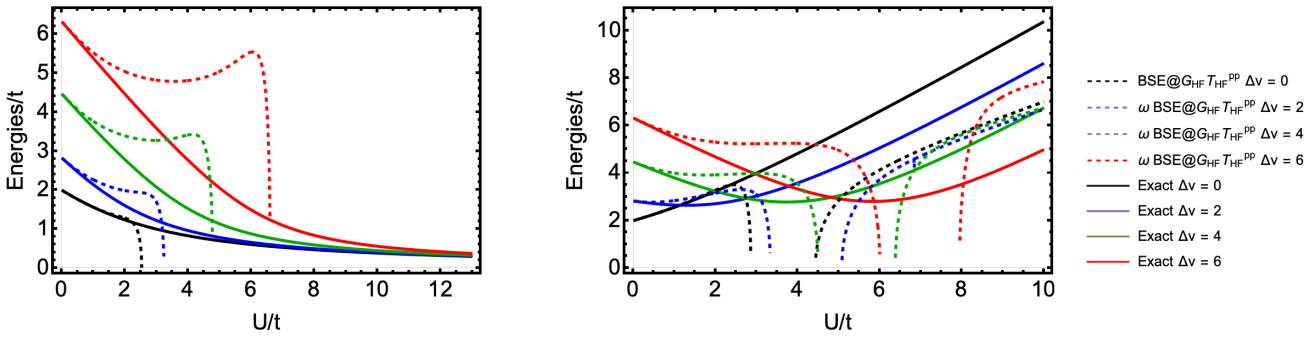

Figure 4.15 – Triplet (left) and singlet (right) BSE@$G_{\mathrm{HF}}T_{\mathrm{HF}}^{pp}$ neutral excitations as functions of U/t for various values of $\Delta v/t$.

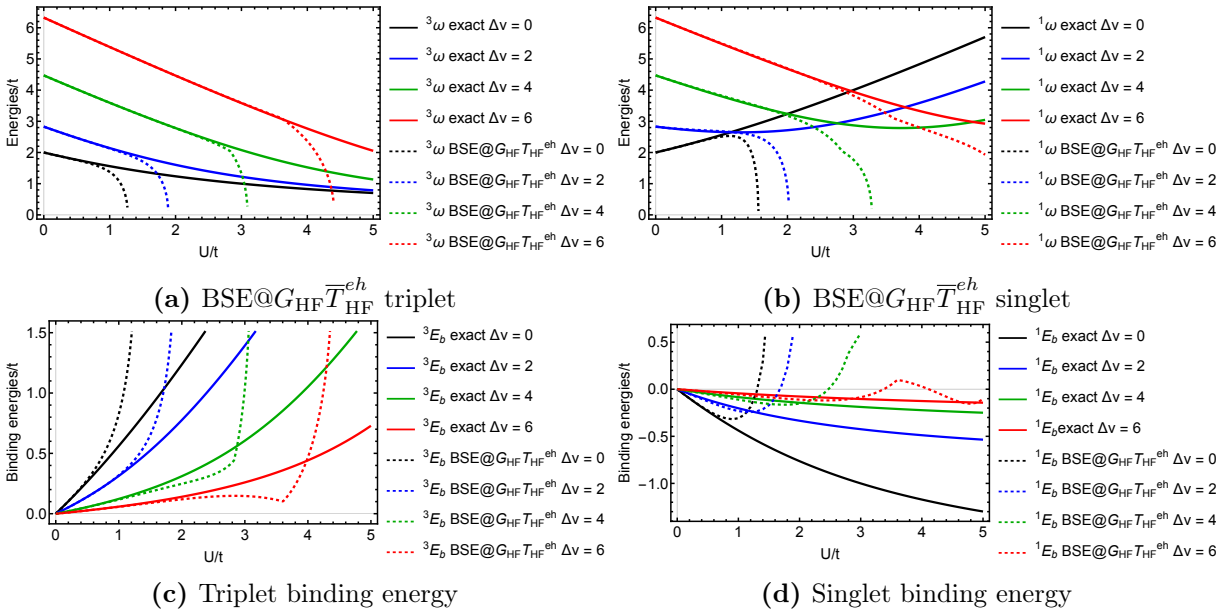

(a) BSE@$G_{\mathrm{HF}}\overline{T}_{\mathrm{HF}}^{eh}$ triplet **(b)** BSE@$G_{\mathrm{HF}}\overline{T}_{\mathrm{HF}}^{eh}$ singlet

(c) Triplet binding energy **(d)** Singlet binding energy

Figure 4.16 – BSE@$G_{\mathrm{HF}}\overline{T}_{\mathrm{HF}}^{eh}$ neutral excitations and their corresponding binding energies as functions of U/t for various values of $\Delta v/t$.

Neutral excitations (U fixed)

In the following, we select a sufficiently large value of U/t to place the system in a strong correlation regime when $\Delta v/t = 0$. As depicted in Fig. 4.1, for a fixed U/t value, when $\Delta v/t > U/t$, the ground state will exhibit a predominant weight on the doubly occupied site:

$$|^1\Psi_0^N\rangle \underset{\Delta v=0}{\approx} c_{10}\,|\uparrow_1\downarrow_2\rangle + c_{20}\,|\downarrow_1\uparrow_2\rangle \xrightarrow[\Delta v\gg U]{} |0_1\ \uparrow\downarrow_2\rangle \tag{4.39}$$

The triplet excited state remains unchanged with variations in U or Δv [see Eq. (4.3)]. Regarding the singlet excited state, we have

$$|^1\Psi_1^N\rangle \underset{\Delta v=0}{=} \frac{|\uparrow\downarrow_1\ 0_2\rangle - |0_1\ \uparrow\downarrow_2\rangle}{\sqrt{2}} \xrightarrow[\Delta v\gg U]{} c_{12}\,|\uparrow_1\downarrow_2\rangle + c_{22}\,|\downarrow_1\uparrow_2\rangle \tag{4.40}$$

In this limit, the singlet excited state wave function, instead of being composed by equally-weighted configurations consisting of electrons located on the same site at $\Delta v = 0$, mix configurations where electrons are located on both sites. Therefore, one could say that the singlet state goes towards a delocalization of particles from one site to another and, as a result, its wave function becomes similar to the one of triplet state. Consequently, both excitations $^3\omega$ and $^1\omega$ merge. In the following "delocalization" will refer to this situation in which singlet and triplet merge.

Furthermore, if we denote φ_b, φ_a as the molecular basis and ϕ_1, ϕ_2 as the site basis, we can express:

$$\varphi_b = c_1\phi_1 + c_2\phi_2 \xrightarrow[\Delta \mathrm{v}\gg \mathrm{U}]{} c_2\phi_2 \tag{4.41}$$

$$\varphi_a = c_1'\phi_1 + c_2'\phi_2 \xrightarrow[\Delta \mathrm{v}\gg \mathrm{U}]{} c_1'\phi_1 \tag{4.42}$$

Here, c_1, c_2, c_1', and c_2' are normalization coefficients that satisfy:

$$c_1^2 + c_2^2 = 1 \qquad (c_1')^2 + (c_2')^2 = 1 \tag{4.43}$$

Consequently, the singlet excited state is initially expressed as a linear combination of doubly occupied site configurations at $\Delta v/t = 0$. As we increase $\Delta v/t$, we progressively

add weight to the singly-occupied site configurations. When $\Delta v/t > U/t$, the particle on site 1 is delocalized to site 2, resulting in the merging of the triplet and singlet states. At this stage, the molecular orbitals resemble atomic orbitals, and the delocalization becomes observable even in the molecular basis.

In Fig. 4.17, we analyze in more detail the trend of the singlet and triplet excitation energies as a function of $\Delta v/t$. Here we only compare GW and GT^{pp} neutral excitations since $G\overline{T}^{eh}$ excitations become complex rather rapidly with increasing U/t. First, we notice that, since the singlet ground- and excited-state wave functions depend on $\Delta v/t$, the transition probabilities to the singlet states also depend on $\Delta v/t$. In particular, the exact transition probabilities

$$f_1 = \langle {}^1\Psi_0^N | \hat{n}_1 - \hat{n}_2 | {}^1\Psi_1^N \rangle \tag{4.44}$$

associated with the singlet excitation is peaked at $\Delta v/t = U/t$, as shown in the second-last panel of Fig. 4.17, which goes with a change in the site occupation numbers of the ground state and the corresponding singlet state ($\langle \hat{n}_i \rangle_0 \equiv \langle {}^1\Psi_0^N | \hat{n}_i | {}^1\Psi_0^N \rangle$ and $\langle \hat{n}_i \rangle_1 \equiv \langle {}^1\Psi_1^N | \hat{n}_i | {}^1\Psi_1^N \rangle$, respectively, with $i = 1$ or 2, indicating the site). We observe that, precisely at the value $\Delta v/t = U/t$, the singlet excitation energy calculated within the GT^{pp} approximation encounters a singularity in the case $U/t = 20$, whereas, for $U/t = 4$, the singularity disappears but the energy becomes complex below $\Delta v/t = 4$. The triplet excitation energy, instead, becomes complex below $\Delta v/t = U/t$. In the case of the GW approximation, the singlet excitation energy is complex over a slightly larger range of $\Delta v/t$ for $U/t = 20$, whereas it remains always real for $U/t = 4$ (see first panel of Fig. 4.17). Overall, for $\Delta v/t \ll U/t$, GW describes better than GT^{pp} the triplet excitation energy for $U/t = 20$ and both the singlet and triplet transitions for $U/t = 4$. The corresponding binding energies, however, suffer from the GW error in the fundamental gap.

For $\Delta v/t \gg U/t$, the exact and approximate kernels of the BSE become negligible so that the triplet and singlet excitation energies tend to the fundamental gap: HF and GW excitation energies merge to the exact ones since the HF and GW fundamental gaps tend also to the exact gap for large $\Delta v/t$ (see Fig. 4.9); instead, the GT^{pp} excitation energies tend to the GT^{pp} fundamental gap, which, as we discussed above, deviates from the exact one. Of course, these trends in the excitation energies influence the quality of the corresponding binding energies, which tend to the exact results in this limit.

In the strongly correlated case ($U/t = 20$ in the left panel of Fig. 4.17), we observe that for GW, the triplet excited state remains real at all times. On the other hand, the singlet excited state remains real throughout, except near the value $\Delta v/t \approx 20$, where a delocalisation occurs in the exact case, in the case of GT^{pp}. During this delocalization, the triplet state becomes real for GT^{pp}, and, slightly later, the same happens with the singlet state for GW. Simultaneously, there is a change in the sign of the binding energies, and they become real. This transition from complex eigenvalues to real eigenvalues may be attributed to the fact that when $\Delta v/t > U/t$, the singlet state becomes similar to the triplet state. Even if we use the exact quasiparticles with the same kernels (as seen in Fig. 4.18), the singlet state is significantly improved for the T^{pp} kernel, but the triplet state remains complex up to the delocalization event. With the W kernel, the singlet state becomes real up to $\Delta v/t \approx 10$, but the triplet state deteriorates.

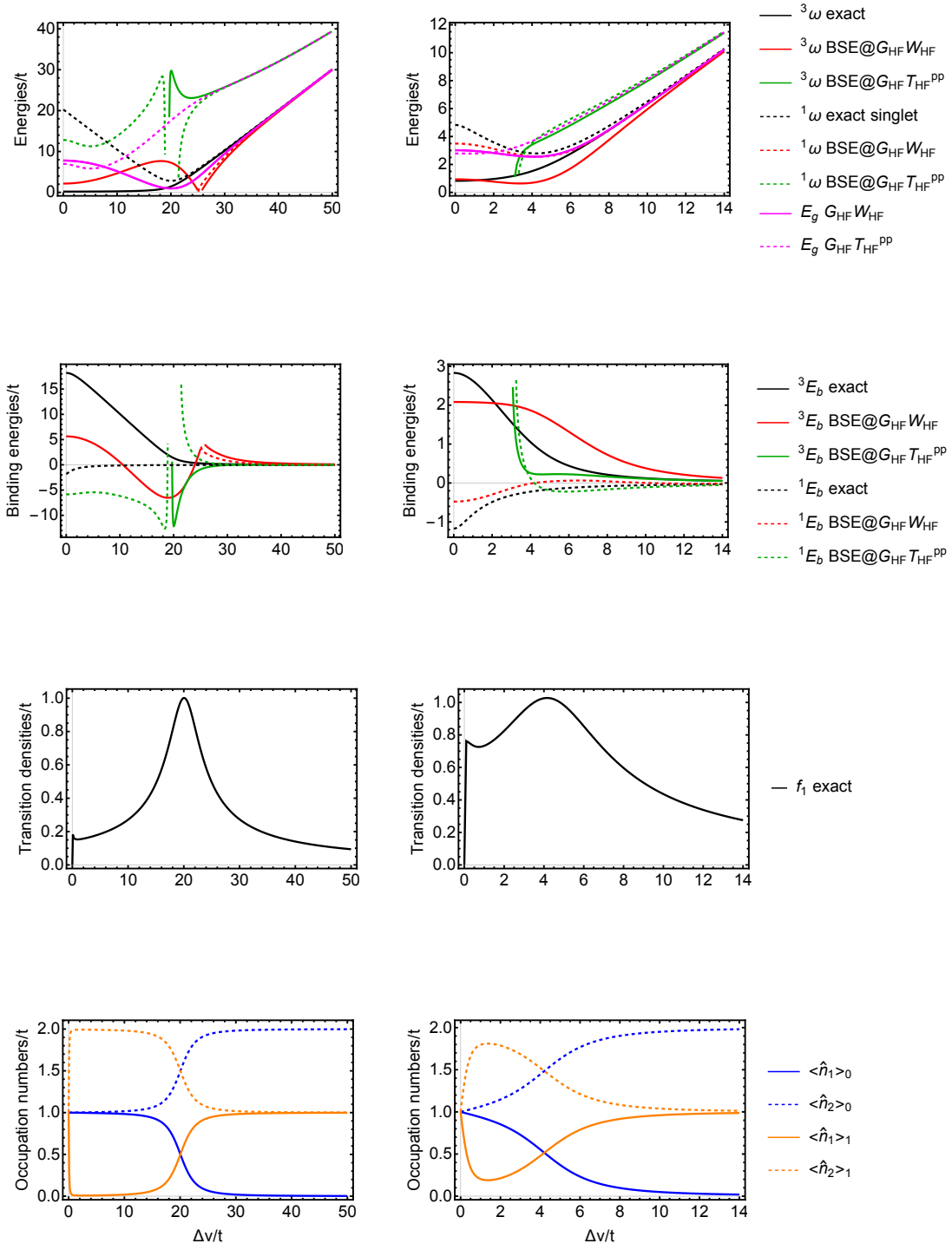

Figure 4.17 – Neutral excitations (first row), binding energies (second row), transitions densities (third row), and occupation numbers (fourth row) of the ground state and the first singlet excited state as functions of $\Delta v/t$. Results obtained for $U/t = 20$ (left column) and $U/t = 4$ (right column).

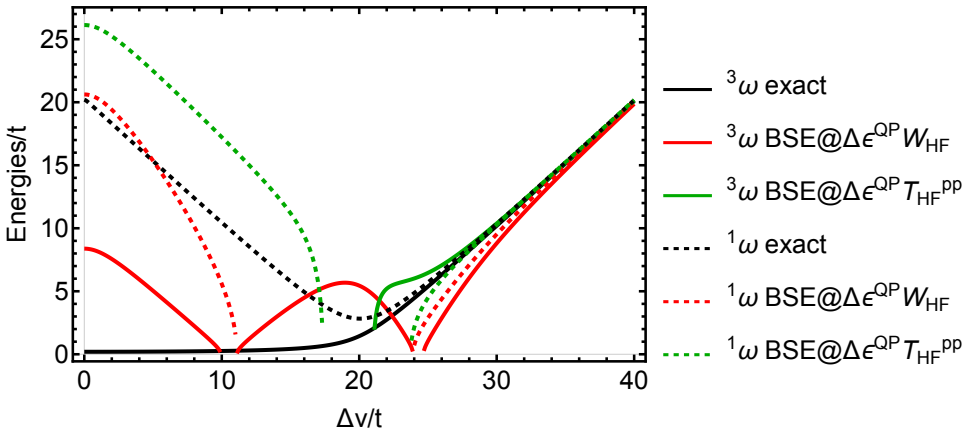

Figure 4.18 – Neutral excitations with exact quasiparticles and two different kernels as functions of $\Delta v/t$ and $U/t = 20$.

Comparison between the isolated and the interacting two-body system

The results we obtained for the symmetric dimer were not influenced by the choice of the Green's function as a starting point for W and $\overline{T}^{eh}$ when the varying parameter was U/t. This might seem unexpected because, when using the non-interacting Green's function, we are essentially studying the neutral excitations of an electron-hole system isolated from the rest of the system. On the other hand, with an interacting Green's function, we include the effects of the system's interaction with the surroundings. This situation suggests that there may exist an invariance and/or symmetry between G_0 and G_{HF} when the varying parameter is U/t. Consequently, it appears as if, in this specific case, whether we include the interaction with the rest of the system or not, we would not observe any significant difference in the behavior of the electron-hole polarizability.

However, when the variation parameter is $\Delta v/t$, we notice that the starting point has a significant impact on both polarizabilities. In Fig. 4.19, we present the neutral excitations and binding energies for $\overline{T}^{eh}$ and W. We begin with the exact results in the right panels of Fig. 4.19, with $U/t = 20$ as our setting. When we examine the exact neutral excitations (Fig. 4.19b), we observe that, prior to the delocalization, the exact triplet binding energy ^3E_b (Fig. 4.19d) is positive, indicating an attraction between the particle and the hole in the case of $^3\omega$. For the singlet, ^1E_b is negative but close to zero, suggesting a weak repulsion between the particle and the hole in the case of $^1\omega$. However, at the moment of delocalization and thereafter, the binding energies tend towards zero, and both excitations merge. In the exact case, when we set $U = 0$ (gray curve), the binding energies are zero, and the neutral excitations merge for all values of $\Delta v/t$ because the delocalization is instantaneous.

When we calculate W with G_0 (as indicated by the blue curves in Fig. 4.19b and Fig. 4.19d), both binding energies are negative and quite close to each other, signifying that the excitations are in close proximity. They merge at $\Delta v/t \approx 10$. However, when we also consider the interaction with the rest of the system (as shown by the red curves), a different pattern emerges. First, the delocalization occurs at $\Delta v/t > U/t$. This indicates that the presence of the second electron, considered in this case, delays the delocalization at higher $\Delta v/t$. Moreover, before the delocalization, the singlet excitation is complex, whereas with G_0, it was real. It is only when $\Delta v/t \approx 25$ that this excitation energy becomes real. After this point, both excitations gradually begin to merge. The influence of the second electron is also evident in the binding energies. ^3E_b changes its sign, ^1E_b becomes complex, and after the delocalization, both binding energies become real and tend toward zero.

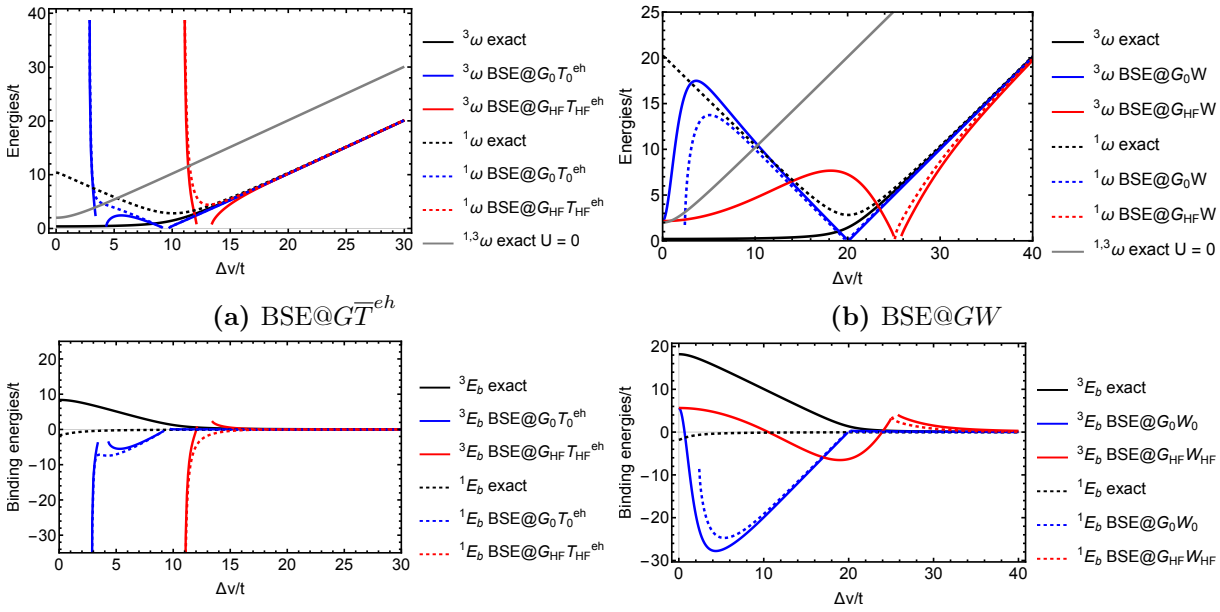

(a) BSE@$G\overline{T}^{eh}$ **(b)** BSE@GW

(c) BSE@$G\overline{T}^{eh}$ binding energies **(d)** BSE@GW binding energies

Figure 4.19 – Neutral excitations (top panels) and binding energies (bottom panels) for the electron-hole T-matrix (left column) and W (right column) for two different starting point as functions of $\Delta v/t$ at $U/t = 10$ for $\overline{T}^{eh}$ and $U/t = 20$ for W.

For $\overline{T}^{eh}$, we set the value $U/t = 10$. This time, with G_0 (as represented by the blue curves in Fig. 4.19a and Fig. 4.19c), we observe a singularity at $\Delta v/t \approx 4$, followed by a discontinuity around $\Delta v/t \approx 10$. With G_{HF} (depicted by the red curves), there is a single singularity that occurs at approximately $\Delta v/t \approx 13$. In both cases, the triplet and singlet eigenvalues merge and remain real, except at the singularities.

Finally, we consider the case of T^{pp}. When examining the neutral excitations (Fig. 4.20), we can see that with the use of G_0, the delocalization occurs at $\Delta v/t \approx 12$. However, with G_{HF}, we encounter a singularity at $\Delta v/t = 20$ which is slightly below the delocalization point of the exact case. Following this singularity, the excitations merge. In summary, we observe that whether we account for the many-body effects or not has a significant influence on the results. The results can shift and even become complex when using G_{HF} instead of G_0.

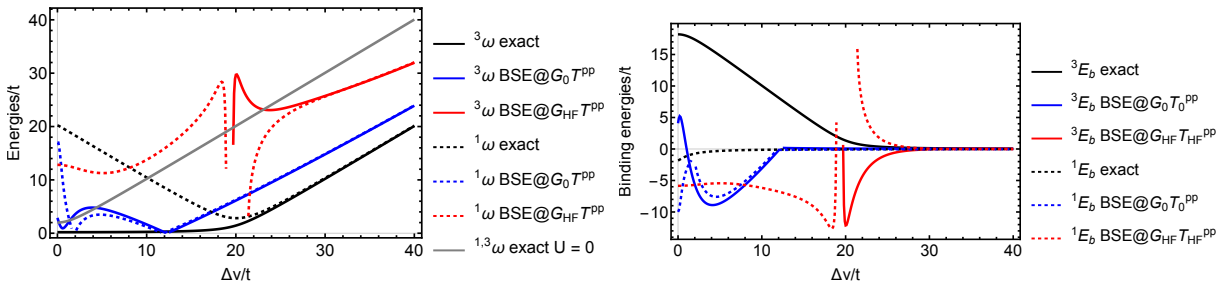

Figure 4.20 – Neutral excitations (top panel) and binding energies (bottom panel) for the particle-particle T-matrix for two different starting points as functions of $\Delta v/t$ at $U/t = 20$.

Chapter 5

The GW, particle-particle, and electron-hole T-matrix self-energies: application to molecular systems

This chapter is based on the following publication: R. Orlando, P. Romaniello, and P. F. Loos, *J. Chem. Phys.* (submitted) arXiv:2309.04167.

5.1 The standard form of Hedin's equations

The quasiparticle picture is a central concept in quantum many-body physics and chemistry as it provides a means to understand the behavior of electrons within a material or a molecule [33, 32, 34]. It emerges as an effective mapping from the complex many-body system to a simplified effective one-body system. Within the quasiparticle framework, the effects of collective excitations are incorporated by adding a dynamical correction to an effective one-body operator obtained from a simpler system, such as the non-interacting system. This correction, which contains Hartree (H), exchange (x), and correlation (c) effects, is known as the self-energy and is denoted as Σ. The famous Hedin equations, a self-consistent set of five integrodifferential equations, provide a route to calculate this self-energy [41]. Their conventional form is

$$\begin{aligned}
\Gamma(123) &= \delta(12)\delta(13) \\
&\quad + \Xi_{\text{xc}}(12;45)G(46)G(75)\Gamma(673) && \text{(5.1a)}\\
P(12) &= -\mathrm{i}G(13)G(41)\Gamma(342) && \text{(5.1b)}\\
W(12) &= v(12) + v(13)P(34)W(42) && \text{(5.1c)}\\
\Sigma_{\text{xc}}(12) &= \mathrm{i}G(14)W(1^+3)\Gamma(423) && \text{(5.1d)}\\
G(12) &= G_{\text{H}}(12) + G_{\text{H}}(13)\Sigma_{\text{xc}}(34)G(42) && \text{(5.1e)}
\end{aligned}$$

where P is the *irreducible* polarizability, W and v are the dynamically screened and bare Coulomb interactions, Γ is the *irreducible* three-point vertex which is completely defined by the four-point exchange-correlation kernel

$$\Xi_{\text{xc}}(12;1'2') = \frac{\delta\Sigma_{\text{xc}}(11')}{\delta G(2'2)} \tag{5.2}$$

In these equations, integrals over repeated indices are assumed, and, for instance, $1 = (\boldsymbol{r}_1, \sigma_1, t_1)$ is a space-spin-time variable and $1^+ = (\boldsymbol{r}_1, \sigma_1, t_1 + \delta)$ with $\delta \to 0^+$. G and G_{H} are the fully-interacting and Hartree Green's functions, respectively, and are linked by a Dyson equation, Eq. (5.1e). The exchange-correlation part of the self-energy is

$$\Sigma_{\text{xc}} = \Sigma_{\text{x}} + \Sigma_{\text{c}} = \Sigma - \Sigma_{\text{H}} \tag{5.3}$$

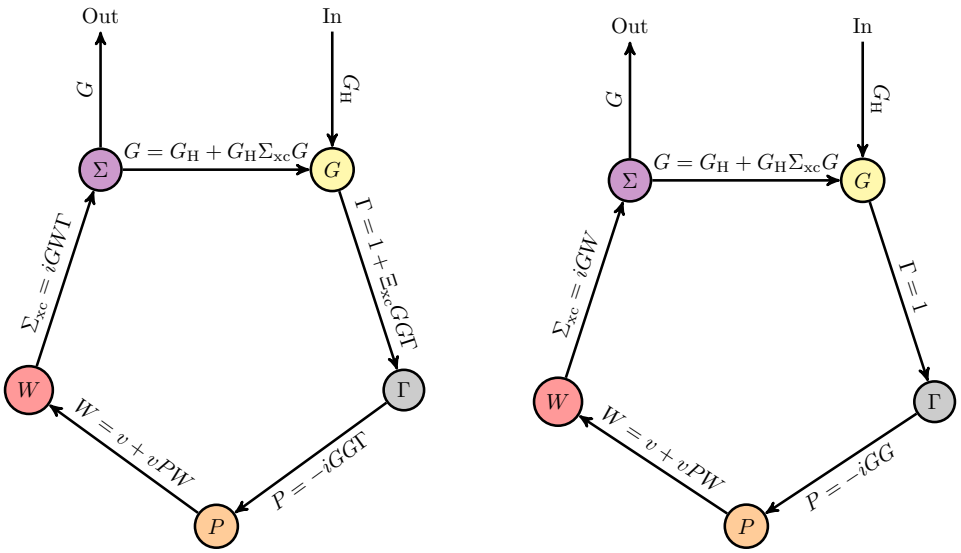

Figure 5.1 – Left: Hedin's pentagon yielding the exact Green's function G. Right: Hedin's pentagon yielding the GW approximation by setting $\Gamma = 1$ in the expression of P and Σ_{xc}.

where the Hartree and exchange components are respectively given by

$$\Sigma_{\text{H}}(12) = -\text{i}\delta(12)v(1^+3)G(33^+) \tag{5.4a}$$

$$\Sigma_{\text{x}}(12) = +\text{i}v(1^+2)G(12) \tag{5.4b}$$

with δ the Dirac delta function.

As shown schematically in Fig. 5.1, one can easily obtain the *GW form* of the self-energy from Hedin's equations by neglecting the vertex corrections, i.e., by setting $\Gamma(123) = \delta(12)\delta(13)$ in Eq. (5.1a), yielding $\Sigma_{\text{xc}}(12) = \text{i}G(12)W(12)$ [35, 1, 36, 37]. The *GW approximation* is obtained by additionally setting $\Gamma(123) = \delta(12)\delta(13)$ in the expression of the irreducible polarizability given in Eq. (5.1b),which reads $P^{\text{eh}}(12) = -\text{i}G(12)G(21)$. Diagrammatically, the GW equations correspond to a resummation of the direct ring (or bubble) diagrams [72] and its central quantity is the two-point dynamically screened Coulomb interaction $W(12) = v(12) + v(13)P^{\text{eh}}(34)W(42)$.

Other types of diagrams can be resummed, such as ladder diagrams [34]. This alternative resummation defines the T-matrix approximation that has the effective four-point interaction $T(12;1'2')$ as a key object [44, 45, 46, 47]. The two types of ladder diagrams, electron-hole (eh) and particle-particle (pp), produce two different channels for the T-matrix that one can write down in terms of Dyson equations with a random-phase approximation (RPA) [73, 74, 75, 76] polarizability as a kernel. It is however not natural to derive the T-matrix approximation from the conventional form of Hedin's equations.

5.2 An alternative form of Hedin's equations

Following Romaniello and coworkers [42] (see also Refs. [77, 78] for an alternative derivation), one can recast Hedin's equations in a more convenient way by considering the Dyson equation that links the non-interacting two-body correlation function

$$L_0(12;1'2') = G(12')G(21') \tag{5.5}$$

to the full two-body correlation function

$$\begin{aligned} L(12;1'2') = {} & L_0(12;1'2') \\ & + L_0(14;1'3)\Xi(35;46)L(62;52') \end{aligned} \tag{5.6}$$

Figure 5.2 – Left: Hedin's "square" yielding the exact Green's function G. Center: Hedin's square yielding the GW approximation by setting $\Xi = -\mathrm{i}V$. Right: Hedin's square yielding the T-matrix approximation by setting $L = L_0$ and $\Xi = \mathrm{i}T$.

with

$$\begin{aligned}\Xi(12;1'2') &= \frac{\delta\Sigma(11')}{\delta G(2'2)} = \Xi_{\mathrm{H}}(12;1'2') + \Xi_{\mathrm{xc}}(12;1'2') \\ &= -\mathrm{i}V(12;1'2') + \Xi_{\mathrm{xc}}(12;1'2')\end{aligned} \tag{5.7}$$

where it is convenient to introduce, at this stage, the four-point version of the bare and dynamically screened Coulomb interactions

$$V(12;1'2') = \delta(11')\delta(22')v(12) \tag{5.8a}$$
$$W(12;1'2') = \delta(12')\delta(1'2)W(12) \tag{5.8b}$$

Equation (5.6) is the Bethe-Salpeter equation of the two-body correlation function which completely defines the dynamically screened interaction via

$$\begin{aligned}W(12;1'2') = V(12;2'1') \\ - \mathrm{i}V(13;2'3')L(34;3'4')V(42;4'1')\end{aligned} \tag{5.9}$$

The latter equation is the four-point extension of the two-point expression $W(12) = v(12) + v(13)\chi(34)v(42)$, with $\chi(12) = -\mathrm{i}L(12;1^+2^+)$ the response function, which can be obtained from Eq. (5.1c) through the link $-\mathrm{i}L = (1 - vP)^{-1}P$. Together with Eqs (5.6) and (5.7), we obtain a more compact form of Hedin's equations (see Fig. 5.2):

$$\Sigma_c(12) = \mathrm{i}G(13)\Xi(35;26)L(64;54)v(14) \tag{5.10a}$$
$$G(12) = G_{\mathrm{Hx}}(12) + G_{\mathrm{Hx}}(13)\Sigma_{\mathrm{c}}(34)G(42) \tag{5.10b}$$

A different derivation of the standard and alternative forms of Hedin's equation is presented in Sec. 5.3 based on the equation-of-motion formalism.

5.3 Hedin's equations from the equation-of-motion formalism

Here, we present a different derivation of the standard (see Sec. 5.1) and alternative (see Sec. 5.2) forms of Hedin's equations. We refer the interested reader to Refs. [42, 34] for additional details.

From the equation-of-motion of the one-body Green's function [34]

$$G(12) = G_0(12) - \mathrm{i}G_0(13)v(34)G_2(34^+;24^{++}) \tag{5.11}$$

and the Dyson equation (5.1e) linking G_0 and G, one gets the following exact expression of the self-energy

$$\Sigma(12) = -\mathrm{i}v(1^+3)G_2(13;43^+)G^{-1}(42) \tag{5.12}$$

where G_2 is the two-body Green's function. One can then employ the Martin-Schwinger relation [79]

$$\frac{\delta G(12;[V_{\mathrm{ext}}])}{\delta V_{\mathrm{ext}}(3)} = -G_2(13;23^+;[V_{\mathrm{ext}}]) + G(12;[V_{\mathrm{ext}}])G(33^+;[V_{\mathrm{ext}}]) \tag{5.13}$$

which relates the one- and two-body Green's functions and the variation of G with respect to a fictitious external potential V_{ext}, to substitute G_2 in the expression of the self-energy. The equilibrium Green's functions are retrieved for $V_{\text{ext}} = 0$, i.e., $G(12, [V_{\text{ext}} = 0]) \equiv G(12)$ and $G_2(12;34;[V_{\text{ext}}] = 0) \equiv G_2(12;34)$. We hence arrive at

$$\Sigma(12) = \Sigma_{\text{H}}(12) + \mathrm{i}v(1^+3) \left.\frac{\delta G(14;[V_{\text{ext}}])}{\delta V_{\text{ext}}(3)}\right|_{V_{\text{ext}}=0} G^{-1}(42) \tag{5.14}$$

For notational convenience, in the following, we drop the functional dependence on V_{ext} and the limit $V_{\text{ext}} = 0$. Using the chain-rule derivative

$$\frac{\delta G(12)}{\delta V_{\text{ext}}(3)} = -G(14)\frac{\delta G^{-1}(45)}{\delta V_{\text{ext}}(3)}G(52) \tag{5.15}$$

we finally obtain

$$\Sigma(12) = \Sigma_{\text{H}}(12) - \mathrm{i}v(1^+3)G(14)\frac{\delta G^{-1}(42)}{\delta V_{\text{ext}}(3)} \tag{5.16}$$

where the second term of the right-hand side corresponds to the exchange-correlation part of the self-energy.

One can then recover Hedin's form of Σ_{xc} [see Eq. (5.1d)] by introducing the total classical potential $V_{\text{tot}} = V_{\text{H}} + V_{\text{ext}}$ [where $V_{\text{H}}(1) = -\mathrm{i}v(1^+2)G(22^+)$ is the local Hartree potential], as follows

$$\begin{aligned}\Sigma_{\text{xc}}(12) &= -\mathrm{i}v(1^+3)G(14)\frac{\delta G^{-1}(42)}{\delta V_{\text{tot}}(5)}\frac{\delta V_{\text{tot}}(5)}{\delta V_{\text{ext}}(3)} \\ &= \mathrm{i}G(14)W(13)\Gamma(423)\end{aligned} \tag{5.17}$$

where $W(12) = \epsilon^{-1}(13)v(32)$ is the dynamically screened Coulomb interaction,

$$\epsilon^{-1}(12) = \frac{\delta V_{\text{tot}}(1)}{\delta V_{\text{ext}}(2)} = \delta(12) + v(13)\chi(32) \tag{5.18}$$

is the inverse dielectric function [with $\chi(32) = -\mathrm{i}\,\delta G(33^+)/\delta V_{\text{ext}}(2)$], and $\Gamma(423) = -\delta G^{-1}(42)/\delta V_{\text{tot}}(3)$ is the *irreducible* vertex function [42, 34].

To recover the alternative form of the self-energy given in Eq. (5.10a), we substitute $G^{-1} = G_0^{-1} - V_{\text{ext}} - \Sigma$ into Eq. (5.17), and this yields

$$\begin{aligned}\Sigma_{\text{xc}}(12) &= \Sigma_{\text{x}}(12) + \mathrm{i}v(13)G(14)\frac{\delta\Sigma(42)}{\delta G(65)}\frac{\delta G(65)}{\delta V_{\text{ext}}(3)} \\ &= \Sigma_{\text{x}}(12) + \mathrm{i}v(13)G(14)\Xi(45;26)L(63;53)\end{aligned} \tag{5.19}$$

with the kernel Ξ given by Eq. (5.7) and the polarization propagator $L(12;32) = \delta G(13)/\delta V_{\text{ext}}(2)$.

5.4 Dyson equations

We are now in a position to explain how to obtain the GW and T-matrix expressions of the self-energy building on the work of Romaniello *et al.* [42] (see also Ref. [34]). Our goal is to approximate the expression of Σ_{c} given in Eq. (5.10a). There are basically two ways of doing this: approximating the kernel Ξ and/or the two-body correlation function L.

First, let us show how to recover the GW form that we have derived in Sec. 5.1. In GW, one assumes a simple local form for the kernel by setting $\Xi = \Xi_{\mathrm{H}} = -\mathrm{i}V$ in Eq. (5.10a). Hence, one gets

$$\Sigma_{\mathrm{c}}(12) = \mathrm{i}G(12)v(13)\chi(34)v(42) = \mathrm{i}G(12)W_c(12) \tag{5.20}$$

where $W_{\mathrm{c}} = v\chi v$ is the correlation part of W.

The GW approximation is obtained by setting $\Xi = \Xi_{\mathrm{H}} = -\mathrm{i}V$ in the expression of the propagator, which yields, thanks to Eq. (5.9), the following Dyson equation for the dynamically screened Coulomb interaction

$$\begin{aligned} W(12;1'2') = V(12;2'1') \\ + V(13;2'3')P^{\mathrm{eh}}(34';3'4)W(42;1'4') \end{aligned} \tag{5.21}$$

with

$$P^{\mathrm{eh}}(12;1'2') = -\mathrm{i}L_0(12;1'2') = -\mathrm{i}G(12')G(21') \tag{5.22}$$

the four-point version of the eh-RPA polarizability. Equations (5.21) and (5.22) are the key equations of the GW formalism and we will further discuss how to calculate these quantities in Sec. 5.5.

One can also include internal and/or external vertex corrections by improving the approximation of Ξ in Eqs. (5.6) and (5.10a), leading to various more involved and expensive approximations [80, 81, 82, 83, 84, 69, 42, 85, 86, 87, 88, 89, 78, 90, 91, 92, 93, 38, 94, 95, 96, 97, 98].

Let us explore the derivation of the T-matrix self-energy from the alternative form of Hedin's equations. The main idea is to rely on a rough approximation, $L = L_0$ in Eq. (5.6), for the response of the system but concentrate on a clever approximation of Ξ. In other words, one neglects the screening effects rather than the (external) vertex corrections. To this end, we introduce an effective four-point interaction T, such that

$$\Sigma(12) = \mathrm{i}G(43)T(13;24) \tag{5.23}$$

where, at this stage, T is an unknown four-point generalized effective interaction that is linked to the kernel through the functional derivative of Σ [see Eq. (5.7)] as follows

$$\Xi(12;1'2') = \mathrm{i}T(12;1'2') + \mathrm{i}G(34)\frac{\delta T(14;23)}{\delta G(2'2)} \tag{5.24}$$

Additionally, we neglect the variation of T with respect to G, i.e., $\delta T/\delta G = 0$, as it is usually done in the Bethe-Salpeter equation formalism [40], which yields $\Xi = \mathrm{i}T$. Using Eqs. (5.4a), (5.4b), and (5.10a), the self-energy then becomes an integral equation for T:

$$\begin{aligned} \Sigma(12) &= \mathrm{i}G(43)T(13;24) \\ &= \Sigma_{\mathrm{Hx}}(12) - v(16)G(13)G(46)G(65)T(35;24) \end{aligned} \tag{5.25}$$

Since $\mathrm{i}G(43)T(13;24)$ cannot be directly inverted to find T, several choices for T yield a suitable form for Σ. More explicitly, by factorizing one of the Green's functions stemming from L_0 or the other, i.e., $G(46)$ or $G(65)$ in Eq. (5.25), one generates the two channels of the T-matrix: the particle-particle T-matrix, T^{pp}, or the electron-hole T-matrix, T^{eh}. (By setting $T(35;24) = -v(35)\delta(32)\delta(54)$ in the right-hand side of Eq. (5.25) and by factorizing $G(12)$, one would recover the GW form of the self-energy.) More explicitly, they are defined via two distinct Dyson equations that read

$$\begin{aligned} T^{\mathrm{pp}}(12;1'2') = &-\overline{V}(12;1'2') \\ &+ \frac{1}{4}\overline{V}(12;34)P^{\mathrm{pp}}(34;56)T^{\mathrm{pp}}(65;1'2') \end{aligned} \tag{5.26a}$$

$$\begin{aligned} T^{\mathrm{eh}}(12;1'2') = &-\overline{V}(12;1'2') \\ &- V(12';34)\overline{P}^{\mathrm{eh}}(36;45)T^{\mathrm{eh}}(52;1'6) \end{aligned} \tag{5.26b}$$

Figure 5.3 – Schematic view of an electron attachment in the case of a closed-shell many-body system. The spin-up electron added to the system (gray) creates electron-hole pairs (wavy lines) in the spin-up and spin-down channels. The three different correlation channels that correspond to three-particle propagations are represented. Left: At the GW level (red), the effective interaction is created by the propagation of the electron-hole pairs. Center: At the pp T-matrix level (yellow), the effective interaction is created by the propagation of the added electron and the spin-up or spin-down excited electron. Right: At the eh T-matrix level (green), the effective interaction is created by the propagation of the added electron and the spin-up or spin-down hole.

where

$$\overline{V}(12;1'2') = V(12;1'2') - V(12;2'1') \tag{5.27}$$

is the four-point antisymmetrized Coulomb operator, and

$$P^{\text{pp}}(12;1'2') = +\text{i}[G(11')G(22') - G(12')G(21')] \tag{5.28a}$$

$$\overline{P}^{\text{eh}}(12;1'2') = -\text{i}G(12')G(21') \tag{5.28b}$$

are the pp-RPA [61] and an eh-RPA-like polarizabilities, respectively. Note that Eq. (5.26a) is a symmetrized version of the standard Dyson equation for T^{pp} given, for example, in Ref. [42]. It is obtained by exploiting the symmetry of the Bethe-Goldstone equation for G_2 with respect to the exchange of the two particles. In other words, the four terms that arise from $\overline{V}P^{\text{pp}}$ on the right-hand side of Eq. (5.26a) are topologically equivalent, which justifies the prefactor 1/4.

One can show that P^{pp} and P^{eh} have the same spin structure, but different time structures, while P^{eh} and $\overline{P}^{\text{eh}}$ have the same time structure, but different spin structures (see Fig. 5.3) [42, 34]. Equations (5.26a), (5.26b), (5.28a), and (5.28b) are the key equations of the T-matrix formalism, and we shall discuss in Sec. 5.5 how to explicitly compute their respective response functions and self-energies.

5.5 Response functions

As derived in Sec. 5.4, the dynamically screened Coulomb interaction W, Eq. (5.21), and the pp and eh T-matrices, Eqs. (5.26a) and (5.26b), are given in terms of Dyson equations, with a RPA polarizability P as kernel [see Eqs. (5.22), (5.28a), and (5.28b)]. However, they can be alternatively expressed in terms of a corresponding RPA response function χ. This provides a formulation for the self-energy in terms of the eigenvalues and eigenvectors of the RPA matrix. This expression is textbook knowledge for W and it has been recently derived for T^{pp} [59]. However, to the best of our knowledge, it is unknown for T^{eh}. In the following, we provide such an expression through a derivation that puts the three approximations on an equal footing.

Let us explain the procedure symbolically by considering generic quantities. We start by writing a general effective interaction Θ as a function of the irreducible polarizability via a Dyson equation, i.e.,

$$\Theta = \widetilde{V} + \widetilde{V}'P\Theta \tag{5.29}$$

where $\widetilde{V}$ and $\widetilde{V}'$ can be equal to $\pm V$ or $\pm\overline{V}$, and $P = P^{\text{eh}}$, P^{pp}, or $\overline{P}^{\text{eh}}$. From Eq. (5.29), one easily gets

$$\Theta = \epsilon^{-1}\widetilde{V} \tag{5.30}$$

where $\epsilon = 1 - \widetilde{V}'P$ is a generalized dielectric function. Substituting the expression of Θ in the right-hand side of Eq. (5.29) by its expression given in Eq. (5.30), we obtain the expression of the effective interaction as a function of the response function, that is,

$$\Theta = \widetilde{V} + \widetilde{V}'\chi\widetilde{V} \tag{5.31}$$

where $\chi = P\epsilon^{-1}$, from which

$$\chi^{-1} = P^{-1} - \widetilde{V}' \tag{5.32}$$

This is the key equation to compute the RPA response function χ for the three channels. In practice, the inversion of χ^{-1} is performed by investigating the eigensystem of its matrix representation. This is the aim of Sec. 5.6.

5.6 Self-energies

Throughout this paper, we assume real spinorbitals $\{\varphi_p(\boldsymbol{x})\}$, where the composite variable $\boldsymbol{x} = (\boldsymbol{r}, \sigma)$ gathers space and spin variables. The indices i, j, k, and l are occupied (hole) orbitals; a, b, c, and d are unoccupied (particle) orbitals; p, q, r, and s indicate arbitrary orbitals; and m and n label single excitations/deexcitations and double electron attachments/detachments, respectively. The one-electron energies, $\{\epsilon_p\}$, are quasiparticle energies and

$$v_{pqrs} = \iint \frac{\varphi_p(\boldsymbol{x}_1)\varphi_q(\boldsymbol{x}_2)\varphi_r(\boldsymbol{x}_1)\varphi_s(\boldsymbol{x}_2)}{|\boldsymbol{r}_1 - \boldsymbol{r}_2|} d\boldsymbol{x}_1 d\boldsymbol{x}_2 \tag{5.33}$$

are the usual bare two-electron integrals in the spinorbital basis. For any two-electron operator $\mathcal{O}$, we follow the same convention for its projection in the spinorbital basis, i.e.,

$$\mathcal{O}_{pqrs} = \iint \varphi_p(\boldsymbol{x}_1)\varphi_q(\boldsymbol{x}_2)\mathcal{O}(\boldsymbol{x}_1, \boldsymbol{x}_2)\varphi_r(\boldsymbol{x}_1)\varphi_s(\boldsymbol{x}_2) d\boldsymbol{x}_1 d\boldsymbol{x}_2 \tag{5.34}$$

5.6.1 *GW* self-energy

As stated previously, the eh polarizability P^{eh} defined in Eq. (5.22) used to compute W within the *GW* approximation [see Eq. (5.21)] is the usual eh-RPA polarizability where one performs a resummation of all direct ring diagrams. The corresponding response function χ^{eh} is constructed via the eigenvalues and eigenvectors of the eh-RPA linear system defined in the basis of excitations ($i \to a$) and deexcitations ($a \to i$) as follows:

$$\begin{pmatrix} \boldsymbol{A}^{\text{eh}} & \boldsymbol{B}^{\text{eh}} \\ -\boldsymbol{B}^{\text{eh}} & -\boldsymbol{A}^{\text{eh}} \end{pmatrix} \begin{pmatrix} \boldsymbol{X}^{\text{eh}} & \boldsymbol{Y}^{\text{eh}} \\ \boldsymbol{Y}^{\text{eh}} & \boldsymbol{X}^{\text{eh}} \end{pmatrix} = \begin{pmatrix} \boldsymbol{X}^{\text{eh}} & \boldsymbol{Y}^{\text{eh}} \\ \boldsymbol{Y}^{\text{eh}} & \boldsymbol{X}^{\text{eh}} \end{pmatrix} \begin{pmatrix} \boldsymbol{\Omega}^{\text{eh}} & \boldsymbol{0} \\ \boldsymbol{0} & -\boldsymbol{\Omega}^{\text{eh}} \end{pmatrix} \tag{5.35}$$

where the diagonal matrix $\boldsymbol{\Omega}^{\text{eh}}$ gathers the positive eigenvalues and the normalization condition is

$$\begin{pmatrix} \boldsymbol{X}^{\text{eh}} & \boldsymbol{Y}^{\text{eh}} \\ \boldsymbol{Y}^{\text{eh}} & \boldsymbol{X}^{\text{eh}} \end{pmatrix}^{\intercal} \begin{pmatrix} \boldsymbol{X}^{\text{eh}} & \boldsymbol{Y}^{\text{eh}} \\ -\boldsymbol{Y}^{\text{eh}} & -\boldsymbol{X}^{\text{eh}} \end{pmatrix} = \begin{pmatrix} \boldsymbol{1} & \boldsymbol{0} \\ \boldsymbol{0} & -\boldsymbol{1} \end{pmatrix} \tag{5.36}$$

The matrix elements of the (anti)resonant block $\boldsymbol{A}^{\text{eh}}$ and the coupling block $\boldsymbol{B}^{\text{eh}}$ read

$$A^{\text{eh}}_{ia,jb} = (\epsilon_a - \epsilon_i)\delta_{ij}\delta_{ab} + v_{ibaj} \tag{5.37a}$$

$$B^{\text{eh}}_{ia,jb} = v_{ijab} \tag{5.37b}$$

Note that, in Eqs. (5.37a) and (5.37b), only the direct Coulomb terms, v_{ibaj} and v_{ijab}, are present. Hence, the RPA eigenvalue problem (5.35) is often referred to as *direct* RPA (dRPA) in contrast to RPA with exchange (RPAx) where the corresponding exchange terms, $-v_{ibja}$ and $-v_{ijba}$, are also included.

Using these quantities, one can compute the elements of the dynamically screened Coulomb interaction as

$$W_{pqrs}(\omega) = v_{pqrs} + \sum_m \left[\frac{M^{\text{eh}}_{pr,n} M^{\text{eh}}_{qs,m}}{\omega - \Omega^{\text{eh}}_m + \mathrm{i}\eta} - \frac{M^{\text{eh}}_{pr,n} M^{\text{eh}}_{qs,m}}{\omega + \Omega^{\text{eh}}_m - \mathrm{i}\eta} \right] \tag{5.38}$$

where the screened two-electron integrals (or transition densities) read

$$M^{\mathrm{eh}}_{pq,m} = \sum_{jb} v_{pjqb}\big(X^{\mathrm{eh}}_{jb,m} + Y^{\mathrm{eh}}_{jb,m}\big) \tag{5.39}$$

and η is a positive infinitesimal. Performing the final convolution of the Green's function and the dynamically screened interaction, the elements of the correlation part of the GW self-energy are found to be

$$\Sigma^{\mathrm{eh}}_{\mathrm{c},pq}(\omega) = \sum_{im} \frac{M^{\mathrm{eh}}_{pi,m} M^{\mathrm{eh}}_{qi,m}}{\omega - \epsilon_i + \Omega^{\mathrm{eh}}_m - \mathrm{i}\eta} + \sum_{am} \frac{M^{\mathrm{eh}}_{pa,m} M^{\mathrm{eh}}_{qa,m}}{\omega - \epsilon_a - \Omega^{\mathrm{eh}}_m + \mathrm{i}\eta} \tag{5.40}$$

In the popular one-shot scheme, known as G_0W_0 in the case of the GW approximation [99, 100, 101, 102, 103, 104, 105], one often considers the diagonal part of the self-energy and performs a single iteration of Hedin's equations. Considering a Hartree-Fock (HF) starting point, the quasiparticle energies are thus obtained by solving the non-linear quasiparticle equation for each orbital p:

$$\omega - \epsilon^{\mathrm{HF}}_p - \mathrm{Re}[\Sigma^{\mathrm{eh}}_{\mathrm{c},pp}(\omega)] = 0 \tag{5.41}$$

It is also practically convenient to compute the renormalization factor Z^{eh}_p that gives the spectral weight of the corresponding quasiparticle solution ϵ_p:

$$\big(Z^{\mathrm{eh}}_p\big)^{-1} = 1 - \left.\frac{\partial\, \mathrm{Re}[\Sigma^{\mathrm{eh}}_{\mathrm{c},pp}(\omega)]}{\partial\omega}\right|_{\omega=\epsilon_p} \tag{5.42}$$

which can easily be shown to be strictly restricted between 0 and 1 in the case of GW. When the so-called quasiparticle approximation holds, the weight of the quasiparticle equation is close to unity, while the remaining weight is distributed among the satellite (or shake-up) transitions.

5.6.2 Particle-particle T-matrix self-energy

The pp response function, χ^{pp}, is built using the eigenvalues and eigenvectors of the pp-RPA problem, a non-Hermitian eigenvalue problem expressed in the basis of double electron attachments (ee) and double electron detachments (hh) [61, 106, 63]:

$$\begin{pmatrix} \boldsymbol{A}^{\mathrm{ee}} & \boldsymbol{B}^{\mathrm{ee,hh}} \\ -(\boldsymbol{B}^{\mathrm{ee,hh}})^{\intercal} & -\boldsymbol{C}^{\mathrm{hh}} \end{pmatrix} \begin{pmatrix} \boldsymbol{X}^{\mathrm{ee}} & \boldsymbol{Y}^{\mathrm{hh}} \\ \boldsymbol{Y}^{\mathrm{ee}} & \boldsymbol{X}^{\mathrm{hh}} \end{pmatrix} = \begin{pmatrix} \boldsymbol{X}^{\mathrm{ee}} & \boldsymbol{Y}^{\mathrm{hh}} \\ \boldsymbol{Y}^{\mathrm{ee}} & \boldsymbol{X}^{\mathrm{hh}} \end{pmatrix} \begin{pmatrix} \boldsymbol{\Omega}^{\mathrm{ee}} & \boldsymbol{0} \\ \boldsymbol{0} & \boldsymbol{\Omega}^{\mathrm{hh}} \end{pmatrix} \tag{5.43}$$

where the diagonal matrices $\boldsymbol{\Omega}^{\mathrm{ee}}$ and $\boldsymbol{\Omega}^{\mathrm{hh}}$ collect the double electron attachment and double electron removal energies, and the normalization condition is

$$\begin{pmatrix} \boldsymbol{X}^{\mathrm{ee}} & \boldsymbol{Y}^{\mathrm{hh}} \\ \boldsymbol{Y}^{\mathrm{ee}} & \boldsymbol{X}^{\mathrm{hh}} \end{pmatrix}^{\intercal} \begin{pmatrix} \boldsymbol{X}^{\mathrm{ee}} & \boldsymbol{Y}^{\mathrm{hh}} \\ -\boldsymbol{Y}^{\mathrm{ee}} & -\boldsymbol{X}^{\mathrm{hh}} \end{pmatrix} = \begin{pmatrix} \boldsymbol{1} & \boldsymbol{0} \\ \boldsymbol{0} & -\boldsymbol{1} \end{pmatrix} \tag{5.44}$$

The matrix elements of the different blocks are

$$A^{\mathrm{ee}}_{ab,cd} = (\epsilon_a + \epsilon_b)\delta_{ac}\delta_{bd} + \overline{v}_{abcd} \tag{5.45a}$$

$$B^{\mathrm{ee,hh}}_{ab,ij} = \overline{v}_{abij} \tag{5.45b}$$

$$C^{\mathrm{hh}}_{ij,kl} = -(\epsilon_i + \epsilon_j)\delta_{ik}\delta_{jl} + \overline{v}_{ijkl} \tag{5.45c}$$

where $\overline{v}_{pqrs} = v_{pqrs} - v_{pqsr}$ are the antisymmetrized two-electron integrals.

As first derived by Zhang *et al.*, the elements of the pp T-matrix are [59]

$$T^{\mathrm{pp}}_{pqrs}(\omega) = \overline{v}_{pqrs} + \sum_{n} \left[\frac{M^{\mathrm{ee}}_{pq,n} M^{\mathrm{ee}}_{rs,n}}{\omega - \Omega^{\mathrm{ee}}_{n} + \mathrm{i}\eta} - \frac{M^{\mathrm{hh}}_{pq,n} M^{\mathrm{hh}}_{rs,m}}{\omega + \Omega^{\mathrm{hh}}_{n} - \mathrm{i}\eta} \right] \tag{5.46}$$

where

$$M^{\mathrm{ee}}_{pq,n} = \sum_{c<d} \overline{v}_{pqcd} X^{\mathrm{ee}}_{cd,n} + \sum_{k<l} \overline{v}_{pqkl} Y^{\mathrm{ee}}_{kl,n} \tag{5.47a}$$

$$M^{\mathrm{hh}}_{pq,n} = \sum_{c<d} \overline{v}_{pqcd} X^{\mathrm{hh}}_{cd,n} + \sum_{k<l} \overline{v}_{pqkl} Y^{\mathrm{hh}}_{kl,n} \tag{5.47b}$$

while the corresponding self-energy elements read

$$\Sigma^{\mathrm{pp}}_{\mathrm{c},pq}(\omega) = \sum_{in} \frac{M^{\mathrm{ee}}_{pi,n} M^{\mathrm{ee}}_{qi,n}}{\omega + \epsilon_i - \Omega^{\mathrm{ee}}_{n} + \mathrm{i}\eta} + \sum_{an} \frac{M^{\mathrm{hh}}_{pa,n} M^{\mathrm{hh}}_{qa,n}}{\omega + \epsilon_a - \Omega^{\mathrm{hh}}_{n} - \mathrm{i}\eta} \tag{5.48}$$

with the renormalization factor fulfilling $0 \leq Z^{\mathrm{pp}}_{p} \leq 1$. As in Sec. 5.6.1, one denotes the one-shot scheme as $G_0 T^{\mathrm{pp}}_{0}$.

5.6.3 Electron-hole T-matrix self-energy

The eh response function, $\overline{\chi}^{\mathrm{eh}}$, is obtained from a distinct RPA problem that is very similar to the usual eh-RPA problem discussed above [see Eq. (5.35)]. However, one has to consider index exchanges between the two coupled single (de)excitations (see Fig. 5.3). More explicitly, it reads

$$\begin{pmatrix} \overline{\boldsymbol{A}}^{\mathrm{eh}} & \overline{\boldsymbol{B}}^{\mathrm{eh}} \\ -\overline{\boldsymbol{B}}^{\mathrm{eh}} & -\overline{\boldsymbol{A}}^{\mathrm{eh}} \end{pmatrix} \begin{pmatrix} \overline{\boldsymbol{X}}^{\mathrm{eh}} & \overline{\boldsymbol{Y}}^{\mathrm{eh}} \\ \overline{\boldsymbol{Y}}^{\mathrm{eh}} & \overline{\boldsymbol{X}}^{\mathrm{eh}} \end{pmatrix} = \begin{pmatrix} \overline{\boldsymbol{X}}^{\mathrm{eh}} & \overline{\boldsymbol{Y}}^{\mathrm{eh}} \\ \overline{\boldsymbol{Y}}^{\mathrm{eh}} & \overline{\boldsymbol{X}}^{\mathrm{eh}} \end{pmatrix} \begin{pmatrix} \overline{\boldsymbol{\Omega}}^{\mathrm{eh}} & \boldsymbol{0} \\ \boldsymbol{0} & -\overline{\boldsymbol{\Omega}}^{\mathrm{eh}} \end{pmatrix} \tag{5.49}$$

with a similar normalization condition as in Eq. (5.36), and where

$$\overline{A}^{\mathrm{eh}}_{ia,jb} = (\epsilon_a - \epsilon_i)\delta_{ij}\delta_{ab} - v_{ibja} \tag{5.50a}$$

$$\overline{B}^{\mathrm{eh}}_{ia,jb} = -v_{ijba} \tag{5.50b}$$

One would notice that it is exactly the "exchange" version of the usual eh-RPA problem defined in Eq. (5.35). After a careful derivation, one eventually ends up with the following expression for the elements of the eh T-matrix

$$T^{\mathrm{eh}}_{pqrs}(\omega) = \overline{v}_{pqrs} - \sum_{m} \left[\frac{L^{\mathrm{eh}}_{ps,m} R^{\mathrm{eh}}_{rq,m}}{\omega - \overline{\Omega}^{\mathrm{eh}}_{m} + \mathrm{i}\eta} - \frac{L^{\mathrm{eh}}_{sp} R^{\mathrm{eh}}_{qr,m}}{\omega + \overline{\Omega}^{\mathrm{eh}}_{m} - \mathrm{i}\eta} \right] \tag{5.51}$$

which has the peculiarity of having numerators composed of two different sets of transition densities:

$$L^{\mathrm{eh}}_{pq,m} = \sum_{jb} \left(v_{pjbq} \overline{X}^{\mathrm{eh}}_{jb,m} + v_{pbjq} \overline{Y}^{\mathrm{eh}}_{jb,m} \right) \tag{5.52a}$$

$$R^{\mathrm{eh}}_{pq,m} = \sum_{jb} \left(\overline{v}_{pjbq} \overline{X}^{\mathrm{eh}}_{jb,m} + \overline{v}_{pbjq} \overline{Y}^{\mathrm{eh}}_{jb,m} \right) \tag{5.52b}$$

Figure 5.4 – Error (in eV) with respect to ΔCCSD(T) in the principal IPs of the $GW20$ set computed at the G_0W_0, $G_0T_0^{\text{pp}}$, and $G_0T_0^{\text{eh}}$ levels with the def2-TVZPP basis. Raw data can be found in Table 5.1.

which are not symmetric with the exchange of the indices p and q. The resulting elements of the correlation part of the eh T-matrix self-energy are

$$\overline{\Sigma}^{\text{eh}}_{\text{c},pq}(\omega) = \sum_{im} \frac{L^{\text{eh}}_{ip,m} R^{\text{eh}}_{iq,m}}{\omega - \epsilon_i + \overline{\Omega}^{\text{eh}}_m - \mathrm{i}\eta} + \sum_{am} \frac{L^{\text{eh}}_{pa,m} R^{\text{eh}}_{qa,m}}{\omega - \epsilon_a - \overline{\Omega}^{\text{eh}}_m + \mathrm{i}\eta} \tag{5.53}$$

Equation (5.53) is the central result of the present manuscript. We denote the corresponding one-shot scheme as $G_0T_0^{\text{eh}}$.

The renormalization factor associated with the eh T-matrix self-energy is expressed as follows:

$$\overline{Z}^{\text{eh}}_p = \frac{1}{1 - \left. \frac{\partial \, \text{Re}[\overline{\Sigma}^{\text{eh}}_{\text{c},pp}(\omega)]}{\partial \omega} \right|_{\omega=\epsilon_p}} \tag{5.54}$$

It is important to note that, unlike in GW and pp T-matrix, $\overline{Z}^{\text{eh}}_p$ is not confined within the interval of 0 to 1, and its values can extend beyond this range, including values below 0 and above 1. Indeed, while the values of the self-energy derivate are always positive for GW and GT^{pp}, negative values can be reached in the GT^{eh} formalism. This can be traced back to the eigenvectors of the eh-RPA-like matrix. Notably, in the work by Muller *et al.* [56], it is mentioned that the spectral function of the eh T-matrix can assume negative values as observed in cases like iron. This phenomenon, linked to the violation of causality, directly arises due to the absence of certain self-energy diagrams. It is acknowledged that these extreme renormalization effects should be regarded as unphysical.

In the context of solids, the eh T-matrix approximation is often used to study electron-magnon scattering processes in ferromagnetic systems [56, 107, 57, 108]. However, to the best of our knowledge, calculations of quasiparticle energies in realistic molecular systems within the eh T-matrix approximation have never been reported in the literature

5.7 Results and discussion

In this study, we exclusively employ the restricted formalism due to all investigated systems possessing a closed-shell singlet ground state. Our calculations are initiated from Hartree-Fock (HF) orbitals and energies. We focus on a set composed by charged excitations where we specifically consider principal ionization potentials (IPs). This set consists of 20 atoms and molecules, known as the $GW20$ set, which is part of the $GW100$ test set [109] and has been previously explored in Refs. [92, 29]. The geometries for the $GW20$ set are extracted from Ref. [109].

Using the def2-TZVPP basis, we employ the three one-shot schemes discussed in the present paper to compute the IPs: G_0W_0, $G_0T_0^{\text{pp}}$, and $G_0T_0^{\text{eh}}$. These three many-body formalisms have been implemented in QUACK, an open-source software for emerging quantum electronic structure methods. For each scheme, we compute the quasiparticle energies as explained in Sec. 5.6.1 using Newton's method. As reference data, we rely on the IPs computed (in the same basis) via energy difference between the cation and the neutral species using coupled cluster singles and doubles with perturbative triples [ΔCCSD(T)] [110]. Throughout our calculations, we set the positive infinitesimal η to zero.

The principal IPs of the $GW20$ test are reported in Table 5.1 and the error with respect to the ΔCCSD(T) reference values are represented in Fig. 5.4. As previously reported

Table 5.1 – Principal IPs (in eV) of the $GW20$ set computed at various levels of theory using the def2-TZVPP basis. The corresponding renormalization factor is reported in parenthesis. The mean absolute error (MAE), mean signed error (MSE), root-mean-square error (RMSE), and maximum error (Max) with respect to the reference ΔCCSD(T) values are reported.

Mol.	G_0W_0	$G_0T_0^{\mathrm{pp}}$	$G_0T_0^{\mathrm{eh}}$	ΔCCSD(T)
He	24.60(0.96)	24.75(0.99)	24.26(0.91)	24.51
Ne	21.35(0.95)	21.02(0.96)	18.69(0.83)	21.32
H_2	16.48(0.95)	16.26(0.99)	17.26(0.86)	16.40
Li_2	5.29(0.92)	5.04(0.98)		5.27
LiH	8.15(0.92)	8.14(0.98)	7.35(0.46)	7.96
HF	16.17(0.94)	15.65(0.95)	13.23(0.76)	16.03
Ar	15.73(0.95)	15.52(0.97)	16.03(0.83)	15.54
H_2O	12.82(0.94)	12.28(0.95)	10.48(0.73)	12.56
LiF	11.31(0.92)	10.88(0.94)	7.98(0.69)	11.32
HCl	12.77(0.95)	12.50(0.96)	13.21(0.79)	12.59
BeO	9.76(0.98)	9.20(0.93)	7.94(0.33)	9.94
CO	15.00(0.93)	14.44(0.95)	15.42(0.24)	14.21
N_2	16.30(0.93)	15.69(0.94)	14.72(0.69)	15.57
CH_4	14.74(0.94)	14.27(0.96)	14.46(0.79)	14.37
BH_3	13.64(0.94)	13.30(0.97)	13.87(0.81)	13.28
NH_3	11.14(0.94)	10.64(0.95)	9.87(0.73)	10.68
BF	11.26(0.94)	10.91(0.98)	16.18(0.65)	11.09
BN	11.69(0.92)	11.11(0.94)		11.89
SH_2	10.48(0.94)	10.17(0.96)	11.28(0.76)	10.31
F_2	16.27(0.93)	15.36(0.93)		15.71
MAE	0.26	0.25	1.59	
MSE	0.22	−0.17	−0.45	
RMSE	0.34	0.32	2.11	
Max	0.79	0.78	5.09	

[a] Calculation of T^{eh} performed in the Tamm-Dancoff approximation due to triplet instabilities.

Figure 5.5 – Self-energy (blue curves) associated with the HOMO orbital of Ar (left) and BeO (right) computed at the G_0W_0 (top), $G_0T_0^{\text{pp}}$ (middle), and $G_0T_0^{\text{eh}}$ (bottom) levels with the def2-TVZPP basis. The solutions of the quasiparticle equation are given by the intersection of the blue and red curves.

in the literature [29], G_0W_0 and $G_0T_0^{\text{pp}}$ have very similar mean absolute errors (MAEs) for this set of small systems (0.26 eV *vs* 0.26 eV), while their respective mean signed errors (MSEs) are almost exactly opposite (0.22 eV *vs* −0.17 eV). The $G_0T_0^{\text{eh}}$ scheme has much larger MAE (1.59 eV) and MSE (−0.45 eV). Figure 5.4 clearly shows that large errors are observed for some systems, like Ne, HF, LiF, BeO, BF, and F_2. Moreover, even at equilibrium geometry, triplet instabilities are encountered for several systems (Li_2, BN, and F_2). This forced us to compute T^{eh} within the Tamm-Dancoff approximation which consists in setting $\overline{\boldsymbol{B}} = \mathbf{0}$ in Eq. (5.49). From these results, it is clear that the performances of $G_0T_0^{\text{eh}}$ are clearly inferior to those of G_0W_0 and $G_0T_0^{\text{pp}}$. This explains the development of the screened version of the eh T-matrix in solid-state calculations [111, 42, 112, 53, 113, 114, 115, 116]. Qualitatively at least, the poor performance of $G_0T_0^{\text{eh}}$ can be explained by the fact that T^{eh} is constructed with the eigenvectors and eigenvalues associated with the triplet states of the system computed at the RPAx level [see Eq. (5.49) and the discussion below it] starting from a singlet HF ground-state reference. It is well known that this usually leads to poorly described triplet states and, often, triplet instabilities [117].

In Fig. 5.5, we plot the variation of the G_0W_0 (top), $G_0T_0^{\text{pp}}$ (middle), and $G_0T_0^{\text{eh}}$ (bottom) self-energies associated with the highest-occupied molecular orbital (HOMO) as functions of ω for two systems: Ar, a weakly correlated system, and BeO, a more strongly correlated system. The solutions of the quasiparticle equation are given by the intersection of the blue and red curves. At the G_0W_0 and $G_0T_0^{\text{pp}}$ levels, the two systems exhibit similar behavior with well-defined quasiparticle solutions with respective weights of 0.95 (0.98) and 0.97 (0.93) for Ar (BeO), as reported in Table 5.1. This is graphically evidenced by the small values of the self-energy derivative in the central region of the graphs. At the $G_0T_0^{\text{eh}}$ level, it is clear that the variations of the self-energy are more pronounced. Contrary to G_0W_0 and $G_0T_0^{\text{pp}}$, the $G_0T_0^{\text{eh}}$ self-energy derivative can take positive values, as mentioned in Sec. 5.6.3. For Ar, the quasiparticle solution has a weight of 0.83 and the behavior of the $G_0T_0^{\text{eh}}$ self-energy is quite standard. The case of BeO is more interesting though as the solution around −8 eV reached from the HF starting value using Newton's method has a small weight (0.33) and cannot really be classified as a quasiparticle solution. Another solution with a similar weight can be located around −22 eV. This example represents a clear breakdown of the quasiparticle approximation.

Chapter 6

Conclusions and Perspectives

In this thesis, we have studied three approximations based on Green's function many-body perturbation theory to obtain the charged and neutral excitations of many-body systems. As a first step, these approximations have been studied, implemented, and tested on a simple model system: the two-site Hubbard model at half-filling. Such types of quantum mechanical models for which it is possible to solve explicitly the Schrödinger equation have ongoing value and are useful both for illuminating more complicated systems and for testing and developing theoretical approaches. We have then extended our analysis to real molecular systems.

Based on the exactly-solvable asymmetric Hubbard dimer model, we have gauged the accuracy of the charged and neutral excitation energies in different correlation regimes obtained with three distinct approximations of the self-energy: the GW, the particle-particle T-matrix, and the particle-hole T-matrix approximations which correspond to a resummation of different families of diagrams. In particular, using these approximate self-energies and their corresponding kernel, excited-state energies were computed within the Bethe-Salpeter formalism. Overall, we have found that the GW approximation works better than the GT approximations both for the quasiparticle energies and the neutral excitation energies as functions of the degree of correlation (U/t) and asymmetry ($\Delta v/t$) in the system. In particular, the GT^{pp} quasiparticle energies do not exhibit the correct behavior as $\Delta v/t \to \infty$. In this limit, correlation becomes negligible in the exact case and in GW, but not in GT, because of the non-vanishing particle-particle polarizability which enters into the T-matrix expression. Because of this, the behavior of the neutral excitation energies is also incorrect in the large $\Delta v/t$ limit, unlike their HF and GW counterparts. This suggests that the quality of the GT results can be sensitive to inhomogeneities in real materials. To shed more light on this issue it would be interesting to analyze this issue in real materials [118, 119]. Moreover, GT seems to be more sensitive to the starting Green's function, at least for the Hubbard dimer, and this can strongly affect the quality of the results.

We have then extended our study to real molecules. In finite systems, the GW self-energy is usually implemented using the response function χ rather than the polarizability P to compute W. While the RPA expression for the electron-hole and particle-particle response functions employed in W and the particle-particle T-matrix, respectively, are known, this is not the case, to the best of our knowledge, for the RPA-like electron-hole response function needed in the electron-hole T-matrix. Therefore, we have derived such equations and put the three approximations on an equal footing. To evaluate the efficacy of these approaches, we have assessed their performances on molecular systems. Specifically, we compute the principal IPs across a collection of 20 small molecules. The outcomes of our computations distinctly indicate that the eh T-matrix formalism falls short when compared to the other two approaches. The subset of diagrams composed by the eh ladder

diagrams is thus less relevant than the two other subsets (direct rings and pp ladders) in the present context. This observation paves the way for an investigation into the screened version of the eh T-matrix, which has demonstrated successes in diverse systems, such as ferromagnetic periodic structures, as reported in prior studies [56, 107, 57, 108]. Another avenue for further exploration involves the combination of these three correlation channels, akin to "fluctuation exchange" (FLEX) [120, 121, 50, 122], the Baym-Kadanoff approximation [44, 45], parquet theory [123, 124], and other similar approaches [42, 125]. Although challenging, this task holds significant promise and represents a potential avenue for our future investigations.

In terms of perspectives, it is advisable to consider investigating the issue of complex eigenvalues within the context of the BSE [126, 127]. This topic has been explored, notably in the field of particle physics, where it has been demonstrated that complex eigenvalues may arise due to a reference problem. This problem can be resolved by correcting the non-interacting Green's function with a self-energy, and in cases where this correction is insufficient, by introducing vertex corrections as well. Furthermore, it has been established that complex eigenvalues can also correspond to the physical process of transitioning from a bound state to a free state. This phenomenon has been rigorously proven in the case of a system comprising two spinless particles with instantaneous interactions [128]. Importantly, this result holds true even in the non-relativistic limit. Additionally, the transition from a bound state to a free state has been observed in the context of dynamical mean-field theory (DMFT), as documented in the literature. It is shown that the kernel of the BSE is intimately connected to the second derivative of the free energy. Consequently, this provides a valuable framework for investigating metal-insulator transitions, including Mott transitions, within the Landau theory of phase transitions [129].

A more comprehensive examination of the T-matrix is warranted. Previous investigations into the T-matrix [130, 131, 132, 133, 134, 135], particularly with a temperature-dependent formalism, have revealed significant insights. These studies have demonstrated that the real part of the T-matrix characterizes bound states involving particle-particle (electron-hole) interactions in the context of T^{pp} (T^{eh}). When the imaginary part of the T-matrix is introduced, it provides valuable information about the scattering component of the spectrum. These findings serve as a foundational basis for exploring the particle-particle BSE with the T-matrix kernel, which in turn can be employed to investigate Mott transitions and related phenomena.

In the Appendix, various methods for studying the BSE in particle physics and electrodynamics are presented. It would be beneficial and intriguing to incorporate these methods, as they offer fresh approaches to tackle integral equations. For example, the techniques that demonstrate how to handle singularities can be applied to recast an integral equation as a Fredholm or Volterra integral, for which established solution methods are available.

Chapter 7

Résumé en français

Introduction

Les électrons déterminent de nombreuses propriétés des matériaux. Par conséquent, pour comprendre les propriétés d'un système à N corps, il faudrait résoudre l'équation de Schrödinger indépendante du temps.

$$\hat{H}\Psi = E\Psi \tag{7.1}$$

afin d'accéder à sa fonction d'onde à plusieurs corps Ψ. L'hamiltonien (électronique) à plusieurs corps est donné par

$$\hat{H} = \hat{T}_e + \hat{T}_n + \hat{V}_{en} + \hat{V}_{ee} + \hat{V}_{nn}, \tag{7.2}$$

où $\hat{T}_e$ représente l'opérateur d'énergie cinétique électronique, $\hat{T}_n$ désigne l'opérateur d'énergie cinétique nucléaire, $\hat{V}_{en}$ est l'interaction électron-noyau, $\hat{V}_{ee}$ est l'interaction électron-électron et $\hat{V}_{nn}$ est l'interaction noyau-noyau. (Tout au long de la thèse, nous utilisons un cadre non relativiste.) Cependant, cette approche n'est pas réalisable car elle nécessite de résoudre un ensemble d'équations couplées avec $4N$ degrés de liberté (provenant des particules N définies par leur position $\boldsymbol{r}$ et leur spin σ). Par conséquent, des approximations de la fonction d'onde à plusieurs corps ou des formalismes alternatifs à plusieurs corps, tels que la théorie fonctionnelle de la densité (DFT) ou la théorie des perturbations à plusieurs corps (MBPT) basées sur les fonctions de Green, doivent être utilisées. Ces derniers formalismes offrent l'avantage de simplifier la complexité du problème en travaillant avec des quantités « réduites » comme la densité électronique ou la fonction de Green à un corps au lieu de la fonction d'onde à plusieurs corps. Ces quantités réduites sont plus simples à gérer que la fonction d'onde à N corps, et pourtant elles contiennent suffisamment d'informations pour déterminer les observables d'intérêt. Cependant, dans les applications pratiques, des approximations des effets dits à N corps du système, qui caractérisent les interactions électroniques, sont nécessaires. De plus, il n'est pas toujours simple d'extraire les propriétés intéressantes de ces quantités réduites.

Dans cette thèse, nous utiliserons le cadre du MBPT pour étudier les excitations neutres ou « états liés » du système. Ces excitations correspondent à des transitions de l'état fondamental à un état excité : le système est excité par un faible champ électrique et il répond à cette perturbation dans le cadre d'une réponse linéaire (signifiant que la réponse du système est directement proportionnelle à la perturbation). Dans une image simplifiée à un électron, les excitations neutres peuvent être décrites par des transitions d'orbitales moléculaires occupées (ou de bandes dans le cas de solides) vers des orbitales inoccupées (voir Fig. 1.7.1). Ces transitions englobent des transitions électron-trou uniques, appelées excitations uniques, ou elles peuvent impliquer plusieurs transitions électron-trou. Un

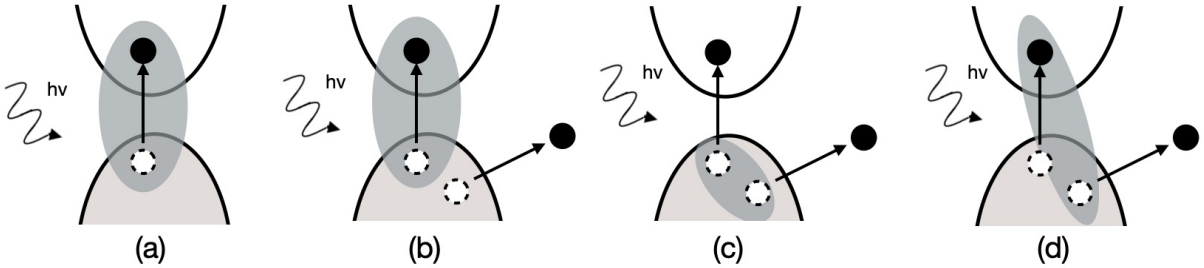

Figure 7.1 – Représentation schématique des excitations neutres et chargées : (a) création de paires électron-trou ; (b) élimination des électrons en GW ; (c) élimination des électrons dans la matrice T particule-particule ; (c) suppression des électrons dans la matrice T électron-trou. La forme ovale ombrée indique le couple de particules qui sont corrélées dans la description théorique.

exemple de cette dernière est la promotion simultanée de deux électrons vers des orbitales inoccupées, appelées doubles excitations.

L'avantage d'utiliser la MBPT pour décrire les excitations neutres est que, contrairement à la DFT et à son extension au domaine temporel, elle offre un cadre physique plus clair pour effectuer des approximations significatives des effets à N corps du système. Des approximations pertinentes sont essentielles pour obtenir des résultats précis. Au sein de la MBPT, la fonction de Green à un corps (1-GF) permet de calculer les énergies des quasiparticules (liées aux potentiels d'ionisation et aux affinités électroniques), qui sont successivement utilisées pour calculer les excitations neutres à travers la fonction de Green à deux corps (2-GF). Chacune de ces GF vérifie une équation de Dyson, qui relie la GF sans interaction à celle interagissante via un noyau. Dans le cas de la 1-GF, ce noyau est appelé self-énergie (Σ), alors que dans le cas de la 2-GF, ce noyau est la dérivée fonctionnelle de la self-énergie par rapport à la 1-GF. En pratique, des approximations de la self-énergie et de sa dérivée sont nécessaires. Les équations de Hedin (voir Fig. 7.2) constituent un bon point de départ pour faire des approximations. Il s'agit d'un ensemble de cinq équations intégro-différentielles qui sont, en principe, exactes, mais qui doivent être approchées en pratique. Une approximation bien connue est l'approximation GW de la self-énergie, qui se lit $\Sigma = v_H + iGW$, où v_H est le potentiel Hartree classique, G est le 1-GF et W le potentiel coulombien filtré dynamiquement. La structure est similaire à l'approximation Hartree-Fock de l'énergie propre ($\Sigma = v_H + iGv_c$, avec v_c le potentiel de Coulomb), mais il y a maintenant une corrélation incluse via W qui représente le fait que l'interaction coulombienne entre les particules du système est écrantée par la présence des autres particules. Il s'agit d'une approximation physiquement valable dans le cas d'un système comportant de nombreux électrons, mais elle montre des échecs à faible densité. Dans ce cas, d'autres approximations, comme l'approximation de la matrice T, qui décrit la diffusion multiple entre deux particules (matrice T pp) ou un électron et un trou (matrice T eh), sont plus adaptées. Les trois approximations peuvent être mises sur un pied d'égalité en examinant le processus de suppression des électrons (ou de manière équivalente le processus d'addition d'électrons) : dans une image simplifiée, l'électron retiré quitte un phototrou qui excite le système (création de paires électron-trou) (voir Fig. . 7.1b-d). Ce processus peut être considéré comme impliquant au moins trois particules qui, dans une description théorique, devraient être corrélées entre elles. Ceci est généralement coûteux et on choisit donc de n'en corréler que deux, ce qui habille donc le troisième. Dans GW, les paires eh créées par le phototrou sont corrélées (Fig. 7.1b), alors que, dans le formalisme de la matrice T, on corrèle les deux trous (Fig. 7.1c) ou le phototrou et l'électron excité (Fig. 7.1d).

Ces méthodes ont été développées dans le domaine de la matière condensée pour étudier les solides. En particulier, la méthode GW a réussi dans de nombreux systèmes pour étudier la structure de bande et les spectres de photoémission ainsi que les spectres

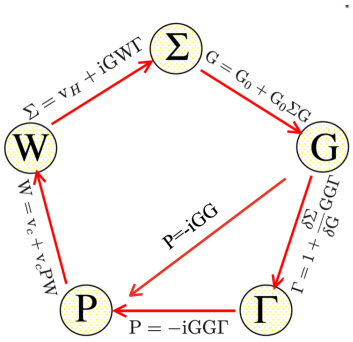

Figure 7.2 – Les cinq équations de Hedin pour la self-énergie (Σ), la fonction de Green à un corps (G), le vertex irréductible ($\tilde{\Gamma}$), la polarisabilité irréductible (P) , et le potentiel coulombien écranté dynamiquement (W), représenté sous la forme d'un pentagone. En mettant le vertex à 1, on obtient l'approximation GW.

optiques en utilisant l'équation de Bethe-Salpeter (BSE) [1]. Plus récemment ce formalisme a été importé en chimie quantique pour étudier les propriétés électroniques des molécules [2, 3, 4, 5, 6, 7, 8, 9, 10, 11, 13, 14, 15, 16, 17, 18, 19, 20, 21, 22, 23, 24]. Cependant, lorsqu'elle est appliquée à des systèmes finis comme les molécules, la méthode GW est souvent considérée comme moins efficace. Cette perception vient du fait que dans l'approximation GW, les effets collectifs qui écrante l'interaction coulombienne sont pris en compte. Bien qu'il s'agisse d'une approximation appropriée pour les solides où les effets d'écrantage jouent un rôle central, elle pourrait être moins applicable aux systèmes plus petits tels que les molécules, qui présentent moins d'effets d'écrantage. En particulier, BSE dans l'approximation GW peut montrer certains échecs, tels que des énergies d'excitation de triplet sous-estimées, un manque de double excitations, des instabilités énergétiques de l'état fondamental dans la limite de dissociation, etc. Néanmoins, dans cette thèse, nous visons à démontrer la pertinence de cette approche dans les systèmes à quelques électrons. Pour illustrer cela, nous étudierons les excitations neutres dans de petites molécules en utilisant BSE dans les approximations de GW, de la matrice pp T et de la matrice eh T.

Le problème à N corps

7.1 L'approximation de Born-Oppenheimer

Dans ce qui suit, nous utilisons les unités atomiques $\hbar = m_e = 1$ (m_e est la masse de l'électron). Lorsque nous voulons étudier un système à N-corps, il faut résoudre l'équation de Schrödinger à plusieurs corps dépendante du temps [30]

$$i\frac{\partial}{\partial t}|\Phi\rangle = H|\Phi\rangle \tag{7.3}$$

où Φ est la fonction d'onde à plusieurs corps du système et H est l'hamiltonien à plusieurs corps (non relativiste) pour une molécule d'électrons N et de noyaux M

$$H = -\sum_{i=1}^{N}\frac{1}{2}\nabla_i^2 - \sum_{A=1}^{M}\frac{1}{2M_A}\nabla_A^2 - \sum_{i=1}^{N}\sum_{A=1}^{M}\frac{Z_A}{r_{iA}} + \sum_{i=1}^{N}\sum_{i>j}^{N}\frac{1}{r_{ij}} + \sum_{A=1}^{M}\sum_{B>A}^{M}\frac{Z_A Z_B}{R_{AB}} \tag{7.4}$$

Le premier terme du membre de droite de (7.4) est l'énergie cinétique des électrons, le deuxième terme est l'énergie cinétique des noyaux, le troisième terme est l'attraction électron-noyau, le quatrième terme est la répulsion coulombienne électron-électron et le cinquième terme est la répulsion noyau-noyau. $r_{iA} = |\mathbf{r}_i - \mathbf{R}_A|$ est la distance entre l'électron en position $\mathbf{r}_i$ et le noyau à la position $\mathbf{R}_A$, $r_{ij} = |\mathbf{r}_i - \mathbf{r}_j|$ est la distance entre l'électron i à la position $\mathbf{r}_i$ et l'électron j à la position $\mathbf{r}_j$, $R_{AB} = |\mathbf{R}_A - \mathbf{R}_B|$ est la distance entre le noyau A à la position $\mathbf{R}_A$ et le noyau B à la position $\mathbf{R}_B$. M_A est le rapport entre la masse du noyau A et la masse d'un électron et Z_A est le numéro atomique du noyau A. L'opérateur laplacien ∇_i se différencie par rapport aux coordonnées de l'électron i et ∇_A se différencie par rapport aux coordonnées du noyau A.

L'état de la molécule est décrit par la fonction d'onde Φ qui dépend des coordonnées des électrons, des coordonnées des noyaux et du temps t,

$$\Phi = \Phi(\{\mathbf{r}_i\}; \{\mathbf{R}_A\}, t) \tag{7.5}$$

Les termes du hamiltonien (7.4) ne dépendent pas du temps ; par conséquent, sans aucune perturbation externe dépendante du temps, nous pouvons séparer la dépendance spatiale et temporelle de (7.3) et étudier l'équation de Schrödinger indépendante du temps

$$H|\Phi\rangle = E|\Phi\rangle \tag{7.6}$$

Puisque cette équation aux valeurs propres est indépendante du temps, ses états propres sont des états stationnaires. Dans (7.6) l'hamiltonien H à plusieurs corps est impossible à résoudre, nous pouvons donc simplifier (7.4) avec l'approximation de Born-Oppenheimer. Nous considérerons que le « mouvement » des électrons est très rapide par rapport au mouvement des noyaux, qui sont beaucoup plus lourds, et donc ils s'adapteront instantanément à un changement de position des noyaux, qui se déplacent très lentement et sont donc considérés comme fixes. Avec cette approximation, le deuxième terme de (7.4) peut être négligé. Le cinquième terme de (7.4) peut être considéré comme constant donc il ne change pas l'opérateur, mais comme nous ne nous intéressons qu'aux propriétés électroniques du système, nous étudierons l'hamiltonien électronique

$$H_{elec} = -\sum_{i=1}^{N}\frac{1}{2}\nabla_i^2 - \sum_{i=1}^{N}\sum_{A=1}^{M}\frac{Z_A}{r_{iA}} + \sum_{i=1}^{N}\sum_{i>j}^{N}\frac{1}{r_{ij}} \tag{7.7}$$

Le problème des valeurs propres (7.6) peut être réécrit avec (**??**) comme

$$H_{elec}\,|\Phi_{elec}\rangle = E_{elec}\,|\Phi_{elec}\rangle \tag{7.8}$$

Φ_{elec} est la fonction d'onde électronique

$$\Phi_{elec} = \Phi_{elec}(\{\mathbf{r}_i\};\{\mathbf{R}_A\}) \tag{7.9}$$

Il décrit le mouvement des électrons, cela dépend de leurs coordonnées $\{\mathbf{r}_i\}$ et cela dépend aussi paramétriquement des coordonnées des noyaux $\{\mathbf{R}_A\}$. Cela signifie que pour chaque ensemble de coordonnées nucléaires $\{\mathbf{R}_A\}$, la fonction d'onde électronique a une dépendance fonctionnelle différente par rapport aux coordonnées électroniques $\{\mathbf{r}_i\}$. L'énergie électronique dépend également de $\{\mathbf{R}_A\}$

$$E_{elec} = E_{elec}(\{\mathbf{R}_A\}) \tag{7.10}$$

Pour obtenir l'énergie totale on ajoute à (7.10) la répulsion nucléaire-nucléaire pour les noyaux fixes

$$E_{tot} = E_{elec} + \sum_{A=1}^{M}\sum_{B>A}^{M}\frac{Z_A Z_B}{R_{AB}} \tag{7.11}$$

7.2 Théorie Hartree-Fock

L'hamiltonien électronique (7.7) ne dépend que des coordonnées spatiales des électrons mais pour les décrire il faut aussi prendre en compte le spin. On note $\alpha(\sigma)$ le spin up et $\beta(\sigma)$ le spin down. Ils doivent vérifier les propriétés d'orthonormalisation

$$\sum_{\sigma}\alpha^*(\sigma)\alpha(\sigma) = \sum_{\sigma}\beta^*(\sigma)\beta(\sigma) = 1 \tag{7.12}$$

$$\sum_{\sigma}\alpha^*(\sigma)\beta(\sigma) = \sum_{\sigma}\beta^*(\sigma)\alpha(\sigma) = 0 \tag{7.13}$$

Les coordonnées d'un électron s'écrivent donc $\mathbf{x} = (\mathbf{r}, \sigma)$ et la fonction d'onde à plusieurs corps du système $\Phi(\mathbf{x}_1, \ldots, \mathbf{x}_N)$. Parce que les électrons sont des fermions, ils doivent vérifier le principe d'exclusion de Pauli selon lequel deux électrons ne peuvent pas être exactement dans le même état quantique. Cela nécessite que la fonction d'onde soit antisymétrique par rapport à l'échange de coordonnées électroniques.

$$\Phi(\mathbf{x}_1, \ldots, \mathbf{x}_i, \ldots, \mathbf{x}_j, \ldots, \mathbf{x}_N) = -\Phi(\mathbf{x}_1, \ldots, \mathbf{x}_j, \ldots, \mathbf{x}_i, \ldots, \mathbf{x}_N) \tag{7.14}$$

Nous définissons une orbitale comme une fonction d'onde pour une seule particule et nous appelons l'orbitale spatiale $\psi_i(\mathbf{r})$ la fonction de la position $\mathbf{r}$ qui décrit la distribution spatiale d'un électron. La probabilité de trouver un électron dans un élément de volume $d\mathbf{r}$ entourant $\mathbf{r}$ est alors $|\psi_i(\mathbf{r})|^2 d\mathbf{r}$. L'ensemble $\{\psi_i\}$ des orbitales spatiales vérifie les propriétés orthonormées

$$\int d\mathbf{r}\psi_i^*(\mathbf{r})\psi_j(\mathbf{r}) = \delta_{ij} \tag{7.15}$$

L'ensemble $\{\psi_i\}$ est infini mais en pratique, nous utiliserons un ensemble fini $\{\psi_i | i = 1, \ldots, K\}$. Par conséquent, nous ne couvrirons qu'une certaine région de l'ensemble complet et les résultats seront exacts dans le sous-espace couvert. Nous pouvons placer un électron

dans une orbitale spatiale $\psi_i(\mathbf{r})$ soit avec un spin haut, soit avec un spin bas, donc pour décrire complètement un électron, nous introduisons les orbitales de spin χ

$$\chi_i(\mathbf{x}) = \begin{cases} \psi_i(\mathbf{r})\alpha(\sigma) \\ \psi_i(\mathbf{r})\beta(\sigma) \end{cases} \tag{7.16}$$

Avec un ensemble d'orbitales spatiales K, nous pouvons former un ensemble d'orbitales de spin $2K$

$$\left.\begin{aligned} \chi_{2i-1}(\mathbf{x}) &= \psi_i(\mathbf{r})\alpha(\sigma) \\ \chi_{2i}(\mathbf{x}) &= \psi_i(\mathbf{r})\beta(\sigma) \end{aligned}\right\} i = 1, 2, \ldots, K \tag{7.17}$$

L'orthonormalité des orbitales spatiales implique

$$\int d\mathbf{x}\chi_i^*(\mathbf{x})\chi_j(\mathbf{x}) = \delta_{ij} \tag{7.18}$$

Dans la théorie de Hartree-Fock, on décrit l'état fondamental d'un système à N corps avec une seule fonction d'onde antisymétrique appelée déterminant de Slater.

$$|\Psi_0\rangle = |\chi_1\chi_2 \cdots \chi_i\chi_j \cdots \chi_N\rangle \tag{7.19}$$

ou

$$\Psi_0\left(\mathbf{x}_1, \mathbf{x}_2, \ldots, \mathbf{x}_N\right) = \frac{1}{\sqrt{N!}} \begin{vmatrix} \chi_1\left(\mathbf{x}_1\right) & \chi_2\left(\mathbf{x}_1\right) & \cdots & \chi_N\left(\mathbf{x}_1\right) \\ \chi_1\left(\mathbf{x}_2\right) & \chi_2\left(\mathbf{x}_2\right) & \cdots & \chi_N\left(\mathbf{x}_2\right) \\ \vdots & \vdots & & \vdots \\ \chi_1\left(\mathbf{x}_N\right) & \chi_2\left(\mathbf{x}_N\right) & \cdots & \chi_N\left(\mathbf{x}_N\right) \end{vmatrix} \tag{7.20}$$

Appliquer cette ansatz au Hamiltonien du système transforme le problème aux valeurs propres en un problème effectif à un électron tel que

$$\begin{aligned} f(\mathbf{r}_1)\psi_j(\mathbf{r}_1) &= h(\mathbf{r}_1)\psi_j(\mathbf{r}_1) \\ &+ 2\sum_k^{N/2} \int d\mathbf{r}_2 \psi_k^*(\mathbf{r}_2) r_{12}^{-1} \psi_k(\mathbf{r}_2)\psi_j(\mathbf{r}_1) - \sum_k^{N/2} \int d\mathbf{r}_2 \psi_k^*(\mathbf{r}_2) r_{12}^{-1} \psi_j(\mathbf{r}_2)\psi_k(\mathbf{r}_1) \end{aligned} \tag{7.21}$$

avec f l'operateur de Fock

$$f(\mathbf{r}_1) = h(\mathbf{r}_1) + \sum_k^{N/2} (2\mathcal{J}_k(\mathbf{r}_1) - \mathcal{K}_k(\mathbf{r}_1)) \tag{7.22}$$

L'operateur de Coulomb

$$\mathcal{J}_j(\mathbf{x}_1)\chi_i(\mathbf{x}_1) = \left[\int d\mathbf{x}_2 \chi_j^*(\mathbf{x}_2) r_{12}^{-1} \chi_j(\mathbf{x}_2)\right] \chi_i(\mathbf{x}_1) \tag{7.23}$$

l'operateur d'échange

$$\mathcal{K}_j(\mathbf{x}_1)\chi_i(\mathbf{x}_1) = \left[\int d\mathbf{x}_2 \chi_j^*(\mathbf{x}_2) r_{12}^{-1} \chi_i(\mathbf{x}_2)\right] \chi_j(\mathbf{x}_1) \tag{7.24}$$

L'énergie Hartree-Fock est

$$E_0 = \langle\Psi_0|H_{elec}|\Psi_0\rangle = 2\sum_i h_{ii} + \sum_{ij}(2\mathcal{J}_{ij} - \mathcal{K}_{ij}) \tag{7.25}$$

et les énergies orbitalaire sont

$$\varepsilon_i = h_{ii} + \sum_j (2\mathcal{J}_{ij} - \mathcal{K}_{ij}) \tag{7.26}$$

Calculs post Hatree-Fock

7.3 Théorie des perturbations à N corps

On fait l'hypothèse que le système vérifie l'approximation dite de la phase aléatoire. Il s'agit d'une théorie classique dans laquelle on suppose que lorsqu'on perturbe faiblement un système à N corps, chacun d'entre eux répond individuellement et independament les uns des autres à la perturbation, mais dans un même mode d'oscillation collectif qu'on appelle la réponse du système.

Pour étudier cette réponse on utilise le formalisme de la fonction de Green à un corps

$$iG_1(1,2) = \Theta(t_1 - t_2) \left\langle \Psi_0^N \right| \hat{\psi}_H(1)\hat{\psi}_H^\dagger(2) \left| \Psi_0^N \right\rangle - \Theta(t_2 - t_1) \left\langle \Psi_0^N \right| \hat{\psi}_H^\dagger(2)\hat{\psi}_H(1) \left| \Psi_0^N \right\rangle \quad (7.27)$$

La fonction de Green à un corps ajoute une particule au système en $2 = (\mathbf{x}_2, t_2, s_2)$, et supprime une particule au système en $1 = (\mathbf{x}_1, t_1, s_1)$ dans le cas où $t_1 > t_2$, ou elle enlève une particule dans $1 = (\mathbf{x}_1, t_1, s_1)$, et ajoute une particule dans $2 = (\mathbf{x}_2, t_2, s_2)$ si $t_2 > t_1$.

A partir de G_1, on peut reécrire les équations du mouvement qu'on a obtenu du Hamiltonien à N corps et de l'expression suivante

$$i\frac{d}{dt}O_H = [O_H, H_H] \quad (7.28)$$

où O_H et H_H sont respectivement l'operateur O et le Hamiltonien en representation de Heisenberg.

$$O_H(t) = e^{iHt}Oe^{-iHt} \quad (7.29)$$

$$H_H(t) = e^{iHt}He^{-iHt} \quad (7.30)$$

On obtient l'expression suivante

$$\left[i\frac{\partial}{\partial t_1} - h(1)\right] G_1(1,2) - \int d3U(1,3)G_1(3,2) + i\int d3v(1,3)G_2(1,3^+;2,3^{++}) = \delta(1,2) \quad (7.31)$$

où G_2 est la fonction de Green à deux corps et U est un potentiel externe tel que

$$U(1,3) = U(\mathbf{x}_1, \mathbf{x}_3; t_1)\delta(t_1 - t_3) \quad (7.32)$$

Ce potentiel externe permet de relier la fonction de Green à deux corps à la fonction de Green à un corps

$$G_2(1,3;2,3^+) = G_1(1,2)G_1(3,3^+) - \frac{\delta G_1(1,2)}{\delta U(3)} \quad (7.33)$$

Dans l'équation (7.33) U est un potential local et avec cette expression, l'équation (7.31) se reécrit

$$\left[i\frac{\partial}{\partial t_1} - h(1) - U(1) + i\int d3v(1,3)G_1(3,3^+)\right] G_1(1,2) - i\int d3v(1^+,3)\frac{\delta G_1(1,2)}{\delta U(3)} = \delta(1,2) \quad (7.34)$$

On définit la self-énergie

$$\Sigma(1,2) = \Sigma_H(1,2) + i\int d34\ \ v(1^+,3)\frac{\delta G_1(1,4)}{\delta U(3)}G_1^{-1}(4,2) \tag{7.35}$$

$$\Sigma_H(1,2) = \delta(1,2)\left[-i\int d3\ \ v(1,3)G_1(3,3^+)\right] \tag{7.36}$$

Σ est un potentiel effectif non-local, non-hermitien, (7.35) est une expression exacte qui permet de prendre en compte les interactions d'une particule avec les autres particules du milieu, réduisant ainsi une équation à plusieurs particules en une équation effective à une particule, avec cette définition l'expression (7.31) devient

$$\left[i\frac{\partial}{\partial t_1} - h(1) - U(1)\right]G_1(1,2) - i\int d3\ \ \Sigma(1,3)G_1(3,2) = \delta(1,2) \tag{7.37}$$

De l'équation (7.37) on obtient l'équation de Dyson

$$G_1(1,2) = G_1^0(1,2) + \int d34\ \ G_1^0(1,3)\Sigma(3,4)G_1(4,2) \tag{7.38}$$

On définit le potentiel total

$$V(1) = U(1) - i\int d3v(1,3)G_1(3,3^+) \tag{7.39}$$

La fonction diélectrique inverse

$$\epsilon^{-1}(1,2) = \frac{\delta V(1)}{\delta U(2)} \tag{7.40}$$

On utilise dans (7.39), le fait que

$$\rho(3) = -iG_1(3,3^+) \tag{7.41}$$

pour réécrire ϵ^{-1}

$$\epsilon^{-1}(1,2) = \delta(1,2) + \int d3v(1,3)\frac{\delta\rho(3)}{\delta U(2)} \tag{7.42}$$

La dérivée fonctionnelle dans le membre de droite peut être exprimée avec la fonction de Green à deux corps et liée à la polarisabilité réductible χ du système avec (7.33)

$$\chi(1,2) = \frac{\delta\rho(1)}{\delta U(2)} = i[G_2(1,2,1^+,2^+) - G_1(1,1^+)G_1(2,2^+)] \tag{7.43}$$

La polarisabilité réductible χ s'exprime en fonction de polarisabilité irréductible $\tilde{\chi}$ de la façon suivante

$$\chi(1,2) = \int d3\frac{\delta\rho(1)}{\delta V(3)}\frac{\delta V(3)}{U(2)} = \tilde{\chi}(1,2) + \int d34\tilde{\chi}(1,3)v(3,4)\chi(4,2) \tag{7.44}$$

où

$$\tilde{\chi}(1,2) = \frac{\delta\rho(1)}{\delta V(2)} \tag{7.45}$$

Avec les propriétés des dérivées fonctionnelles, nous pouvons exprimer Σ en termes de V

$$\Sigma(1,2) = \Sigma_H(1,2) - i\int d345\ \ v(1^+,3)G_1(1,4)\frac{\delta G_1^{-1}(4,2)}{\delta V(5)}\frac{\delta V(5)}{\delta U(3)} \tag{7.46}$$

on note

$$\Sigma_{xc}(1,2) = -i\int d345 v(1^+,3)G_1(1,4)\frac{\delta G_1^{-1}(4,2)}{\delta V(5)}\frac{\delta V(5)}{\delta U(3)} \tag{7.47}$$

où Σ_{xc} est la partie d'échange-corrélation de la self-énergie, et nous définissons la fonction vertex telle que

$$\tilde{\Gamma}(1,2,3) = -\frac{\delta G_1^{-1}(1,2)}{\delta V(3)} = \delta(1,3)\delta(2,3) + \frac{\delta\Sigma_{xc}(1,2)}{\delta V(3)} \tag{7.48}$$

on fait une autre dérivation fonctionnelle

$$\tilde{\Gamma}(1,2,3) = \delta(1,3)\delta(2,3) + \int d4567\frac{\delta\Sigma_{xc}(1,2)}{\delta G_1(4,5)}G_1(4,6)G_1(7,5)\tilde{\Gamma}(6,7,3) \tag{7.49}$$

nous pouvons également relier la polarisabilité irréductible à la fonction de vertex par

$$\tilde{\chi}(1,2) = -i\int d34 G_1(1,3)G_1(4,1)\tilde{\Gamma}(3,4,2) \tag{7.50}$$

Enfin, nous introduisons l'interaction de Coulomb écranté dynamiquement W

$$\begin{aligned} W(1,2) &= \int d3\epsilon^{-1}(1,3)v(3,2) \\ &= v(1,2) + \int d34 v(1,3)\chi(3,4)v(4,2) \\ &= v(1,2) + \int d34 v(1,3)\tilde{\chi}(3,4)W(4,2) \end{aligned} \tag{7.51}$$

W décrit le fait que lorsqu'une particule interagit avec une autre dans un milieu, puisque les deux particules ne sont pas seules, l'interaction coulombienne entre elles n'est pas l'interaction coulombienne nue mais une interaction coulombienne écrantée et l'écrantage provient de l'interaction avec le reste du système. Avec ces expressions, l'opérateur de masse peut s'écrire

$$\Sigma_{xc}(1,2) = i\int d34 G_1(1,4)W(1^+,3)\tilde{\Gamma}(4,2,3) \tag{7.52}$$

Les équations (7.38), (7.48), (7.49), (7.50) et (7.52) forment un ensemble d'équations couplées appelées équations de Hedin et peuvent être représentées sur un diagramme en forme de pentagone (voir Fig.7.2)

Dans ce pentagone, nous avons choisi comme point de départ la fonction de Green, qui est généralement une fonction de Green à champ moyen telle que la fonction de Hartree-Fock Green G^{HF} ou la fonction de Kohn-Sham Green G^{KS}. À partir de ce point de départ, nous devons ensuite calculer le vertex, la polarisabilité réductible, l'interaction de Coulomb écrantée, la self-énergie et itérer de manière auto-cohérente jusqu'à ce que la convergence soit atteinte.

7.3.1 Approximations sur la self-énergie

En pratique, nous effectuons rarement la procédure auto-cohérente complète, nous effectuons un seul cycle sur le pentagone appelé "one-shot". Ensuite, nous faisons une approximation appelée approximation de phase aléatoire (RPA) qui consiste à considérer que lorsque l'on excite un système à N corps avec un champ externe, chaque particule répond indépendamment des autres à cette perturbation. Dans cette approximation, nous prenons la correction de vertex $\Gamma \approx 1$. Dans cette procédure, nous faisons une théorie des perturbations au premier ordre. Nous corrigeons les énergies mais pas les orbitales, les résultats obtenus dépendent donc de la référence choisie comme point de départ.

Approximation *GW*

Dans l'approximation GW, la partie échange-corrélation de la self-énergie s'écrit comme

$$\Sigma_{xc}^{GW} = iGW \tag{7.53}$$

où W est construit à partir de la polarisabilité RPA

$$P(1,2) \approx -iG_1(1,2^+)G_1(2,1^+) \tag{7.54}$$

qui décrit la propagation indépendante de paires particule-trou dans un milieu. La polarisabilité irréductible RPA est représentée par des diagrammes à bulles et la polarisabilité réductible

$$\chi(1,2) = P(1,2) + \int d34 P(1,3)v(3,4)\chi(4,2) \tag{7.55}$$

est une sommation infinie de cette classe particulière de diagrammes. Mais si l'on veut prendre en compte d'autres types d'interaction, il faut exprimer la self-énergie comme un potentiel généralisé à partir duquel on pourra faire d'autres approximations, on part de l'équation (7.35) et après quelques dérivations on a

$$\begin{aligned}\Sigma(1,2) &= \Sigma_H(1,2) + i\int d34\ \ v(1^+,3)\frac{\delta G_1(1,4)}{\delta U(3)}G_1^{-1}(4,2) \\ &= \Sigma_H(1,2) + iv(1,2^+)G_1(1,2) + i\int d2'345\ \ v(1,2'^+)G_1(1,3)\frac{\delta\Sigma(3,2)}{\delta G_1(4,5)}\frac{\delta G_1(4,5)}{\delta U(2')}\Big|_{U=0} \\ &= \Sigma_H(1,2) + iv(1,2^+)G_1(1,2) + i\int d2'345\ \ v(1,2'^+)G_1(1,3)\Xi(3,5,2,4)L(4,2',5,2'^+)\end{aligned} \tag{7.56}$$

où $\Xi(3,5,2,4) = \frac{\delta\Sigma(3,2)}{\delta G_1(4,5)}$ est appelé le noyau,

et $L(4,2',5,2'^+) = \frac{\delta G_1(4,5)}{\delta G_1(2',2')}$ est une fonction de réponse généralisée.

La dernière expression décrit les effets physiques suivants : le terme Hartree Σ_H est l'interaction d'une particule avec la densité du système, le terme $\Sigma_x(1,2) = iv(1,2^+)G_1(1,2)$ échange deux particules avec le même spin, le dernier terme (Σ_c) est celui de corrélation et peut être considéré comme non local induit généralisé potentiel, provoqué par la propagation d'une particule. Si dans le noyau nous approximons la self-énergie comme le terme Hartree

$$\Xi(3,5,2,4) = \frac{\delta\Sigma(3,2)}{\delta G_1(4,5)} \approx \frac{\delta\Sigma_H(3,2)}{\delta G_1(4,5)} = -iv(3,4^+)\delta(4^+,5)\delta(3,2) \tag{7.57}$$

on obtient

$$\begin{aligned}\Sigma(1,2) &= \Sigma_H(1,2) + iv(1,2^+)G_1(1,2) + i\int d2'345\ \ v(1,2'^+)G_1(1,3)\Xi(3,5,2,4)L(4,2',5,2'^+)\\ &\approx \Sigma_H(12) + iv(12^+)G_1(12) + i\int d2'345 v(12'^+)G(13)\left[-iv(34^+)\delta(4^+5)\delta(32)L(42'4^+2'^+)\right]\\ &= \Sigma_H(1,2) + iv(1,2^+)G_1(1,2) + i\int d2'4 v(2,4^+)\chi(4,2')v(2'^+,1)G(1,2)\\ &= \Sigma_H(1,2) + iG_1(1,2)\left[\underbrace{v(1,2^+) + \int d2'4 v(1,2'^+)\chi(2',4)v(4^+,2)}_{W(1,2^+)}\right]\end{aligned} \tag{7.58}$$

où $\chi(1,2) = -iL(1,2,1^+,2^+)$, qui est la forme GW de la self-énergie. Notons qu'ici χ n'est pas nécessairement la fonction de réponse RPA mais peut également inclure les corrections de vertex.

Approximation GT

Une autre classe de diagrammes que nous pourrions considérer sont les diagrammes d'échelles, pour les obtenir, dans la première ligne de (7.58) nous faisons l'approximation suivante

$$L(4,2',5,2'^+) \approx G_1(4,2'^+)G_1(2',5) \tag{7.59}$$

Cela donne

$$\Sigma(1,2) = \Sigma_H(1,2) + \Sigma_x(1,2) + i\int d2'345\ \ v(1,2'^+)G_1(1,3)\frac{\delta\Sigma(3,1')}{\delta G_1(4,5)}G_1(4,2')G_1(2',5) \tag{7.60}$$

À partir de cette expression, nous définissons la matrice T comme une quantité à quatre points telle que

$$\Sigma^{GT}(1,2) = \int d2'4 G_1(4,2')T(1,2',2,4) \tag{7.61}$$

Lorsque l'on dérive la self-énergie par rapport à G_1, nous obtenons $\frac{\delta\Sigma}{\delta G_1} = \frac{\delta G_1}{\delta G_1}T + G_1\frac{\delta T}{\delta G_1}$, mais nous négligerons la dérivée de T par rapport à G_1 car elle donne des termes de deuxième ordre. On obtient alors

$$\frac{\delta\Sigma}{\delta G_1} \approx T \tag{7.62}$$

L'expression (7.61) donne respectivement la particule-particule (pp) T-matrice T^{pp} et la particule-trou (ph) T-matrice $\overline{T}^{ph}$

$$T_1^{pp}(1,2,1',2') = -iv(12)\delta(11')\delta(22') + iv(12)\int d35 G(13)G(25)T_1^{pp}(3,5,1',2') \tag{7.63}$$

$$T_2^{pp}(1,2,1',2') = iv(12)\delta(21')\delta(12') + iv(12)\int d35 G_1(13)G_1(25)T_2^{pp}(3,5,1',2') \tag{7.64}$$

$$\overline{T}_1^{eh}(1,2,1',2') = -iv(1'2')\delta(11')\delta(22') + iv(12')\int d35 G_1(13)G_1(52')\overline{T}_1^{eh}(3,2,1',5) \tag{7.65}$$

$$\overline{T}_2^{eh}(1,2,1',2') = -iv(1'2')\delta(21')\delta(12') + iv(12')\int d35 G_1(13)G_1(52')\overline{T}_2^{eh}(3,2,1',5) \tag{7.66}$$

où T_1 est le terme direct, T_2 est le terme d'échange et T s'écrit

$$T = T_1 + T_2 \tag{7.67}$$

7.3.2 Calcul de la réponse depuis la polarisabilité reductible χ

On dérive la réponse d'un système à partir des équations de Hedin en RPA, on explique la procédure de façon symbolique. On écrit Ξ un terme effectif d'interaction à deux corps qui peut s'écrire sous la forme d'une équation intégrale

$$\Xi = \tilde{v} + \tilde{v}P\Xi \tag{7.68}$$

où $\tilde{v}$ peut être le terme Hartree ou Hartree-Fock et P est la polarisabilité irréductible associée à Ξ. On ferme cette équation

$$\Xi = \epsilon^{-1}\tilde{v} \tag{7.69}$$

où ϵ^{-1} est la fonction diélectrique inverse qui caractérise la réponse du système à un champ électrique externe

$$\epsilon = 1 - \tilde{v}P \tag{7.70}$$

on remplace (7.69) dans (7.68), cela donne

$$\Xi = \tilde{v} + \tilde{v}\chi\tilde{v} \tag{7.71}$$

où

$$\chi = P\epsilon^{-1} \tag{7.72}$$

qui donnera

$$\chi^{-1} = P^{-1} \pm \tilde{v} \tag{7.73}$$

Une fois que nous avons cette expression, selon que P soit une polarisabilité particule-trou ou particule-particule, nous utiliserons la représentation spectrale associée. Dans le cas particule-trou cela s'écrit

$$L^{eh}(\mathbf{x}_1, \mathbf{x}_2, \mathbf{x}_1, \mathbf{x}_2; \tau_1, \tau_2, \omega) = \frac{1}{i}\sum_{n\neq 0} \frac{X_n(\mathbf{x}_{1'}, \mathbf{x}_1, \tau_1)\tilde{X}_n(\mathbf{x}_2, \mathbf{x}_{2'}, \tau_2)\,\mathrm{sgn}(\omega_n)}{\omega - \omega_n + i\eta\,\mathrm{sgn}(\omega_n)}. \tag{7.74}$$

où

$$\begin{aligned} X_n(\mathbf{x}_1, \mathbf{x}_{1'}; \tau) &= \chi_n(\mathbf{x}_1, \mathbf{x}_{1'}; \tau) \quad \text{for} \quad \omega_n > 0 \\ X_n(\mathbf{x}_1, \mathbf{x}_{1'}; \tau) &= \tilde{\chi}_n(\mathbf{x}_1, \mathbf{x}_{1'}; \tau) \quad \text{for} \quad \omega_n < 0 \end{aligned} \tag{7.75}$$

et

$$\begin{aligned} \tilde{X}_n(\mathbf{x}_1, \mathbf{x}_{1'}; \tau) &= \tilde{\chi}_n(\mathbf{x}_1, \mathbf{x}_{1'}; \tau) \quad \text{for} \quad \omega_n > 0 \\ \tilde{X}_n(\mathbf{r}_1, \mathbf{x}_{1'}; \tau) &= \chi_n(\mathbf{x}_1, \mathbf{x}_{1'}; \tau) \quad \text{for} \quad \omega_n < 0 \end{aligned} \tag{7.76}$$

et

$$\begin{aligned} \chi_n(\mathbf{x}_1, \mathbf{x}_{1'}; \tau_1) = \Theta(\tau_1)e^{i(E_0^N + E_n^N)\frac{\tau_1}{2}} \left\langle \Psi_0^N \middle| \psi(\mathbf{x}_1)e^{-iH\tau_1}\psi^\dagger(\mathbf{x}_{1'}) \middle| \Psi_n^N \right\rangle \\ - \Theta(-\tau_1)e^{-i(E_0^N + E_n^N)\frac{\tau_1}{2}} \left\langle \Psi_0^N \middle| \psi^\dagger(\mathbf{x}_{1'})e^{iH\tau_1}\psi(\mathbf{x}_1) \middle| \Psi_n^N \right\rangle \end{aligned} \tag{7.77}$$

avec $\tau_1 = t_1 - t_{1'}$

Pour la polarisabilité particule-particule, nous dériverons une représentation spectrale similaire.

GW

Pour GW, tous calculs effectués, on obtient

$$\chi_{(pq)(rs)} = [(\varepsilon_n - \varepsilon_{n'} - \omega)\delta_{nm}\delta_{n'm'} + (f_{m'}^{\sigma_{m'}} - f_n^{\sigma_n})v_{nn'm'm}]^{-1}_{(pq)(rs)}(f_s^{\sigma_s} - f_r^{\sigma_r}) \tag{7.78}$$

ou

$$\begin{pmatrix} \boldsymbol{A}^{\text{eh}} & \boldsymbol{B}^{\text{eh}} \\ -\boldsymbol{B}^{\text{eh}} & -\boldsymbol{A}^{\text{eh}} \end{pmatrix} \begin{pmatrix} \boldsymbol{X}_\nu^N \\ \boldsymbol{Y}_\nu^N \end{pmatrix} = \Omega_\nu^N \begin{pmatrix} \boldsymbol{X}_\nu^N \\ \boldsymbol{Y}_\nu^N \end{pmatrix} \tag{7.79}$$

avec

$$A^{\text{eh}}_{ia,jb} = (\varepsilon_a - \varepsilon_i)\delta_{ij}\delta_{ab} + \langle ib|aj\rangle \tag{7.80a}$$
$$B^{\text{eh}}_{ia,jb} = \langle ij|ab\rangle \tag{7.80b}$$

L'expression de W est

$$W_{pqrs} = v_{pqrs} + \lim_{\eta\to 0^+} \sum_\nu \left\langle pr\middle|\chi_\nu^N\right\rangle \left\langle qs\middle|\chi^N{}_{nu}\right\rangle \left[\frac{1}{\omega - \Omega_\nu^N + i\eta} - \frac{1}{\omega + \Omega_\nu^N - i\eta}\right] \tag{7.81}$$

avec

$$\left\langle pr\middle|\chi_\nu^N\right\rangle = \sum_{bj} \left[X^N_{bj,\nu} + Y^N_{bj,\nu}\right] v_{pjrb} \tag{7.82}$$

et

$$\Sigma^c_{ps}(\omega) = \sum_{i\nu} \frac{\left\langle pi\middle|\chi_\nu^N\right\rangle \left\langle is\middle|\chi_\nu^N\right\rangle}{\omega - \varepsilon_i + \Omega_\nu^N - i\eta} - \sum_{a\nu} \frac{\left\langle pa\middle|\chi_\nu^N\right\rangle \left\langle as\middle|\chi_\nu^N\right\rangle}{\omega - \varepsilon_a - \Omega_\nu^N + i\eta} \tag{7.83}$$

GT$^{\text{pp}}$

Pour GT^{pp} nous avons

$$\overline{\chi}_{(pq)(rs)} = [\delta_{n_1n_3}\delta_{n_2n_4}\left[\omega - (\varepsilon_{n_1}^{\sigma_1} + \varepsilon_{n_2}^{\sigma_2})\right] - \left[1 - (f_{n_1}^{\sigma_1} + f_{n_2}^{\sigma_2})\right]\overline{v}_{(n_1n_2)(n_3n_4)}]^{-1}_{(pq)(rs)}\left[1 - (f_r^{\sigma_3} + f_s^{\sigma_4})\right] \tag{7.84}$$

or

$$\begin{pmatrix} \boldsymbol{A}^{\text{pp}} & \boldsymbol{B}^{\text{pp}} \\ -\boldsymbol{B}^{\text{pp}} & -\boldsymbol{C}^{\text{pp}} \end{pmatrix} \begin{pmatrix} X_\nu^{N\pm2} \\ Y_\nu^{N\pm2} \end{pmatrix} = \Omega_\nu^{N\pm2} \begin{pmatrix} X_\nu^{N\pm2} \\ Y_\nu^{N\pm2} \end{pmatrix} \tag{7.85}$$

avec

$$A^{\text{pp}}_{ab,cd} = (\varepsilon_a + \varepsilon_b)\delta_{ac}\delta_{bd} + \langle ab||cd\rangle \tag{7.86a}$$
$$B^{\text{pp}}_{ab,ij} = \langle ab||ij\rangle \tag{7.86b}$$
$$C^{\text{pp}}_{ij,kl} = -(\varepsilon_i + \varepsilon_j)\delta_{ik}\delta_{jl} + \langle ij||kl\rangle \tag{7.86c}$$

L'expression de T^{pp} est

$$T^{pp}_{pqrs} = \overline{v}_{pqrs} + \sum_\nu \left[\frac{\left\langle pq\middle|\chi_\nu^{N+2}\right\rangle \left\langle \chi_\nu^{N+2}\middle|rs\right\rangle}{\omega - \Omega_\nu^{N+2} + i\eta} - \frac{\left\langle pq\middle|\chi_\nu^{N-2}\right\rangle \left\langle \chi_\nu^{N-2}\middle|rs\right\rangle}{\omega - \Omega_\nu^{N-2} - i\eta}\right] \tag{7.87}$$

avec

$$\langle pq|\chi_\nu^{N\pm2}\rangle = \sum_{c<d} \langle pq||cd\rangle\, X^{N\pm2}_{cd,\nu} + \sum_{k<l} \langle pq||kl\rangle\, Y^{N\pm2}_{kl,\nu} \tag{7.88}$$

et

$$\Sigma^c_{pr}(\omega) = \sum_{i\nu} \frac{\left\langle pi\middle|\chi_\nu^{N+2}\right\rangle \left\langle \chi_\nu^{N+2}\middle|ri\right\rangle}{\omega - \varepsilon_i - \Omega_\nu^{N+2} + i\eta} + \sum_{a\nu} \frac{\left\langle pa\middle|\chi_\nu^{N-2}\right\rangle \left\langle \chi_\nu^{N-2}\middle|ra\right\rangle}{\omega + \varepsilon_a - \Omega_\nu^{N-2} - i\eta} \tag{7.89}$$

$\mathbf{G\overline{T}^{eh}}$

Pour $G\overline{T}^{eh}$ nous avons

$$\overline{\chi}^{eh}_{(pq)(rs)} = [(\varepsilon_n - \varepsilon_{n'} - \omega)\delta_{nm}\delta_{n'm'} - (f^{\sigma_{m'}}_{m'} - f^{\sigma_n}_{n})v_{mm'nn'}]^{-1}_{(pq)(rs)}(f^{\sigma_s}_{s} - f^{\sigma_r}_{r}) \tag{7.90}$$

ou

$$\begin{pmatrix} \overline{\mathbf{A}}^{\text{eh}} & \overline{\mathbf{B}}^{\text{eh}} \\ -\overline{\mathbf{B}}^{\text{eh}*} & -\overline{\mathbf{A}}^{\text{eh}*} \end{pmatrix} \begin{pmatrix} \mathbf{X}^N_\nu \\ \mathbf{Y}^N_\nu \end{pmatrix} = \Omega^N_\nu \begin{pmatrix} \mathbf{X}^N_\nu \\ \mathbf{Y}^N_\nu \end{pmatrix} \tag{7.91}$$

avec

$$\begin{aligned} \overline{A}^{\text{eh}}_{(ia)(jb)} &= (\varepsilon_a - \varepsilon_i)\delta_{ij}\delta_{ab} - \langle bi|aj\rangle \\ \overline{B}^{\text{eh}}_{(ia)(jb)} &= -\langle ji|ab\rangle \end{aligned} \tag{7.92}$$

L'expression de $\overline{T}^{eh}$ est

$$\overline{T}^{eh}_{pqrs} = -i\overline{v}_{pqrs} + i\lim_{\eta\to 0^+}\sum_\nu \left[\frac{\langle ps|\chi^N_\nu\rangle \langle rq||\chi^N_\nu\rangle^*}{\omega - \overline{\Omega}^N_\nu + i\eta} - \frac{\langle qr||\chi^N_\nu\rangle \langle sp|\chi^N_\nu\rangle^*}{\omega + \overline{\Omega}^N_\nu - i\eta}\right] \tag{7.93}$$

où

$$\langle ps|\chi^N_\nu\rangle = \sum_{bj}\left[X^N_{bj,\nu}v_{pjbs} + Y^N_{bj,\nu}v_{pbjs}\right] \tag{7.94}$$

$$\langle rq||\chi^N_\nu\rangle = \sum_{bj}\left[X^N_{bj,\nu}v_{rjbq} + Y^N_{bj,\nu}v_{rbjq}\right] - \sum_{bj}\left[X^N_{bj,\nu} + Y^N_{bj,\nu}\right]v_{jrbq} \tag{7.95}$$

et

$$\overline{\Sigma}^c_{pr}(\omega) = \sum_{i\nu}\frac{\langle ir||\chi^N_\nu\rangle \langle ip|\chi^N_\nu\rangle^*}{\omega - \varepsilon_i + \overline{\Omega}^N_\nu - i\eta} + \sum_{a\nu}\frac{\langle ap|\chi^N_\nu\rangle^* \langle ar||\chi^N_\nu\rangle}{\omega - \varepsilon_a - \overline{\Omega}^N_\nu + i\eta} \tag{7.96}$$

Une fois que l'on a calculé la self-énergie, on l'introduit dans l'équation de Schrödinger effective comme correction sur l'opérateur de Fock

$$(F + \Sigma(\omega))\psi^{QP}(\omega) = \omega\psi^{QP}(\omega) \tag{7.97}$$

où ψ^{QP} et ω (ou encore ε^{QP}) sont respectivement la fonction d'onde de la quasi-particule et l'énergie de la quasi-particule. Σ introduit un décalage dans les énergies tel que

$$\omega = \varepsilon + \Sigma(\omega) \tag{7.98}$$

et transforme l'équation aux valeurs propres en un problème aux valeurs propres non linéaire. Cela est dû au fait que lorsqu'on ajoute ou enlève une particule au système, cela peut donner des excitations supplémentaires appelées satellites qui correspondent à des états excités du système à N+1 ou N−1-corps. En pratique pour simplifier ce problème, nous supposons qu'à la résonance de la quasi-particule, la partie imaginaire de Σ est "petite", donc

$$\omega = \varepsilon + Re[\Sigma(\omega)] \tag{7.99}$$

Ensuite, nous supposons que la partie réelle de Σ est linéaire à l'énergie de la quasi-particule, nous pouvons donc faire un développement de Taylor

$$Re[\Sigma(\omega)] \approx Re[\Sigma(\varepsilon)] + (\omega - \varepsilon)\frac{\partial Re[\Sigma(\omega)]}{\partial\omega}\Big|_{\omega=\varepsilon} \tag{7.100}$$

On définit le facteur de renormalisation Z

$$Z = \frac{1}{1 - \frac{\partial Re[\Sigma(\omega)]}{\partial\omega}\Big|_{\omega=\varepsilon}} \tag{7.101}$$

Ce qui permet d'obtenir les énergies des quasi-particules dans l'approximation linéaire

$$\varepsilon^{QP} = \varepsilon + Z\Sigma(\omega = \varepsilon) \tag{7.102}$$

7.4 La fonction de Green à deux corps

La fonction de Green à deux corps est une fonction de corrélation qui permet d'étudier la corrélation entre une particule et un trou ou deux particules (trous) au sein d'un système qui contient d'autres particules, elle est définit de la façon suivante

$$i^2 G_2\left(1,2,1',2'\right) = \left\langle \Psi_0^N \right| T[\hat{\psi}_H(1)\hat{\psi}(2)\hat{\psi}_H^\dagger\left(2'\right)\hat{\psi}_H^\dagger\left(1'\right)] \left| \Psi_0^N \right\rangle \tag{7.103}$$

Elle contient quatre opérateurs de champ dont nous devons choisir l'ordonnancement temporel tel que cela corresponde aux corrélations du canal que nous voulons étudier. Nous avons six ordonnancements possible, comme nous souhaitons etudier l'interaction entre la particule et le trou que nous avons précedemment habillés, nous choisissons le canal particule-trou qui correspond aux fonctions G_2^I and G_2^{II}, telles que $t_1, t_{1'} > t_2, t_{2'}$ et $t_2, t_{2'} > t_1, t_{1'}$.

$$\begin{aligned} G_2^{\mathrm{I}}\left(1,2;1',2'\right) &= (-i)^2 \left\langle \Psi_0^N \right| T[\hat{\psi}_H(1)\hat{\psi}_H^\dagger\left(1'\right)] T[\hat{\psi}_H(2)\hat{\psi}_H^\dagger\left(2'\right)] \left| \Psi_0^N \right\rangle \\ &\quad \cdot \Theta\left(\tau - \frac{1}{2}\left|\tau_1\right| - \frac{1}{2}\left|\tau_2\right|\right) \end{aligned} \tag{7.104a}$$

$$\begin{aligned} G_2^{\mathrm{II}}\left(1,2;1',2'\right) &= (-i)^2 \left\langle \Psi_0^N \right| T[\hat{\psi}_H(2)\hat{\psi}_H^\dagger\left(2'\right)] T[\hat{\psi}_H(1)\hat{\psi}_H^\dagger\left(1'\right)] \left| \Psi_0^N \right\rangle \\ &\quad \cdot \Theta\left(-\tau - \frac{1}{2}\left|\tau_1\right| - \frac{1}{2}\left|\tau_2\right|\right) \end{aligned} \tag{7.104b}$$

où $\tau_1 = t_1 - t_{1'}$, $\tau_2 = t_2 - t_{2'}$, $\tau = t^1 - t^2$, $t^1 = \frac{t_1 + t_{1'}}{2}$ et $t^2 = \frac{t_2 + t_{2'}}{2}$

Ces fonctions peuvent se mettre sous la forme suivante

$$G_2^I(1,2;1',2') = (-i)^2 \sum_n \chi_n(\mathbf{x}_1, \mathbf{x}_{1'}, \tau_1)\widetilde{\chi}_n(\mathbf{x}_2, \mathbf{x}_{2'}, \tau_2) e^{-i(E_n^N - E_0^N)\tau} \Theta\left(\tau - \frac{1}{2}|\tau_1| - \frac{1}{2}|\tau_2|\right) \tag{7.105}$$

et

$$G_2^{II}(1,2;1',2') = (-i)^2 \sum_n \widetilde{\chi}_n(\mathbf{x}_1, \mathbf{x}_{1'}, \tau_1)\chi_n(\mathbf{x}_2, \mathbf{x}_{2'}, \tau_2) e^{i(E_n^N - E_0^N)\tau} \Theta\left(-\tau - \frac{1}{2}|\tau_1| - \frac{1}{2}|\tau_2|\right) \tag{7.106}$$

avec

$$\chi_n(1,1') = \left\langle \Psi_0^N \right| T[\hat{\psi}_H(\mathbf{x}_1)\hat{\psi}_H^\dagger\left(\mathbf{x}_{1'}\right)] \left| \Psi_n^N \right\rangle e^{-i\frac{(E_n^N - E_0^N)}{2}(t_1 + t_{1'})} \tag{7.107}$$

$$\tilde{\chi}_n(2,2') = \left\langle \Psi_n^N \right| T[\hat{\psi}_H(\mathbf{x}_2)\hat{\psi}_H^\dagger\left(\mathbf{x}_{2'}\right)] \left| \Psi_0^N \right\rangle e^{i\frac{(E_n^N - E_0^N)}{2}(t_2 + t_{2'})} \tag{7.108}$$

La fonction de Green à deux corps, dans le canal particule-trou s'écrit

$$G_2^{eh}(1,2;1',2') = G_2^I(1,2;1',2') + G_2^{II}(1,2;1',2') \tag{7.109}$$

Nous définissons maintenant la fonction de corrélation à deux corps

$$L^{eh}(1,2;1',2') = -G_2^{eh}(1,2;1',2') + G_1(1,1')G_1(2,2') \tag{7.110}$$

La transformée de Fourier de L^{eh} par rapport à τ est

$$L^{eh}(\mathbf{x}_1, \mathbf{x}_2, \mathbf{x}_{1'}, \mathbf{x}_{2'}; \tau_1, \tau_2, \omega) = \int \frac{d\omega}{2\pi}(L^I + L^{II})(\mathbf{x}_1, \mathbf{x}_2, \mathbf{x}_{1'}, \mathbf{x}_{2'}; \tau_1, \tau_2, \tau) e^{-i\omega\tau} \tag{7.111}$$

on obtient

$$L^{eh}(\tau_1,\tau_2,\omega) = \tag{7.112}$$
$$-i\lim_{\eta\to 0^+}\sum_{n\neq 0}\left[\frac{e^{\frac{i}{2}[\omega-(E_n^N-E_0^N)][|\tau_1|+|\tau_2|]}}{\omega-(E_n^N-E_0^N)+i\eta}-\frac{e^{-\frac{i}{2}[\omega+(E_n^N-E_0^N)][|\tau_1|+|\tau_2|]}}{\omega+(E_n^N-E_0^N)-i\eta}\right]\chi_n(\mathbf{x}_1,\mathbf{x}_{1'},\tau_1)\widetilde{\chi}_n(\mathbf{x}_2,\mathbf{x}_{2'},\tau_2)$$

On prend les limites $\tau_1\to 0^-$ et $\tau_2\to 0^-$

$$L^{eh}(\omega) = \tag{7.113}$$
$$-i\lim_{\eta\to 0^+}\sum_{n\neq 0}\left[\frac{1}{\omega-(E_n^N-E_0^N)+i\eta}-\frac{1}{\omega+(E_n^N-E_0^N)-i\eta}\right]\chi_n(\mathbf{x}_1,\mathbf{x}_{1'})\widetilde{\chi}_n(\mathbf{x}_2,\mathbf{x}_{2'})$$

C'est la définition exacte. Nous avons cependant besoin d'une équation pratique pour calculer L^{eh}, on dérive donc une nouvelle expression pour L^{eh} à partir de (7.33)

$$\begin{aligned}L^{eh}(1,2;1',2') &= -\int d34 G_1(1,3)\frac{\delta G_1^{-1}(3,4)}{\delta U(2',2)}G_1(4,1') \qquad (7.114)\\ &= \int d34 G_1(1,3)\left[\delta(3,2')\delta(4,2)\delta(t_4-t_2)\frac{\delta\Sigma(3,4)}{\delta U(2',2)}\right]G_1(4,1')\\ &= G_1(1,2')G_1(2,1')+\int d3456 G_1(1,3)G_1(4,1')\frac{\delta\Sigma(3,4)}{\delta G_1(6,5)}L^{eh}(6,2;5,2')\end{aligned}$$

where the external potential U is supposed instantaneous, or for any variable t_2 and $t_{2'}$

$$L^{eh}(1,2;1',2') = L^0(1,2;1',2')+\int d3456 L^0(1,4;1',3)\Xi(3,5;4,6)L^{eh}(6,2;5,2') \tag{7.115}$$

avec

$$L^0(1,2;1',2') = G_1(1,2')G_1(2,1') \tag{7.116}$$

Cette équation de Dyson s'appelle l'équation de Bethe-Salpeter (BSE) [64]. Le premier membre du membre de droite est le terme non homogène. Il représente deux corps se propageant librement sans interagir entre eux mais chacun interagissant avec l'environnement. Le deuxième membre du membre de droite est le terme homogène, il représente l'interaction des deux corps.

7.4.1 La réponse libre du système à deux corps

La transformée de Fourier de L_0 s'écrit

$$L_0(\mathbf{x}_1,\mathbf{x}_2;\mathbf{x}_{1'},\mathbf{x}_{2'},\omega) = \int\frac{d\omega'}{2\pi i}G_1(\mathbf{x}_1,\mathbf{x}_{2'},\omega'+\frac{\omega}{2})G_1(\mathbf{x}_2,\mathbf{x}_{1'},\omega'-\frac{\omega}{2})e^{i\omega'\eta} \tag{7.117}$$

nous exprimons la fonction de Green à un corps dans l'approximation de la quasi-particule

$$G_1(\mathbf{x}_1,\mathbf{x}_2,\omega) = \sum_n\frac{\phi_n(\mathbf{x}_1)\phi_n^*(\mathbf{x}_2)}{\omega-\varepsilon_n^{QP}+i\eta\,\mathrm{sgn}(\varepsilon_n^{QP}-\mu)} \tag{7.118}$$

nous obtenons

$$L_0(\mathbf{x}_1,\mathbf{x}_2;\mathbf{x}_{1'},\mathbf{x}_{2'},\omega) = \sum_{nn'}\frac{(f_n-f_{n'})\phi_n(\mathbf{x}_1)\phi_n^*(\mathbf{x}_{2'})\phi_{n'}(\mathbf{x}_2)\phi_{n'}^*(\mathbf{x}_{1'})}{\varepsilon_n^{QP}-\varepsilon_{n'}^{QP}-\omega+i\eta\,\mathrm{sgn}(\varepsilon_{n'}^{QP}-\varepsilon_n^{QP})} \tag{7.119}$$

Les pôles résonants de L^0 s'écrivent sous la forme $\omega=\varepsilon_{n'}^{QP}-\varepsilon_n^{QP}$. Si nous utilisons pour les énergies des quasiparticules ε^{QP} les énergies de la fonction de Green sans interaction G_1^0, L^0 représente la propagation libre d'un système de trous de particules isolés. Si vous utilisez une fonction de Green en interaction, ces pôles représentent la libre propagation d'un système particule-trou interagissant uniquement avec le milieu.

7.4.2 La réponse totale du système à deux corps avec un noyau statique

Dans cette section nous ajoutons à la propagation indépendante de la quasiparticule et du quasitrou l'interaction entre eux, pour ce faire nous gardons dans le membre droit de l'équation de Bethe-Salpeter, le terme homogène et non homogène. Nous devons inverser cette équation, mais si nous écrivons sa transformée de Fourier, qui est

$$L^{eh}(\omega,\omega',\omega'') = L^0(\omega,\omega',\omega'') + \int \frac{d\omega'''d\omega^{IV}}{(2\pi)^2} L^0(\omega,\omega',\omega''')\Xi(\omega,\omega''',\omega^{IV})L^{eh}(\omega,\omega^{IV},\omega'') \tag{7.120}$$

on ne peut intégrer que sur ω' et ω'' car ces variables sont libres, alors L^{eh} dépend de ω à gauche et des deux fréquences ω et ω^{IV} du côté droit, donc on ne peut pas fermer l'équation. Pour rendre l'équation inversible on fait une approximation statique sur le noyau, que l'on va considérer indépendant de la fréquence $\Xi(\omega,\omega''',\omega^{IV}) \approx \Xi$ et on ce qui permet d'intégrer sur les deux dernières fréquences

$$L^{eh}(\omega) = L_0(\omega) + L_0(\omega)\Xi L^{eh}(\omega) \tag{7.121}$$

Dans la base des orbitales à une particule cette équation s'écrit

$$L^{eh}_{(pq)(rs)} = L^0_{(pq)(rs)} + \sum_{(ij)(kl)} L^0_{(pq)(ij)}\Xi_{(ij)(kl)}L^{eh}_{(kl)(rs)} \tag{7.122}$$

où

$$L^{eh}_{(pq)(rs)} = L^{eh}_{qrps} = \int dx_1 dx_2 dx_{1'} dx_{2'} L^{eh}(x_1,x_2,x_{1'},x_{2'})\phi^*_q(x_1)\phi^*_r(x_2)\phi_p(x_{1'})\phi_s(x_{2'}) \tag{7.123}$$

nous utilisons la même définition pour L^0 et Ξ, nous inversons (7.122)

$$L^{eh,-1}_{(pq)(rs)} = L^{0,-1}_{(pq)(rs)} - \Xi_{(pq)(rs)} \tag{7.124}$$

Si on utilise la base qui diagonalise L^0 on arrive à

$$-iL^{eh}_{(pq)(rs)} = [(\varepsilon^{QP}_n - \varepsilon^{QP}_{n'} - \omega)\delta_{nm}\delta_{n'm'} + (f^{\sigma_{m'}}_{m'} - f^{\sigma_n}_n)\Xi_{nn'm'm}]^{-1}_{(pq)(rs)}(f^{\sigma_s}_s - f^{\sigma_r}_r) \tag{7.125}$$

cela peut se réécrire comme une équation aux valeurs propres matricielles

$$\begin{pmatrix} \boldsymbol{\mathcal{A}}^{\text{eh}} & \boldsymbol{\mathcal{B}}^{\text{eh}} \\ -\boldsymbol{\mathcal{B}}^{\text{eh}} & -\boldsymbol{\mathcal{A}}^{\text{eh}} \end{pmatrix} \begin{pmatrix} \boldsymbol{X}_n \\ \boldsymbol{Y}_n \end{pmatrix} = \omega_n \begin{pmatrix} \boldsymbol{X}_n \\ \boldsymbol{Y}_n \end{pmatrix} \tag{7.126}$$

La structure est similaire à l'équation matricielle GW en RPA mais les quantités sont différentes. Le noyau Ξ va au-delà de la RPA puisqu'il contient les effets d'échange et de corrélation. Il s'agit également d'un problème de valeurs propres non-hermitien, donc les valeurs propres peuvent devenir complexes.

Résultats

Nous étudions dans ce chapitre les approximations GW et T appliquées au dimère de Hubbard à deux électrons. Ce paradigme est largement utilisé dans la littérature pour tester des méthodes à N corps. [136, 137, 138, 139, 54, 69, 42] Par exemple, Carrascal *et al.* ont étudié l'état fondamental [71] dans le cadre de la théorie fonctionnelle de la densité (DFT) de Kohn-Sham (KS) et les propriétés d'état excité en TD-DFT (dépendant du temps) [140] en utilisant le dimère asymétrique de Hubbard. Les approximations GW [69, 141, 142] et de la matrice T [44, 45, 54, 42, 70, 59] ont également été étudiées à l'aide de ce modèle omniprésent. Ici, nous utilisons le dimère asymétrique de Hubbard, qui peut être résolu de façon exacte et, par conséquent, offre la possibilité de comprendre les tendances observées dans les énergies d'excitation chargées et neutres dans les approximations de la GW et de la matrice T. En particulier, nous aborderons la qualité des énergies d'excitation triplet dans les deux approximations et l'apparition d'énergies d'excitation complexes dans BSE.

7.5 Le Hamiltonien du dimère de Hubbard

Le Hamiltonien du dimère asymétrique est

$$\hat{H} = -t \sum_{\sigma=\uparrow,\downarrow} \left(\hat{a}^\dagger_{1\sigma} \hat{a}_{2\sigma} + \hat{a}^\dagger_{2\sigma} \hat{a}_{1\sigma} \right) + U \sum_{i=1}^{2} \hat{n}_{i\uparrow} \hat{n}_{i\downarrow} + \Delta v \frac{\hat{n}_2 - \hat{n}_1}{2} \tag{7.127}$$

où $t > 0$ est le paramètre de saut, $U \geq 0$ l'interaction de Coulomb local, $\hat{n}_{i\sigma} = \hat{a}^\dagger_{i\sigma} \hat{a}_{i\sigma}$ l'operateur de densité de spin par site i, $\hat{n}_i = \hat{n}_{i\uparrow} + \hat{n}_{i\downarrow}$ est l'operateur densité par site i, et $\Delta v = v_1 - v_2$ (avec $v_1 > v_2$ et $v_1 + v_2 = 0$) est la différence de potentiel entre deux sites. L'operateur $\hat{a}^\dagger_{i\sigma}$ ($\hat{a}_{i\sigma}$) créé (annihile) un electron de spin σ sur le site i. Dans la suite, toutes les quantités sont reportées en unités réduites ou, de façon équivalente, en unité de t.

Pour $N = 2$, le Hamiltonien dans la base des sites $|\uparrow_1\downarrow_2\rangle$, $|\uparrow\downarrow_1\, 0_2\rangle$, $|0_1\, \uparrow\downarrow_2\rangle$, $|\downarrow_1\uparrow_2\rangle$, s'écrit

$$H^{N=2} = \begin{array}{c} \begin{array}{cccc} |\uparrow_1\downarrow_2\rangle & |\uparrow\downarrow_1\, 0_2\rangle & |0_1\, \uparrow\downarrow_2\rangle & |\downarrow_1\uparrow_2\rangle \end{array} \\ \begin{pmatrix} 0 & -t & -t & 0 \\ -t & U + \Delta v & 0 & t \\ -t & 0 & U - \Delta v & t \\ 0 & t & t & 0 \end{pmatrix} \end{array} \tag{7.128}$$

La fonction d'onde de l'état excité du triplet est

$$|^3\Psi^N\rangle = \frac{|\uparrow_1\downarrow_2\rangle + |\downarrow_1\uparrow_2\rangle}{\sqrt{2}} \tag{7.129}$$

alors que la fonction de d'onde du singulet ($n = 0$) et de l'état excité ($n = 1$ and 2) sont de la forme

$$|^1\Psi^N_n\rangle = c_{1n} |\uparrow_1\downarrow_2\rangle + c_{2n} |\downarrow_1\uparrow_2\rangle + c_{3n} |0_1\, \uparrow\downarrow_2\rangle + c_{4n} |\uparrow\downarrow_1\, 0_2\rangle \tag{7.130}$$

avec

$$c_{1n} = -c_{2n} = \frac{1}{\mathcal{N}_n} \tag{7.131a}$$

$$c_{3n} = \frac{1}{\mathcal{N}_n} \frac{2t}{U - \Delta v - E_n^N} \tag{7.131b}$$

$$c_{4n} = \frac{1}{\mathcal{N}_n} \frac{2t}{U + \Delta v - E_n^N} \tag{7.131c}$$

et

$$\mathcal{N}_n = \sqrt{2 + \left(\frac{2t}{U - \Delta v - E_n^N}\right)^2 + \left(\frac{2t}{U + \Delta v - E_n^N}\right)^2} \tag{7.132}$$

où les E_n^N's sont les energies (exactes) of Eq. (7.127). Les différences entre les énergies à N électrons permettent de calculer les excitations neutres exactes du système de la façon suivante :

$$^3\omega = E_1^{N=2} - E_0^{N=2} \tag{7.133}$$

$$^1\omega = E_2^{N=2} - E_0^{N=2} \tag{7.134}$$

alors que les énergies d'ionisation (IP) et d'attachements (EA) sont calculées comme les différences d'énergie par rapport aux systèmes avec $N-1$ et $N+1$ électrons

$$\text{IP} = E_0^{N-1} - E_0^N = -\varepsilon_i \tag{7.135}$$

$$\text{EA} = E_0^N - E_0^{N+1} = -\varepsilon_a \tag{7.136}$$

7.5.1 Dimère de Hubbard symétrique

Quasiparticules

Nous étudions le dimère symétrique en premier (i.e., $\Delta v = 0$) car celui-ci peut se résoudre analytiquement dans le cas d'un point de départ non-interagissant ou HF, G_0 et G_{HF}, respectivement, ce qui permet d'étudier l'influence de la fonction de Green de départ.

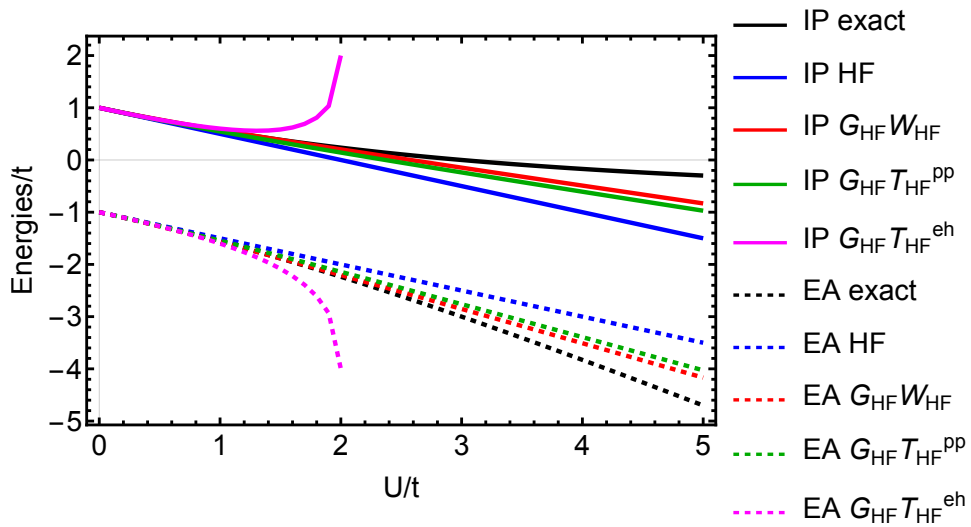

Figure 7.3 – IP et EA en fonction de U/t pour le dimère de Hubbard symétrique obtenues à différends niveaux de théorie: exacte (noire), HF (bleu), $G_{\text{HF}}W$ (rouge), $G_{\text{HF}}T^{pp}$ (verte) and $G_{\text{HF}}\overline{T}^{eh}$ (magenta).

Dans le régime de corrélation faible (c'est-à-dire petit U/t), toutes les approximations sont en bon accord avec les résultats exacts. Dans le régime de forte corrélation (c'est-à-dire de grand U/t), les approximations GW et de la matrice T^{pp} sous-estiment le gap fondamental de manière assez significative, tandis que l'approximation T^{eh} surestime le gap qui devient complexe.

Excitations neutres

Nous nous concentrons maintenant sur les excitations neutres du dimère symétrique de Hubbard. Les énergies d'excitation sont présentées sur la Fig. 7.4 aux côtés des énergies de liaison des énergies d'excitation singulet et triplet.

L'approximation GW (courbes rouges) décrit mieux l'énergie d'excitation exacte du triplet, ${}^3\omega$, que l'énergie d'excitation exacte du singulet, ${}^1\omega$. Entre $U/t \approx 7$ et $U/t \approx 12$, cependant, ${}^3\omega^{GW}$ (courbe rouge continue) devient complexe en raison d'une instabilité triplet dans la matrice BSE. Fait intéressant, dans cette même plage, l'énergie de liaison GW ${}^3E_\mathrm{b}$ (courbe bleue continue) atteint le gap fondamental GW (ligne magenta continue). De plus, à $U/t \approx 7$, ${}^1\omega^{GW}$ (courbe rouge en pointillés) devient inférieur au gap fondamental et, par conséquent, devient, par définition, une état « lié », tandis que, à $U/t \approx 12$, il devient complexe (instabilité du singulet) lorsque ${}^1E_\mathrm{b}$ (courbe bleue en pointillés) atteint le gap fondamental GW (ligne magenta en pointillés) .

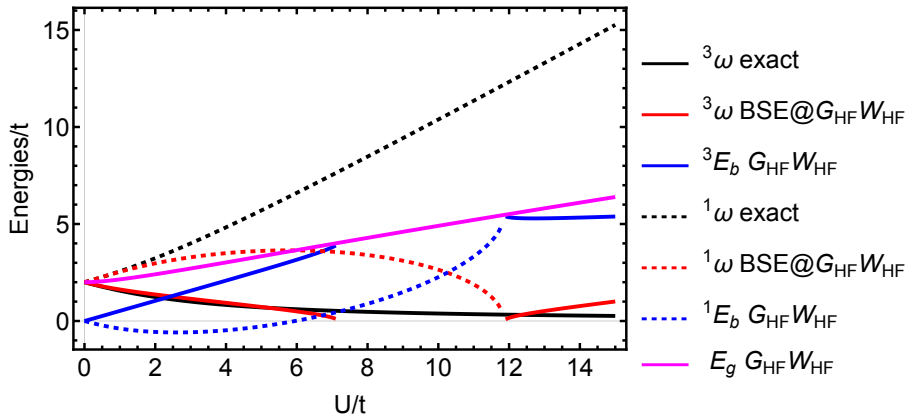

Figure 7.4 – Energies d'excitation neutres (rouge), énergies de liaison (bleu), et gap fondamental (magenta) en fonctions de U/t pour le dimère de Hubbard symétrique ($\Delta v = 0$) pour les états excités du triplet (solide) et du singulet (pointillés) à différends niveaux de théorie: exacte (noire) et BSE@$G_\mathrm{HF}W_\mathrm{HF}$.

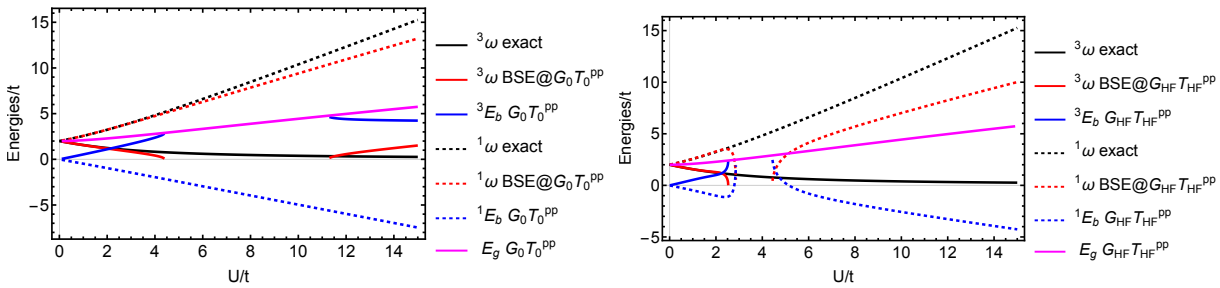

(a) Neutral excitation energies with G_0 **(b)** Neutral excitation energies with G_HF

Figure 7.5 – Energies d'excitation neutres (rouge), énergies de liaison (bleu), et gap fondamental (magenta) en fonctions de U/t pour le dimère de Hubbard symétrique ($\Delta v = 0$) pour les états excités du triplet (solide) et du singulet (pointillés) à différends niveaux de théorie: exacte (noire) et BSE@GT^{pp}.

Les énergies d'excitation sont représentées sur les Fig. 7.5a, Fig. 7.5b et Fig. 7.6 en fonctions de U/t. Pour le cas de BSE@$G_{\mathrm{HF}}T^{pp}_{\mathrm{HF}}$, les transitions exactes singulet et triplet (courbes noires) sont bien décrites par ${}^1\omega^{G_{\mathrm{HF}}T^{pp}_{\mathrm{HF}}}$ et ${}^3\omega^{G_{\mathrm{HF}}T^{pp}_{\mathrm{HF}}}$ (courbes rouges) jusqu'à $U/t \approx 3$. Après cela, elles deviennent toutes deux complexes, ${}^1\omega^{G_{\mathrm{HF}}T^{pp}_{\mathrm{HF}}}$ devenant à nouveau réel à $U/t \approx 4,5$. Comme avant ${}^1\omega^{G_{\mathrm{HF}}T^{pp}_{\mathrm{HF}}}$ et ${}^3\omega^{G_{\mathrm{HF}}T^{pp}_{\mathrm{HF}}}$ deviennent complexes lorsque leur énergie de liaison respective, ${}^1E_{\mathrm{b}}$ et ${}^3E_{\mathrm{b}}$ (courbes magenta), atteint la valeur du gap fondamental.

Enfin, dans le cas d'un calcul BSE@$G_{\mathrm{HF}}\overline{T}^{eh}_{\mathrm{HF}}$, il est important de noter que, les pôles de la fonction de réponse deviennent complexes lorsque $U > 2t$.

Dans l'ensemble, BSE@GW fournit une meilleure description des excitations de triplet par rapport à BSE@GT^{pp}. Pour les excitations singulet, nous avons l'inverse. Dans le cas de T^{pp} et de $\overline{T}^{eh}$, nous rencontrons des singularités.

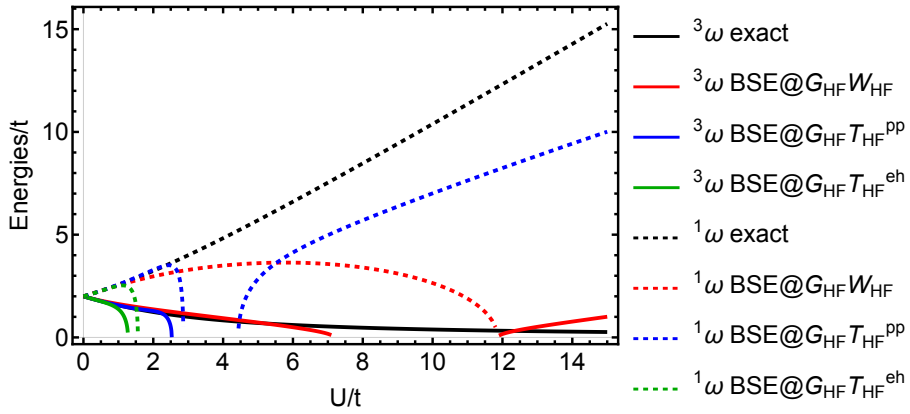

Figure 7.6 – Energies d'excitation neutres : exacte (noire), BSE@GW (rouge), BSE@GT^{pp} (bleu) and BSE@$G\overline{T}^{eh}$ (verte) en fonctions de U/t opur le dimère asymétrique ($\Delta v = 0$) pour les états excités du triplet (solide) et du singulet (pointillés).

7.5.2 Dimère de Hubbard asymétrique

Excitations chargés

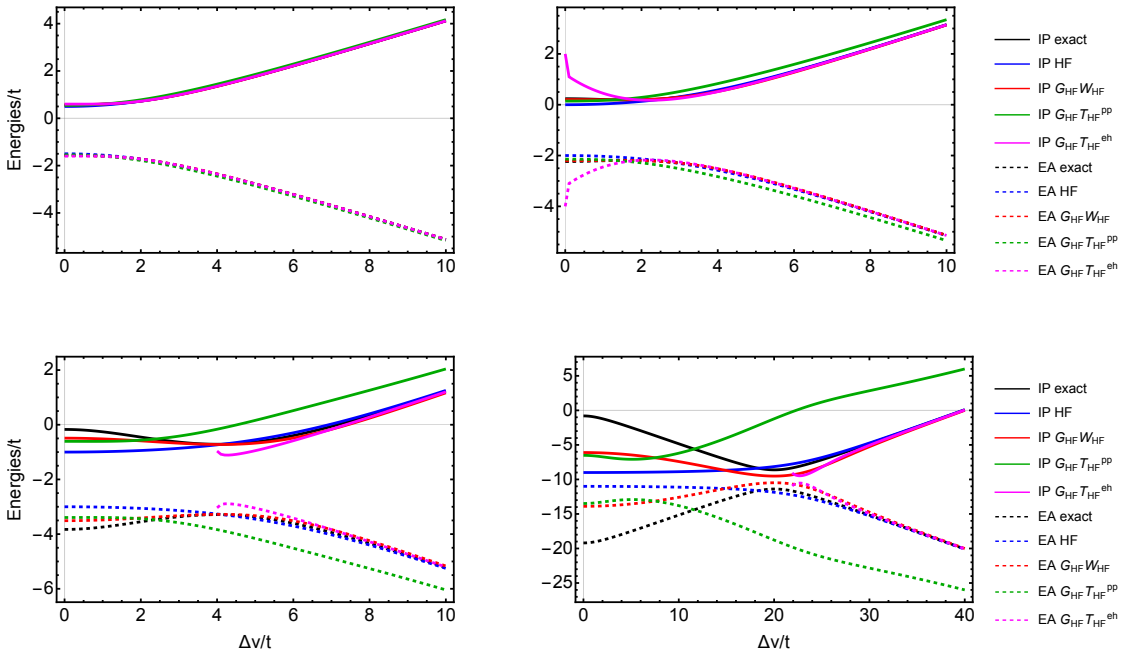

Figure 7.7 – IP et EA en fonctions de $\Delta v/t$ dans le cas du dimère asymétrique pour $U/t = 1$ (panneau haut gauche), $U/t = 2$ (panneau haut droit), $U/t = 4$ (panneau bas gauche) et $U/t = 20$ (panneau bas droit) obtenus à différend niveaux de théorie: exacte (noire), HF (bleu), $G_{\mathrm{HF}}W_{\mathrm{HF}}$ (rouge), $G_{\mathrm{HF}}T^{pp}_{\mathrm{HF}}$ (verte) et $G_{\mathrm{HF}}\overline{T}^{eh}_{\mathrm{HF}}$ (magenta).

Dans la Fig. 7.7, nous rapportons l'IP et l'EA en fonction de $\Delta v/t$. Le rapport U/t est fixé à différentes valeurs. Par exemple, si nous définissons $U/t = 20$, pour $\Delta v/t < 20$ (panneau inférieur droit de la Fig. 7.7), nous pouvons supposer que le système est dans un régime fortement corrélé, alors que, pour $\Delta v/t > 20$, la corrélation électronique est faible. Quant au cas symétrique, nous montrons que, dans le régime fortement corrélé, toutes les approximations sous-estiment le gap fondamental exact, avec une performance légèrement meilleure de GW (courbes rouges) par rapport à GT^{pp} (courbes vertes) et $G\overline{T}^{eh}$ (courbes magenta). Pour $\Delta v/t > U/t$, HF, GW et GT^{eh} tendent vers les valeurs exactes, tandis que GT^{pp} s'écarte du résultat exact. Enfin, $G\overline{T}^{eh}$ produit des pôles complexes pour $\Delta v/t$ inférieur à une valeur critique.

Excitations neutres (Δv fixé)

Nous commençons par analyser l'excitation du triplet. La fonction d'onde à l'état excité triplet $|^3\Psi^N\rangle$ [voir Eq. (7.129)] ne dépend pas de Δv, contrairement au singulet ground-fonction d'onde d'état $|^1\Psi_0^N\rangle$. À $\Delta v = 0$ et $U = 0$, $|^1\Psi_0^N\rangle$ est une combinaison linéaire de $|\uparrow_1\downarrow_2\rangle$, $|\downarrow_1\uparrow_2\rangle$, $|\uparrow\downarrow_1\ 0_2\rangle$ et $|0_1\ \uparrow\downarrow_2\rangle$ avec des poids égaux. La contribution des occupations doubles, $|\uparrow\downarrow_1\ 0_2\rangle$ et $|0_1\ \uparrow\downarrow_2\rangle$, diminue en augmentant U/t et augmente en augmentant $\Delta v/t$. Cette énergie d'excitation est bien décrite par GW jusqu'à $U/t \approx 5$ pour $\Delta v = 0$, comme le montre la Fig. 7.8 (panneau supérieur gauche); l'erreur par rapport au résultat exact augmente avec $\Delta v/t$ (voir le panneau supérieur droit de la Fig. 7.8). Dans le cas de l'énergie d'excitation singulet, nous observons que l'erreur GW diminue en augmentant

$\Delta v/t$ (voir les panneaux inférieurs de la Fig. 7.8). Pour la matrice T particule-particule, les résultats sont présentés dans la Fig. 7.9. Pour les énergies de transition triplet et singulet, l'erreur augmente avec Δv.

Lorsque nous traçons les excitations neutres de la matrice T électron-trou en fonction de U/t pour différentes valeurs de $\Delta v/t$, on observe que ces excitations neutres deviennent complexes à mesure que U/t se rapproche de la valeur de $\Delta v/t$. Ce comportement est cohérent dans tous les cas et se produit lorsque l'énergie de liaison associée à l'excitation neutre commence à augmenter rapidement. Cette augmentation indique un renforcement significatif de l'interaction électron-trou, et elle est observée à la fois pour les transitions triplet et singulet. Auparavant, nous avons constaté que GW fournit une meilleure description des transitions triplet par rapport aux transitions singulet. Cependant, pour T^{pp}, la tendance inverse est observée. Dans le cas de $\overline{T}^{eh}$, les deux types d'excitations sont décrits avec à peu près le même niveau de précision.

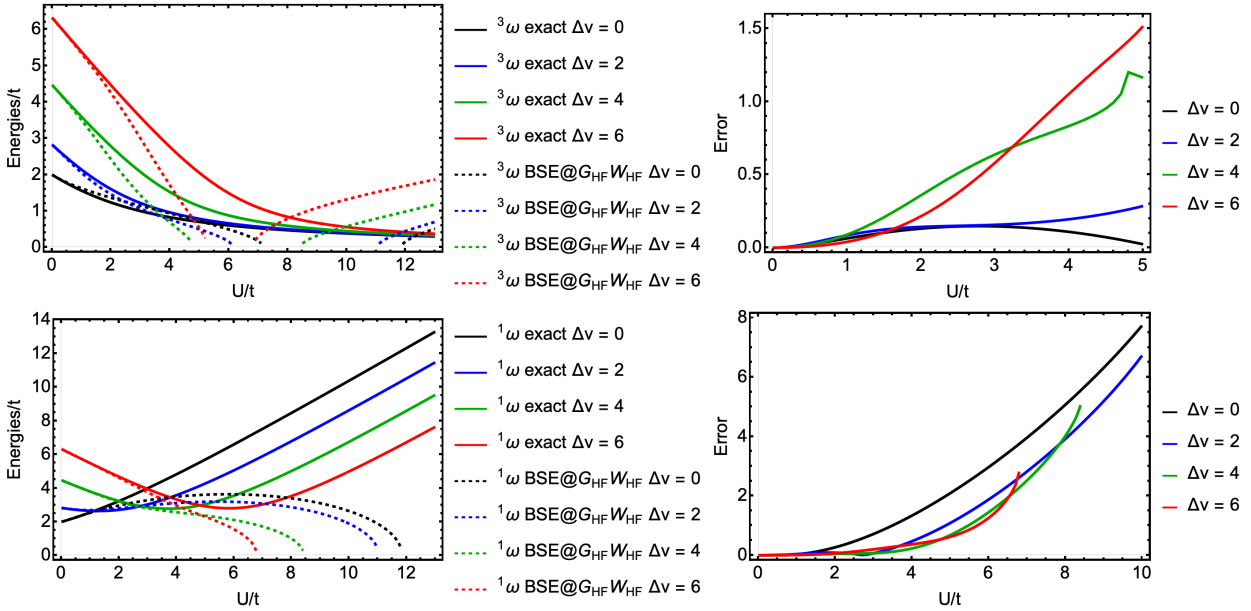

Figure 7.8 – Triplet (haut) et singulet (bas), excitations neutres BSE@$G_{\mathrm{HF}}W_{\mathrm{HF}}$ (gauche) et leur erreur correspondante par rapport au résultat exact (droite) en fonctions de U/t pour différentes valeurs de $\Delta v/t$.

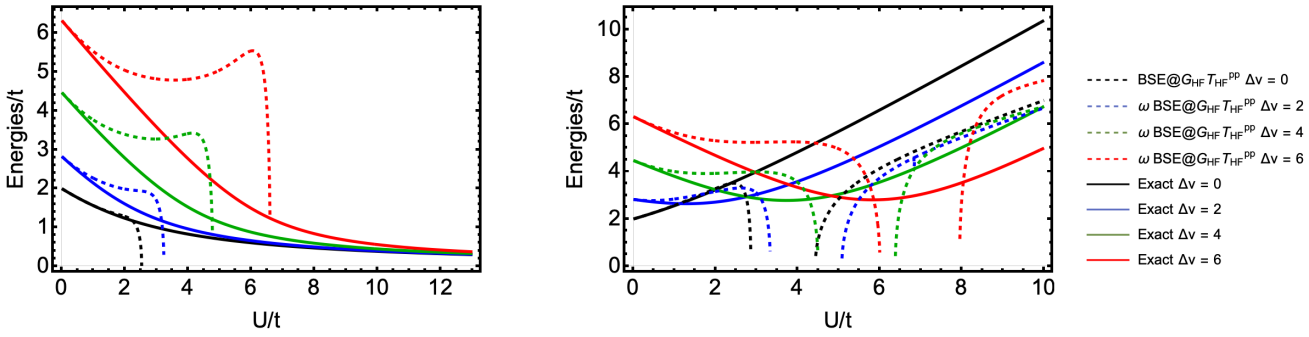

Figure 7.9 – Triplet (gauche) et singulet (droite), excitations neutres BSE@$G_{\mathrm{HF}}T_{\mathrm{HF}}^{pp}$ en fonctions de U/t pour différentes valeurs de $\Delta v/t$.

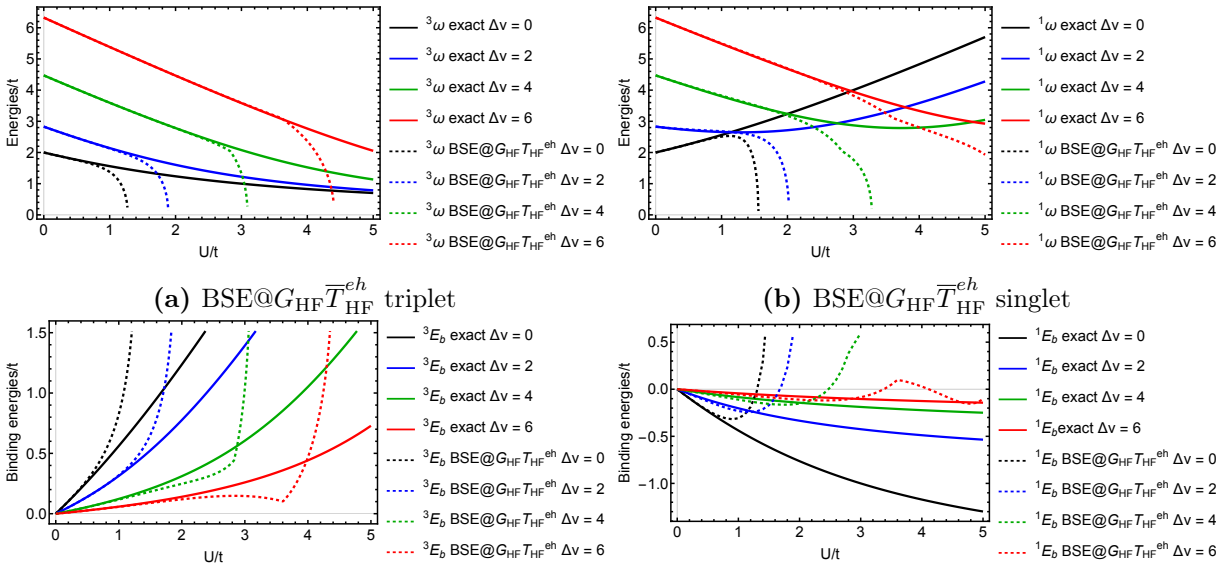

(a) BSE@$G_{\mathrm{HF}}\overline{T}^{eh}_{\mathrm{HF}}$ triplet

(b) BSE@$G_{\mathrm{HF}}\overline{T}^{eh}_{\mathrm{HF}}$ singlet

(c) Energie de liaison du triplet

(d) Energie de liaison du singulet

Figure 7.10 – Excitations neutres BSE@$G_{\mathrm{HF}}\overline{T}^{eh}_{\mathrm{HF}}$ et leur energie de liaison correspondante en fonctions de U/t pour différentes valeurs de $\Delta v/t$.

Excitations neutres (U fixé)

Dans ce qui suit, nous choisissons une valeur suffisamment grande de U/t pour placer le système dans un régime de forte corrélation lorsque $\Delta v/t = 0$. Pour une valeur U/t fixe, lorsque $\Delta v/t > U/t$, l'état fondamental présentera un poids prédominant sur le site doublement occupé :

$$|^1\Psi_0^N\rangle \underset{\Delta v=0}{\approx} c_{10}\,|\uparrow_1\downarrow_2\rangle + c_{20}\,|\downarrow_1\uparrow_2\rangle \xrightarrow[\Delta v\gg U]{} |0_1\ \uparrow\downarrow_2\rangle \tag{7.137}$$

L'état excité du triplet reste inchangé avec des variations de U ou Δv [voir Eq. (7.129)]. Concernant l'état excité singulet, nous avons

$$|^1\Psi_1^N\rangle \underset{\Delta v=0}{=} \frac{|\uparrow\downarrow_1\ 0_2\rangle - |0_1\ \uparrow\downarrow_2\rangle}{\sqrt{2}} \xrightarrow[\Delta v\gg U]{} c_{12}\,|\uparrow_1\downarrow_2\rangle + c_{22}\,|\downarrow_1\uparrow_2\rangle \tag{7.138}$$

Dans cette limite, la fonction d'onde de l'état excité singulet, au lieu d'être composée de configurations équipondérées constituées d'électrons situés sur le même site à $\Delta v = 0$, mélange des configurations où les électrons sont situés sur les deux sites. On pourrait donc dire que l'état singulet va vers une délocalisation des particules d'un site à un autre et, par conséquent, sa fonction d'onde devient similaire à celle de l'état triplet. Par conséquent, les deux excitations $^3\omega$ et $^1\omega$ fusionnent. Dans ce qui suit, «délocalisation» fera référence à cette situation dans laquelle le singulet et le triplet fusionnent.

Sur la Fig. 7.11, nous analysons plus en détail l'évolution des énergies d'excitation singulet et triplet en fonction de $\Delta v/t$. Ici, nous comparons uniquement les excitations neutres GW et GT^{pp} puisque les excitations $G\overline{T}^{eh}$ deviennent complexes assez rapidement avec l'augmentation de U/t. Tout d'abord, nous remarquons que, puisque les fonctions d'onde des états fondamental et excité du singulet dépendent de $\Delta v/t$, les probabilités de transition vers les états singulet dépendent également de $\Delta v/t$. En particulier, la probabilité transition exacte

$$f_1 = \langle^1\Psi_0^N|\hat{n}_1 - \hat{n}_2|^1\Psi_1^N\rangle \tag{7.139}$$

associée à l'excitation du singulet culmine à $\Delta v/t = U/t$, comme le montre l'avant-dernier panneau de la Fig. 7.11, ce qui accompagne un changement dans les nombres d'occupation du site de l'état fondamental et de l'état singulet correspondant ($\langle \hat{n}_i \rangle_0 \equiv \langle {}^1\Psi_0^N | \hat{n}_i | {}^1\Psi_0^N \rangle$ et $\langle \hat{n}_i \rangle_1 \equiv \ mel * {}^1\Psi_1^N \hat{n}_i {}^1\Psi_1^N$, respectivement, avec $i = 1$ ou 2, indiquant le site). On observe que, précisément à la valeur $\Delta v/t = U/t$, l'énergie d'excitation singulet calculée dans l'approximation GT^{pp} rencontre une singularité dans le cas $U/t = 20$, alors que , pour $U/t = 4$, la singularité disparaît mais l'énergie devient complexe en dessous de $\Delta v/t = 4$. L'énergie d'excitation triplet, au contraire, devient complexe en dessous de $\Delta v/t = U/t$. Dans le cas de l'approximation GW, l'énergie d'excitation singulet est complexe sur une plage légèrement plus grande de $\Delta v/t$ pour $U/t = 20$, alors qu'elle reste toujours réelle pour $U/t = 4$ (voir premier panneau de la Fig. 7.11). Dans l'ensemble, pour $\Delta v/t \ll U/t$, GW décrit mieux que GT^{pp} l'énergie d'excitation triplet pour $U/t = 20$ et les transitions singulet et triplet pour $U/t = 4$. Les énergies de liaison correspondantes souffrent cependant de l'erreur GW au niveau du gap fondamental.

Pour $\Delta v/t \gg U/t$, les noyaux exacts et approximatifs de BSE deviennent négligeables de sorte que les énergies d'excitation triplet et singulet tendent vers l'écart fondamental : les énergies d'excitation HF et GW se fondent avec le gap fondamental exacte pour les grands $\Delta v/t$; au lieu de cela, les énergies d'excitation GT^{pp} tendent vers le gap fondamental GT^{pp}, qui, comme nous l'avons discuté ci-dessus, s'écarte du gap exact. Bien entendu, ces évolutions des énergies d'excitation influencent la qualité des énergies de liaison correspondantes, qui tendent vers les résultats exacts dans cette limite.

Dans le cas fortement corrélé ($U/t = 20$ dans le panneau de gauche de la Fig. 7.11), nous observons que pour GW, l'état excité du triplet reste réel à tout moment. En revanche, l'état excité singulet reste réel partout, sauf près de la valeur $\Delta v/t \approx 20$, où une délocalisation se produit dans le cas exact et dans le cas de GT^{pp}. Lors de cette délocalisation, l'état triplet devient réel pour GT^{pp}, et, un peu plus tard, la même chose se produit avec l'état singlet pour GW. Simultanément, il y a un changement dans le signe des énergies de liaison, et elles deviennent réelles. Cette transition de valeurs propres complexes à des valeurs propres réelles peut être attribuée au fait que lorsque $\Delta v/t > U/t$, l'état singulet devient similaire à l'état triplet.

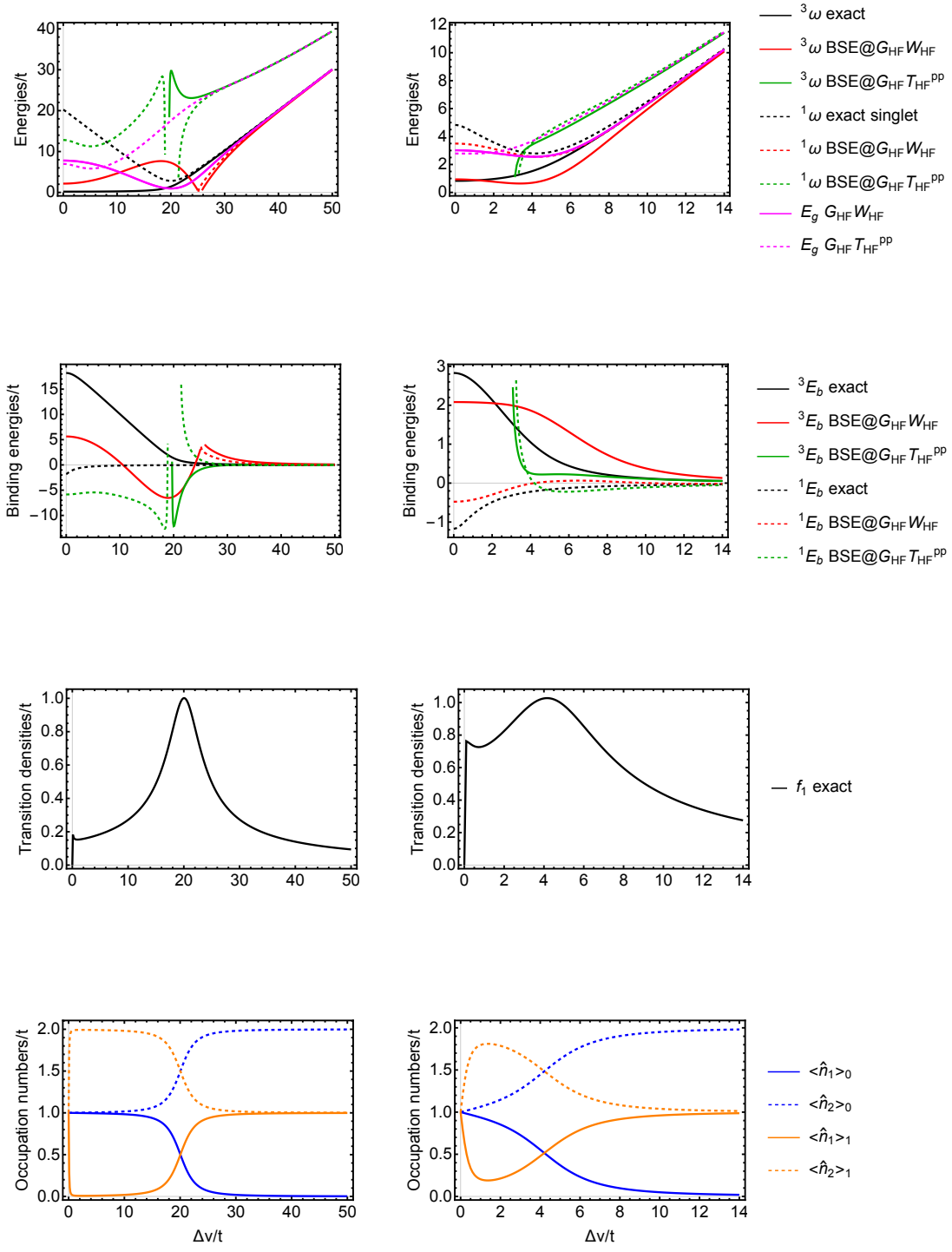

Figure 7.11 – Neutral excitations (first row), binding energies (second row), transitions densities (third row), and occupation numbers (fourth row) of the ground state and the first singlet excited state as functions of $\Delta v/t$. Results obtained for $U/t = 20$ (left column) and $U/t = 4$ (right column).

Conclusions et Perspectives

Dans cette thèse, nous avons étudié trois approximations basées sur la théorie des perturbations à N corps de la fonction de Green pour obtenir les excitations chargées et neutres de systèmes à N corps. Dans un premier temps, ces approximations ont été étudiées, implémentées et testées sur un système modèle simple : le modèle de Hubbard à deux sites à demi-remplie. Ces types de modèles en mécanique quantique pour lesquels il est possible de résoudre explicitement l'équation de Schrödinger sont utiles à la fois pour comprendre des systèmes plus complexes et pour tester et développer des approches théoriques. Nous avons ensuite étendu notre analyse à de véritables systèmes moléculaires.

Sur la base du modèle du dimère asymétrique de Hubbard, résoluble exactement, nous avons évalué la précision des énergies d'excitation chargées et neutres dans différents régimes de corrélation obtenus avec trois approximations distinctes de la self-énergie: GW, la matrice T particule-particule et la matrice T particule-trou qui correspondent à une sommation de différentes familles de diagrammes. En particulier, en utilisant ces self-énergies approximatives et leur noyau correspondant, les énergies des états excités ont été calculées dans le cadre du formalisme de Bethe-Salpeter. Dans l'ensemble, nous avons constaté que l'approximation GW fonctionne mieux que les approximations GT à la fois pour les énergies des quasiparticules et les énergies d'excitation neutres en fonction du degré de corrélation (U/t) et d'asymétrie ($\Delta v/t$) dans le système. En particulier, les énergies des quasiparticules GT^{pp} ne présentent pas le comportement correct comme $\Delta v/t \to \infty$. Dans cette limite, la corrélation devient négligeable dans le cas exact et dans GW, mais pas dans GT, en raison de la polarisabilité particule-particule non nulle qui entre dans l'expression de la matrice T. De ce fait, le comportement des énergies d'excitation neutres est également incorrect dans la grande limite $\Delta v/t$, contrairement à leurs homologues HF et GW. Cela suggère que la qualité des résultats GT peut être sensible aux inhomogénéités des matériaux réels. Pour apporter plus de lumière sur cette question, il serait intéressant d'analyser cette question dans des matériaux réels [118, 119]. De plus, GT semble être plus sensible à la fonction de Green de départ, du moins pour le dimère de Hubbard, et cela peut fortement affecter la qualité des résultats.

Nous avons ensuite étendu notre étude à des molécules réelles. Dans les systèmes finis, la self-énergie GW est généralement implémentée en utilisant la fonction de réponse χ plutôt que la polarisabilité P pour calculer W. Bien que l'expression RPA pour les fonctions de réponse électron-trou et particule-particule utilisées respectivement dans W et la matrice particule-particule T sont connus, ce n'est pas le cas, à notre connaissance, pour la fonction de réponse RPA électron-trou. Par conséquent, nous avons dérivé ces équations et mis les trois approximations sur un pied d'égalité. Pour évaluer l'efficacité de ces approches, nous avons évalué leurs performances sur des systèmes moléculaires. Plus précisément, nous calculons les principales IP sur une collection de 20 petites molécules. Les résultats de nos calculs indiquent clairement que le formalisme de la matrice eh T est insuffisant par rapport aux deux autres approches. Le sous-ensemble de diagrammes composé des diagrammes à contacts eh est donc moins pertinent que les deux autres sous-ensembles (anneaux directs et échelles pp) dans le contexte présent. Cette observation ouvre la voie à une étude sur la version écrantée de la matrice eh T, qui a démontré des succès dans divers systèmes, tels que les structures périodiques ferromagnétiques, comme indiqué dans des études antérieures [56, 107, 57, 108]. Une autre piste d'exploration plus approfondie implique la combinaison de ces trois canaux de corrélation, semblable à « l'échange de fluctuation » (FLEX) [120, 121, 50, 122], l'approximation de Baym-Kadanoff [44, 45], la théorie du parquet [123, 124], et d'autres approches similaires [42, 125]. Bien que difficile, cette tâche est très prometteuse et représente une voie potentielle pour nos

futures études.

En termes de perspectives, il est conseillé d'envisager d'étudier la question des valeurs propres complexes dans le contexte de BSE [126, 127]. Ce sujet a été exploré, notamment dans le domaine de la physique des particules, où il a été démontré que des valeurs propres complexes peuvent apparaître en raison d'un problème de référence. Ce problème peut être résolu en corrigeant la fonction de Green sans interaction avec une self-énergie, et dans les cas où cette correction est insuffisante, en introduisant également des corrections de vertex. De plus, il a été établi que des valeurs propres complexes peuvent également correspondre au processus physique de transition d'un état lié à un état libre. Ce phénomène a été rigoureusement prouvé dans le cas d'un système comprenant deux particules sans spin avec des interactions instantanées [128]. Il est important de noter que ce résultat reste vrai même dans la limite non relativiste. De plus, la transition d'un état lié à un état libre a été observée dans le contexte de la théorie dynamique du champ moyen (DMFT), comme documenté dans la littérature. Il est montré que le noyau de BSE est intimement lié à la dérivée seconde de l'énergie libre. Par conséquent, cela fournit un cadre précieux pour étudier les transitions métal-isolant (Mott), dans le cadre de la théorie de Landau des transitions de phase [129].

Remerciements

Je remercie Monsieur Pierre-François Loos et Madame Pina Romaniello, pour tout ce que j'ai appris grâce à eux et pour leurs contributions aux discussions, les calculs, le code, l'écriture et la correction du manuscrit et des articles, sans lesquelles cette thèse n'aurait pas aboutie. Je remercie Monsieur Thierry Leininger, qui a accepté en fin de deuxième année de me laisser terminer la thèse. Je remercie Monsieur Julien Toulouse et Monsieur Francesco Sottile d'avoir accepté d'être rapporteurs, d'avoir pris le temps de lire et corriger le manuscrit et des questions qu'ils m'ont posé, ainsi que Madame Nadine Halberstadt et Madame Elisa Rebolini d'avoir accepté d'être rapporteur, d'avoir lu et posé des questions sur le manuscrit.
Je remercie Monsieur Hagop Szadjian et Madame Luisa Fermo d'avoir pris le temps d'échanger avec moi et de me recevoir ainsi que Monsieur Michael Urban pour la discussion que nous avons eue.
Je remercie Kevin Levesque-Simon qui est quelqu'un de très déterminé et de très engagé dans son travail avec les personnes avec qui ils collaborent, et qui a de grandes qualités humaines. Il aide et rend service aux autres, par pur altruisme et cela même quand il ne peut pas forcement se le permettre. Pendant la thèse et même avant, il prenait régulièrement de mes nouvelles et me remontait le moral lors des moments difficiles ("répète après moi : je suis une putain de légende").
Enfin je remercie aussi ceux que j'ai rencontré à Toulouse, notamment dans cette petite salle de sport de l'allée Jean Jaurès, qui avec le temps est devenu comme une grande famille, ils ont été une source d'inspiration, de motivation et ma bouteille d'oxygène dans cette inertie morose de ces années covid.

Bibliography

[1] G. Onida, L. Reining, and A. Rubio, "Electronic excitations: Density-functional versus many-body green's function approaches," *Rev. Mod. Phys.*, vol. 74, pp. 601–659, 2002.

[2] M. Rohlfing and S. G. Louie, "Optical excitations in conjugated polymers," *Phys. Rev. Lett.*, vol. 82, pp. 1959–1962, Mar 1999. [Online]. Available: https://link.aps.org/doi/10.1103/PhysRevLett.82.1959

[3] J.-W. van der Horst, P. A. Bobbert, M. A. J. Michels, G. Brocks, and P. J. Kelly, "Ab initio calculation of the electronic and optical excitations in polythiophene: Effects of intra- and interchain screening," *Phys. Rev. Lett.*, vol. 83, pp. 4413–4416, Nov 1999. [Online]. Available: https://link.aps.org/doi/10.1103/PhysRevLett.83.4413

[4] P. Puschnig and C. Ambrosch-Draxl, "Suppression of electron-hole correlations in 3d polymer materials," *Phys. Rev. Lett.*, vol. 89, p. 056405, Jul 2002. [Online]. Available: https://link.aps.org/doi/10.1103/PhysRevLett.89.056405

[5] M. L. Tiago, J. E. Northrup, and S. G. Louie, "Ab initio calculation of the electronic and optical properties of solid pentacene," *Phys. Rev. B*, vol. 67, p. 115212, Mar 2003. [Online]. Available: https://link.aps.org/doi/10.1103/PhysRevB.67.115212

[6] D. Rocca, D. Lu, and G. Galli, "Ab initio calculations of optical absorption spectra: Solution of the bethe–salpeter equation within density matrix perturbation theory," *J. Chem. Phys.*, vol. 133, no. 16, p. 164109, 2010.

[7] P. Boulanger, D. Jacquemin, I. Duchemin, and X. Blase, "Fast and accurate electronic excitations in cyanines with the many-body bethe-salpeter approach," *J. Chem. Theory Comput.*, vol. 10, no. 3, pp. 1212–1218, 2014.

[8] D. Jacquemin, I. Duchemin, and X. Blase, "Benchmarking the Bethe–Salpeter Formalism on a Standard Organic Molecular Set," *J. Chem. Theory Comput.*, vol. 11, no. 7, pp. 3290–3304, Jul. 2015.

[9] F. Bruneval, S. M. Hamed, and J. B. Neaton, "A systematic benchmark of the ab initio bethe-salpeter equation approach for low-lying optical excitations of small organic molecules," *J. Chem. Phys.*, vol. 142, no. 24, p. 244101, 2015.

[10] D. Jacquemin, I. Duchemin, and X. Blase, "0–0 energies using hybrid schemes: Benchmarks of td-dft, cis(d), adc(2), cc2, and bse/gw formalisms for 80 real-life compounds," *J. Chem. Theory Comput.*, vol. 11, no. 11, pp. 5340–5359, 2015.

[11] D. Hirose, Y. Noguchi, and O. Sugino, "All-electron gw+bethe-salpeter calculations on small molecules," *Phys. Rev. B*, vol. 91, p. 205111, May 2015. [Online]. Available: https://link.aps.org/doi/10.1103/PhysRevB.91.205111

[12] D. Jacquemin, I. Duchemin, and X. Blase, "Is the bethe–salpeter formalism accurate for excitation energies? comparisons with td-dft, caspt2, and eom-ccsd," *J. Phys. Chem. Lett.*, vol. 8, no. 7, pp. 1524–1529, 2017.

[13] D. Jacquemin, I. Duchemin, A. Blondel, and X. Blase, "Benchmark of bethe-salpeter for triplet excited-states," *J. Chem. Theory Comput.*, vol. 13, no. 2, pp. 767–783, 2017.

[14] T. Rangel, S. M. Hamed, F. Bruneval, and J. B. Neaton, "An assessment of low-lying excitation energies and triplet instabilities of organic molecules with an *ab initio* Bethe-Salpeter equation approach and the Tamm-Dancoff approximation," *J. Chem. Phys.*, vol. 146, no. 19, p. 194108, May 2017.

[15] K. Krause and W. Klopper, "Implementation of the bethe-salpeter equation in the turbomole program," *J. Comput. Chem.*, vol. 38, no. 6, pp. 383–388, 2017.

[16] X. Gui, C. Holzer, and W. Klopper, "Accuracy assessment of gw starting points for calculating molecular excitation energies using the bethe–salpeter formalism," *J. Chem. Theory Comput.*, vol. 14, no. 4, pp. 2127–2136, 2018.

[17] X. Blase, I. Duchemin, and D. Jacquemin, "The bethe–salpeter equation in chemistry: relations with td-dft, applications and challenges," *Chem. Soc. Rev.*, vol. 47, pp. 1022–1043, 2018. [Online]. Available: http://dx.doi.org/10.1039/C7CS00049A

[18] C. Liu, J. Kloppenburg, Y. Yao, X. Ren, H. Appel, Y. Kanai, and V. Blum, "All-electron ab initio bethe-salpeter equation approach to neutral excitations in molecules with numeric atom-centered orbitals," *J. Chem. Phys.*, vol. 152, p. 044105, 2020.

[19] X. Blase, I. Duchemin, D. Jacquemin, and P.-F. Loos, "The bethe–salpeter equation formalism: From physics to chemistry," *J. Phys. Chem. Lett.*, vol. 11, no. 17, pp. 7371–7382, 2020.

[20] C. Holzer and W. Klopper, "Communication: A hybrid bethe–salpeter/time-dependent density-functional-theory approach for excitation energies," *J. Chem. Phys.*, vol. 149, no. 10, p. 101101, 2018.

[21] C. Holzer, X. Gui, M. E. Harding, G. Kresse, T. Helgaker, and W. Klopper, "Bethe–salpeter correlation energies of atoms and molecules," *J. Chem. Phys.*, vol. 149, p. 144106, 2018.

[22] P.-F. Loos, A. Scemama, I. Duchemin, D. Jacquemin, and X. Blase, "Pros and cons of the bethe–salpeter formalism for ground-state energies," *J. Phys. Chem. Lett.*, vol. 11, no. 9, pp. 3536–3545, 2020.

[23] P.-F. Loos, M. Comin, X. Blase, and D. Jacquemin, "Reference energies for intramolecular charge-transfer excitations," *J. Chem. Theory Comput.*, vol. 17, no. 6, pp. 3666–3686, 2021.

[24] C. A. McKeon, S. M. Hamed, F. Bruneval, and J. B. Neaton, "An optimally tuned range-separated hybrid starting point for ab initio gw plus bethe–salpeter equation calculations of molecules," *J. Chem. Phys.*, vol. 157, no. 7, p. 074103, 2022.

[25] L. Hedin and J. Lee, "Sudden approximation in photoemission and beyond," *Journal of electron spectroscopy and related phenomena*, vol. 124, no. 2-3, pp. 289–315, 2002.

[26] F. Reinert and S. Hüfner, "Photoemission spectroscopy—from early days to recent applications," *New Journal of Physics*, vol. 7, no. 1, p. 97, 2005.

[27] M. Govoni and G. Galli, "Gw100: Comparison of methods and accuracy of results obtained with the west code," *J. Chem. Theory Comput.*, vol. 14, pp. 1895–1909, 2018.

[28] M. J. van Setten, R. Costa, F. Viñes, and F. Illas, "Assessing *GW* Approaches for Predicting Core Level Binding Energies," *J. Chem. Theory Comput.*, vol. 14, no. 2, pp. 877–883, Feb. 2018.

[29] E. Monino and P.-F. Loos, "Connections and performances of green's function methods for charged and neutral excitations," *J. Chem. Phys.*, vol. 159, no. 3, p. 034105, Jul. 2023. [Online]. Available: https://doi.org/10.1063/5.0159853

[30] A. Szabo and N. S. Ostlund, *Modern quantum chemistry.* New York: McGraw-Hill, 1989.

[31] E. K. Gross and E. Runge, "Many-particle theory," 1986.

[32] A. L. Fetter and J. D. Waleck, *Quantum Theory of Many Particle Systems.* McGraw Hill, San Francisco, 1971.

[33] G. Csanak, H. Taylor, and R. Yaris, "Green's function technique in atomic and molecular physics," in *Advances in atomic and molecular physics.* Elsevier, 1971, vol. 7, pp. 287–361.

[34] R. M. Martin, L. Reining, and D. M. Ceperley, *Interacting Electrons: Theory and Computational Approaches.* Cambridge University Press, 2016.

[35] F. Aryasetiawan and O. Gunnarsson, "The gw method," *Rep. Prog. Phys.*, vol. 61, pp. 237–312, 1998.

[36] L. Reining, "The GW approximation: Content, successes and limitations: The GW approximation," *Wiley Interdiscip. Rev. Comput. Mol. Sci.*, vol. 8, p. e1344, 2017.

[37] D. Golze, M. Dvorak, and P. Rinke, "The gw compendium: A practical guide to theoretical photoemission spectroscopy," *Front. Chem.*, vol. 7, p. 377, 2019.

[38] F. Bruneval, N. Dattani, and M. J. van Setten, "The gw miracle in many-body perturbation theory for the ionization potential of molecules," *Front. Chem.*, vol. 9, p. 749779, 2021.

[39] R. M. Richard, M. S. Marshall, O. Dolgounitcheva, J. V. Ortiz, J.-L. Brédas, N. Marom, and C. D. Sherrill, "Accurate Ionization Potentials and Electron Affinities of Acceptor Molecules I. Reference Data at the CCSD(T) Complete Basis Set Limit," *J. Chem. Theory Comput.*, vol. 12, no. 2, pp. 595–604, Feb. 2016.

[40] G. Strinati, "Application of the Green's functions method to the study of the optical properties of semiconductors," *Riv. Nuovo Cimento*, vol. 11, pp. 1–86, 1988.

[41] L. Hedin, "New method for calculating the one-particle Green's function with application to the electron-gas problem," *Phys. Rev.*, vol. 139, no. 3A, p. A796, 1965.

[42] P. Romaniello, F. Bechstedt, and L. Reining, "Beyond the G W approximation: Combining correlation channels," *Phys. Rev. B*, vol. 85, no. 15, p. 155131, 2012.

[43] H. A. Bethe and J. Goldstone, "Effect of a repulsive core in the theory of complex nuclei," *Proc. Math. Phys. Eng. Sci.*, vol. 238, no. 1215, pp. 551–567, 1957. [Online]. Available: http://www.jstor.org/stable/100108

[44] G. Baym and L. P. Kadanoff, "Conservation laws and correlation functions," *Phys. Rev.*, vol. 124, pp. 287–299, Oct 1961. [Online]. Available: https://link.aps.org/doi/10.1103/PhysRev.124.287

[45] G. Baym, "Self-Consistent Approximations in Many-Body Systems," *Phys. Rev.*, vol. 127, no. 4, pp. 1391–1401, Aug. 1962.

[46] P. Danielewicz, "Quantum theory of nonequilibrium processes, i," *Ann. Phys.*, vol. 152, no. 2, pp. 239–304, 1984. [Online]. Available: https://www.sciencedirect.com/science/article/pii/0003491684900927

[47] ——, "Quantum theory of nonequilibrium processes ii. application to nuclear collisions," *Ann. Phys.*, vol. 152, no. 2, pp. 305–326, 1984. [Online]. Available: https://www.sciencedirect.com/science/article/pii/0003491684900939

[48] A. Liebsch, "Ni *d*-band self-energy beyond the low-density limit," *Phys. Rev. B*, vol. 23, pp. 5203–5212, May 1981. [Online]. Available: https://link.aps.org/doi/10.1103/PhysRevB.23.5203

[49] N. Bickers and D. Scalapino, "Conserving approximations for strongly fluctuating electron systems. i. formalism and calculational approach," *Ann. Phys.*, vol. 193, no. 1, pp. 206–251, 1989. [Online]. Available: https://www.sciencedirect.com/science/article/pii/000349168990359X

[50] N. E. Bickers and S. R. White, "Conserving approximations for strongly fluctuating electron systems. ii. numerical results and parquet extension," *Phys. Rev. B*, vol. 43, pp. 8044–8064, Apr 1991. [Online]. Available: https://link.aps.org/doi/10.1103/PhysRevB.43.8044

[51] M. I. Katsnelson and A. I. Lichtenstein, "LDA approach to the electronic structure of magnets: correlation effects in iron," *J. Phys. Condens. Matter*, vol. 11, no. 4, pp. 1037–1048, jan 1999.

[52] M. Katsnelson and A. Lichtenstein, "Electronic structure and magnetic properties of correlated metals," *Eur. Phys. J. B*, vol. 30, pp. 9–15, 2002.

[53] V. P. Zhukov, E. V. Chulkov, and P. M. Echenique, "GW + T theory of excited electron lifetimes in metals," *Phys. Rev. B*, vol. 72, no. 15, p. 72.155109, Oct. 2005.

[54] M. Puig von Friesen, C. Verdozzi, and C.-O. Almbladh, "Kadanoff-baym dynamics of hubbard clusters: Performance of many-body schemes, correlation-induced damping and multiple steady and quasi-steady states," *Phys. Rev. B*, vol. 82, p. 155108, Oct 2010. [Online]. Available: https://link.aps.org/doi/10.1103/PhysRevB.82.155108

[55] J. Gukelberger, L. Huang, and P. Werner, "On the dangers of partial diagrammatic summations: Benchmarks for the two-dimensional hubbard model in the weak-coupling regime," *Phys. Rev. B*, vol. 91, p. 235114, Jun 2015.

[56] M. C. T. D. Müller, S. Blügel, and C. Friedrich, "Electron-magnon scattering in elementary ferromagnets from first principles: Lifetime broadening and band anomalies," *Phys. Rev. B*, vol. 100, p. 045130, Jul 2019. [Online]. Available: https://link.aps.org/doi/10.1103/PhysRevB.100.045130

[57] C. Friedrich, "Tetrahedron integration method for strongly varying functions: Application to the *gt* self-energy," *Phys. Rev. B*, vol. 100, p. 075142, Aug 2019. [Online]. Available: https://link.aps.org/doi/10.1103/PhysRevB.100.075142

[58] T. Biswas and A. Singh, "Excitonic effects in absorption spectra of carbon dioxide reduction photocatalysts," *npj Comput. Mater.*, vol. 7, p. 189, 2021.

[59] D. Zhang, N. Q. Su, and W. Yang, "Accurate Quasiparticle Spectra from the T-Matrix Self-Energy and the Particle–Particle Random Phase Approximation," *J. Phys. Chem. Lett.*, vol. 8, no. 14, pp. 3223–3227, Jul. 2017.

[60] J. Li, Z. Chen, and W. Yang, "Renormalized singles green's function in the t-matrix approximation for accurate quasiparticle energy calculation," *J. Phys. Chem. Lett.*, vol. 12, no. 26, pp. 6203–6210, 2021.

[61] P. Ring and P. Schuck, *The Nuclear Many-Body Problem*. Springer, 2004.

[62] W. Greiner, J. A. Maruhn *et al.*, *Nuclear models*. Springer, 1996.

[63] G. E. Scuseria, T. M. Henderson, and I. W. Bulik, "Particle-particle and quasiparticle random phase approximations: Connections to coupled cluster theory," *J. Chem. Phys.*, vol. 139, no. 10, p. 104113, 2013.

[64] E. E. Salpeter and H. A. Bethe, "A relativistic equation for bound-state problems," *Phys. Rev.*, vol. 84, p. 1232, 1951.

[65] F. Sottile, "Response functions of semiconductors and insulators: from the bethe-salpeter equation to time-dependent density functional theory," Ph.D. dissertation, Ecole Polytechnique X, 2003.

[66] J. G. Angyan, R.-F. Liu, J. Toulouse, and G. Jansen, "Correlation energy expressions from the adiabatic-connection fluctuation dissipation theorem approach," *J. Chem. Theory Comput.*, vol. 7, pp. 3116–3130, 2011.

[67] F. Bruneval, "Optimized virtual orbital subspace for faster GW calculations in localized basis," *J. Chem. Phys.*, vol. 145, no. 23, p. 234110, Dec. 2016.

[68] E. Monino and P.-F. Loos, "Spin-conserved and spin-flip optical excitations from the bethe–salpeter equation formalism," *J. Chem. Theory Comput.*, vol. 17, no. 5, pp. 2852–2867, 2021.

[69] P. Romaniello, S. Guyot, and L. Reining, "The self-energy beyond GW: Local and nonlocal vertex corrections," *J. Chem. Phys.*, vol. 131, p. 154111, 2009.

[70] P.-F. Loos and P. Romaniello, "Static and dynamic bethe–salpeter equations in the t-matrix approximation," *J. Chem. Phys.*, vol. 156, no. 16, p. 164101, 2022.

[71] D. J. Carrascal, J. Ferrer, J. C. Smith, and K. Burke, "The Hubbard dimer: A density functional case study of a many-body problem," *J. Phys. Condens. Matter*, vol. 27, no. 39, p. 393001, Oct. 2015.

[72] M. Gell-Mann and K. A. Brueckner, "Correlation energy of an electron gas at high density," *Phys. Rev.*, vol. 106, no. 2, pp. 364–368, 1957.

[73] D. Bohm and D. Pines, "A collective description of electron interactions. i. magnetic interactions," *Phys. Rev.*, vol. 82, pp. 625–634, Jun 1951. [Online]. Available: https://link.aps.org/doi/10.1103/PhysRev.82.625

[74] D. Pines and D. Bohm, "A collective description of electron interactions: Ii. collective vs individual particle aspects of the interactions," *Phys. Rev.*, vol. 85, pp. 338–353, Jan 1952. [Online]. Available: https://link.aps.org/doi/10.1103/PhysRev.85.338

[75] D. Bohm and D. Pines, "A collective description of electron interactions: Iii. coulomb interactions in a degenerate electron gas," *Phys. Rev.*, vol. 92, pp. 609–625, Nov 1953. [Online]. Available: https://link.aps.org/doi/10.1103/PhysRev.92.609

[76] P. Nozières and D. Pines, "Correlation energy of a free electron gas," *Phys. Rev.*, vol. 111, pp. 442–454, Jul 1958. [Online]. Available: https://link.aps.org/doi/10.1103/PhysRev.111.442

[77] R. Starke and G. Kresse, "Self-consistent green function equations and the hierarchy of approximations for the four-point propagator," *Phys. Rev. B*, vol. 85, p. 075119, Feb 2012. [Online]. Available: https://link.aps.org/doi/10.1103/PhysRevB.85.075119

[78] E. Maggio and G. Kresse, "Gw vertex corrected calculations for molecular systems," *J. Chem. Theory Comput.*, vol. 13, no. 10, pp. 4765–4778, 2017.

[79] P. C. Martin and J. Schwinger, "Theory of Many-Particle Systems. I," *Phys. Rev.*, vol. 115, no. 6, pp. 1342–1373, Sep. 1959.

[80] R. Del Sole, L. Reining, and R. W. Godby, "GwΓ approximation for electron self-energies in semiconductors and insulators," *Phys. Rev. B*, vol. 49, pp. 8024–8028, Mar 1994. [Online]. Available: https://link.aps.org/doi/10.1103/PhysRevB.49.8024

[81] E. L. Shirley, "Self-consistent gw and higher-order calculations of electron states in metals," *Phys. Rev. B*, vol. 54, pp. 7758–7764, Sep 1996. [Online]. Available: https://link.aps.org/doi/10.1103/PhysRevB.54.7758

[82] A. Schindlmayr and R. W. Godby, "Systematic vertex corrections through iterative solution of Hedin's equations beyond the GW approximation," *Phys. Rev. Lett.*, vol. 80, no. 8, p. 1702, 1998.

[83] A. J. Morris, M. Stankovski, K. T. Delaney, P. Rinke, P. García-González, and R. W. Godby, "Vertex corrections in localized and extended systems," *Phys. Rev. B*, vol. 76, p. 155106, Oct 2007. [Online]. Available: https://link.aps.org/doi/10.1103/PhysRevB.76.155106

[84] M. Shishkin, M. Marsman, and G. Kresse, "Accurate quasiparticle spectra from self-consistent gw calculations with vertex corrections," *Phys. Rev. Lett.*, vol. 99, p. 246403, Dec 2007. [Online]. Available: https://link.aps.org/doi/10.1103/PhysRevLett.99.246403

[85] A. Grüneis, G. Kresse, Y. Hinuma, and F. Oba, "Ionization potentials of solids: The importance of vertex corrections," *Phys. Rev. Lett.*, vol. 112, p. 096401, Mar 2014. [Online]. Available: https://link.aps.org/doi/10.1103/PhysRevLett.112.096401

[86] W. Chen and A. Pasquarello, "Accurate band gaps of extended systems via efficient vertex corrections in *gw*," *Phys. Rev. B*, vol. 92, p. 041115, 2015.

[87] X. Ren, N. Marom, F. Caruso, M. Scheffler, and P. Rinke, "Beyond the G W approximation: A second-order screened exchange correction," *Phys. Rev. B*, vol. 92, no. 8, p. 081104, Aug. 2015.

[88] F. Caruso, M. Dauth, M. J. van Setten, and P. Rinke, "Benchmark of gw approaches for the gw100 test set," *J. Chem. Theory Comput.*, vol. 12, p. 5076, 2016.

[89] L. Hung, F. Bruneval, K. Baishya, and S. Öğüt, "Benchmarking the *GW* Approximation and Bethe–Salpeter Equation for Groups IB and IIB Atoms and Monoxides," *J. Chem. Theory Comput.*, vol. 13, no. 5, pp. 2135–2146, May 2017.

[90] B. Cunningham, M. Grüning, P. Azarhoosh, D. Pashov, and M. van Schilfgaarde, "Effect of ladder diagrams on optical absorption spectra in a quasiparticle self-consistent *GW* framework," *Phys. Rev. Mater.*, vol. 2, p. 034603, 2018.

[91] V. Vlček, "Stochastic vertex corrections: Linear scaling methods for accurate quasiparticle energies," *J. Chem. Theory Comput.*, vol. 15, no. 11, pp. 6254–6266, 2019.

[92] A. M. Lewis and T. C. Berkelbach, "Vertex corrections to the polarizability do not improve the gw approximation for the ionization potential of molecules," *J. Chem. Theory Comput.*, vol. 15, p. 2925, 2019.

[93] Y. Wang, P. Rinke, and X. Ren, "Assessing the g0w00(1) approach: Beyond g0w0 with hedin's full second-order self-energy contribution," *J. Chem. Theory Comput.*, vol. 17, no. 8, pp. 5140–5154, 2021.

[94] C. Mejuto-Zaera and V. c. v. Vlček, "Self-consistency in $gw\Gamma$ formalism leading to quasiparticle-quasiparticle couplings," *Phys. Rev. B*, vol. 106, p. 165129, Oct 2022. [Online]. Available: https://link.aps.org/doi/10.1103/PhysRevB.106.165129

[95] Y. Wang and X. Ren, "Vertex effects in describing the ionization energies of the first-row transition-metal monoxide molecules," *J. Chem. Theory Comput.*, vol. 157, no. 21, p. 214115, 2022.

[96] A. Förster and L. Visscher, "Exploring the statically screened $g3w2$ correction to the gw self-energy: Charged excitations and total energies of finite systems," *Phys. Rev. B*, vol. 105, p. 125121, 2022.

[97] N. Dadkhah, W. R. L. Lambrecht, D. Pashov, and M. van Schilfgaarde, "Improved quasiparticle self-consistent electronic band structure and excitons in $\beta-\mathrm{ligao}_2$," *Phys. Rev. B*, vol. 107, p. 165201, 2023.

[98] M. Grzeszczyk, S. Acharya, D. Pashov, Z. Chen, K. Vaklinova, M. van Schilfgaarde, K. Watanabe, T. Taniguchi, K. S. Novoselov, M. I. Katsnelson, and M. Koperski, "Strongly correlated exciton-magnetization system for optical spin pumping in crbr3 and cri3." *Adv. Mater.*, vol. 35, no. 17, p. 2209513, 2023.

[99] G. Strinati, H. J. Mattausch, and W. Hanke, "Dynamical correlation effects on the quasiparticle bloch states of a covalent crystal," *Phys. Rev. Lett.*, vol. 45, pp. 290–294, Jul 1980. [Online]. Available: http://link.aps.org/doi/10.1103/PhysRevLett.45.290

[100] M. S. Hybertsen and S. G. Louie, "First-Principles Theory of Quasiparticles: Calculation of Band Gaps in Semiconductors and Insulators," *Phys. Rev. Lett.*, vol. 55, no. 13, pp. 1418–1421, Sep. 1985.

[101] R. W. Godby, M. Schlüter, and L. J. Sham, "Self-energy operators and exchange-correlation potentials in semiconductors," *Phys. Rev. B*, vol. 37, pp. 10 159–10 175, Jun 1988. [Online]. Available: http://link.aps.org/doi/10.1103/PhysRevB.37.10159

[102] W. von der Linden and P. Horsch, "Precise quasiparticle energies and hartree-fock bands of semiconductors and insulators," *Phys. Rev. B*, vol. 37, pp. 8351–8362, May 1988. [Online]. Available: https://link.aps.org/doi/10.1103/PhysRevB.37.8351

[103] J. E. Northrup, M. S. Hybertsen, and S. G. Louie, "Many-body calculation of the surface-state energies for si(111)2×1," *Phys. Rev. Lett.*, vol. 66, pp. 500–503, Jan 1991. [Online]. Available: https://link.aps.org/doi/10.1103/PhysRevLett.66.500

[104] X. Blase, X. Zhu, and S. G. Louie, "Self-energy effects on the surface-state energies of h-si(111)1×1," *Phys. Rev. B*, vol. 49, pp. 4973–4980, Feb 1994. [Online]. Available: https://link.aps.org/doi/10.1103/PhysRevB.49.4973

[105] M. Rohlfing, P. Krüger, and J. Pollmann, "Efficient scheme for gw quasiparticle band-structure calculations with aapplications to bulk si and to the si(001)-(2×1) surface," *Phys. Rev. B*, vol. 52, pp. 1905–1917, Jul 1995. [Online]. Available: https://link.aps.org/doi/10.1103/PhysRevB.52.1905

[106] D. Peng, S. N. Steinmann, H. van Aggelen, and W. Yang, "Equivalence of particle-particle random phase approximation correlation energy and ladder-coupled-cluster doubles," *J. Chem. Phys.*, vol. 139, no. 10, p. 104112, Sep. 2013.

[107] E. Młyńczak, M. C. T. D. Müller, P. Gospodarič, T. Heider, I. Aguilera, G. Bihlmayer, M. Gehlmann, M. Jugovac, G. Zamborlini, C. Tusche, S. Suga, V. Feyer, L. Plucinski, C. Friedrich, S. Blügel, and C. M. Schneider, "Kink far below the fermi level reveals new electron-magnon scattering channel in fe," *Nat. Comm.*, vol. 10, no. 1, p. 505, Jan. 2019. [Online]. Available: https://doi.org/10.1038/s41467-019-08445-1

[108] D. Nabok, S. Blügel, and C. Friedrich, "Electron–plasmon and electron–magnon scattering in ferromagnets from first principles by combining GW and GT self-energies," *npj Computational Materials*, vol. 7, no. 1, p. 178, Nov. 2021. [Online]. Available: https://doi.org/10.1038/s41524-021-00649-8

[109] M. J. van Setten, F. Caruso, S. Sharifzadeh, X. Ren, M. Scheffler, F. Liu, J. Lischner, L. Lin, J. R. Deslippe, S. G. Louie, C. Yang, F. Weigend, J. B. Neaton, F. Evers, and P. Rinke, "GW 100: Benchmarking G_0W_0 for Molecular Systems," *J. Chem. Theory Comput.*, vol. 11, no. 12, pp. 5665–5687, Dec. 2015.

[110] K. Krause, M. E. Harding, and W. Klopper, "Coupled-cluster reference values for the gw27 and gw100 test sets for the assessment of gw methods," *Mol. Phys.*, vol. 113, p. 1952, 2015.

[111] M. Springer, F. Aryasetiawan, and K. Karlsson, "First-principles T-matrix theory with application to the 6 ev satellite in ni," *Phys. Rev. Lett.*, vol. 80, pp. 2389–2392, Mar 1998. [Online]. Available: https://link.aps.org/doi/10.1103/PhysRevLett.80.2389

[112] V. P. Zhukov, E. V. Chulkov, and P. M. Echenique, "Lifetimes of excited electrons in fe and ni: First-principles gw and the t-matrix theory," *Phys. Rev. Lett.*, vol. 93, p. 096401, Aug 2004. [Online]. Available: https://link.aps.org/doi/10.1103/PhysRevLett.93.096401

[113] ——, "Lifetimes and inelastic mean free path of low-energy excited electrons in fe, ni, pt, and au: Ab initio GW + T calculations," *Phys. Rev. B*, vol. 73, p. 125105, Mar 2006. [Online]. Available: https://link.aps.org/doi/10.1103/PhysRevB.73.125105

[114] I. A. Nechaev and E. V. Chulkov, "Multiple electron-hole scattering effect on quasiparticle properties in a homogeneous electron gas," *Phys. Rev. B*, vol. 73, p. 165112, Apr 2006. [Online]. Available: https://link.aps.org/doi/10.1103/PhysRevB.73.165112

[115] I. A. Nechaev, I. Y. Sklyadneva, V. M. Silkin, P. M. Echenique, and E. V. Chulkov, "Theoretical study of quasiparticle inelastic lifetimes as applied to aluminum," *Phys. Rev. B*, vol. 78, p. 085113, Aug 2008. [Online]. Available: https://link.aps.org/doi/10.1103/PhysRevB.78.085113

[116] A. Mönnich, J. Lange, M. Bauer, M. Aeschlimann, I. A. Nechaev, V. P. Zhukov, P. M. Echenique, and E. V. Chulkov, "Experimental time-resolved photoemission and ab initio study of lifetimes of excited electrons in mo and rh," *Phys. Rev. B*, vol. 74, p. 035102, Jul 2006. [Online]. Available: https://link.aps.org/doi/10.1103/PhysRevB.74.035102

[117] A. Dreuw and M. Head-Gordon, "Single-Reference ab Initio Methods for the Calculation of Excited States of Large Molecules," *Chem. Rev.*, vol. 105, pp. 4009–4037, 2005.

[118] M. C. T. D. Müller, S. Blügel, and C. Friedrich, "Electron-magnon scattering in elementary ferromagnets from first principles: Lifetime broadening and band anomalies," *Phys. Rev. B*, vol. 100, p. 045130, Jul 2019. [Online]. Available: https://link.aps.org/doi/10.1103/PhysRevB.100.045130

[119] D. Nabok, S. Blügel, and C. Friedrich, "Electron–plasmon and electron–magnon scattering in ferromagnets from first principles by combining gw and gt self-energies," *npj Comput. Mater.*, vol. 7, p. 178, 2021. [Online]. Available: https://doi.org/10.1038/s41524-021-00649-8

[120] N. E. Bickers, D. J. Scalapino, and S. R. White, "Conserving approximations for strongly correlated electron systems: Bethe-salpeter equation and dynamics for the two-dimensional hubbard model," *Phys. Rev. Lett.*, vol. 62, pp. 961–964, Feb 1989. [Online]. Available: https://link.aps.org/doi/10.1103/PhysRevLett.62.961

[121] N. Bickers and D. Scalapino, "Conserving approximations for strongly fluctuating electron systems. i. formalism and calculational approach," *Ann. Phys.*, vol. 193, no. 1, pp. 206–251, 1989. [Online]. Available: https://www.sciencedirect.com/science/article/pii/000349168990359X

[122] N. E. Bickers, *Self-Consistent Many-Body Theory for Condensed Matter Systems*. Springer New York, 2004, pp. 237–296. [Online]. Available: https://doi.org/10.1007/0-387-21717-7_6

[123] C. De Dominicis and P. C. Martin, "Stationary entropy principle and renormalization in normal and superfluid systems. i. algebraic formulation," *J. Math. Phys.*, vol. 5, no. 1, pp. 14–30, 1964.

[124] ——, "Stationary entropy principle and renormalization in normal and superfluid systems. ii. diagrammatic formulation," *J. Math. Phys.*, vol. 5, no. 1, pp. 31–59, 1964.

[125] J. J. Shepherd, T. M. Henderson, and G. E. Scuseria, "Range-separated brueckner coupled cluster doubles theory," *Phys. Rev. Lett.*, vol. 112, p. 133002, Apr 2014. [Online]. Available: https://link.aps.org/doi/10.1103/PhysRevLett.112.133002

[126] N. Nakanishi, "A general survey of the theory of the bethe-salpeter equation," *Progress of Theoretical Physics Supplement*, vol. 43, pp. 1–81, 1969.

[127] S. Ahlig and R. Alkofer, "(in-) consistencies in the relativistic description of excited states in the bethe–salpeter equation," *Annals of Physics*, vol. 275, no. 1, pp. 113–147, 1999.

[128] R. Cutkosky, "Solutions of a bethe-salpeter equation," *Physical Review*, vol. 96, no. 4, p. 1135, 1954.

[129] E. G. van Loon, F. Krien, and A. A. Katanin, "Bethe-salpeter equation at the critical end point of the mott transition," *Physical Review Letters*, vol. 125, no. 13, p. 136402, 2020.

[130] M. Schmidt and G. Röpke, "The pair correlation function and mott transition in two-component fermi systems," *physica status solidi (b)*, vol. 139, no. 2, pp. 441–455, 1987.

[131] H. Stolz and R. Zimmermann, "Correlated pairs and a mass action law in two-component fermi systems excitons in an electron-hole plasma," *physica status solidi (b)*, vol. 94, no. 1, pp. 135–146, 1979.

[132] R. Zimmermann and H. Stolz, "The mass action law in two-component fermi systems revisited excitons and electron-hole pairs," *physica status solidi (b)*, vol. 131, no. 1, pp. 151–164, 1985.

[133] R. Zimmermann, K. Kilimann, W. Kraeft, D. Kremp, and G. Röpke, "Dynamical screening and self-energy of excitons in the electron–hole plasma," *physica status solidi (b)*, vol. 90, no. 1, pp. 175–187, 1978.

[134] D. Kremp, W. Kraeft, and A. Lambert, "Equation of state and ionization equilibrium for nonideal plasmas," *Physica A Statistical Mechanics and its Applications*, vol. 127, no. 1, pp. 72–86, 1984.

[135] R. Jost and A. Pais, "On the scattering of a particle by a static potential," *Physical review*, vol. 82, no. 6, p. 840, 1951.

[136] C. Verdozzi, R. W. Godby, and S. Holloway, "Evaluation of *GW* approximations for the self-energy of a hubbard cluster," *Phys. Rev. Lett.*, vol. 74, pp. 2327–2330, Mar 1995. [Online]. Available: https://link.aps.org/doi/10.1103/PhysRevLett.74.2327

[137] A. Schindlmayr, T. J. Pollehn, and R. W. Godby, "Spectra and total energies from self-consistent many-body perturbation theory," *Phys. Rev. B*, vol. 58, pp. 12 684–12 690, Nov 1998. [Online]. Available: https://link.aps.org/doi/10.1103/PhysRevB.58.12684

[138] T. J. Pollehn, A. Schindlmayr, and R. W. Godby, "Assessment of theGWapproximation using hubbard chains," *Journal of Physics: Condensed Matter*, vol. 10, no. 6, pp. 1273–1283, feb 1998. [Online]. Available: https://doi.org/10.1088/0953-8984/10/6/011

[139] M. P. von Friesen, C. Verdozzi, and C.-O. Almbladh, "Successes and failures of kadanoff-baym dynamics in hubbard nanoclusters," *Phys. Rev. Lett.*, vol. 103, p. 176404, Oct 2009. [Online]. Available: https://link.aps.org/doi/10.1103/PhysRevLett.103.176404

[140] D. J. Carrascal, J. Ferrer, N. Maitra, and K. Burke, "Linear response time-dependent density functional theory of the Hubbard dimer," *Eur. Phys. J. B*, vol. 91, p. 142, 2018.

[141] M. Vanzini, L. Reining, and M. Gatti, "Spectroscopy of the Hubbard dimer: The spectral potential," *Eur. Phys. J. B*, vol. 91, no. 8, Aug. 2018.

[142] S. Di Sabatino, P.-F. Loos, and P. Romaniello, "Scrutinizing gw-based methods using the hubbard dimer," *Front. Chem.*, vol. 9, p. 751054, 2021.

[143] C. Schwartz and C. Zemach, "Theory and calculation of scattering with the bethe-salpeter equation," *Physical review*, vol. 141, no. 4, p. 1454, 1966.

[144] W. B. Kaufmann, "Numerical solutions of the bethe-salpeter equation," *Physical Review*, vol. 187, no. 5, p. 2051, 1969.

[145] M. Harada and Y. Yoshida, "Solving the homogeneous bethe-salpeter equation," *Physical Review D*, vol. 53, no. 3, p. 1482, 1996.

[146] U. D. Jentschura and G. S. Adkins, *Quantum Electrodynamics: Atoms, Lasers and Gravity*. World Scientific, 2022.

Appendices

Appendix A

Asymmetric dimer

The Hamiltonian of the asymmetric Hubbard dimer is

$$H = \sum_{\sigma} \left[\frac{\Delta v}{2}(n_{1\sigma} - n_{2\sigma}) - t(c^{\dagger}_{1\sigma}c_{2\sigma} + c^{\dagger}_{2\sigma}c_{1\sigma}) + \frac{U}{2}(n_{1\sigma}n_{1\bar{\sigma}} + n_{2\sigma}n_{2\bar{\sigma}}) \right] \tag{A.1}$$

A.1 One electron

The Hamiltonian of the system is written as

$$H^{N=1} = \begin{array}{c} \\ \langle\uparrow_1\, 0_2| \\ \langle 0_1\, \uparrow_2| \\ \langle\downarrow_1\, 0_2| \\ \langle 0_1\, \downarrow_2| \end{array} \begin{array}{c} \begin{array}{cccc} |\uparrow_1\, 0_2\rangle & |0_1\, \uparrow_2\rangle & |\downarrow_1\, 0_2\rangle & |0_1\, \downarrow_2\rangle \end{array} \\ \begin{pmatrix} \frac{\Delta v}{2} & -t & 0 & 0 \\ -t & -\frac{\Delta v}{2} & 0 & 0 \\ 0 & 0 & \frac{\Delta v}{2} & -t \\ 0 & 0 & -t & -\frac{\Delta v}{2} \end{pmatrix} \end{array} \tag{A.2}$$

The eigenvalues are

$$E_1^{N=1} = \sqrt{t^2 + \left(\frac{\Delta v}{2}\right)^2} \tag{A.3}$$

$$E_0^{N=1} = -\sqrt{t^2 + \left(\frac{\Delta v}{2}\right)^2} \tag{A.4}$$

The eigenvectors are

$$\left|\Psi_n^{N=1}\right\rangle = \cos\rho_n \left|\uparrow_1\, 0_2\right\rangle + \sin\rho_n \left|0_1\, \uparrow_2\right\rangle \tag{A.5}$$

$$\cos\rho_n = \frac{1}{\sqrt{1 + \left(\frac{\Delta v}{2t} - \frac{E_n}{t}\right)^2}} \quad \sin\rho_n = \frac{\frac{\Delta v}{2t} - \frac{E_n}{t}}{\sqrt{1 + \left(\frac{\Delta v}{2t} - \frac{E_n}{t}\right)^2}} \tag{A.6}$$

A.2 Two electrons

The Hamiltonian of the system is written as

$$H^{N=2} = \begin{array}{c} \begin{array}{cccc} |\uparrow_1\downarrow_2\rangle & |\uparrow\downarrow_1\, 0_2\rangle & |0_1\, \uparrow\downarrow_2\rangle & |\downarrow_1\uparrow_2\rangle \end{array} \\ \begin{pmatrix} 0 & -t & -t & 0 \\ -t & U + \Delta v & 0 & t \\ -t & 0 & U - \Delta v & t \\ 0 & t & t & 0 \end{pmatrix} \end{array} \tag{A.7}$$

The characterisitc polynomial is

$$\chi(z) = z(z^3 - 2Uz^2 + (U^2 - \Delta v^2 - 4t^2)z + 4Ut^2) \tag{A.8}$$

To find the roots of the polynomial we use the Tschirnaus-Vieta's approach

$$ax^3 + bx^2 + cx + d = 0 \tag{A.9}$$

We set $x = t + B$

$$t^3 + \left(3B + \frac{b}{a}\right)t^2 + \left(3B^2 + \frac{c + 2bB}{a}\right)t + \left(B^3 + \frac{bB^2 + cB + d}{a}\right) = 0 \tag{A.10}$$

We set $B = -\frac{b}{3a}$ to make disappear the term in t^2, which gives

$$t^3 + pt + q = 0 \tag{A.11}$$

With $p = \frac{3ac - b^2}{3a^2}$ and $q = \frac{2b^3 - 9abc + 27a^2d}{27a^3}$

Then we set $t = A\cos\theta$ and we multiply by $\frac{4}{A^3}$ in order to use the trigonometric relation

$$\cos 3\theta = 4\cos^3\theta - 3\cos\theta \tag{A.12}$$

This gives

$$4\cos^3\theta + \frac{4p}{A^2}\cos\theta + \frac{4}{A^3}q = 0 \tag{A.13}$$

$\frac{4p}{A^2} = -3 \Rightarrow A = 2\sqrt{\frac{-p}{3}}$, so p is negative and we obtain

$$4\cos^3\theta - 3\cos\theta - \frac{3q}{Ap} = 0 \tag{A.14}$$

With the trigonometric relation we can write

$$\cos 3\theta = \frac{3q}{Ap} \tag{A.15}$$

We set $\phi = \arccos\frac{3q}{Ap}$, so

$$\theta = \frac{\phi + 2k\pi}{3} \tag{A.16}$$

hence $x = t + B = A\cos\theta + B$

We apply this procedure to the following polynomial

$$z^3 - 2Uz^2 + (U^2 - \Delta v^2 - 4t^2)z + 4Ut^2 = 0 \tag{A.17}$$

Setting $z = \lambda + B$ gives

$$\lambda^3 + (3B - 2U)\lambda^2 + (3B - 4BU + U^2 - \Delta v^2 - 4t^2)\lambda + B^3 - 2UB^2 + (U^2 - \Delta v^2 - 4t^2)B + 4Ut^2 = 0 \tag{A.18}$$

We choose $B = \frac{2U}{3}$ so we have

$$\lambda^3 + p\lambda + q = 0 \tag{A.19}$$

with $p = -\frac{U^2}{3} - \Delta v^2 - 4t^2$ and $q = \frac{2}{27}U^3 + \frac{2U}{3}(2t^2 - \Delta v^2)$, so $A = \frac{2}{3}\sqrt{U^2 + 3\Delta v^2 + 12t^2}$

$$\cos 3\theta = \frac{3q}{Ap} = -U\frac{18t^2 + U^2 - 9\Delta v^2}{(12t^2 + U^2 + 3\Delta v^2)^{3/2}} = -U\frac{s^2}{r^3} \tag{A.20}$$

with $s^2 = 18t^2 + U^2 - 9\Delta v^2$ and $r = 12t^2 + U^2 + 3\Delta v^2$

Thus $\phi = \arccos\left(-U\frac{s^2}{r^3}\right)$, $\theta_n = \frac{\phi+2n\pi}{3}$, $\lambda_n = A\cos\theta_n$

$$z_n = \frac{2}{3}U + \frac{2}{3}\left(\sqrt{12t^2 + U^2 + 3\Delta v^2}\cos\theta_n\right) \tag{A.21}$$

We replace z by E and k by λ

$$\begin{aligned} E_1^{N=2} &= 0 \\ E_{n\neq 1}^{N=2} &= \frac{2}{3}\left(U + r\cos\theta_n\right) \end{aligned} \tag{A.22}$$

The eigenvectors are

$$\left|\Psi_1^{N=2}\right\rangle = \frac{1}{\sqrt{2}}(|\uparrow_1\downarrow_2\rangle + |\downarrow_1\uparrow_2\rangle) \tag{A.23}$$

$$\left|\Psi_{n\neq 1}^{N=2}\right\rangle = \frac{1}{N_{2n}}\left(-|\downarrow_1\uparrow_2\rangle + |\uparrow_1\downarrow_2\rangle + \frac{2t}{U - \Delta v - E_n^{N=2}}|0_1\uparrow\downarrow_2\rangle + \frac{2t}{U + \Delta v - E_n^{N=2}}|\uparrow\downarrow_1 0_2\rangle\right)$$

with

$$N_{2n} = \sqrt{2 + \left(\frac{2t}{U - \Delta v - E_n^{N=2}}\right)^2 + \left(\frac{2t}{U + \Delta v - E_n^{N=2}}\right)^2} \tag{A.24}$$

A.3 Three electrons

The Hamiltonian of the system is written as

$$H^{N=3} = \begin{array}{c} \\ \langle\downarrow_1\uparrow\downarrow_2| \\ \langle\uparrow\downarrow_1\downarrow_2| \\ \langle\uparrow_1\uparrow\downarrow_2| \\ \langle\uparrow\downarrow_1\uparrow_2| \end{array} \begin{array}{c} \begin{array}{cccc} |\downarrow_1\uparrow\downarrow_2\rangle & |\uparrow\downarrow_1\downarrow_2\rangle & |\uparrow_1\uparrow\downarrow_2\rangle & |\uparrow\downarrow_1\uparrow_2\rangle \end{array} \\ \begin{pmatrix} -\frac{\Delta v}{2} + U & t & 0 & 0 \\ t & \frac{\Delta v}{2} + U & 0 & 0 \\ 0 & 0 & -\frac{\Delta v}{2} + U & t \\ 0 & 0 & t & \frac{\Delta v}{2} + U \end{pmatrix} \end{array} \tag{A.25}$$

The eigenvalues are

$$E_1^{N=3} = U + \sqrt{t^2 + \left(\frac{\Delta v}{2}\right)^2} \qquad E_0^{N=3} = U - \sqrt{t^2 + \left(\frac{\Delta v}{2}\right)^2} \tag{A.26}$$

The eigenvectors are

$$\left|\Psi_0^{N=3}\right\rangle = \frac{1}{N_{30}}\left(\left(-\frac{\Delta v}{2t} - \sqrt{1 + \left(\frac{\Delta v}{2t}\right)^2}\right)|\uparrow_1\uparrow\downarrow_2\rangle + |\uparrow\downarrow_1\uparrow_2\rangle\right) \tag{A.27}$$

$$\left|\Psi_1^{N=3}\right\rangle = \frac{1}{N_{31}}\left(\left(-\frac{\Delta v}{2t} + \sqrt{1 + \left(\frac{\Delta v}{2t}\right)^2}\right)|\uparrow_1\uparrow\downarrow_2\rangle + |\uparrow\downarrow_1\uparrow_2\rangle\right)$$

with

$$N_{30} = \sqrt{1 + \left(\frac{\Delta v}{2t} + \sqrt{1 + \left(\frac{\Delta v}{2t}\right)^2}\right)^2} \quad N_{31} = \sqrt{1 + \left(-\frac{\Delta v}{2} + \sqrt{1 + \left(\frac{\Delta v}{2t}\right)^2}\right)^2} \tag{A.28}$$

Appendix B

The electron-hole RPA

The particle-hole polarizability is

$$P^{eh}(34) = -iG(34)G(43) \tag{B.1}$$

We calculate its Fourier transform

$$\begin{aligned} P^{eh}(34) &= -i \int \frac{d\omega}{2\pi} \frac{d\omega'}{2\pi} G(\omega)G(\omega')e^{-i\omega(t_3-t_4)}e^{-i\omega'(t_4-t_3)} \\ &= -i \int \frac{d\omega}{2\pi} \frac{d\omega'}{2\pi} G(\omega)G(\omega')e^{-i(t_3-t_4)(\omega-\omega')} \end{aligned} \tag{B.2}$$

$$\begin{aligned} P^{eh}(\widetilde{\omega}) &= \int d(t_3-t_4)\, P(34)e^{i\widetilde{\omega}(t_3-t_4)} \\ &= -i \int d(t_3-t_4) \int \frac{d\omega}{2\pi} \frac{d\omega'}{2\pi} G(\omega)G(\omega')e^{-i(t_3-t_4)(\omega-\omega')}e^{i\widetilde{\omega}(t_3-t_4)} \end{aligned} \tag{B.3}$$

We obtain

$$P^{eh}(\omega) = \int \frac{d\omega'}{2\pi i} G(\omega')G(\omega'-\omega)e^{i\omega'\eta} \tag{B.4}$$

We project in the one-particle orbital basis

$$\begin{aligned} P^{eh}_{ijkl}(\omega) &= \int \frac{d\omega'}{2\pi i} G_{ij}(\omega')G_{kl}(\omega'-\omega)e^{i\omega'\eta} \\ &= \int \frac{d\omega'}{2\pi i} \left[\frac{\delta_{ij}}{\omega'-\varepsilon_v-i\eta} + \frac{\delta_{ij}}{\omega'-\varepsilon_c+i\eta}\right] \left[\frac{\delta_{kl}}{\omega'-\omega-\varepsilon_v-i\eta} + \frac{\delta_{kl}}{\omega'-\omega-\varepsilon_c+i\eta}\right] \end{aligned}$$

This gives

$$P^{eh}_{ijkl}(\omega) = \frac{\delta_{ij}\delta_{kl}}{-\omega+\varepsilon_v-\varepsilon_c+i\eta} + \frac{\delta_{ij}\delta_{kl}}{\omega+\varepsilon_v-\varepsilon_c+i\eta} = \frac{\delta_{ij}\delta_{kl}(f_i^{\sigma_i}-f_k^{\sigma_k})}{\varepsilon_i-\varepsilon_k-\omega+2i\eta\,\mathrm{sgn}(\varepsilon_i-\varepsilon_k)} \tag{B.5}$$

In electron-hole RPA, the expression of the polarizabilty is

$$\chi^{eh}(3'4'34) = \lim_{\eta\to 0^+} \sum_n \left[\frac{\rho_n(3'3)\rho_n^*(44')}{\omega-\Omega_n^{eh}+i\eta} - \frac{\rho_n(4'4)\rho_n^*(33')}{\omega+\Omega_n^{eh}-i\eta}\right] \tag{B.6}$$

where

$$\rho_n(3'3) = \left\langle \Psi_0^N \middle| \psi^\dagger(3)\psi(3') \middle| \Psi_n^N \right\rangle \tag{B.7}$$

B.1 GW

The screened Coulomb interaction is written

$$W(12) = v(12) + \int d34 v(13) P^{eh}(34) W(42) \tag{B.8}$$

We close the equation

$$\int d4 \left[\delta(14) - \int d3 v(13) P^{eh}(34) \right] W(42) = v(12) \tag{B.9}$$

We set $\epsilon(14) = \delta(14) - \int d3 v(13) P^{eh}(34)$ and we isolate W

$$W(42) = \int d1 \epsilon^{-1}(41) v(12) \tag{B.10}$$

We replace this expression in the right hand side of (B.8), we get

$$W(12) = v(12) + \int d35 v(13) \chi^{eh}(35) v(52) \tag{B.11}$$

where

$$\chi^{eh}(35) = \int d4 P^{eh}(34) \epsilon^{-1}(45) \tag{B.12}$$

We inverse (B.12) to obtain

$$\chi(34) = P^{eh}(34) + \int d56 \chi^{eh}(35) v(56) P(64) \tag{B.13}$$

We express χ and P as a four point quantities

$$\chi^{eh}(1234) = P^{eh}(1234) + \int d55'66' \chi^{eh}(1535') v(56) \delta(55') \delta(66') P(626'4) \tag{B.14}$$

This gives for W

$$W(12) = v(12) + \int d33'44' v(13) \chi^{eh}(3'4'34) \delta(33') \delta(44') v(42) \tag{B.15}$$

In the one-particle orbital basis we use for χ^{eh} the following definition

$$\chi^{eh}_{(ia)(jb)} = \int d33'44' \phi^*_a(x_{3'}) \phi_i(x_3) \chi^{eh}(3'4'34) \phi^*_j(x_{4'}) \phi_b(x_4) \tag{B.16}$$

anf for P^{eh}

$$P^{eh}_{nmn'm'} = \int d1234 P^{eh}(1234) \phi^*_n(x_1) \phi_m(x_4) \phi^*_{n'}(x_2) \phi_{m'}(x_3) = P^{eh}_{(m'n)(n'm)} \tag{B.17}$$

With these definitions, we have in the matrix notations

$$\chi^{eh}_{(pq)(rs)} = P^{eh}_{(pq)(rs)} + \sum_{(ia)(jb)} \chi^{eh}_{(pq)(ia)} v_{(ia)(jb)} P^{eh}_{(jb)(rs)} \tag{B.18}$$

We inverse the equation

$$\chi^{eh,-1}_{(pq)(rs)} = P^{eh,-1}_{(pq)(rs)} - v_{(pq)(rs)} \tag{B.19}$$

We use (B.5)

$$\chi^{eh,-1}_{(pq)(rs)} = \left[\frac{\delta_{qs}\delta_{rp}(f_q^{\sigma_q} - f_r^{\sigma_r})}{\varepsilon_q - \varepsilon_r - \omega + 2i\eta\,\mathrm{sgn}(\varepsilon_q - \varepsilon_r)}\right]^{-1} - v_{qrps} \tag{B.20}$$

This gives

$$\chi^{eh,-1}_{(pq)(rs)}(f_q^{\sigma_q} - f_p^{\sigma_p}) = M_{(pq)(rs)} \tag{B.21}$$

with $M_{(pq)(rs)} = \delta_{pr}\delta_{qs}(\varepsilon_q - \varepsilon_r) - (f_q^{\sigma_q} - f_p^{\sigma_p})v_{qrps}$, we inverse χ^{eh}

$$\chi^{eh}_{(pq)(rs)} = M^{-1}_{(pq)(rs)}(f_s^{\sigma_s} - f_r^{\sigma_r}) \tag{B.22}$$

or

$$\chi^{eh}_{(pq)(rs)} = [(\varepsilon_n - \varepsilon_{n'} - \omega)\delta_{nm}\delta_{n'm'} - (f_n^{\sigma_n} - f_{m'}^{\sigma_{m'}})v_{nn'm'm}]^{-1}_{(pq)(rs)}(f_s^{\sigma_s} - f_r^{\sigma_r}) \tag{B.23}$$

$$\chi^{eh}_{(pq)(rs)} = [(\varepsilon_n - \varepsilon_{n'} - \omega)\delta_{nm}\delta_{n'm'} + (f_{m'}^{\sigma_{m'}} - f_n^{\sigma_n})v_{nn'm'm}]^{-1}_{(pq)(rs)}(f_s^{\sigma_s} - f_r^{\sigma_r}) \tag{B.24}$$

This gives the following eigenvalue problem

$$\begin{pmatrix} \mathbf{A}^{\mathrm{eh}} & \mathbf{B}^{\mathrm{eh}} \\ -\mathbf{B}^{\mathrm{eh}*} & -\mathbf{A}^{\mathrm{eh}*} \end{pmatrix} \begin{pmatrix} \mathbf{X}^N_\nu \\ \mathbf{Y}^N_\nu \end{pmatrix} = \Omega^N_\nu \begin{pmatrix} \mathbf{X}^N_\nu \\ \mathbf{Y}^N_\nu \end{pmatrix} \tag{B.25}$$

where

$$\begin{aligned} A^{\mathrm{eh}}_{(ia),(jb)} &= (\varepsilon_a - \varepsilon_i)\delta_{ij}\delta_{ab} + \langle ib|aj\rangle \\ B^{\mathrm{eh}}_{(ia),(jb)} &= \langle ij|ab\rangle \end{aligned} \tag{B.26}$$

For W (and v), we use the definition

$$W_{pqrs} = \int dx_1 dx_2 \phi_p^*(x_1)\phi_q^*(x_2)W(12)\phi_r(x_1)\phi_s(x_2) \tag{B.27}$$

We obtain

$$W_{pqrs} = v_{pqrs} + \sum_{(ia)(jb)} v_{pira}\chi^{eh}_{(ia)(jb)}v_{bqjs} \tag{B.28}$$

Or, in matrix notations

$$W_{(rp)(qs)} = v_{(rp)(qs)} + \sum_{(ia)(jb)} v_{(rp)(ia)}\chi^{eh}_{(ia)(jb)}v_{(jb)(qs)} \tag{B.29}$$

with $W_{(rp)(qs)} = W_{pqrs}$ and $v_{(rp)(qs)} = v_{pqrs}$.

In (B.15) we integrate over $3'$ and $4'$ and use (B.6), we obtain for (B.29)

$$W_{pqrs} = v_{pqrs} + \sum_{iajb} v_{pira}\int d34 \lim_{\eta\to 0^+}\sum_n \left[\frac{\rho_n(3'3)\rho_n^*(44')}{\omega - \Omega^{eh}_n + i\eta} - \frac{\rho_n(4'4)\rho_n^*(33')}{\omega + \Omega^{eh}_n - i\eta}\right]\phi_a^*(x_3)\phi_i(x_3)\phi_j^*(x_4)\phi_b(x_4)v_{bqjs}$$

We calculate the right hand side

$$\begin{aligned}\sum_{ia} v_{pira}\int d3\rho_n(3)\phi_i(x_3)\phi_a^*(x_3) &= \sum_{ia}\int dx_1x_23\phi_p^*(x_1)\phi_i^*(x_2)v(x_1,x_2)\phi_r(x_1)\phi_a(x_2)\rho_n(3)\phi_i(x_3)\phi_a^*(x_3)\\ &= \int dx_1x_2\phi_p^*(x_1)\phi_r(x_1)v(x_1,x_2)\rho_n(x_2)\\ &= \left\langle pr\middle|\chi_\nu^N\right\rangle\end{aligned}$$

and

$$\begin{aligned}\sum_{jb}\int d4\rho_n^*(4)v_{bqjs}\phi_b(x_4)\phi_j^*(x_4) &= \sum_{jb}\int dx_1x_24\rho_n^*(4)\phi_b^*(x_1)\phi_q^*(x_2)v(x_1,x_2)\phi_j(x_1)\phi_s(x_2)\phi_b(x_4)\phi_j^*(x_4)\\ &= \int dx_1x_2\left[\phi_s^*(x_1)\phi_q(x_2)v(x_1,x_2)\rho_n(x_1)\right]^*\\ &= \left\langle sq\middle|\chi_\nu^N\right\rangle^*\end{aligned}$$

where in both case we used $\sum_n \phi_n(x_1)\phi_n(x_2)^* = \delta(x_1-x_2)$, the expression of W is then

$$W_{pqrs} = v_{pqrs} + \lim_{\eta\to 0^+}\sum_n \left\langle pr\middle|\chi_\nu^N\right\rangle\left\langle qs\middle|\chi_\nu^N\right\rangle\left[\frac{1}{\omega-\Omega_n^{eh}+i\eta}-\frac{1}{\omega+\Omega_n^{eh}-i\eta}\right] \tag{B.30}$$

where we used $\left\langle sq\middle|\chi_\nu^N\right\rangle^* = \left\langle qs\middle|\chi_\nu^N\right\rangle$, to implement these amplitudes, we need to express them in terms of eigenvectors

$$\begin{aligned}\left\langle pr\middle|\chi_\nu^N\right\rangle &= \int dx_1x_2\phi_p^*(x_1)\phi_r(x_1)v(x_1,x_2)\rho_n(x_2)\\ &= \int dx_1x_2\phi_p^*(x_1)\phi_r(x_1)v(x_1,x_2)\sum_{bj}\left[X_{bj,\nu}^N\phi_b(x_2)\phi_j^*(x_2)+Y_{bj,\nu}^N\phi_j(x_2)\phi_b^*(x_2)\right]\\ &= \sum_{bj}\left[X_{bj,\nu}^N v_{pjrb}+Y_{bj,\nu}^N v_{pbrj}\right]\\ &= \sum_{bj}\left[X_{bj,\nu}^N+Y_{bj,\nu}^N\right]v_{pjrb}\end{aligned}$$

To calculate the GW self-energy, we use

$$\Sigma_{ps}(\omega) = -\sum_{rq}\int\frac{d\omega'}{2\pi i}G_{rq}(\omega')W_{pqrs}(\omega-\omega')e^{i\omega'\eta} \tag{B.31}$$

We keep only the correlation part written Σ^c

$$\Sigma_{ps}^c(\omega) = \sum_{in}\frac{\left\langle pi\middle|\chi_\nu^N\right\rangle\left\langle is\middle|\chi_\nu^N\right\rangle}{\omega-\varepsilon_i+\Omega_n^{eh}-i\eta} - \sum_{an}\frac{\left\langle pa\middle|\chi_\nu^N\right\rangle\left\langle as\middle|\chi_\nu^N\right\rangle}{\omega-\varepsilon_a-\Omega_n^{eh}+i\eta} \tag{B.32}$$

B.2 $G\overline{T}^{eh}$

$$\overline{T}^{eh}(121'2') = -i\overline{v}(1'2'12) + iv(12')\int d34G(13)G(42')\overline{T}^{eh}(321'4) \tag{B.33}$$

where $\overline{v}(121'4) = v(12)[\delta(11')\delta(24) - \delta(14)\delta(21')]$

We use the definition

$$\overline{T}^{eh}_{pqrs} = \int dx_1 dx_2 \phi^*_p(x_1)\phi^*_q(x_2)\overline{T}^{eh}(121'2')\phi_r(x_{1'})\phi_s(x_{2'}) \tag{B.34}$$

We obtain

$$\overline{T}^{eh}_{pqrs} = -i\overline{v}_{pqrs} - \sum_{iajb} v_{pibs}\overline{P}^{eh}_{bjai}\overline{T}^{eh}_{jqra} \tag{B.35}$$

where $\overline{v}_{pqrs} = v_{pqrs} - v_{pqsr}$, we use the notation

$$\overline{P}^{eh}_{bjai} = \overline{P}^{eh}_{(ib)(aj)} \tag{B.36}$$

To rewrite the integral equation

$$\overline{T}^{eh}_{(sp)(qr)} = -i\overline{v}_{(sp)(qr)} - \sum_{(ib)(aj)} v_{(sp)(ib)}\overline{P}^{eh}_{(ib)(aj)}\overline{T}^{eh}_{(aj)(qr)} \tag{B.37}$$

where $\overline{T}^{eh}_{(sp)(qr)} = \overline{T}^{eh}_{pqrs}$ and $v_{(sp)(qr)} = v_{pqrs}$

We close the equation

$$\sum_{(aj)}\left[\delta_{sa}\delta_{pj} + \sum_{(ib)} v_{(sp)(ib)}\overline{P}^{eh}_{(ib)(aj)}\right]\overline{T}^{eh}_{(aj)(qr)} = -i\overline{v}_{(sp)(qr)} \tag{B.38}$$

We set

$$\epsilon_{(sp)(aj)} = \delta_{sa}\delta_{pj} + \sum_{(ib)} v_{(sp)(ib)}\overline{P}^{eh}_{(ib)(aj)} \tag{B.39}$$

We obtain

$$\overline{T}^{eh}_{(aj)(qr)} = -i\sum_{(sp)} \epsilon^{-1}_{(aj)(sp)}\overline{v}_{(sp)(qr)} \tag{B.40}$$

We replace this expression in (B.37) to obtain

$$\overline{T}^{eh}_{(sp)(qr)} = -i\overline{v}_{(sp)(qr)} + i\sum_{(ab)(ij)} v_{(sp)(ab)}\overline{\chi}^{eh}_{(ab)(ij)}\overline{v}_{(ij)(qr)} \tag{B.41}$$

with

$$\overline{\chi}^{eh}_{(ib)(aj)} = \sum_{(cd)} \overline{P}^{eh}_{(ib)(cd)}\epsilon^{-1}_{(cd)(aj)} \tag{B.42}$$

with these definitions, we have in the matrix notations

$$\overline{\chi}^{eh}_{(ib)(aj)} = \overline{P}^{eh}_{(ib)(aj)} - \sum_{(cd)(kl)} \overline{\chi}^{eh}_{(ib)(cd)}v_{(cd)(kl)}\overline{P}^{eh}_{(kl)(aj)} \tag{B.43}$$

We inverse the equation

$$\overline{\chi}^{eh,-1}_{(pq)(rs)} = \overline{P}^{eh,-1}_{(pq)(rs)} + v_{(pq)(rs)} \tag{B.44}$$

or

$$\overline{\chi}^{eh,-1}_{(pq)(rs)} = \overline{P}^{eh,-1}_{qsrp} + v_{spqr} \tag{B.45}$$

Similar calculations to the ones done for GW leads to

$$\overline{\chi}^{eh}_{(pq)(rs)} = [(\varepsilon_n - \varepsilon_{n'} - \omega)\delta_{nm}\delta_{n'm'} - (f^{\sigma_{m'}}_{m'} - f^{\sigma_n}_{n})v_{mm'nn'}]^{-1}_{(pq)(rs)}(f^{\sigma_s}_{s} - f^{\sigma_r}_{r}) \tag{B.46}$$

This gives the following eigenvalue problem

$$\begin{pmatrix} \overline{\mathbf{A}}^{\mathrm{eh}} & \overline{\mathbf{B}}^{\mathrm{eh}} \\ -\overline{\mathbf{B}}^{\mathrm{eh}*} & -\overline{\mathbf{A}}^{\mathrm{eh}*} \end{pmatrix} \begin{pmatrix} \mathbf{X}^N_\nu \\ \mathbf{Y}^N_\nu \end{pmatrix} = \Omega^N_\nu \begin{pmatrix} \mathbf{X}^N_\nu \\ \mathbf{Y}^N_\nu \end{pmatrix} \tag{B.47}$$

where

$$\begin{aligned} \overline{A}^{\mathrm{eh}}_{(ia)(jb)} &= (\varepsilon_a - \varepsilon_i)\delta_{ij}\delta_{ab} - \langle bi|aj\rangle \\ \overline{B}^{\mathrm{eh}}_{(ia)(jb)} &= -\langle ji|ab\rangle \end{aligned} \tag{B.48}$$

We use

$$\overline{P}^{eh}_{(ib)(aj)} = \overline{P}^{eh}_{bjai} = \int dx_1x_2x_3x_4\overline{P}^{eh}(343'4')\phi^*_b(x_3)\phi_j(x_{4'})\phi^*_a(x_4)\phi_i(x_{3'}) \tag{B.49}$$

$$\overline{\chi}^{eh}_{(ib)(aj)} = \overline{\chi}^{eh}_{jiab} = \int dx_1x_2x_3x_4\overline{\chi}^{eh}(343'4')\phi^*_b(x_3)\phi_j(x_{4'})\phi^*_a(x_4)\phi_i(x_{3'}) \tag{B.50}$$

To write

$$\overline{T}^{eh}_{pqrs} = -i\overline{v}_{pqrs} + i\sum_{abij} v_{pabs}\overline{\chi}^{eh}_{jaib}\overline{v}_{jqri} \tag{B.51}$$

$$\overline{T}^{eh}_{pqrs} = -i\overline{v}_{pqrs} + \sum_{abij} v_{pabs}\int d343'4' \lim_{\eta\to 0^+}\sum_n \left[\frac{\rho_n(33')\rho^*_n(4'4)}{\omega - \overline{\Omega}^{eh}_n + i\eta} - \frac{\rho_n(44')\rho^*_n(3'3)}{\omega + \overline{\Omega}^{eh}_n - i\eta}\right]\phi^*_b(x_3)\phi_j(x_{4'})\phi^*_a(x_4)\phi_i(x_{3'})\overline{v}_{jqri}$$

We calculate the right-hand side

$$\begin{aligned} \sum_{ab} v_{pabs}\int d33'\rho_n(33')\phi^*_b(x_3)\phi_a(x_{3'}) &= \sum_{ab}\int dx_1x_233'\phi^*_p(x_1)\phi^*_i(x_2)v(x_1,x_2)\phi_r(x_1)\phi_a(x_2)\rho_n(33')\phi^*_b(x_3)\phi_a \\ &= \int dx_1x_2\phi^*_p(x_1)\phi_s(x_2)v(x_1,x_2)\rho_n(x_1,x_2) \\ &= \left\langle ps\middle|\chi^N_\nu\right\rangle \end{aligned}$$

and

$$\begin{aligned} \sum_{ij}\int d44'\rho^*_n(4'4)\overline{v}_{jqri} &= \int dx_1x_2\left[\phi^*_r(x_1)\phi_q(x_2)v(x_1,x_2)\rho_n(x_1,x_2)\right]^* \\ &\quad - \int dx_1x_3\left[\phi^*_r(x_3)\phi_q(x_3)v(x_1,x_3)\rho_n(x_1,x_1)\right]^* \\ &= \left\langle rq\middle|\middle|\chi^N_\nu\right\rangle^* \end{aligned}$$

The expression of $\overline{T}^{eh}$ is then

$$\overline{T}^{eh}_{pqrs} = -i\overline{v}_{pqrs} + i\lim_{\eta\to 0^+}\sum_n\left[\frac{\left\langle ps\middle|\chi^N_\nu\right\rangle\left\langle rq\middle|\middle|\chi^N_\nu\right\rangle^*}{\omega - \overline{\Omega}^{eh}_n + i\eta} - \frac{\left\langle qr\middle|\middle|^N_\nu\right\rangle\left\langle sp\middle|\chi^N_\nu\right\rangle^*}{\omega + \overline{\Omega}^{eh}_n - i\eta}\right] \tag{B.52}$$

To implement these amplitudes, we need to express them in terms of eigenvectors

$$\begin{aligned}\left\langle ps\middle|\chi_\nu^N\right\rangle &= \int dx_1 x_2 \phi_p^*(x_1)\phi_s(x_2)v(x_1,x_2)\rho_n(x_1,x_2) \\ &= \int dx_1 x_2 \phi_p^*(x_1)\phi_s(x_2)v(x_1,x_2)\sum_{bj}\left[X_{bj,\nu}^N\phi_b(x_1)\phi_j^*(x_2)+Y_{bj,\nu}^N\phi_j(x_1)\phi_b^*(x_2)\right] \\ &= \sum_{bj}\left[X_{bj,\nu}^N v_{pjbs}+Y_{bj,\nu}^N v_{pbjs}\right]\end{aligned}$$

and

$$\left\langle rq\middle|\middle|\chi_\nu^N\right\rangle = \sum_{bj}\left[X_{bj,\nu}^N v_{rjbq}+Y_{bj,\nu}^N v_{rbjq}\right]-\sum_{bj}\left[X_{bj,\nu}^N+Y_{bj,\nu}^N\right]v_{jrbq} \tag{B.53}$$

To calculate the $G\overline{T}^{eh}$ self-energy, we use

$$\Sigma_{pr}(\omega) = -\sum_{sq}\int\frac{d\omega'}{2\pi i}G_{sq}(\omega')\overline{T}_{pqrs}^{eh}(\omega-\omega')e^{i\omega'\eta} \tag{B.54}$$

We keep only the correlation part written Σ^c

$$\Sigma_{pr}^c(\omega) = \sum_{in}\frac{\left\langle ir\middle|\middle|\chi_\nu^N\right\rangle\left\langle ip\middle|\chi_\nu^N\right\rangle^*}{\omega-\varepsilon_i+\overline{\Omega}_n^{eh}-i\eta}+\sum_{an}\frac{\left\langle ap\middle|\chi_\nu^N\right\rangle^*\left\langle ar\middle|\middle|\chi_\nu^N\right\rangle}{\omega-\varepsilon_a-\overline{\Omega}_n^{eh}+i\eta} \tag{B.55}$$

Appendix C

The particle-particle RPA

The particle-particle T-matrix is written

$$T^{pp}(121'4) = -i\overline{v}(121'4) \tag{C.1}$$
$$+\frac{i}{4}\int d33'55'67\overline{v}(1267)G(63)G(75)\overline{\delta(33')\delta(55')}T^{pp}(3'5'1'4)$$

where $\overline{v}(121'4) = v(12)[\delta(11')\delta(24) - \delta(14)\delta(21')]$ and $\overline{\delta(33')\delta(55')} = \delta(35')\delta(53') - \delta(17)\delta(26)$.

We will project this equation on the one-particle basis with the following definition

$$T^{pp}_{pqrs} = \int dx_1 dx_2 dx_{1'} dx_4 \phi^*_p(x_1)\phi^*_q(x_2)T^{pp}(121'4)\phi_r(x_{1'})\phi_s(x_4) \tag{C.2}$$

We obtain

$$T^{pp}_{pqrs} = -i\overline{v}_{pqrs} + \frac{i}{4}\sum_{abij}\overline{v}_{pqab}\left(G_{ai}G_{bj} - G_{aj}G_{bi}\right)T^{pp}_{ijrs} \tag{C.3}$$

To get rid of the factor $1/4$ we can impose the restriction $b < a$ and $j < i$, then we set

$$P^{pp}_{(ab)(ij)} = iG_{ai}G_{bj} \tag{C.4}$$

and

$$\overline{P}^{pp}_{(ab)(ij)} = P^{pp}_{(ab)(ij)} - P^{pp}_{(ab)(ji)} \tag{C.5}$$

So we can rewritte (C.3)

$$T^{pp}_{(pq)(rs)} = -i\overline{v}_{(pq)(rs)} + \sum_{(ab)(ij)}\overline{v}_{(pq)(ab)}\overline{P}^{pp}_{(ab)(ij)}T^{pp}_{(ij)(rs)} \tag{C.6}$$

where $\overline{v}_{(pq)(ab)} = \overline{v}_{pqab} = \langle pq||ab\rangle$.

We close this equation to obtain T^{pp}

$$T^{pp}_{(ij)(rs)} = -i\sum_{(ab)(kl)}\epsilon^{-1}_{(ij)(kl)}\overline{v}_{(kl)(rs)} \tag{C.7}$$

$$\epsilon_{(ij)(kl)} = \delta_{ik}\delta_{jl} - \sum_{(ab)}\overline{v}_{(ij)(ab)}\overline{P}^{pp}_{(ab)(kl)} \tag{C.8}$$

We replace (C.7) in (C.6), this gives

$$T^{pp}_{(pq)(rs)} = -i\overline{v}_{(pq)(rs)} - i\sum_{(ab)(kl)} \overline{v}_{(pq)(ab)}\overline{\chi}^{pp}_{(ab)(kl)}\overline{v}_{(kl)(rs)} \tag{C.9}$$

where

$$\overline{\chi}^{pp}_{(ab)(kl)} = \sum_{(ij)} \overline{P}^{pp}_{(ab)(ij)}\epsilon^{-1}_{(ij)(kl)} \tag{C.10}$$

This can be rewritten

$$\overline{\chi}^{pp}_{(ab)(ij)} = \overline{P}^{pp}_{(ab)(ij)} + \sum_{(kl)(cd)} \overline{\chi}^{pp}_{(ab)(kl)}\overline{v}_{(kl)(cd)}\overline{P}^{pp}_{(cd)(ij)} \tag{C.11}$$

with the restriction $k < l$ and $c < d$. We write the inverse of χ

$$\overline{\chi}^{pp,-1}_{(ab)(ij)} = \overline{P}^{pp,-1}_{(ab)(ij)} - \overline{v}_{(ab)(ij)} \tag{C.12}$$

To calculate (C.12), we have to determine $\overline{P}^{pp}$ first, to do so we use the Fourier transform

$$P^{pp}_{(ij)(kl)}(\omega) = -\int \frac{d\omega'}{2\pi i} G_{ik}(\omega')G_{jl}(\omega-\omega')e^{-i\omega'\eta} \tag{C.13}$$

We obtain

$$P^{pp}_{(ij)(kl)}(\omega) = \frac{\delta_{ik}\delta_{jl}\left[1-(f_i^{\sigma_i}+f_j^{\sigma_j})\right]}{\omega-(\varepsilon_i^{\sigma_i}+\varepsilon_j^{\sigma_j})+i\eta\,\mathrm{sgn}(\varepsilon_i^{\sigma_i}-\mu)} \tag{C.14}$$

where μ is the chemical potential. The second term of $\overline{P}_{(ab)(ij)}$ will not appear in the Fourier transform because of the restriction on the indices, we obtain

$$\left[1-(f_{n_1}^{\sigma_1}+f_{n_2}^{\sigma_2})\right]\overline{\chi}^{pp,-1}_{(n_1n_2)(n_3n_4)} = \mathcal{M}_{(n_1n_2)(n_3n_4)} \tag{C.15}$$

or

$$\overline{\chi}^{pp}_{(n_1n_2)(n_3n_4)} = \mathcal{M}^{-1}_{(n_1n_2)(n_3n_4)}\left[1-(f_{n_3}^{\sigma_3}+f_{n_4}^{\sigma_4})\right] \tag{C.16}$$

with

$$\mathcal{M}_{(n_1n_2)(n_3n_4)} = \delta_{n_1n_3}\delta_{n_2n_4}\left[\omega-(\varepsilon_{n_1}^{\sigma_1}+\varepsilon_{n_2}^{\sigma_2})+i\eta\,\mathrm{sgn}(\varepsilon_{n_2}^{\sigma_2}-\mu)\right]-\left[1-(f_{n_1}^{\sigma_1}+f_{n_2}^{\sigma_2})\right]\overline{v}_{(n_1n_2)(n_3n_4)} \tag{C.17}$$

This gives the following eigenvalue problem

$$\begin{pmatrix} \boldsymbol{A}^{\mathrm{pp}} & \boldsymbol{B}^{\mathrm{pp}} \\ -\boldsymbol{B}^{\mathrm{pp}} & -\boldsymbol{C}^{\mathrm{pp}} \end{pmatrix}\begin{pmatrix} X^{N\pm2}_\nu \\ Y^{N\pm2}_\nu \end{pmatrix} = \Omega^{N\pm2}_\nu \begin{pmatrix} X^{N\pm2}_\nu \\ Y^{N\pm2}_\nu \end{pmatrix} \tag{C.18}$$

where

$$A^{\mathrm{pp}}_{ab,cd} = (\varepsilon_a+\varepsilon_b)\delta_{ac}\delta_{bd} + \langle ab||cd\rangle \tag{C.19a}$$
$$B^{\mathrm{pp}}_{ab,ij} = \langle ab||ij\rangle \tag{C.19b}$$
$$C^{\mathrm{pp}}_{ij,kl} = -(\varepsilon_i+\varepsilon_j)\delta_{ik}\delta_{jl} + \langle ij||kl\rangle \tag{C.19c}$$

Then we write the two-body Green's function in the particle-particle (pp) and hole-hole (hh) channels

$$i^2G_2^{pp}(121'2') = \sum_n \mathcal{X}_n^{N+2}(x_1,x_2,t_1-t_2)\tilde{\mathcal{X}}_n^{N+2}(x_{2'},x_{1'},t_{2'}-t_{1'})\Theta\left(t_\alpha-\frac{1}{2}|\tau_\alpha|-\frac{1}{2}|T_\alpha|\right) \tag{C.20}$$

where

$$\mathcal{X}_n^{N+2}(x_1,x_2,t_1-t_2)=\left\langle\Psi_0^N\right|T\left[\psi(x_1)\psi(x_2)\right]\left|\Psi_n^{N+2}\right\rangle e^{i\omega_n^{N+2}(t_1+t_2)/2} \tag{C.21}$$

$$\tilde{\mathcal{X}}_n^{N+2}(x_{2'},x_{1'},t_{2'}-t_{1'})=\left\langle\Psi_n^{N+2}\right|T\left[\psi^\dagger(x_{2'})\psi^\dagger(x_{1'})\right]\left|\Psi_0^N\right\rangle e^{-i\omega_n^{N+2}(t_{2'}+t_{1'})/2} \tag{C.22}$$

$$\omega_n^{N+2}=E_n^{N+2}-E_0^N \tag{C.23}$$

We use

$$\Theta(t)=-\frac{1}{2\pi i}\lim_{\eta\to+0}\int_{-\infty}^{\infty}d\omega\frac{1}{\omega+i\eta}e^{-i\omega t} \tag{C.24}$$

In the expression (C.26)

$$iG_2^{pp}(x_1,x_2,x_{1'},x_{2'},\omega)=\sum_n\frac{\mathcal{X}_n^{N+2}(x_1,x_2,t_1-t_2)\tilde{\mathcal{X}}_n^{N+2}(x_{2'},x_{1'},t_{2'}-t_{1'})}{\omega-\omega_n^{N+2}+i\eta}e^{-i(\omega-\omega_n^{N+2})(-\frac{1}{2}|\tau_\alpha|-\frac{1}{2}|T_\alpha|)} \tag{C.25}$$

Once we have the Fourier transform we choose the time $t_2\to t_1$ and $t_{1'}\to t_{2'}$, so the exponential factor disappear. We do the same for

$$i^2G_2^{hh}(121'2')=\sum_n\mathcal{X}_n^{N-2}(x_{2'},x_{1'},t_{2'}-t_{1'})\tilde{\mathcal{X}}_n^{N-2}(x_1,x_2,t_1-t_2)\Theta\left(-t_\alpha-\frac{1}{2}|\tau_\alpha|-\frac{1}{2}|T_\alpha|\right) \tag{C.26}$$

We obtain

$$iG_2^{hh}(x_1,x_2,x_{1'},x_{2'},\omega)=-\sum_n\frac{\mathcal{X}_n^{N-2}(x_{2'},x_{1'},t_{2'}-t_{1'})\tilde{\mathcal{X}}_n^{N-2}(x_1,x_2,t_1-t_2)}{\omega-\omega_n^{N-2}-i\eta}e^{-i(\omega-\omega_n^{N-2})(-\frac{1}{2}|\tau_\alpha|-\frac{1}{2}|T_\alpha|)} \tag{C.27}$$

We express the bound state amplitudes in the one-particle orbital basis

$$\mathcal{X}_n^{N+2}(x_1,x_2)=\left\langle\Psi_0^N\right|\psi(x_1)\psi(x_2)\left|\Psi_n^{N+2}\right\rangle=\sum_{uv}\mathcal{X}_{uv,n}^{N+2}\phi_u(x_1)\phi_v(x_2) \tag{C.28}$$

$$\tilde{\mathcal{X}}_n^{N+2}(x_{2'},x_{1'})=\left\langle\Psi_n^{N+2}\right|\psi^\dagger(x_{2'})\psi^\dagger(x_{1'})\left|\Psi_0^N\right\rangle=\sum_{u'v'}(\mathcal{X}_{u'v',n}^{N+2})^*\phi_{v'}^*(x_{2'})\phi_{u'}^*(x_{1'}) \tag{C.29}$$

$$\tilde{\mathcal{X}}_n^{N-2}(x_1,x_2)=\left\langle\Psi_n^{N-2}\right|\psi(x_1)\psi(x_2)\left|\Psi_0^N\right\rangle=\sum_{uv}\mathcal{X}_{uv,n}^{N-2}\phi_u(x_1)\phi_v(x_2) \tag{C.30}$$

$$\mathcal{X}_n^{N-2}(x_{2'},x_{1'})=\left\langle\Psi_0^N\right|\psi^\dagger(x_{2'})\psi^\dagger(x_{1'})\left|\Psi_n^{N-2}\right\rangle=\sum_{u'v'}(\mathcal{X}_{u'v',n}^{N-2})^*\phi_{v'}^*(x_{2'})\phi_{u'}^*(x_{1'}) \tag{C.31}$$

With these notations (C.9) can be written as

$$T_{(pq)(rs)}^{pp}=-i\overline{v}_{(pq)(rs)}-i\sum_{(uv)(u'v')}\overline{v}_{(pq)(uv)}\sum_n\left[\frac{\mathcal{X}_{uv,n}^{N+2}(\mathcal{X}_{u'v',n}^{N+2})^*}{\omega-\omega_n^{N+2}+i\eta}-\frac{\mathcal{X}_{uv,n}^{N-2}(\mathcal{X}_{u'v',n}^{N-2})^*}{\omega-\omega_n^{N-2}-i\eta}\right]\overline{v}_{(u'v')(rs)} \tag{C.32}$$

We introduce new notations

$$\left\langle pq\right|\left.\chi_n^{N+2}\right\rangle=\sum_{c<d}\overline{v}_{pqcd}X_{cd,n}^{N+2}+\sum_{k<l}\overline{v}_{pqkl}Y_{kl,n}^{N+2} \tag{C.33}$$

$$\left\langle\chi_n^{N+2}\right|\left.rs\right\rangle=\sum_{c<d}\left(X_{cd,n}^{N+2}\right)^*\overline{v}_{cdrs}+\sum_{k<l}\left(Y_{kl,n}^{N+2}\right)^*\overline{v}_{klrs} \tag{C.34}$$

$$\left\langle pq\right|\left.\chi_n^{N-2}\right\rangle=\sum_{c<d}\overline{v}_{pqcd}X_{cd,n}^{N-2}+\sum_{k<l}\overline{v}_{pqkl}Y_{kl,n}^{N-2} \tag{C.35}$$

$$\left\langle \chi_n^{N-2} \middle| rs \right\rangle = \sum_{c<d} \left(X_{cd,n}^{N-2} \right)^* \overline{v}_{cdrs} + \sum_{k<l} \left(Y_{kl,n}^{N-2} \right)^* \overline{v}_{klrs} \tag{C.36}$$

$$T_{pqrs}^{pp} = \overline{v}_{pqrs} + \sum_n \left[\frac{\left\langle pq \middle| \chi_n^{N+2} \right\rangle \left\langle \chi_n^{N+2} \middle| rs \right\rangle}{\omega - \omega_n^{N+2} + i\eta} - \frac{\left\langle pq \middle| \chi_n^{N-2} \right\rangle \left\langle \chi_n^{N-2} \middle| rs \right\rangle}{\omega - \omega_n^{N-2} - i\eta} \right] \tag{C.37}$$

Appendix D

Quasiparticles and neutral excitations of the symmetric Hubbard dimer

D.1 Quasiparticles

The expression of the one-body non-interacting Green's function is

$$G_{0,ij} = \frac{(-1)^{i-j}}{2}\left[\frac{1}{\omega-(\varepsilon+t)+i\eta}+\frac{(-1)^{i-j}}{\omega-(\varepsilon-t)-i\eta}\right] \tag{D.1}$$

$$G_0 = \begin{pmatrix} \frac{\omega-\varepsilon}{d} & -\frac{t}{d} \\ -\frac{t}{d} & \frac{\omega-\varepsilon}{d} \end{pmatrix} \tag{D.2}$$

where $d = [\omega-(\varepsilon+t)]\,[\omega-(\varepsilon-t)]$

The inverse of this matrix is

$$G_0^{-1} = \begin{pmatrix} \omega-\varepsilon & t \\ t & \omega-\varepsilon \end{pmatrix} \tag{D.3}$$

To calculate the interacting Green's function, we use the Dyson equation that we invert

$$G^{-1} = G_0^{-1} - \Sigma = \begin{pmatrix} \omega-\varepsilon-\Sigma_{11} & t-\Sigma_{12} \\ t-\Sigma_{12} & \omega-\varepsilon-\Sigma_{11} \end{pmatrix} \tag{D.4}$$

With the Hartre-Fock self-energy $\Sigma_{ij}^{HF} = \frac{U}{2}\delta_{ij}$, we obtain the Hartre-Fock Green's function

$$G_{\mathrm{HF},ij} = \frac{(-1)^{i-j}}{2}\left[\frac{1}{\omega-(\varepsilon+t+\frac{U}{2})+i\eta}+\frac{(-1)^{i-j}}{\omega-(\varepsilon-t+\frac{U}{2})-i\eta}\right] \tag{D.5}$$

We want to obtain the poles of G which amounts to solve

$$\det\left(G^{-1}\right) = 0 \tag{D.6}$$

This gives two solutions

$$\omega_1 = \varepsilon + t + \Sigma_{11}(\omega_1) - \Sigma_{12}(\omega_1) \tag{D.7}$$

$$\omega_2 = \varepsilon - t + \Sigma_{11}(\omega_2) + \Sigma_{12}(\omega_2) \tag{D.8}$$

We compute the quasiparticles with three different approximations on the self-energy. We can do a static approximation where we set $\omega_1 = \varepsilon + t$ and $\omega_2 = \varepsilon - t$ in Σ, we can solve the two non-linear equations that we got on ω_1 and ω_2, or we can linearize these two equations by renormalizing them with a weight factor Z.

D.1.1 *GW* Quasiparticles

The expression of the self-energy for the Hubbard dimer in the *GW* approximation is

$$\Sigma_{ij}^{G_0W_0} = \frac{U}{2}\delta_{ij} + \frac{U^2 t}{2\Omega^{eh}}\left[\frac{1}{\omega - (\varepsilon + t + \Omega^{eh}) + i\eta} + \frac{(-1)^{i-j}}{\omega - (\varepsilon - t - \Omega^{eh}) - i\eta}\right] \tag{D.9}$$

This gives for the quasiparticles (with a static self-energy)

$$\varepsilon_a^{QP} = \varepsilon + t + \frac{U}{2} - \frac{U^2 t}{\Omega^{eh}}\frac{1}{\varepsilon - (2t + \Omega^{eh})} \tag{D.10}$$

$$\varepsilon_i^{QP} = \varepsilon - t + \frac{U}{2} - \frac{U^2 t}{\Omega^{eh}}\frac{1}{\varepsilon + \Omega^{eh}} \tag{D.11}$$

With a dynamical self-energy, we obtain

$$\varepsilon_a^{QP} = \varepsilon + \frac{U}{4} - \frac{\Omega^{eh}}{2} \pm \frac{1}{2}\sqrt{\left(2t + \frac{U}{2} + \Omega^{eh}\right)^2 + \frac{4U^2 t}{\Omega^{eh}}} \tag{D.12}$$

$$\varepsilon_i^{QP} = \varepsilon + \frac{U}{4} + \frac{\Omega^{eh}}{2} \pm \frac{1}{2}\sqrt{\left(2t + \frac{U}{2} + \Omega^{eh}\right)^2 + \frac{4U^2 t}{\Omega^{eh}}} \tag{D.13}$$

We keep the solutions such as

$$\varepsilon_a^{QP}(U = 0) = \varepsilon + t \tag{D.14}$$

and

$$\varepsilon_i^{QP}(U = 0) = \varepsilon - t \tag{D.15}$$

Which are

$$\varepsilon_a^{QP} = \varepsilon + \frac{U}{4} - \frac{\Omega^{eh}}{2} + \frac{1}{2}\sqrt{\left(2t + \frac{U}{2} + \Omega^{eh}\right)^2 + \frac{4U^2 t}{\Omega^{eh}}} \tag{D.16}$$

$$\varepsilon_i^{QP} = \varepsilon + \frac{U}{4} + \frac{\Omega^{eh}}{2} - \frac{1}{2}\sqrt{\left(2t + \frac{U}{2} + \Omega^{eh}\right)^2 + \frac{4U^2 t}{\Omega^{eh}}} \tag{D.17}$$

D.1.2 *GT*^{pp} Quasiparticles

The expression of the self-energy for the Hubbard dimer in the *GW* approximation is

$$\Sigma_{0,ij}^{G_0T_0^{pp}} = \frac{U}{2}\delta_{ij} + \frac{U^2 t}{4\Omega^{pp}}\left[\frac{1}{\omega + \varepsilon - (t + \Omega^{pp}) + i\eta} + \frac{(-1)^{i-j}}{\omega + \varepsilon + (t + \Omega^{pp}) - i\eta}\right] \tag{D.18}$$

This gives for the quasiparticles (with a static self-energy)

$$\varepsilon_a^{QP} = \varepsilon + t + \frac{U}{2} + \frac{U^2 t}{2\Omega^{pp}}\frac{1}{\varepsilon + 2t + \Omega^{pp}} \tag{D.19}$$

$$\varepsilon_i^{QP} = \varepsilon - t + \frac{U}{2} + \frac{U^2 t}{2\Omega^{pp}}\frac{1}{\varepsilon - (2t + \Omega^{pp})} \tag{D.20}$$

With a dynamical self-energy, we obtain

$$\varepsilon_a^{QP} = \frac{1}{2}\left(\frac{U}{2} - \Omega^{pp} \pm \sqrt{\left(2\varepsilon + 2t + \frac{U}{2} + \Omega^{pp}\right)^2 + \frac{2U^2 t}{\Omega^{pp}}}\right) \tag{D.21}$$

$$\varepsilon_i^{QP} = \frac{1}{2}\left(\frac{U}{2} + \Omega^{pp} \pm \sqrt{\left(2\varepsilon - 2t + \frac{U}{2} - \Omega^{pp}\right)^2 + \frac{2U^2t}{\Omega^{pp}}}\right) \tag{D.22}$$

The solutions are

$$\varepsilon_a^{QP} = \frac{1}{2}\left(\frac{U}{2} - \Omega^{pp} + \sqrt{\left(2\varepsilon + 2t + \frac{U}{2} + \Omega^{pp}\right)^2 + \frac{2U^2t}{\Omega^{pp}}}\right) \tag{D.23}$$

$$\varepsilon_i^{QP} = \frac{1}{2}\left(\frac{U}{2} + \Omega^{pp} - \sqrt{\left(2\varepsilon - 2t + \frac{U}{2} - \Omega^{pp}\right)^2 + \frac{2U^2t}{\Omega^{pp}}}\right) \tag{D.24}$$

D.1.3 $G\overline{T}^{eh}$ Quasiparticles

The expression of the self-energy for the Hubbard dimer in the GW approximation is

$$\Sigma_{ij}^{G_0\overline{T}_0^{eh}} = \frac{U}{2}\delta_{ij} + \frac{U^2t}{4\overline{\Omega}^{eh}}\left[\frac{1}{\omega - (\varepsilon + t + \overline{\Omega}^{eh}) + i\eta} + \frac{(-1)^{i-j}}{\omega - (\varepsilon - t - \overline{\Omega}^{eh}) - i\eta}\right] \tag{D.25}$$

This gives for the quasiparticles (with a static self-energy)

$$\varepsilon_a^{QP} = \varepsilon + t + \frac{U}{2} - \frac{U^2t}{2\overline{\Omega}^{eh}}\frac{1}{\varepsilon - (2t + \overline{\Omega}^{eh})} \tag{D.26}$$

$$\varepsilon_i^{QP} = \varepsilon - t + \frac{U}{2} + \frac{U^2t}{2\overline{\Omega}^{eh}}\frac{1}{\varepsilon + 2t + \overline{\Omega}^{eh}} \tag{D.27}$$

With a dynamical self-energy, we obtain

$$\varepsilon_a^{QP} = \varepsilon + \frac{U}{4} - \frac{\overline{\Omega}^{eh}}{2} \pm \frac{1}{2}\sqrt{\left(2t + \frac{U}{2} + \overline{\Omega}^{eh}\right)^2 + \frac{2U^2t}{\overline{\Omega}^{eh}}} \tag{D.28}$$

$$\varepsilon_i^{QP} = \varepsilon + \frac{U}{4} + \frac{\overline{\Omega}^{eh}}{2} \pm \frac{1}{2}\sqrt{\left(-2t + \frac{U}{2} - \overline{\Omega}^{eh}\right)^2 + \frac{2U^2t}{\overline{\Omega}^{eh}}} \tag{D.29}$$

The solutions are

$$\varepsilon_a^{QP} = \varepsilon + \frac{U}{4} - \frac{\overline{\Omega}^{ph}}{2} + \frac{1}{2}\sqrt{\left(2t + \frac{U}{2} + \overline{\Omega}^{eh}\right)^2 + \frac{2U^2t}{\overline{\Omega}^{eh}}} \tag{D.30}$$

$$\varepsilon_i^{QP} = \varepsilon + \frac{U}{4} + \frac{\overline{\Omega}^{eh}}{2} - \frac{1}{2}\sqrt{\left(-2t + \frac{U}{2} - \overline{\Omega}^{eh}\right)^2 + \frac{2U^2t}{\overline{\Omega}^{eh}}} \tag{D.31}$$

D.2 Bethe-Salpeter calculation in the GW approximation

The screened Coulomb interaction W is defined by

$$W(12) = v(12) + \int d34\, v(13) P^{eh}(34) W(42) \tag{D.32}$$

where P is the particle-hole polarisability such that

$$P^{eh}(34) = -iG(34)G(43) \tag{D.33}$$

To express this integral equation in the one particle orbital basis, we use the definition

$$W_{ijkl}^{\sigma_i\sigma_j\sigma_k\sigma_l} = \int dx_1 dx_2\, \phi^*_{i\sigma_i}(x_1)\phi^*_{j\sigma_j}(x_2) W(12) \phi_{k\sigma_k}(x_1)\phi_{l\sigma_l}(x_2) \tag{D.34}$$

where $x_a = (r_a, \sigma_a)$, we obtain for W

$$W_{ijkl}^{\sigma_i\sigma_j\sigma_k\sigma_l} = v_{ijkl}\delta_{\sigma_i\sigma_k}\delta_{\sigma_j\sigma_l} - 2i \sum_{aba'b'} v_{ib'ka} G_{ab}^{\sigma_a\sigma_a} G_{a'b'}^{\sigma_{a'}\sigma_{a'}} W_{bja'l}^{\sigma_i\sigma_j\sigma_k\sigma_l} \tag{D.35}$$

with $v_{ijkl} = \int dx_1 dx_2\, \phi^*_{i\sigma_i}(x_1)\phi^*_{j\sigma_j}(x_2) v(12) \phi_{k\sigma_k}(x_1)\phi_{l\sigma_l}(x_2)$

We close the equation

$$\sum_{ba'} \left[\delta_{ib}\delta_{ka'} + 2i \sum_{ab'} v_{ib'ka} G_{ib}^{\sigma_i\sigma_i} G_{bi}^{\sigma_i\sigma_i} \right] W_{bja'l}^{\sigma_i\sigma_j\sigma_k\sigma_l} = v_{ijkl}\delta_{\sigma_i\sigma_k}\delta_{\sigma_j\sigma_l} \tag{D.36}$$

This can be rewrite

$$W_{cjdl}^{\sigma_i\sigma_j\sigma_i\sigma_j} = \sum_{ik} [\epsilon^{-1}]_{(cd)(ik)} v_{ijkl}\delta_{\sigma_i\sigma_k}\delta_{\sigma_j\sigma_l} \tag{D.37}$$

with

$$\epsilon_{(cd)(ik)} = \delta_{ci}\delta_{dk} - 2\sum_{ab'} v_{cb'da} P_{aikb'}^{eh\ \sigma_i\sigma_k} \tag{D.38}$$

For the Hubbard dimer the Coulomb interaction is local, $v(1,2) = U\delta(1,2)$ with this we have

$$W_{ijkl}^{\sigma_i\sigma_j\sigma_k\sigma_l} = \delta_{ik} \overline{W}_{ijil}^{\ \sigma_i\sigma_j\sigma_k\sigma_l} \tag{D.39}$$

where

$$\overline{W}_{ijil}^{\ \sigma_i\sigma_j\sigma_k\sigma_l} = U\delta_{ij}\delta_{il}\delta_{\sigma_i\sigma_k}\delta_{\sigma_j\sigma_l} - 2i\sum_b U G_{ib}^{\sigma_i\sigma_i} G_{bi}^{\sigma_i\sigma_i} \overline{W}_{bjbl}^{\ \sigma_i\sigma_j\sigma_k\sigma_l} \tag{D.40}$$

So we get

$$\overline{W}_{ijij}^{\ \sigma_i\sigma_j\sigma_i\sigma_j} = [\epsilon^{-1}]_{ij} U \delta_{\sigma_i\sigma_k}\delta_{\sigma_j\sigma_l} \tag{D.41}$$

and

$$\epsilon_{ij} = \delta_{ij} - 2UP_{ijji}^{eh} \tag{D.42}$$

To obtain the matrix $\boldsymbol{\epsilon}$, we calculate first the polarisability with

$$P_{ijji}^{eh}(\omega) = \int \frac{d\omega'}{2\pi i} G_{ij}(\omega') G_{ji}(\omega' - \omega) e^{i\omega'\eta} \tag{D.43}$$

which gives (with $\varepsilon = 0$ and $G = G_{0/\mathrm{HF}}$)

$$P^{eh}_{ijji} = \frac{(-1)^{i-j}}{4}\left[\frac{1}{\omega - 2t + 2i\eta} - \frac{1}{\omega + 2t - 2i\eta}\right] = (-1)^{i-j}P^0 \tag{D.44}$$

with $P^0 = \frac{1}{4}\left[\frac{1}{\omega-2t+2i\eta} - \frac{1}{\omega+2t-2i\eta}\right]$

then

$$\epsilon^{-1} = \frac{1}{1-4UP_0}\begin{pmatrix} 1-2UP_0 & -2UP_0 \\ -2UP_0 & 1-2UP_0 \end{pmatrix} = \begin{pmatrix} 1+\frac{2Ut}{\omega^2-4t^2-4Ut} & -\frac{2Ut}{\omega^2-4t^2-4Ut} \\ -\frac{2Ut}{\omega^2-4t^2-4Ut} & 1+\frac{2Ut}{\omega^2-4t^2-4Ut} \end{pmatrix}$$

$$[\epsilon^{-1}]_{ij} = \delta_{ij} + (-1)^{i-j}\frac{2Ut}{\omega^2 - 4t^2 - 4Ut} \tag{D.45}$$

Therefore the expression of W is

$$\overline{W}^{\sigma_i\sigma_j\sigma_k\sigma_l}_{ijij}(\omega) = \left[U\delta_{ij} + (-1)^{i-j}\frac{U^2t}{\Omega^{eh}}\left(\frac{1}{\omega - \Omega^{eh} + i\eta} - \frac{1}{\omega + \Omega^{eh} - i\eta}\right)\right]\delta_{\sigma_i\sigma_k}\delta_{\sigma_j\sigma_l} \tag{D.46}$$

where $\Omega^{eh} = \sqrt{4t^2 + 4Ut}$

with the two-body interaction W we calculate the self-energy from

$$\Sigma^{GW}(12) = iG(12)W(12^+) \tag{D.47}$$

The Fourier transform of Σ^{GW} is

$$\Sigma^{GW}_{ij}(\omega) = -\int \frac{d\omega'}{2\pi i}G_{ij}(\omega - \omega')W_{ijij}(\omega')e^{i\omega'\eta} \tag{D.48}$$

which gives

$$\Sigma^{GW}_{ij}(\omega) = \frac{U}{2}\delta_{ij} + \frac{U^2t}{2\Omega^{eh}}\left[\frac{1}{\omega - (t + \Omega^{eh}) + i\eta} + \frac{(-1)^{i-j}}{\omega + (t + \Omega^{eh}) - i\eta}\right] \tag{D.49}$$

The charged excitations are

$$\omega = \varepsilon^0_b + \Sigma_{bb}(\omega) \tag{D.50}$$

$$\omega = \varepsilon^0_a + \Sigma_{aa}(\omega) \tag{D.51}$$

We linearize the two previous equation so we get

$$\varepsilon^{QP}_b = \varepsilon^0_b + Z_b\Sigma_{bb}(\omega = \varepsilon^0_b) \tag{D.52}$$

$$\varepsilon^{QP}_a = \varepsilon^0_a + Z_a\Sigma_{aa}(\omega = \varepsilon^0_a) \tag{D.53}$$

where $Z_p = (1 - \partial_\omega\Sigma_{pp}(\omega)|_{\omega=\varepsilon^0_p})^{-1}$ is the weight factor and ε^{QP}_p are the quasi-particle energies.

$$\Delta\varepsilon^{QP} = \varepsilon^{QP}_b - \varepsilon^{QP}_a \tag{D.54}$$

We calculate now the elements of the effective two-body interaction Ξ

$$\Xi(1234) = \delta(13)\delta(24)v(14) - \delta(14)\delta(23)W(13) \tag{D.55}$$

we use the following definitions

$$\Xi_{ijkl} = \int dx_1dx_2dx_3dx_4\phi^*_i(x_1)\phi^*_j(x_2)\Xi(x_1, x_2, x_3, x_4)\phi_k(x_4)\phi_l(x_3) \tag{D.56}$$

$$\int dx_1 dx_2 dx_3 dx_4 \phi_i^*(x_1)\phi_j^*(x_2)\delta(13)\delta(24)v(14)\phi_k(x_4)\phi_l(x_3) = v_{ijkl}\delta_{\sigma_i\sigma_l}\delta_{\sigma_j\sigma_k} \tag{D.57}$$

We then obtain

$$\int dx_1 dx_2 dx_3 dx_4 \phi_i^*(x_1)\phi_j^*(x_2)\delta(14)\delta(23)W(13)\phi_k(x_4)\phi_l(x_3) = W_{ijlk}\delta_{\sigma_i\sigma_k}\delta_{\sigma_j\sigma_l} \tag{D.58}$$

$$\Xi_{ijkl}^{\sigma_i\sigma_j\sigma_k\sigma_l} = v_{ijkl}\delta_{\sigma_i\sigma_l}\delta_{\sigma_j\sigma_k} - W_{ijlk}^{\sigma_i\sigma_j\sigma_k\sigma_l}\delta_{\sigma_i\sigma_k}\delta_{\sigma_j\sigma_l} \tag{D.59}$$

For the Hubbard dimer this becomes

$$\begin{aligned}\Xi_{ijkl}^{\sigma_i\sigma_j\sigma_k\sigma_l} &= U\delta_{ij}\delta_{ik}\delta_{il}\delta_{\sigma_i\sigma_l}\delta_{\sigma_j\sigma_k} - \delta_{ik}\delta_{jl}\overline{W}_{ijij}\delta_{\sigma_i\sigma_k}\delta_{\sigma_j\sigma_l} \\ &= \delta_{ik}\delta_{jl}\left[U\delta_{ij}\delta_{\sigma_i\sigma_l}\delta_{\sigma_j\sigma_k} - \overline{W}_{ijij}\delta_{\sigma_i\sigma_k}\delta_{\sigma_j\sigma_l}\right] \\ &= \delta_{ik}\delta_{jl}\widetilde{\Xi}_{ijij}^{\sigma_i\sigma_j\sigma_k\sigma_l}\end{aligned} \tag{D.60}$$

We express these matrix elements in the bonding anti-bonding basis with

$$\Xi_{(v\sigma_1 c\sigma_2)(v'\sigma_{1'}c'\sigma_{2'})} = \int dx_1 dx_2 dx_3 dx_4 \phi_{v\sigma_1}(x_3)\phi_{c\sigma_2}^*(x_1)\Xi(1234)\phi_{v'\sigma_{1'}}^*(x_2)\phi_{c'\sigma_{2'}}(x_4) \tag{D.61}$$

$$\Xi_{(v\sigma_1 c\sigma_2)(c'\sigma_{2'}v'\sigma_{1'})} = \int dx_1 dx_2 dx_3 dx_4 \phi_{v\sigma_1}(x_3)\phi_{c\sigma_2}^*(x_1)\Xi(1234)\phi_{c'\sigma_{2'}}^*(x_2)\phi_{v'\sigma_{1'}}(x_4) \tag{D.62}$$

We obtain

$$\Xi_{(v\sigma_1 c\sigma_2)(v'\sigma_{1'}c'\sigma_{2'})} = \frac{1}{2}[U\delta_{\sigma_2\sigma_1}\delta_{\sigma_{2'}\sigma_{1'}} - U\delta_{\sigma_2\sigma_{2'}}\delta_{\sigma_{1'}\sigma_1}] \tag{D.63}$$

$$\Xi_{(v\sigma_1 c\sigma_2)(c'\sigma_{2'}v'\sigma_{1'})} = \frac{1}{2}[U\delta_{\sigma_2\sigma_1}\delta_{\sigma_{2'}\sigma_{1'}} - \frac{Ut}{t+U}\delta_{\sigma_2\sigma_{1'}}\delta_{\sigma_{2'}\sigma_1}] \tag{D.64}$$

$$\begin{aligned}\Xi(1,2,3,4) &= i\frac{\delta\Sigma(1,3)}{\delta G(4,2)} \\ &= i\left[\frac{\delta v_H(1)}{\delta G(4,2)}\delta(1,3) + \frac{\delta\, iG(1,3)W(1,3^+)}{\delta G(4,2)}\right] \\ &\approx i\left[-i\int dx\; v_H(1,x)\frac{\delta G(x,x))}{\delta G(4,2)}\delta(1,3) + i\delta(1,4)\delta(3,2)W(1,3^+)\right] \\ &= i\left[-i\int dx\; v_H(1,x)\delta(x,2)\delta(x,4)\delta(1,3) + i\delta(1,4)\delta(3,2)W(1,3^+)\right]\end{aligned} \tag{D.65}$$

$$\Xi_{(v\sigma_1 c\sigma_2)(v'\sigma_{1'}c'\sigma_{2'})} = \frac{1}{4}[\Xi_{1111}^{\sigma_2\sigma_{1'}\sigma_{2'}\sigma_1} + \Xi_{2222}^{\sigma_2\sigma_{1'}\sigma_{2'}\sigma_1} + \Xi_{1212}^{\sigma_2\sigma_{1'}\sigma_{2'}\sigma_1} + \Xi_{2121}^{\sigma_2\sigma_{1'}\sigma_{2'}\sigma_1}] \tag{D.66}$$

$$\Xi_{(v\sigma_1 c\sigma_2)(v'\sigma_{1'}c'\sigma_{2'})} = \frac{1}{2}[U\delta_{\sigma_2\sigma_1}\delta_{\sigma_{2'}\sigma_{1'}} - U\delta_{\sigma_2\sigma_{2'}}\delta_{\sigma_{1'}\sigma_1}] \tag{D.67}$$

$$\Xi_{(v\sigma_1 c\sigma_2)(c'\sigma_{2'}v'\sigma_{1'})} = \frac{1}{2}[\Xi_{1111}^{\sigma_2\sigma_{2'}\sigma_{1'}\sigma_1} - \Xi_{1212}^{\sigma_2\sigma_{2'}\sigma_{1'}\sigma_1}] \tag{D.68}$$

$$\Xi_{(v\sigma_1 c\sigma_2)(c'\sigma_{2'}v'\sigma_{1'})} = \frac{1}{2}[U\delta_{\sigma_2\sigma_1}\delta_{\sigma_{2'}\sigma_{1'}} - \frac{Ut}{t+U}\delta_{\sigma_2\sigma_{1'}}\delta_{\sigma_{2'}\sigma_1}] \tag{D.69}$$

$${}^3\boldsymbol{H}_{\text{exc}}^{G_{\text{HF}}W_{\text{HF}}} = \begin{pmatrix} E_{\text{g}}^{G_{\text{HF}}W_{\text{HF}}} - \frac{U}{2} & \frac{U}{2}\left(\frac{U}{t+U} - 1\right) \\ -\frac{U}{2}\left(\frac{U}{t+U} - 1\right) & -\left(E_{\text{g}}^{G_{\text{HF}}W_{\text{HF}}} - \frac{U}{2}\right) \end{pmatrix} \tag{D.70a}$$

$${}^1\boldsymbol{H}_{\text{exc}}^{G_{\text{HF}}W_{\text{HF}}} = \begin{pmatrix} E_{\text{g}}^{G_{\text{HF}}W_{\text{HF}}} + \frac{U}{2} & \frac{U}{2}\left(\frac{U}{t+U} + 1\right) \\ -\frac{U}{2}\left(\frac{U}{t+U} + 1\right) & -\left(E_{\text{g}}^{G_{\text{HF}}W_{\text{HF}}} + \frac{U}{2}\right) \end{pmatrix} \tag{D.70b}$$

D.3 Bethe-Salpeter calculation in the GT^{pp} approximation

The particle-particle polarizability is (for time variables)

$$P^{pp}(1-3) = -iG(1-3)G(1^+-3) \tag{D.71}$$

We calculate its Fourier transform

$$\begin{aligned} P^{pp}(1-3) &= -i\int \frac{d\omega}{2\pi}\frac{d\omega'}{2\pi}\, G(\omega)G(\omega')e^{-i\omega(t_1-t_3)}e^{-i\omega'(t_1^+-t_3)} \\ &= -i\int \frac{d\omega}{2\pi}\frac{d\omega'}{2\pi}\, G(\omega)G(\omega')e^{-i(t_1-t_3)(\omega+\omega')}e^{-i\omega'\eta} \end{aligned}$$

$$\begin{aligned} P^{pp}(\widetilde{\omega}) &= \int d(t_1-t_3)\, P^{pp}(1-3)e^{i\widetilde{\omega}(t_1-t_3)} \\ &= -i\int d(t_1-t_3)\int \frac{d\omega}{2\pi}\frac{d\omega'}{2\pi}G(\omega)G(\omega')e^{i(t_1-t_3)(\widetilde{\omega}-\omega-\omega')}e^{-i\omega'\eta} \end{aligned}$$

We obtain

$$P^{pp}(\omega) = \int \frac{d\omega'}{2\pi i}G(\omega-\omega')G(\omega')e^{-i\omega'\eta} \tag{D.72}$$

The particle-particle T-matrix is defined by

$$T^{pp} = T_1^{pp} + T_2^{pp} \tag{D.73}$$

with

$$T_1^{pp}(1,2,1',2') = -iv(12)\delta(11')\delta(22') + iv(12)\int d35G(13)G(25)T_1^{pp}(3,5,1',2') \tag{D.74}$$

and

$$T_2^{pp}(1,2,1',2') = iv(12)\delta(21')\delta(12') + iv(12)\int d35G_1(13)G_1(25)T_2^{pp}(3,5,1',2') \tag{D.75}$$

To express these integral equations in the one particle orbital basis, we use the definition

$$T^{pp\ \sigma_p\sigma_q\sigma_r\sigma_s}_{pqrs} = \int dx_1dx_2dx_{1'}dx_{2'}\ \phi^*_{p\sigma_p}(x_1)\phi^*_{q\sigma_q}(x_2)T^{pp}\phi_{r\sigma_r}(x_{1'})\phi_{s\sigma_s}(x_{2'}) \tag{D.76}$$

We obtain

$$T^{pp\ \sigma_p\sigma_q\sigma_r\sigma_s}_{1,pqrs} = -iv_{pqrs}\delta_{\sigma_p\sigma_r}\delta_{\sigma_q\sigma_s} + i\sum_{ijkl\sigma_p\sigma_q} v_{pqik}G^{\sigma_p\sigma_p}_{ij}G^{\sigma_q\sigma_q}_{kl}T^{pp\ \sigma_i\sigma_j\sigma_r\sigma_s}_{1,jlrs} \tag{D.77}$$

$$T^{pp\ \sigma_p\sigma_q\sigma_r\sigma_s}_{2,pqrs} = iv_{pqsr}\delta_{\sigma_p\sigma_s}\delta_{\sigma_q\sigma_r} + i\sum_{ijkl\sigma_p\sigma_q} v_{pqik}G^{\sigma_p\sigma_p}_{ij}G^{\sigma_q\sigma_q}_{kl}T^{pp\ \sigma_i\sigma_j\sigma_r\sigma_s}_{2,jlrs} \tag{D.78}$$

In matrix notations

$$T^{pp\ \sigma_p\sigma_q\sigma_r\sigma_s}_{1,(pq)(rs)} = -iv_{(pq)(rs)} - \sum_{(ik)(jl)} v_{(pq)(ik)}P^{pp}_{(ik)(jl)}T^{pp\ \sigma_i\sigma_j\sigma_r\sigma_s}_{1,(jl)(rs)} \tag{D.79}$$

with $v_{(pq)(rs)} = v_{pqrs}\delta_{\sigma_p\sigma_r}\delta_{\sigma_q\sigma_s}$ and $P^{pp}_{(ik)(jl)} = P^{pp}_{ijkl} = -iG^{\sigma_p\sigma_p}_{ij}G^{\sigma_q\sigma_q}_{kl}$.

We close the equation

$$T^{pp\ \sigma_p\sigma_q\sigma_p\sigma_q}_{1,(pq)(rs)} = \sum_{nm}[\epsilon^{\sigma_p\sigma_q-1}]_{(pq)(nm)}v_{(nm)(rs)} \tag{D.80}$$

with

$$\epsilon^{\sigma_p\sigma_q}_{(pq)(nm)} = \delta_{pn}\delta_{qm} + \sum_{ik} v_{(pq)(ik)}P^{\sigma_p\sigma_q}_{(ik)(nm)} \tag{D.81}$$

For the Hubbard dimer the Coulomb interaction is local, $v(1,2) = U\delta(1,2)$, therefore

$$T^{pp\ \sigma_p\sigma_q\sigma_r\sigma_s}_{1,pqrs} = -i\delta_{pq}\overline{T}^{pp\ \sigma_p\sigma_q\sigma_r\sigma_s}_{1,pqrs} \tag{D.82}$$

where

$$\overline{T}^{pp\ \sigma_p\sigma_q\sigma_r\sigma_s}_{1,pqrs} = U\delta_{pr}\delta_{ps}\delta_{\sigma_p\sigma_r}\delta_{\sigma_q\sigma_s} + iU\sum_l G^{\sigma_p\sigma_p}_{pl}G^{\sigma_p\sigma_p}_{pl}\overline{T}^{pp\ \sigma_p\sigma_q\sigma_r\sigma_s}_{llrs} \tag{D.83}$$

So we get

$$\overline{T}^{pp\ \sigma_p\sigma_q\sigma_r\sigma_s}_{1,pqrs} = -i\delta_{pq}\delta_{rs}\overline{T}^{pp\ \sigma_p\sigma_q\sigma_r\sigma_s}_{pprr}\delta_{\sigma_p\sigma_r}\delta_{\sigma_q\sigma_s} \tag{D.84}$$

or

$$\overline{T}^{pp\ \sigma_p\sigma_q\sigma_r\sigma_s}_{1,pqrs} = [\epsilon^{-1}]_{ij}U\delta_{\sigma_i\sigma_k}\delta_{\sigma_j\sigma_l} \tag{D.85}$$

and

$$\epsilon_{pq} = \delta_{pq} + UP^{pp}_{(pp)(qq)} \tag{D.86}$$

To obtain the matrix $\boldsymbol{\epsilon}$, we calculate first the polarizability with

$$P^{pp}_{ijij}(\omega) = \int \frac{d\omega'}{2\pi i}G_{ij}(\omega-\omega')G_{ij}(\omega')e^{-i\omega'\eta} \tag{D.87}$$

which gives (with $\varepsilon = 0$ and $G = G_{\mathrm{HF}}$)

$$P^{pp}_{ijij} = -\frac{1}{4}\left[\frac{1}{\omega-(2t+U)+2i\eta} - \frac{1}{\omega+(2t-U)-2i\eta}\right] \tag{D.88}$$

Then

$$[\epsilon^{-1}]_{ij} = \delta_{ij} + \frac{Ut}{2\Omega^{pp}}\left(\frac{1}{\omega-U-\Omega^{pp}+i\eta} - \frac{1}{\omega-U+\Omega^{pp}-i\eta}\right) \tag{D.89}$$

where $\Omega^{pp} = \sqrt{4t^2+2Ut}$

Therefore the expression of $\overline{T}^{pp\ \sigma_p\sigma_q\sigma_r\sigma_s}_1$ is

$$\overline{T}^{pp\ \sigma_p\sigma_q\sigma_r\sigma_s}_{1,pprr}(\omega) = \left[U\delta_{ij} + \frac{U^2t}{2\Omega^{pp}}\left(\frac{1}{\omega-U-\Omega^{pp}+i\eta} - \frac{1}{\omega-U+\Omega^{pp}-i\eta}\right)\right]\delta_{\sigma_i\sigma_k}\delta_{\sigma_j\sigma_l} \tag{D.90}$$

and $\overline{T}^{pp}_2 = \overline{T}^{pp}_1$

from this we calculate the self-energy from

$$\Sigma^{GT^{pp}}_{ij}(\omega) = \int \frac{d\omega'}{2\pi i}G_{ij}(\omega')T^{pp}_{iijj}(\omega+\omega')e^{i\omega'\eta} \tag{D.91}$$

which gives

$$\Sigma_{ij}^{GT^{pp}}(\omega) = \frac{U}{2}\delta_{ij} + \frac{U^2 t}{4\Omega^{pp}}\left[\frac{1}{\omega - (t + \frac{U}{2} + \Omega^{pp}) + i\eta} + \frac{(-1)^{i-j}}{\omega + (t - \frac{U}{2} + \Omega^{pp}) - i\eta}\right] \tag{D.92}$$

Then we express the self-energy in the bonding (b) anti-bonding (a) basis

$$\Sigma_{bb} = \Sigma_{11} + \Sigma_{22} \tag{D.93}$$

$$\Sigma_{aa} = \Sigma_{11} - \Sigma_{22} \tag{D.94}$$

The charged excitations can be calculated as

$$\omega = \varepsilon_b^0 + \Sigma_{bb}(\omega) \tag{D.95}$$

$$\omega = \varepsilon_a^0 + \Sigma_{aa}(\omega) \tag{D.96}$$

where the ε_p^0 are the poles of the Green's function that we choose as a starting point, in our case $\varepsilon_b^0 = -t + \frac{U}{2}$ and $\varepsilon_a^0 = t + \frac{U}{2}$.

We linearize the two previous equation so we get

$$\varepsilon_b^{QP} = \varepsilon_b^0 + Z_b \Sigma_{bb}(\omega = \varepsilon_b^0) \tag{D.97}$$

$$\varepsilon_a^{QP} = \varepsilon_a^0 + Z_a \Sigma_{aa}(\omega = \varepsilon_a^0) \tag{D.98}$$

where $Z_p = (1 - \partial_\omega \Sigma_{pp}(\omega)|_{\omega=\varepsilon_p^0})^{-1}$ is the weight factor and ε_p^{QP} are the quasi-particle energies.

From this we calculate the approximate gap $\Delta\epsilon^{QP}$

$$\Delta\varepsilon^{QP} = \varepsilon_b^{QP} - \varepsilon_a^{QP} \tag{D.99}$$

We calculate now the elements of the effective two-body interaction Ξ

$$\Xi(1234) = iT^{pp}(1234) \tag{D.100}$$

$$\begin{aligned}
\Xi(1,2,3,4) &= i\frac{\delta\Sigma(1,3)}{\delta G(4,2)} \\
&= i\frac{\delta \int d5d6\, G(5,6)T^{pp}(1,5,3,6)}{\delta G(4,2)} \\
&\approx i\int d5d6\, \frac{\delta G(5,6)}{\delta G(4,2)} T^{pp}(1,5,3,6) \\
&= i\int d5d6\, \delta(5,4)\delta(6,2)T^{pp}(1,5,3,6)
\end{aligned} \tag{D.101}$$

$$\Xi_{(v\sigma_1 c\sigma_2)(v'\sigma_{1'}c'\sigma_{2'})} = \frac{1}{2}[U\delta_{\sigma_1\sigma_2}\delta_{\sigma_{1'}\sigma_{2'}} - U\delta_{\sigma_1\sigma_{1'}}\delta_{\sigma_2\sigma_{2'}}] \tag{D.102}$$

$$\Xi_{(v\sigma_1 c\sigma_2)(c'\sigma_{2'}v'\sigma_{1'})} = \frac{U}{2}\delta_{\sigma_2\sigma_1}\delta_{\sigma_{2'}\sigma_{1'}} - \frac{U^2 t}{(\Omega^{pp})^2 - U^2}\delta_{\sigma_2\sigma_{1'}}\delta_{\sigma_{2'}\sigma_1} \tag{D.103}$$

$${}^3\boldsymbol{H}_{\text{exc}}^{G_{\text{HF}}T_{\text{HF}}^{pp}} = \begin{pmatrix} E_{\text{g}}^{G_{\text{HF}}T_{\text{HF}}^{pp}} - \frac{U}{2} & \frac{U}{2}\left(\frac{Ut/2}{(\Omega^{pp})^2 - U^2} - 1\right) \\ -\frac{U}{2}\left(\frac{Ut/2}{(\Omega^{pp})^2 - U^2} - 1\right) & -\left(E_{\text{g}}^{G_{\text{HF}}T_{\text{HF}}^{pp}} - \frac{U}{2}\right) \end{pmatrix} \tag{D.104a}$$

$${}^1\boldsymbol{H}_{\text{exc}}^{G_{\text{HF}}T_{\text{HF}}^{pp}} = \begin{pmatrix} E_{\text{g}}^{G_{\text{HF}}T_{\text{HF}}^{pp}} + \frac{U}{2} & -\frac{U}{2}\left(\frac{Ut/2}{(\Omega^{pp})^2 - U^2} - 1\right) \\ \frac{U}{2}\left(\frac{Ut/2}{(\Omega^{pp})^2 - U^2} - 1\right) & -\left(E_{\text{g}}^{G_{\text{HF}}T_{\text{HF}}^{pp}} + \frac{U}{2}\right) \end{pmatrix} \tag{D.104b}$$

D.3.1 GW for the asymetric dimer

With the convention that $\Delta v = v_1 - v_2$ and $v_1 > v_2$, the one-body non-interacting Green's function for the half-filled asymmetric Hubbard dimer is

$$\begin{aligned} G^0_{11\uparrow}(\omega) &= \left(\frac{1}{2} - \frac{\Delta v}{2d}\right)\frac{1}{\omega + \frac{d}{2} - i\eta} + \left(\frac{1}{2} + \frac{\Delta v}{2d}\right)\frac{1}{\omega - \frac{d}{2} + i\eta} \\ G^0_{22\uparrow}(\omega) &= \left(\frac{1}{2} + \frac{\Delta v}{2d}\right)\frac{1}{\omega + \frac{d}{2} - i\eta} + \left(\frac{1}{2} - \frac{\Delta v}{2d}\right)\frac{1}{\omega - \frac{d}{2} + i\eta} \\ G^0_{12\uparrow}(\omega) &= \frac{t}{d}\left(\frac{1}{\omega + \frac{d}{2} - i\eta} - \frac{1}{\omega - \frac{d}{2} + i\eta}\right) \end{aligned} \tag{D.105}$$

so the matrix of G^0 is

$$G^0 = \frac{1}{\omega^2 - \frac{d^2}{4}} \begin{pmatrix} \omega + \frac{\Delta v}{2} & -t \\ -t & \omega - \frac{\Delta v}{2} \end{pmatrix} \tag{D.106}$$

with $d = \sqrt{4t^2 + \Delta v^2}$, and its inverse is

$$G^{0,-1} = \begin{pmatrix} \omega - \frac{\Delta v}{2} & t \\ t & \omega + \frac{\Delta v}{2} \end{pmatrix} \tag{D.107}$$

Then we calculate the particle-hole polarizability with

$$P^{pp}_{ijji}(\omega) = \sum_\sigma \int \frac{d\omega'}{2\pi i} G_{ij\sigma}(\omega + \omega') G_{ji\sigma}(\omega') e^{i\omega'\eta} \tag{D.108}$$

we obtain

$$\begin{aligned} P^0_{11}(\omega) &= \left(\frac{2t^2}{d^2}\right)\left(\frac{1}{\omega - d + 2i\eta} - \frac{1}{\omega + d - 2i\eta}\right) \\ P^0_{12}(\omega) &= \left(\frac{-2t^2}{d^2}\right)\left(\frac{1}{\omega - d + 2i\eta} - \frac{1}{\omega + d - 2i\eta}\right) \end{aligned} \tag{D.109}$$

we deduce the dielectric function matrix and its inverse

$$\epsilon = \begin{pmatrix} 1 - UP^0_{11} & -UP^0_{12} \\ -UP^0_{12} & 1 - UP^0_{11} \end{pmatrix} \tag{D.110}$$

$$\epsilon^{-1} = \frac{1}{1 - U(P^0_{11} - P^0_{12})} \begin{pmatrix} 1 - UP^0_{11} & UP^0_{12} \\ UP^0_{12} & 1 - UP^0_{11} \end{pmatrix} \tag{D.111}$$

or

$$[\epsilon^{-1}]_{ij} = \delta_{ij} + (-1)^{i-j} \frac{2Ut^2}{d\tilde{d}} \left[\frac{1}{\omega - \tilde{d} + i\eta} - \frac{1}{\omega + \tilde{d} - i\eta}\right] \tag{D.112}$$

From this we calculate W

$$W_{ijij} = U\delta_{ij} + (-1)^{i-j}\frac{2U^2t^2}{d\tilde{d}}\left[\frac{1}{\omega - \tilde{d} + i\eta} - \frac{1}{\omega + \tilde{d} - i\eta}\right] \tag{D.113}$$

with $\tilde{d} = \sqrt{d^2 + \frac{8Ut^2}{d}}$. The GW self-energy is given by

$$\Sigma^{GW}_{ij\sigma}(\omega) = i\int \frac{d\omega'}{2\pi} G_{ij\sigma}(\omega + \omega')W_{ijij\sigma}(\omega')e^{i\omega'\eta} \tag{D.114}$$

We obtain

$$\Sigma^{GW}_{11}(\omega) = \left(1 - \frac{\Delta v}{d}\right)\frac{U}{2} + \frac{U^2t^2}{d\tilde{d}}\left[\frac{1 + \frac{\Delta v}{d}}{\omega - (\frac{d}{2} + \tilde{d}) + 2i\eta} + \frac{1 - \frac{\Delta v}{d}}{\omega + (\frac{d}{2} + \tilde{d}) - 2i\eta}\right] \tag{D.115}$$

$$\Sigma^{GW}_{22}(\omega) = \left(1 + \frac{\Delta v}{d}\right)\frac{U}{2} + \frac{U^2t^2}{d\tilde{d}}\left[\frac{1 - \frac{\Delta v}{d}}{\omega - (\frac{d}{2} + \tilde{d}) + 2i\eta} + \frac{1 + \frac{\Delta v}{d}}{\omega + (\frac{d}{2} + \tilde{d}) - 2i\eta}\right]$$

$$\Sigma^{GW}_{12}(\omega) = \frac{2U^2t^3}{d^2\tilde{d}}\left[\frac{1}{\omega - (\frac{d}{2} + \tilde{d}) + 2i\eta} - \frac{1}{\omega + (\frac{d}{2} + \tilde{d}) - 2i\eta}\right] \tag{D.116}$$

Appendix E

Resolution methods of a Bethe-Salpeter equation

In this section we present how the Bethe-Salpeter equation is solved in other fields such as particle physics and DMFT (dynamical mean field theory) and what is the physical interpretation given to these solutions.

E.0.1 Quantum field theory

In a relativistic quantum field theory the Bethe-Salpeter equation is used to study two-body bound states. It is written as an non-homogeneous integral equation whose resonances are the bound state masses of the system and it is studied in what is called the ladder approximation. In this case the homogeneous Bethe-Salpeter equation has the form of an eigenvalue problem where the eigenvalue is the square of the coupling constant and the bound state mass has to be tuned such that the eigenvalue corresponds to the value of this constant.

The only model exactly solved is the Wick-Cutkosky model [128] where we study the bound states of two spinless particles, if we note m_a and m_b the masses of the two particles, we have a bound state if

$$E = m_a + m_b - B < m_a + m_b \tag{E.1}$$

where E is the total energy and B is the binding energy. For $E = 0$ the Bethe-Salpeter equation has the form

$$(p^2 + m_a^2)(p^2 + m_b^2)\phi(p) = \frac{\lambda}{\pi^2}\int \frac{d^4k}{(p-k)^2 + \kappa^2}\phi(k) \tag{E.2}$$

where κ is the photon mass and the interaction constant λ is the eigenvalue of the equation, one method to study this equation is to do a change of variable to transform into a symmetric integral equation of the form

$$v(x) = \lambda \int_0^a K(x,y)v(y)dy \tag{E.3}$$

we can then apply Fredholm's theory to obtain the eigenvalue spectrum. In (E.2) the right hand-side can be abbreviated by $\lambda I_\kappa \phi$, so for $\kappa = 0$ and $m_a = m_b = m$, the equation takes the form

$$(p^2 + m^2)^2\phi(p) = \lambda I_0 \phi(p) \tag{E.4}$$

the eigenvalue obtained is $\lambda = 2m^2$. For $E \neq 0$ all calculation done we obtain

$$\lambda = \frac{2}{\pi}\sqrt{1 - \eta^2} \tag{E.5}$$

where

$$\eta = \frac{E}{m_a + m_b} \tag{E.6}$$

we see that the eigenvalue turns complex when (E.1) is not verified anymore which means the system undergoes a transition from a bound state to a scattering state.

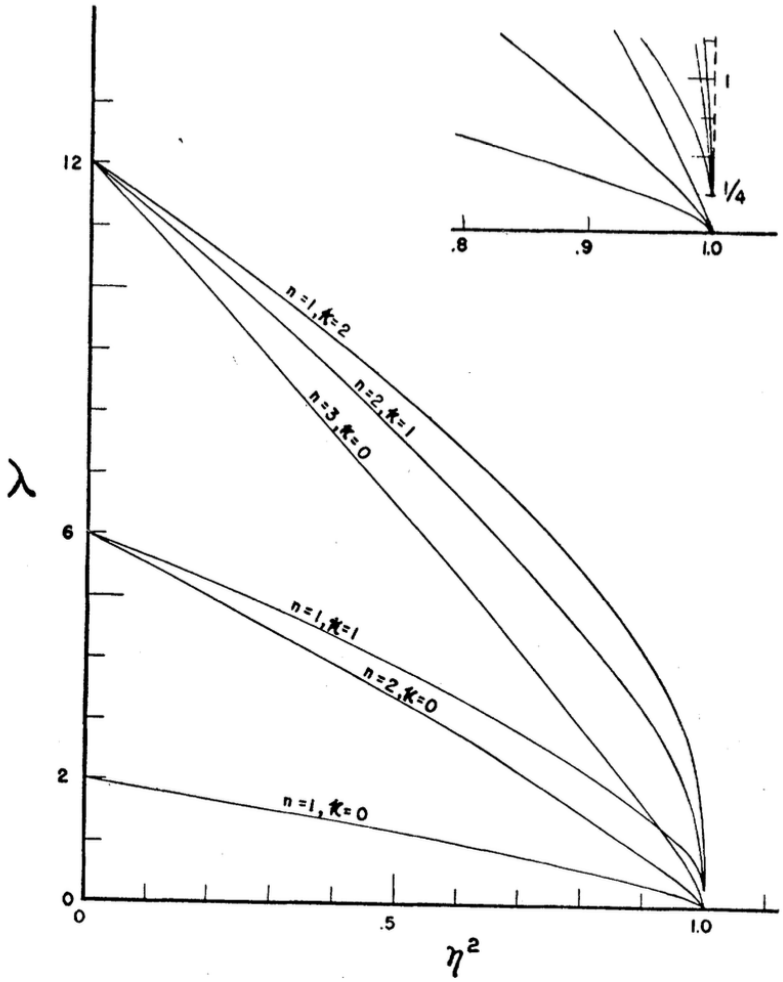

Figure E.1 – variation of λ with respect to η^2. (This picture is taken from [128])

The solutions for which $\lambda = 1/4$ when $\eta^2 = 1$ are called abnormal states, they are non-physical solutions due to relativistic effects.

We can also study the scattering bound states of the non-homogeneous equation [143], we write the integral Schrödinger equation

$$\psi(\boldsymbol{r}) = \psi_0(\boldsymbol{r}) + \int d\boldsymbol{r}' G_0(\boldsymbol{r}, \boldsymbol{r}') V(\boldsymbol{r}') \psi(\boldsymbol{r}') \tag{E.7}$$

$$G_0(\boldsymbol{r}, \boldsymbol{r}') = -\left(\frac{2m}{4\pi}\right) \frac{e^{ik|\boldsymbol{r}-\boldsymbol{r}'|}}{|\boldsymbol{r}-\boldsymbol{r}'|} \tag{E.8}$$

where $\psi(\boldsymbol{r})$, $V(\boldsymbol{r})$ and $G_0(\boldsymbol{r}, \boldsymbol{r}')V(\boldsymbol{r}')$ are respectively the position probability amplitude, the interaction and the free propagator, which we will compare to the Bethe-Salpeter

equation (in the non-relativistic limit)

$$\Psi(x_1,x_2) = \Psi_0(x_1,x_2) + \int G_1(x_1,x_{1'})G_1(x_2,x_{2'})I(x_{1'},x_{2'},x_{1''},x_{2''})\Psi(x_{1''},x_{2''}) \times dx_{1'}dx_{2'}dx_{1''}dx_{2''} \tag{E.9}$$

where $x_i = (\boldsymbol{r_i}, t_i)$

$\Psi(x_1,x_2)$ is the two-body wave function corresponding to the joint probability amplitude that two particles are located in $\boldsymbol{r_1}$ and $\boldsymbol{r_2}$ at the times t_1 and t_2. For $t_1 = t_2$ this equation has the meaning of a Schrödinger wave function. The interaction I represents the sum of irreducible diagrams contributing to the interaction of two particles, in the ladder approximation $I(x_1,x_2,x_{1'},x_{2'}) = I(x_1-x_2)\delta(x_1-x_{1'})\delta(x_2-x_{2'})$ and

$$I(x_1-x_2) = \frac{-i\lambda}{\pi^2}\int \frac{d^4q e^{iq(x_1-x_2)}}{q^2+M^2-i\epsilon} \tag{E.10}$$

where M is the mass of the exchanged particle.

By expressing (E.9) with the coordinates in the center of mass and with some change of variables, this can be rewritten

$$\psi(x) = \psi_0(x) + \int d^4x' G(x,x')I(x')\psi(x') \tag{E.11}$$

where $\psi_0(x) = e^{i\boldsymbol{kr}}$ and x is the relative coordinate. One can show that after a rotation in the complex plane, in the non-relativistic limit this equation reduces to

$$\varphi(\boldsymbol{r}) = e^{i\boldsymbol{k}.\boldsymbol{r}} + \frac{2\lambda}{E}\int d\boldsymbol{r'}\frac{e^{ik|\boldsymbol{r}-\boldsymbol{r'}|}}{|\boldsymbol{r}-\boldsymbol{r'}|}\frac{e^{-Mr'}}{r'}\varphi(\boldsymbol{r'}) \tag{E.12}$$

when we set $E = m_1 + m_2$, the Bethe-Salpeter equation is identical to the Schrödinger equation with a Yukawa potential

$$V(r) = \left(\frac{-\pi\lambda}{m_1 m_2}\right)\frac{e^{-Mr}}{r} \tag{E.13}$$

if

$$M \ll m_{1,2} \tag{E.14}$$

Another method [144] to obtain the bound state spectrum is doing a variational principle, starting from the integral equation

$$\psi_{kK}(x_1,x_2) = \psi_{kK^0}(x_1,x_2) + \lambda\int G_1(x_1-x_{1'})G_1(x_2-x_{2'})V(x_{1''}-x_{2''})\psi_{kK}(x_{1''}-x_{2''})d^4x_{1'}d^4x_{2'} \tag{E.15}$$

with

$$V(x) = \frac{1}{\pi^2}\int d^4q\frac{e^{-i\boldsymbol{qr}}}{q^2+M^2} \tag{E.16}$$

using the boundary condition

$$(p_i^2 + m_i^2)G_1(x) = \delta^4(x) \tag{E.17}$$

(E.15) can be written in a more compact form

$$L(p)\psi_{kK}(x) = \psi_{kK}(x)\lambda\hat{V}(x)\hat{\psi}_{kK}(x) \tag{E.18}$$

defining the following scalar products

$$(\phi_1, \phi_2)_1 = \int \phi_1^*(x)\phi_2(x)d^4x \tag{E.19}$$

$$(\phi_1, \phi_2)_2 = \int \phi_1^*(-x)\phi_2(x)d^4x \tag{E.20}$$

we obtain

$$(\lambda_1 - \lambda_2^*)_1(\psi_1, V\psi_2)_1 = 0 \tag{E.21}$$

if we take $\psi_1 = \psi_2$, then $\lambda_1 = \lambda_2^* = \lambda_1^*$, so λ_1 is real when $(\psi_1, V\psi_2)_1$ is non zero, which is true since V is positive.

The eigenvalue is given by

$$\lambda[\psi_T] = \frac{(\psi_T, L\psi_T)_2}{(\psi_T, V\psi_T)_2} \tag{E.22}$$

where $(\psi, V\phi)$ are T-matrix elements.

One can then decompose the wave function in an even and odd part

$$\psi = \alpha\psi_e + \beta\psi_o \tag{E.23}$$

we have

$$\begin{array}{ll} (\psi_e, V\psi_o) = 0 & (\psi_e, V\psi_e) = 1 \\ (\psi_o, V\psi_o) = 1 & (\psi_0, V\phi) = 0 \\ (\psi_e, V\phi) = t & \end{array} \tag{E.24}$$

we write the Bethe-Salpeter equation in a matrix form

$$\begin{pmatrix} \alpha \\ \beta \end{pmatrix} = \begin{pmatrix} t \\ 0 \end{pmatrix} + \begin{pmatrix} K_{ee} & K_{eo} \\ K_{oe} & K_{oo} \end{pmatrix} \begin{pmatrix} \alpha \\ \beta \end{pmatrix} \tag{E.25}$$

with

$$K_{eo} = \int U_e(x)G(x - x')U_o(x')d^4xd^4x' \tag{E.26}$$

and $U_{e,o} = V\psi_{e,o}$

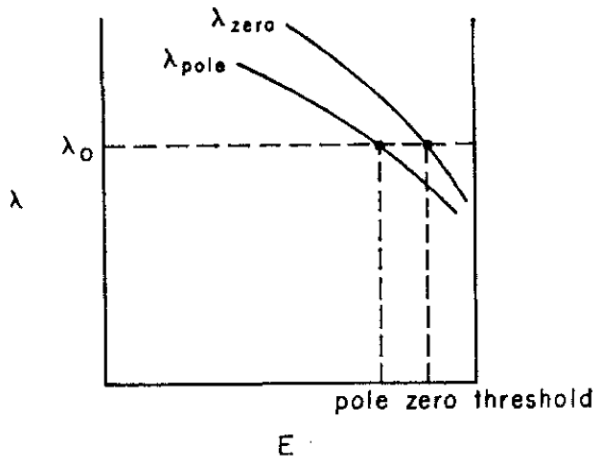

Figure E.2 – Pole and zero of the T-matrix. The poles λ_{pole} are the bound states of the T-matrix and λ_{zero} is its physical scattering region. (This picture is taken from [144])

For a fixed value of λ_0 we will have a bound state or a scattering state depending of the energy E which corresponds to the bound state mass of the system.

A method to solve the homogeneous equation is to solve a fictious eigenvalue problem, with the notations used for (3.256), the bound state equation can be written

$$L_0^{-1}\chi = \Xi\chi \tag{E.27}$$

where χ is the two-body bound state, then we introduce a fictious eigenvalue λ to study this equation as an eigenvalue problem

$$L_0^{-1}\chi = \lambda\Xi\chi \tag{E.28}$$

The eigenvalue λ will depend of the bound state mass M_V, but only the values of M_V for which $\lambda = 1$ are the physical solutions. In [145], the bound state norm is defines as $\langle\langle\chi_{n'}|(-L_0^{-1})|\chi_{n'}\rangle\rangle$ and we have the relation

$$\left(\frac{1}{\lambda_{n'}} - \frac{1}{\lambda^*_{m'}}\right)\langle\langle\chi_{m'}|(-L_0^{-1})|\chi_{n'}\rangle\rangle = 0 \tag{E.29}$$

this means that the eigenvalues are real, otherwise the norm is zero, we consider only the solutions where $\lambda = 1$ and the mass is real. For the case of the orthopositronium in the weak coupling limit, we obtain for the nonrelativistic case

$$M_V^{(n)} = 2m - \frac{m\alpha^2}{4n^2} \tag{E.30}$$

where m is the mass of the fermion and antifermion, and n is a quantum number, the second member of the right hand-side of (E.30) is the binding energy also written $B^{(n)}$. On the other hand solving (E.28) gives

$$\lambda_{n'}(M_V) = \frac{2n}{\alpha}\sqrt{\frac{2m - M_V}{m}} \tag{E.31}$$

we observe that the eigenvalues are real when $0 < M_V < 2m$, when $M_V > 2m$ we have a scattering state and the eigenvalue becomes complex. For $\lambda_{n'}(M_V) = 1$ we retrieve the nonrelativistic results.

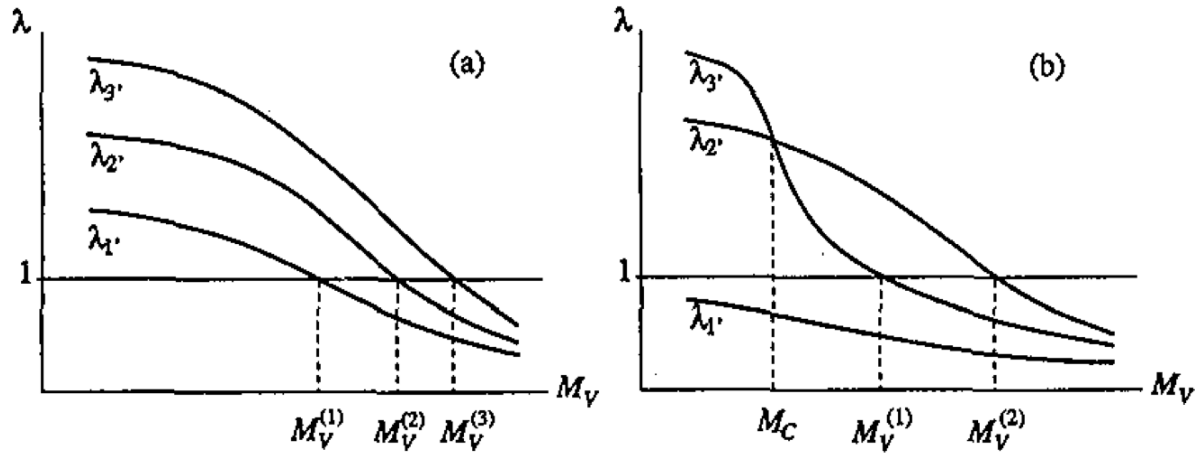

Figure E.3 – Eigenvalues λ with respect to the bound mass M_V. (This picture is taken from [145])

We observe that not every equation $\lambda_{n'}(M_V) = 1$ has a solution, for instance in Fig. E.3(b), the eigenvalue and the corresponding state $(\lambda_{1'}, \chi_{1'})$ have no physical correspondence.

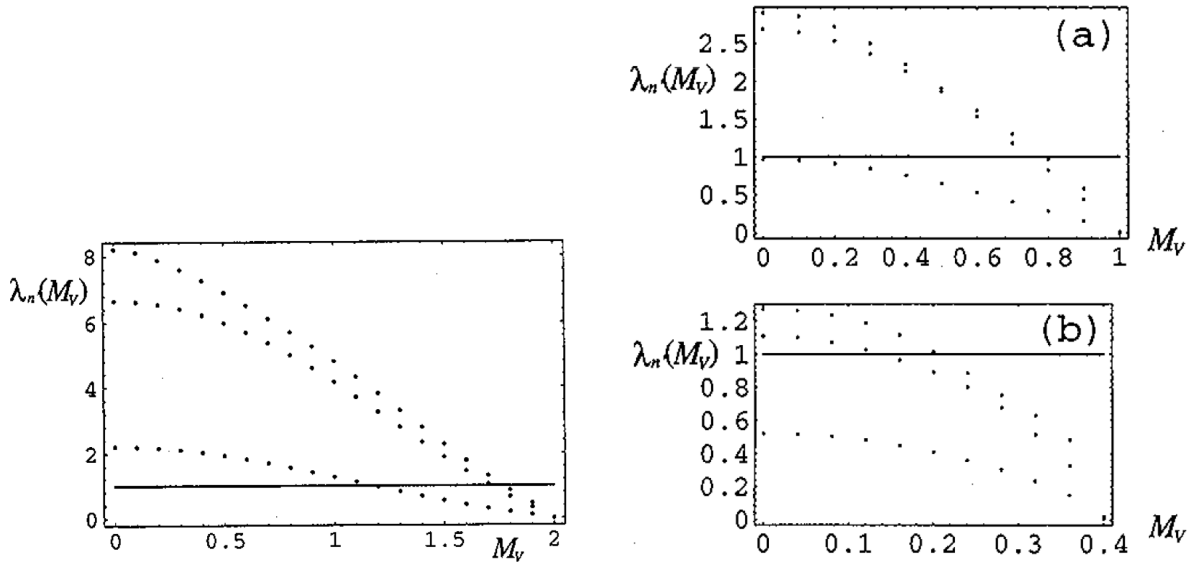

Figure E.4 – The smallest three eigenvalues λ with respect to the bound mass M_V with a mass $m = 1.0$ on the left, $m = 0.5$ in (a) and $m = 0.2$ in (b). (This picture is taken from [145])

On the left panel of Fig. E.4 when $M_V = 2m$, we have $\lambda = 0$ which correspond to free-state solutions of $L_0^{-1}\chi = 0$. On Fig. E.4(a) $m = 0.5$, the lowest eigenvalue $\lambda_{1'}(M_V) = 1$ when $M_V = 0$, this means that this value of m is a critical value and if we chose a value $m < 0.5$ there is no physical solution as we observe on Fig. E.4(b) and Fig. E.5.

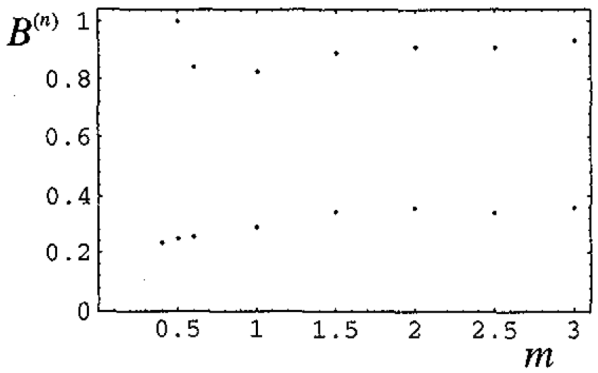

Figure E.5 – Binding energies $B^{(1)}$ in the upper half data and $B^{(2)}$ in the lower half data for several fermion masses m. (This picture is taken from [145])

E.0.2 DMFT

In DMFT [129] the study of the eigenvalues and eigenvectors of the Bethe-Salpeter equation for the two dimensional square lattice Hubbard model at half-filling allowed to observe a metal-insulator (Mott) phase transition in a similar manner that phase transitions are observed in Landau's theory. The free energy F is defined in terms of the exact Green's function G, the non-interacting Green's function G^0, and a potential Φ which is a functional of G

$$F[G] = tr(ln(G)) - tr((G^{0,-1} - G^{-1})G) + \Phi[G] \tag{E.32}$$

and the self-energy by

$$\Sigma[G] = \frac{1}{T}\frac{\delta\Phi[G]}{\delta G} \tag{E.33}$$

The stationary points of (E.32) given by $\frac{\delta F}{\delta G} = 0$ yields the Dyson equation and the second derivative of F which we use to find the critical point of a phase transition is therefore related to the kernel of the Bethe-Salpeter equation.

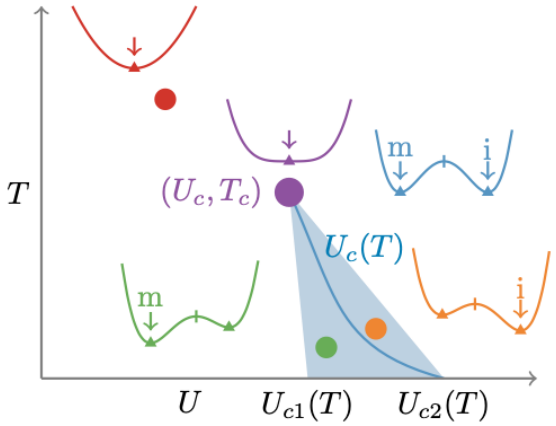

Figure E.6 – Phase diagram of the Hubbard model in DMFT. At low temperature we have a metallic phase for $U < U_{c1}(T)$ and an insulating phase for $U > U_{c2}(T)$. For $U_{c1}(T) < U(T) < U_{c2}(T)$ we have both phases. (This picure is taken from [129])

The second derivative of the free energy is proportional to the Bethe-Salpeter kernel written $\hat{\mathcal{D}}$

$$\frac{\delta^2 F}{\delta\Delta_\nu \Delta_{\nu'}} \propto (\hat{1} - \hat{\mathcal{D}}) \tag{E.34}$$

The kernel determines two stability criteria, the thermodynamic stability which informs on the phase the system is in and the iterative criteria, which is related to the fixed point equation which is solved to obtain the one-particle Green's function, to see if this equation converges to a fixed point we calculate the jacobian's eigenvalue of the variation of the equation with respect to the study parameter, if the eigenvalue is smaller than one, the fixed point is attractive, if it is greater than one it is repulsive, both criteria are related to the kernel. The critical point is reached when the second derivative of F (Hessian) is zero which means that the eigenvalue of the kernel is $\hat{1}$.

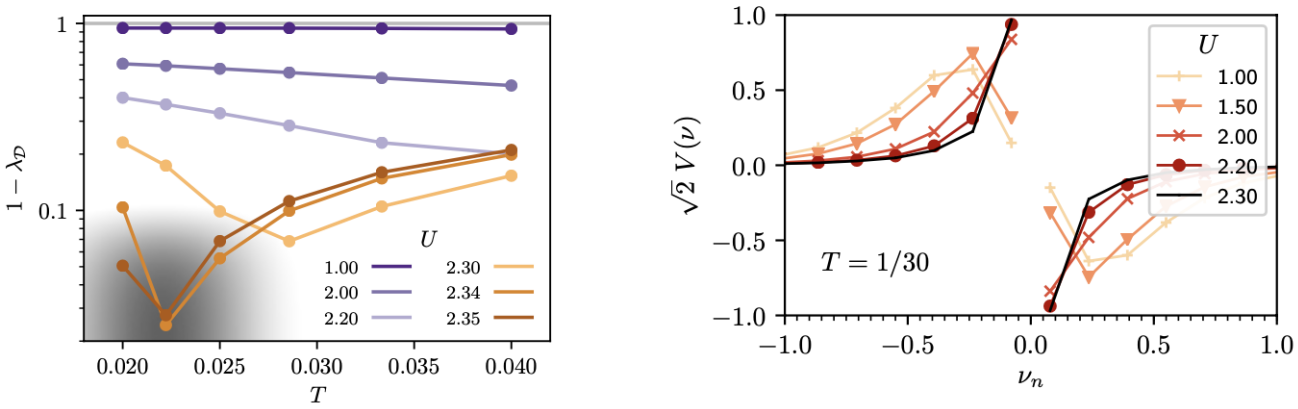

Figure E.7 – On the left the leading eigenvalue of $\hat{\mathcal{D}}$ approaches unity close to the critical point, $2.3 < U_c < 2.35$ and $0.02 < T_c < 0.025$. On the right, the leading right eigenvector V of the non-local Bethe-Salpeter kernel $\hat{\mathcal{D}}$, for T just above T_c. As U increases and the Mott transition is approached, the eigenvector localizes around $\nu = 0$ and $\lambda \to 1$. (This picure is taken from [129])

In Fig. E.7 we see that, for $T < T_c$ and $U_{c1} < U < U_{c2}$, the Bethe-Salpeter equation is convergent (and the iterative process is attractive) at both the metallic and the insulating solutions $\lambda < 1$, and divergent (repulsive) at the unstable fixed point, $\lambda > 1$.

E.0.3 Quantum electrodynamics

The following procedure [146] is used to study the hydrogen system but it could be applied also to obtain the bound state energy of other two-spin 1/2 constituents. The two-body Green's function is defined as

$$G\left(x_1, x_2, y_1, y_2\right) = \langle 0| T\psi_1(x_1)\psi_2(x_2)\overline{\psi}_1(y_1)\overline{\psi}_2(y_2)\,|0\rangle \tag{E.35}$$

we change the coordinates of the individual particles to the ones in the center of mass (CM)

$$X = \xi_1 x_1 + \xi_2 x_2 \qquad x = x_1 - x_2 \tag{E.36a}$$
$$x_1 = X + \xi_2 x \qquad x_2 = X - \xi_1 x \tag{E.36b}$$

where

$$\xi_1 = \frac{m_1}{M} \qquad \xi_2 = \frac{m_2}{M} \qquad M = m_1 + m_2 \tag{E.37}$$

we change the coordinates to the CM in momentum space

$$P = p_1 + p_2 \qquad p = \xi_2 p_1 - \xi_1 p_2 \tag{E.38a}$$
$$p_1 = \xi_1 P + p \qquad p_2 = \xi_2 P - p \tag{E.38b}$$

we have the relation $x_1 \cdot p_1 + x_2 \cdot p_2 = X \cdot P + x \cdot p$. The Fourier transform of the two-body Green's function in the momentum space is

$$\begin{aligned}\overline{G}(p_1, p_2; q_1, q_2) &= \int d^4x_1 d^4x_2 d^4y_1 d^4y_2 e^{i(p_1\cdot x_1 + p_2\cdot x_2 - q_1\cdot y_1 - q_2\cdot y_2)} G\left(x_1, x_2; y_1, y_2\right) \\ &= \int d^4X d^4x d^4Y d^4y e^{i(P\cdot X + p\cdot x - Q\cdot Y - q\cdot y)} \tilde{G}\left(X, x; Y, y\right)\end{aligned} \tag{E.39}$$

where $\tilde{G}\left(X, x; Y, y\right) = G\left(X + \xi_2 x, X - \xi_1 x; Y + \xi_2 y, Y - \xi_1 y\right)$, we have a translation invariance so we have energy-momentum conservation $\delta^4(P - Q)$

$$\overline{G}(p_1, p_2; q_1, q_2) = (2\pi)^4 \delta^4(P - Q) G(P; p, q) \tag{E.40}$$

where

$$G(P;p,q) = \int d^4X d^4x d^4y e^{i(P\cdot X + p\cdot x - q\cdot y)} G(X,x;0,y) \tag{E.41}$$

we choose times such taht $x_1^0, x_2^0 > y_1^0, y_2^0$, we introduce a complete set of two-particle bound states $|\vec{P},n,k\rangle$ of mass M_n with energy

$$\omega_n(\vec{P}) = \sqrt{M_n^2 + \vec{P}^2} \tag{E.42}$$

M_n is the physical mass of the bound system, n is the principal quantum number and k contains the additional quantum numbers which specify the state. The two-body Green's function in the particle-particle channel is

$$\begin{aligned} G\left(x_1,x_2,y_1,y_2\right) =& \Theta(X^0 - Y^0) \sum_{nk} \int \frac{d^3P}{(2\pi)^3 2\omega_n(\vec{P})} \\ & \times \langle 0| T\psi_1(x_1)\psi_2(x_2)|\vec{P},n,k\rangle\langle \vec{P},n,k|T\overline{\psi}_1(y_1)\overline{\psi}_2(y_2)\,|0\rangle \end{aligned} \tag{E.43}$$

we set

$$\Psi_{nk}(\vec{P};x_1,x_2) = \langle 0|\, T\psi_1(x_1)\psi_2(x_2)|\vec{P},n,k\rangle \tag{E.44}$$

$$\overline{\Psi}_{nk}(\vec{P};y_1,y_2) = \langle \vec{P},n,k|T\overline{\psi}_1(y_1)\overline{\psi}_2(y_2)\,|0\rangle \tag{E.45}$$

These are called Bethe-Salpeter wave function, we express them in the CM

$$\begin{aligned} \Psi_{nk}(\vec{P};x_1,x_2) &= \langle 0|\, T\psi_1(X+\xi_2 x)\psi_2(X-\xi_1 x)|\vec{P},n,k\rangle \\ &= \langle 0|\, T e^{i\hat{P}\cdot X}\psi_1(\xi_2 x)e^{-i\hat{P}\cdot X}e^{i\hat{P}\cdot X}\psi_2(-\xi_1 x)e^{-i\hat{P}\cdot X}|\vec{P},n,k\rangle \\ &= e^{-iP_n\cdot X}\Psi_{nk}(\vec{P};\xi_2 x,-\xi_1 x) \end{aligned} \tag{E.46}$$

and

$$\overline{\Psi}_{nk}(\vec{P};y_1,y_2) = e^{iP_n\cdot Y}\overline{\Psi}_{nk}(\vec{P};\xi_2 y,-\xi_1 y) \tag{E.47}$$

using the fact that

$$\Theta(t_1-t_2)f(E)e^{-iE(t_1-t_2)} = i\int \frac{dk_0}{2\pi} e^{-ik_0(t_1-t_2)} \frac{1}{k_0 - E + i\epsilon} f(k_0) \tag{E.48a}$$

$$\Theta(t_2-t_1)f(E)e^{iE(t_1-t_2)} = -i\int \frac{dk_0}{2\pi} e^{-ik_0(t_1-t_2)} \frac{1}{k_0 + E - i\epsilon} f(-k_0) \tag{E.48b}$$

with $E=0$ and $f(E)=1$, (E.43) can be written

$$\begin{aligned} G\left(x_1,x_2,y_1,y_2\right) &= i\int \frac{dP^0}{2\pi} \frac{e^{-iP^0(X^0-Y^0)}}{P^0 + i\epsilon} \sum_{nk} \int \frac{d^3P}{(2\pi)^3 2\omega_n(\vec{P})} \\ &\quad \times \Psi_{nk}(\vec{P};\xi_2 x,-\xi_1 x)\overline{\Psi}_{nk}(\vec{P};\xi_2 y,-\xi_1 y) \\ &= i\sum_{nk}\int \frac{d^4P}{(2\pi)^4 2\omega_n(\vec{P})} \frac{e^{-iP\cdot(X-Y)}}{P^0 - \omega_n(\vec{P}) + i\epsilon} \\ &\quad \times \Psi_{nk}(\vec{P};\xi_2 x,-\xi_1 x)\overline{\Psi}_{nk}(\vec{P};\xi_2 y,-\xi_1 y) \end{aligned} \tag{E.49}$$

we did the change of vairiable $P^0 \to P^0 - \omega_n(\vec{P})$ and $P_n = (\omega_n(\vec{P}), \vec{P}) = (\sqrt{M_n^2 + \vec{P}^2}, \vec{P})$ is the physical momentum. We write the Fourier transform of the Bethe-Salpeter wave function in the momentum space

$$\Psi_{nk}(\vec{P}, p) = \int d^4x e^{ip\cdot x} \frac{\Psi_{nk}(\vec{P}; \xi_2 x, -\xi_1 x)}{\sqrt{2\omega_n(\vec{P})}} \tag{E.50}$$

$$\overline{\Psi}_{nk}(\vec{P}, q) = \int d^4y e^{-iq\cdot y} \frac{\overline{\Psi}_{nk}(\vec{P}; \xi_2 y, -\xi_1 y)}{\sqrt{2\omega_n(\vec{P})}} \tag{E.51}$$

we replace these expressions in (E.49) we get

$$G\,(P; p, q) = i \sum_{nk} \frac{\Psi_{nk}(\vec{P}, p)\overline{\Psi}_{nk}(\vec{P}, q)}{P^0 - \omega_n(\vec{P}) + i\epsilon} \tag{E.52}$$

The bound state pole is given by (E.42), but in the CM frame with $\vec{P} = \vec{0}$, the pole is at $\omega_n = M_n$. Then we derive the Bethe-Salpeter equation from a diagrammatic method

$$G(P; p, q) = S(P; p, q) + \int \frac{d^4l}{(2\pi)^4} \frac{d^4k}{(2\pi)^4} S(P; p, l) K(P; l, k) G(P; k, q) \tag{E.53}$$

Since there is no relative momentum between the electron and the proton in S

$$S(P; p, q) = (2\pi)^4 \delta^4(p - q) S(P; p) \tag{E.54}$$

this simplify (E.53)

$$G(P; p, q) = S(P; p, q) + S(P; p) \int \frac{d^4k}{(2\pi)^4} K(P; l, k) G(P; k, q) \tag{E.55}$$

or

$$G = S + SKG \tag{E.56}$$

we replace (E.52) in (E.53) and we use the residue theorem at $\omega_n(\vec{P}) = (M_n^2 + \vec{P}^2)^{1/2}$ to obtain the homogeneous bound state equation

$$\Psi_{nk}(\vec{P}; p) = S(P_n; p) \int \frac{d^4l}{(2\pi)^4} K(P_n; p, l) \Psi_{nk}(\vec{P}; l) \tag{E.57}$$

The solution of (E.53) is given by

$$G = (S^{-1} - K)^{-1} \tag{E.58}$$

or

$$G = (1 - SK)^{-1} S = S(1 - KS)^{-1} \tag{E.59}$$

from these last expressions we can do a Taylor expansion

$$G = S + SKS + SKSKS + \cdots \tag{E.60}$$

we can also define the truncated Green's function

$$G = S + SG_T S \tag{E.61}$$

where G_T satisfies

$$G_T = K + KSG_T \tag{E.62}$$

the solutions are

$$G_T = (1 - KS)^{-1}K = K(1 - SK)^{-1} \tag{E.63}$$

which leads to the geometric expansion

$$G_T = K + KSK + KSKSK + \cdots \tag{E.64}$$

To derive the orthonormality condition of the Bethe-Salpeter wave functions we start by expanding G^{-1}

$$G^{-1}(P^0) = G^{-1}(P_n^0) + (P^0 - P_n^0)\frac{d}{dP^0}G^{-1}(P^0)\Big|_{P_n^0} + \mathcal{O}(P^0 - P_n^0)^2 \tag{E.65}$$

replacing this expression in the identity $G = GG^{-1}G$ and applying residue theorem at the bound state pole P_n^0 on both side of the identity gives

$$i\sum_k \Psi_{nk}\overline{\Psi}_{nk} = i\sum_r \Psi_{nr}\overline{\Psi}_{nr}\frac{d}{dP^0}G^{-1}(P^0)\Big|_{P_n^0} i\sum_s \Psi_{ns}\overline{\Psi}_{ns} \tag{E.66}$$

or

$$\delta_{rs} = i\overline{\Psi}_{nr}\frac{d}{dP^0}G^{-1}(P^0)\Big|_{P_n^0}\Psi_{ns} \tag{E.67}$$

In the following a method which allows to use a simpler form for the non-interacting propagator S_0 instead of S is presented. In order that this change does not modify the bound-state energies we have to the modifications in such a way that the truncated Green's function G_T remains the same, because G and G_T have the same poles. So to maintain G_T unaltered whereas we use another two-body propagator, we have to proceed to another modification which compensates the one we did on the propagator, this is done by defining a new kernel $\overline{K}$ such that

$$G_T = \overline{K} + \overline{K}S_0G_T \tag{E.68}$$

with the expressions (E.62) and (E.68) we deduce an expression for $\overline{K}$

$$\overline{K} = \left(1 - K(S - S_0)\right)^{-1}K = K + K(S - S_0)K + \cdots \tag{E.69}$$

or we can also write

$$G = S_0 + S_0\overline{K}G \tag{E.70}$$

and using (E.56) and (E.70) we get

$$\overline{K} = K + S_0^{-1} + S^{-1} \tag{E.71}$$

But in order to use (E.71), one needs that S_0 is invertible, if it not the case then one uses (E.69) obtained from the truncated Green's function

To calculate the higher-order terms one needs to start from a lowest order, or reference with an exact solution which will be the foundation of perturbative calculation. The approximated kernel associated to S_0 is written K_0 and verify

$$G_0 = S_0 + S_0K_0G_0 \tag{E.72}$$

where G_0 is the reference Green's function. In (E.70) and (E.72) we multiply by S_0^{-1} on the left and G^{-1} or G_0^{-1} on the right to obtain

$$S_0^{-1} = G^{-1} + \overline{K} \tag{E.73}$$

and

$$S_0^{-1} = G_0^{-1} + K_0 \tag{E.74}$$

we equalize the two equations

$$G^{-1} + \overline{K} = G_0^{-1} + K_0 \tag{E.75}$$

and from this we deduce the following expression

$$G = G_0 + G_0 \delta K G \tag{E.76}$$

where $\delta K = \overline{K} - K_0$. We note E^0, Ψ^0 and $\overline{\Psi}^0$, the energies and Bethe-Salpeter wave functions of the reference, the exact quantities are related to the ones of the reference in a perturbative expansion

$$E_n = E_n^0 + E_n^1 + \cdots \tag{E.77a}$$
$$\Psi_{nk} = \Psi_{nk}^0 + \Psi_{nk}^1 + \cdots \tag{E.77b}$$
$$\overline{\Psi}_{nk} = \overline{\Psi}_{nk}^0 + \overline{\Psi}_{nk}^1 + \cdots \tag{E.77c}$$

For the left side of (E.76) we have

$$\begin{aligned} G(E) &= i\frac{\Psi_{nk}\overline{\Psi}_{nk}}{E - E_n} = i\frac{(\Psi_{nk}^0 + \Psi_{nk}^1 + \cdots)(\overline{\Psi}_{nk}^0 + \overline{\Psi}_{nk}^1 + \cdots)}{(E_n - E_n^0)\left(1 - \frac{E_n^1 + E_n^2 + \cdots}{E_n - E_n^0}\right)} \\ &= i\frac{\Psi_{nk}^0\overline{\Psi}_{nk}^0}{E - E_n^0} + \left\{ i\frac{E_n^1\Psi_{nk}^0\overline{\Psi}_{nk}^0}{(E - E_n^0)^2} + i\frac{\Psi_{nk}^1\overline{\Psi}_{nk}^0 + \Psi_{nk}^0\overline{\Psi}_{nk}^1}{E - E_n^0} \right\} \\ &+ \left\{ i\frac{(E_n^1)^2\Psi_{nk}^0\overline{\Psi}_{nk}^0}{(E - E_n^0)^3} + i\frac{E_n^2\Psi_{nk}^0\overline{\Psi}_{nk}^0 + E_n^1(\Psi_{nk}^1\overline{\Psi}_{nk}^0 + \Psi_{nk}^0\overline{\Psi}_{nk}^1)}{(E - E_n^0)^2} \right. \\ &+ \left. i\frac{\Psi_{nk}^2\overline{\Psi}_{nk}^0 + (\Psi_{nk}^1\overline{\Psi}_{nk}^1 + \Psi_{nk}^0\overline{\Psi}_{nk}^2)}{(E - E_n^0)} + \mathcal{O}(\delta K)^3 \right. \end{aligned} \tag{E.78}$$

Then we expand the right side of (E.76). We write

$$G_0(E) = i\frac{\Psi_{nk}^0\overline{\Psi}_{nk}^0}{E - E_n^0} + \hat{G}_0(E) = i\frac{\Psi_{nk}^0\overline{\Psi}_{nk}^0}{E - E_n^0} + \hat{G}_0 + (E - E_n^0)\hat{G}_0' + \mathcal{O}(E - E_n^0)^2 \tag{E.79}$$

with

$$\hat{G}_0(E) = G_0(E) - i\frac{\Psi_{nk}^0\overline{\Psi}_{nk}^0}{E - E_n^0} \quad \hat{G}_0 = \hat{G}_0(E_n^0) \quad \hat{G}_0' = \frac{d}{dE}\hat{G}_0\Big|_{E_n^0} \tag{E.80}$$

and for δK

$$\delta K(E) = \delta K_0 + (E - E_n^0)\frac{d}{dE}\delta K\Big|_{E_n^0} + \mathcal{O}(E - E_n^0)^2 \tag{E.81}$$

with $\delta K_0 = \delta K(E_n^0)$. We obtain

$$\begin{aligned} G(E) &= G_0 + G_0\delta K G_0 + G_0\delta K G_0 \delta K G_0 + \mathcal{O}(\delta K)^3 \\ &= \left(i\frac{\Psi_{nk}^0\overline{\Psi}_{nk}^0}{E - E_n^0} + \hat{G}_0(E)\right) + \left(i\frac{\Psi_{nk}^0\overline{\Psi}_{nk}^0}{E - E_n^0} + \hat{G}_0(E)\right)\delta K(E)\left(i\frac{\Psi_{nk}^0\overline{\Psi}_{nk}^0}{E - E_n^0} + \hat{G}_0(E)\right) \\ &+ \left(i\frac{\Psi_{nk}^0\overline{\Psi}_{nk}^0}{E - E_n^0} + \hat{G}_0(E)\right)\delta K(E)\left(i\frac{\Psi_{nk}^0\overline{\Psi}_{nk}^0}{E - E_n^0} + \hat{G}_0(E)\right)\delta K(E) \\ &\times \left(i\frac{\Psi_{nk}^0\overline{\Psi}_{nk}^0}{E - E_n^0} + \hat{G}_0(E)\right) + \mathcal{O}(\delta K)^3 \end{aligned} \tag{E.82}$$

we use (E.81) in (E.82)

$$
\begin{aligned}
G(E) = &\left\{ i\frac{\Psi^0_{nk}\overline{\Psi}^0_{nk}}{E-E^0_n} \right\} + \left\{ i\frac{\Psi^0_{nk}\langle i\delta K\rangle\overline{\Psi}^0_{nk}}{(E-E^0_n)^2} \right. \\
&+ \frac{\hat{G}_0\delta K_0 i\Psi^0_{nk}\overline{\Psi}^0_{nk} + i\Psi^0_{nk}\overline{\Psi}^0_{nk}\delta K_0\hat{G}_0 + i\Psi^0_{nk}\langle i\delta K\rangle'\overline{\Psi}^0_{nk}}{(E-E^0_n)} \\
&\left\{ i\frac{\Psi^0_{nk}\langle i\delta K\rangle^2\overline{\Psi}^0_{nk}}{(E-E^0_n)^3} + \frac{1}{(E-E^0_n)^2}\left[\hat{G}_0\delta K_0 i\Psi^0_{nk}\langle i\delta K\rangle\overline{\Psi}^0_{nk}\right.\right. \\
&+ i\Psi^0_{nk}\langle i\delta K\rangle\overline{\Psi}^0_{nk}\delta K_0\hat{G}_0 + i\Psi^0_{nk}\langle i\delta K\hat{G}_0\delta K\rangle\overline{\Psi}^0_{nk} + 2i\Psi^0_{nk}\langle i\delta K\rangle\langle i\delta K\rangle'\overline{\Psi}^0_{nk} \\
&+ \frac{1}{E-E^0_n}\left[i\Psi^0_{nk}\overline{\Psi}^0_{nk}\{\langle i\delta K\rangle\langle i\delta K\rangle'' + (\langle i\delta K\rangle')^2 + \langle i\delta K\hat{G}_0\delta K\rangle'\}\right. \\
&+ i\hat{G}_0\delta K_0\Psi^0_{nk}\overline{\Psi}^0_{nk}\delta K_0\hat{G}_0 + i\hat{G}_0\delta K_0\Psi^0_{nk}\overline{\Psi}^0_{nk}\langle i\delta K\rangle' + i[\hat{G}_0\delta K]'\Psi^0_{nk}\overline{\Psi}^0_{nk}\langle i\delta K\rangle \\
&+ i\hat{G}_0\delta K_0\hat{G}_0\delta K_0\Psi^0_{nk}\overline{\Psi}^0_{nk} + i\Psi^0_{nk}\overline{\Psi}^0_{nk}\delta K_0\hat{G}_0\langle i\delta K\rangle' + i\Psi^0_{nk}\overline{\Psi}^0_{nk}[\delta K\hat{G}_0]'\langle i\delta K\rangle \\
&\left.\left.\left. + i\Psi^0_{nk}\overline{\Psi}^0_{nk}\delta K_0\hat{G}_0\delta K_0\hat{G}_0 + \mathcal{O}(\delta K)^3 + \mathcal{O}(E-E^0_n)^0 \right.\right.\right. \qquad \text{(E.83)}
\end{aligned}
$$

where

$$\langle iX\rangle = i\overline{\Psi}^0_{nk}X(E^0_n)\Psi^0_{nk} \qquad \langle iX\rangle' = i\overline{\Psi}^0_{nk}\frac{dX}{dE}\Big|_{E^0_n}\Psi^0_{nk} \qquad \text{(E.84a)}$$

$$\langle iX\rangle'' = i\overline{\Psi}^0_{nk}\frac{d^2X}{dE^2}\Big|_{E^0_n}\Psi^0_{nk} \qquad [Y]' = \frac{dY}{dE}\Big|_{E^0_n} \qquad \text{(E.84b)}$$

we identify (E.78) and (E.83), this leads to

$$E_n = E^0_n + \langle i\delta K\rangle + \langle i\delta K\hat{G}_0\delta K\rangle + \langle i\delta K\rangle\langle i\delta K\rangle' + \mathcal{O}(\delta K)^3 \qquad \text{(E.85a)}$$

$$\Psi_{nk} = \Psi^0_{nk} + \hat{G}_0\delta K\Psi^0_{nk} + \frac{1}{2}\langle i\delta K\rangle'\Psi^0_{nk} + \mathcal{O}(\delta K)^2 \qquad \text{(E.85b)}$$

$$\overline{\Psi}_{nk} = \overline{\Psi}^0_{nk} + \overline{\Psi}^0_{nk}\delta K\hat{G}_0 + \frac{1}{2}\langle i\delta K\rangle'\overline{\Psi}^0_{nk} + \mathcal{O}(\delta K)^2 \qquad \text{(E.85c)}$$